

DTIC FILE COPY

AD-A204 034

TR FILE

ESL-TR-87-15

FILE # 1

DEVELOPMENT OF A PAVEMENT EVALUATION METHOD FOR LOW-VOLUME AIRFIELD PAVEMENTS

A.J. BUSH III

US ARMY ENGINEER WATERWAYS EXPERIMENT STATION
PO BOX 631
VICKSBURG MS 39180-0631

SEPTEMBER 1987

FINAL REPORT

SEPTEMBER 1985 - MAY 1987

DTIC
ELECTE
DEC 12 1988
S D

APPROVED FOR PUBLIC RELEASE: DISTRIBUTION UNLIMITED



ENGINEERING & SERVICES LABORATORY
AIR FORCE ENGINEERING & SERVICES CENTER
TYNDALL AIR FORCE BASE, FLORIDA 32403

8 8 12 9 0 5 3

NOTICE

PLEASE DO NOT REQUEST COPIES OF THIS REPORT FROM
HQ AFESC/RD (ENGINEERING AND SERVICES LABORATORY).
ADDITIONAL COPIES MAY BE PURCHASED FROM:

NATIONAL TECHNICAL INFORMATION SERVICE
5285 PORT ROYAL ROAD
SPRINGFIELD, VIRGINIA 22161

FEDERAL GOVERNMENT AGENCIES AND THEIR CONTRACTORS
REGISTERED WITH DEFENSE TECHNICAL INFORMATION CENTER
SHOULD DIRECT REQUESTS FOR COPIES OF THIS REPORT TO:

DEFENSE TECHNICAL INFORMATION CENTER
CAMERON STATION
ALEXANDRIA, VIRGINIA 22314

UNCLASSIFIED

SECURITY CLASSIFICATION OF THIS PAGE

ADA204034

REPORT DOCUMENTATION PAGE				Form Approved OMB No. 0704-0188	
1a. REPORT SECURITY CLASSIFICATION UNCLASSIFIED		1b. RESTRICTIVE MARKINGS			
2a. SECURITY CLASSIFICATION AUTHORITY		3. DISTRIBUTION / AVAILABILITY OF REPORT Approved for public release; distribution is unlimited.			
2b. DECLASSIFICATION / DOWNGRADING SCHEDULE					
4. PERFORMING ORGANIZATION REPORT NUMBER(S)		5. MONITORING ORGANIZATION REPORT NUMBER(S) ESL-TR-87-15			
6a. NAME OF PERFORMING ORGANIZATION US Army Engineer Waterways Experiment Station		6b. OFFICE SYMBOL (If applicable) WESGP-IP	7a. NAME OF MONITORING ORGANIZATION Air Force Engineering and Services Center (RDCP)		
6c. ADDRESS (City, State, and ZIP Code) PO Box 631 Vicksburg, Mississippi 39180-0631		7b. ADDRESS (City, State, and ZIP Code) Tyndall AFB, Florida 32403-6001			
8a. NAME OF FUNDING / SPONSORING ORGANIZATION Air Force Engineering and Services Center		8b. OFFICE SYMBOL (If applicable) RDCP	9. PROCUREMENT INSTRUMENT IDENTIFICATION NUMBER MIPR N 85-42 dated Jan 85 as amended		
8c. ADDRESS (City, State, and ZIP Code) Tyndall AFB, Florida 32403-6001		10. SOURCE OF FUNDING NUMBERS			
		PROGRAM ELEMENT NO. 64617F	PROJECT NO. 2621	TASK NO. 40	WORK UNIT ACCESSION NO. 20
11. TITLE (Include Security Classification) (U) DEVELOPMENT OF A PAVEMENT EVALUATION METHOD FOR LOW-VOLUME AIRFIELD PAVEMENTS					
12. PERSONAL AUTHOR(S) Albert J. Bush III					
13a. TYPE OF REPORT Final Report		13b. TIME COVERED FROM 85 09 TO 87 05		14. DATE OF REPORT (Year, Month, Day) September 1987	15. PAGE COUNT 226
16. SUPPLEMENTARY NOTATION Availability of this report is specified on reverse of front cover.					
17. COSATI CODES			18. SUBJECT TERMS (Continue on reverse if necessary and identify by block number)		
FIELD 13	GROUP 02	SUB-GROUP	Airfield pavements, ALRS, Alternate Launch and Recovery Surfaces, Deflection measurements, Nondestructive testing, Traffic test section		
19. ABSTRACT (Continue on reverse if necessary and identify by block number) The US Air Force has a need to predict the number of aircraft operations to failure on marginal flexible pavements. Alternate Launch and Recovery Surfaces (ALRS) are being constructed for use only when the mission-essential runways are destroyed during an attack. Since ALRS pavements will only be used in contingency situations, an evaluation procedure is required to ensure that the pavements will support a limited number of operations. The purpose of this study was to develop a falling weight deflectometer (FWD) based evaluation procedure to predict the allowable F-4 aircraft load and the allowable aircraft passes for marginal flexible pavements. Data from 11 pavement test sections that were trafficked to failure with an F-4 load cart were used to develop the evaluation methodology. Four of the test sections were constructed for the purpose of evaluating thin → (Continued)					
20. DISTRIBUTION / AVAILABILITY OF ABSTRACT <input type="checkbox"/> UNCLASSIFIED/UNLIMITED <input checked="" type="checkbox"/> SAME AS RPT. <input type="checkbox"/> DTIC USERS			21. ABSTRACT SECURITY CLASSIFICATION UNCLASSIFIED		
22a. NAME OF RESPONSIBLE INDIVIDUAL Capt Martin D. Lewis		22b. TELEPHONE (Include Area Code) (904)283-6317		22c. OFFICE SYMBOL HQ AFESC/RDCP	

DD Form 1473, JUN 86

Previous editions are obsolete.

SECURITY CLASSIFICATION OF THIS PAGE

1

UNCLASSIFIED

UNCLASSIFIED

19. ABSTRACT (Continued).

asphalt concrete (AC) surfaces. Seven test sections were environmentally aged pavements from 9 to 30 years old located in non traffic areas of airfields.

The FWD Impulse Stiffness Modulus (ISM) was selected as the best estimator for predicting the pavement performance for low-volume airfield pavements. A method for correcting the ISM for temperature of the AC layer was developed. For evaluation, when California Bearing Ratio (CBR) is measured on all pavement layers, the Corps of Engineers CBR procedure is the next best estimator of performance of low-volume pavements. (SDW)K

PREFACE

This report was submitted as a thesis to the University of Illinois at Urbana-Champaign and funded under Military Interdepartmental Purchase Request (MIPR) Number N-85-42 by the Air Force Engineering and Services Center, Engineering and Services Laboratory, Tyndall Air Force Base, Florida 32403-6001.

This thesis is being published in its original format by this laboratory because of its interest to the worldwide scientific and engineering community. It covers work performed between September 1985 and May 1987. HQ AFESC/RDC project officers were Lt Col Robert R. Costigan and Capt Martin D. Lewis.

This report has been reviewed by the Public Affairs Officer (PA) and is releasable to the National Technical Information Service (NTIS). At NTIS, it will be available to the general public, including foreign nationals.

This technical report has been reviewed and is approved for publication.


MARTIN D. LEWIS, Capt, USAF
Project Officer


ROBERT R. COSTIGAN, Lt Col, USAF
Chief, Engineering Research
Division


GEORGE E. WALROND, Maj, USAF
Chief, Pavement Technology
Branch


LAWRENCE D. HOKANSON, Col, USAF
Director, Engineering and Services
Laboratory



Accession For	
NTIS CRA&I	<input checked="" type="checkbox"/>
DTIC TAB	<input type="checkbox"/>
Unannounced	<input type="checkbox"/>
Justification	
By	
Distribution/	
Availability Codes	
Dist	Avail and/or Special
A-1	

TABLE OF CONTENTS

SECTION	Title	Page
I	INTRODUCTION	1
	A. BACKGROUND	1
	B. PURPOSE	3
	C. SCOPE	4
	D. THESIS FORMAT	4
II	PERFORMANCE PREDICTION	6
	A. PAVEMENT PROPERTIES AFFECTING PERFORMANCE	6
	1. Distresses	6
	2. Granular Layers	7
	3. Subgrades	11
	4. Summary	14
	B. DESTRUCTIVE EVALUATION METHODS	14
	1. California Bearing Ratio (CBR)	14
	2. Rut Depth Prediction	16
	C. NONDESTRUCTIVE EVALUATION METHODS	18
	1. DSM Procedure	19
	2. Wave Propagation Methods	19
	3. Deflection Basin Methods	20
	a. Surface/Base Curvature Index Methods	21
	b. Area/DO Concepts	21
	c. Back Calculation Methods	22
	D. METHODS SELECTED	23
	1. Field Procedure	23
	2. Mechanistic Analysis	23
III	FIELD TESTS	31
	A. INTRODUCTION	31
	B. PAVEMENT CHARACTERISTICS	32
	1. WES Test Items	32
	2. Wright-Patterson and Whiteman Test Items.....	34
	3. North Field Test Section	35
	C. TEST CONDITIONS AND PROCEDURES	36
	1. Instrumentation	36
	2. Nondestructive Testing	37
	3. F-4 Load Cart	39
	4. Traffic Pattern	39
	5. Failure Criteria	40
	6. Other Data	41
IV	ANALYSIS OF DATA	69
	A. FALLING WEIGHT DEFLECTOMETER	69
	1. Verification of Deflections	69
	2. Effects of Force Level	70

TABLE OF CONTENTS (CONCLUDED)

SECTION	Title	Page
	3. Effects of Temperature	73
	4. Effects of Traffic on ISM and Deflection Basin Descriptors	76
	B. USE OF DEFLECTION BASIN DESCRIPTORS	77
	1. Surface/Base Curvature	77
	2. Nonlinear Subgrade Modulus	77
	C. RESULTS FROM BACK CALCULATION PROCEDURE	78
	1. Verification of Modulus Values and Resulting Stress Calculations	79
	2. Effects of Traffic on Modulus Values	80
V	ANALYSIS OF PERFORMANCE OF TRAFFIC TEST ITEMS	132
	A. PERFORMANCE OF TRAFFIC TEST SECTIONS	132
	1. Cracking	132
	2. Rutting	133
	B. ESTIMATE OF PERFORMANCE USING CBR PROCEDURE	133
	C. LAYERED ELASTIC ESTIMATE OF PERFORMANCE	134
	1. Subgrade Vertical Strain	134
	2. Base Course Vertical Strain	135
	D. RUT DEPTH PREDICTIONS	135
VI	NEW PREDICTION MODELS	153
	A. ESTIMATES OF PERFORMANCE	153
	1. Rut Depth	153
	2. Coverages to 3-inch Rut Depth	155
	3. Coverages to 1-inch Rut Depth	157
	B. SELECTION OF BEST ESTIMATOR OF PERFORMANCE	159
	C. VALIDATION OF MODEL	159
	D. EVALUATION PROCEDURE	160
VII	CONCLUSIONS AND RECOMMENDATIONS	171
	A. CONCLUSIONS	171
	B. RECOMMENDATIONS	172
APPENDIX		
	A. FALLING WEIGHT DEFLECTOMETER DEFLECTION BASIN DATA	174
	B. BISDEF PROGRAM	192
	C. PROGRAM FOR CORRECTING FWD ISM DATA FOR TEMPERATURE	203
	REFERENCES	205
	VITA	211

LIST OF TABLES

TABLE	TITLE	PAGE
III-1	SUMMARY OF CBR, DENSITY, AND WATER CONTENT DATA FOR SUBGRADE AND BASE ON WES TEST ITEMS	42
III-2	AS-BUILT LAYER THICKNESS FOR WES TEST ITEMS	43
III-3	PAVEMENT CONSTRUCTION HISTORY	44
III-4	BASE COURSE AND SUBGRADE PROPERTIES FOR WRIGHT- PATTERSON AFB AND WHITEMAN AFB ITEMS	45
III-5	SUMMARY OF CBR, DENSITY, AND WATER CONTENT FOR NORTH FIELD TEST ITEM	46
IV-1	LAYER MODULUS VALUES BACK CALCULATED FROM FWD 9-KIP DATA USING BISDEF	82
IV-2	STRESSES AND STRAINS FOR F-4 LOADING	84
V-1	RUTTING AND CRACKING PROGRESSION OF TEST ITEMS	138
V-2	SUMMARY OF CHARACTERISTICS OF TRAFFIC TEST ITEMS	141
VI-1	DATA BASE FOR RUT DEPTH PREDICTION	162
VI-2	DATA BASE FOR PREDICTING COVERAGES	164
A-1	FALLING WEIGHT DEFLECTOMETER DEFLECTION BASIN DATA ...	175
A-2	FALLING WEIGHT DEFLECTOMETER DEFLECTION BASIN DATA NORTH FIELD	189

LIST OF FIGURES

FIGURE	TITLE	PAGE
II-1	Stable versus Unstable Behavior (Reference 19)	24
II-2	Relationship Between Permanent Strain versus Cycles of Load (Reference 25)	25
II-3	Logarithmic Relationships of Permanent Strain and Cycles (Reference 25)	26
II-4	Limiting Subgrade Strain Criteria for Conventional Flexible Pavements with a 20 Year Life (Reference 30)	27
II-5	Use of Deflection Basin Parameters to Analyze Pavement Structural Layers (Reference 40)	28
II-6	Area of Deflection Basin (Reference 12)	29
II-7	Typical Resilient Modulus - Repeated Deviator Stress Relation (Reference 12)	30
III-1	Layout of WES Test Items	47
III-2	Grain Size Distributions for Subgrade and Base for WES Test Item	48
III-3	Laboratory Compaction and CBR's for WES Test Item Subgrade	49
III-4	Laboratory Compaction and CBR's for WES Test Item Base Course	50
III-5	Layout of Airfield Pavements Showing Location of Test Items, Wright-Patterson AFB, Ohio	51
III-6	Layout of Airfield Pavements Showing Location of Test Items, Whiteman AFB, Missouri	52
III-7	Structure of Wright-Patterson and Whiteman AFB Test Items	53
III-8	Gradation Curves for Wright-Patterson AFB Materials ..	54
III-9	Gradation Curves for Whiteman AFB Materials	55
III-10	Laboratory CE55 Compaction and Unsoaked CBR's for WP-1 Base Course	56

LIST OF FIGURES
(Continued)

FIGURE	TITLE	PAGE
III-11	Laboratory CE55 Compaction and Unsoaked CBR's for WP-2 Base Course	57
III-12	Laboratory CE55 Compaction and Unsoaked CBR's for WP-3 Base Course	58
III-13	Laboratory CE55 Compaction and Unsoaked CBR's for WP-4 Base Course	59
III-14	Laboratory CE55 Compaction and Unsoaked CBR's for W-1 Base Course	60
III-15	Laboratory CE55 Compaction and Unsoaked CBR's for W-2 Base Course	61
III-16	Laboratory CE55 Compaction and Unsoaked CBR's for W-3 Base Course	62
III-17	Layout of North Field	63
III-18	Grain Size Distribution of North Field Base and Subgrade Material	64
III-19	Laboratory Compaction Results for North Field Base Course Material	65
III-20	Laboratory Compaction Results for North Field Subgrade	66
III-21	North Field Instrumentation Layout	67
III-22	Traffic Distribution Pattern	68
IV-1	FWD Velocity Transducer Response	86
IV-2	Time History Output from FWD Load Cell and Velocity Transducers	87
IV-3	Load/Deflection Response of FWD Over Full Range of Deflections	88
IV-4	ISM/Force Relationship on WES and NFF4 Items	89
IV-5	ISM/Force Relationship on Wright-Patterson and Whiteman AFB Items	90

LIST OF FIGURES
(Continued)

FIGURE	TITLE	PAGE
IV-6	Load/Deflection Response on WES Test Item Clay Subgrade	91
IV-7	Load/Deflection Response on WES Test Item Base Course	92
IV-8	Load/Deflection Response on WES 1 Pavement	93
IV-9	Response on WES1 from Subgrade, Base, and Pavement ...	94
IV-10	Response on NFF4 from Subgrade, Base, and Pavement ...	95
IV-11	Modulus-Temperature Relationships for Asphaltic Concrete (Reference 54)	96
IV-12	Structure of Temperature Test Site	97
IV-13	Comparison of Predicted to Measured Mean Pavement Temperature	98
IV-14	Stiffness Values for Temperature Site 1	99
IV-15	Stiffness Values for Temperature Site 2	100
IV-16	Stiffness Values for Temperature Site 3	101
IV-17	Stiffness Values for Temperature Site 4	102
IV-18	Stiffness Values for Temperature Site 5	103
IV-19	Stiffness Values for Temperature Site 6	104
IV-20	Stiffness Values for Temperature Site 7	105
IV-21	Stiffness Values for Temperature Site 8	106
IV-22	Stiffness Values for Temperature Site 9	107
IV-23	Falling Weight Deflectometer ISM Temperature Correction Factors	108
IV-24	Temperature Factors for Site 1	109
IV-25	Temperature Factors for Site 6	110
IV-26	Temperature Factors for Site 7	111

LIST OF FIGURES
(Continued)

FIGURE	TITLE	PAGE
IV-27	Temperature Factors for Site 8	112
IV-28	ISM versus Coverages for WES1 Item	113
IV-29	ISM versus Coverages for NFF4 Item	114
IV-30	Area versus Coverages for WES1 Item	115
IV-31	Area versus Coverages for NFF4 Item	116
IV-32	Surface Curvature Index versus Coverages for WES1 Item	117
IV-33	Surface Curvature Index versus Coverages for NFF4 Item	118
IV-34	Base Curvature Index versus Coverages for WES1 Item ..	119
IV-35	Base Curvature Index versus Coverages for NFF4 Item ..	120
IV-36	Spreadability versus Coverages for WES1 Item	121
IV-37	Spreadability versus Coverages for NFF4 Item	122
IV-38	Comparison of ERI and BISDEF Subgrade Modulus Values .	123
IV-39	ERI versus Coverages for WES1 Item	124
IV-40	Laboratory Resilient Modulus Test Results on NFF4 Subgrade	125
IV-41	Measured and Predicted Stresses on NFF4 Items for F-4 Loading	126
IV-42	Location of Stress and Strain Calculation Points	127
IV-43	Subgrade Modulus versus Coverages for WES1 Item	128
IV-44	Subgrade Modulus versus Coverages for NFF4 Item	129
IV-45	Base Modulus versus Coverages for WES1 Item	130
IV-46	Base Modulus versus Coverages for NFF4 Item	131
V-1	Rutting Types Indicating Failure Location	142
V-2	Rut Depth Progression of WES1	143

LIST OF FIGURES
(Continued)

FIGURE	TITLE	PAGE
V-3	Rut Depth Progression of WES2	143
V-4	Rut Depth Progression of WP-1	144
V-5	Rut Depth Progression of WP-2	144
V-6	Rut Depth Progression of WP-3	145
V-7	Rut Depth Progression of WP-4	145
V-8	Rut Depth Progression of NFF4	146
V-9	Rut Depth Progression of W1	146
V-10	Rut Depth Progression of W2	147
V-11	Rut Depth Progression of W3	147
V-12	Comparison of Predictions with CBR Procedure	148
V-13	Relationship Between Vertical Strain at Subgrade Surface and Performance of Pavement Under Single-Wheel Loads (Reference 59)	149
V-14	Relationship Between Vertical Strain at Subgrade Surface and Performance of Pavements	150
V-15	Relationship Between Vertical Strain at the Base Course Surface and Performance of Pavements	151
V-16	Comparison of Measured Rut Depth to Predicted Rut Depth Using Barber Model	152
VI-1	Logarithmic Relationship between Rut Depth and Coverages	165
VI-2	Estimates of Coverages to a 3-inch Rut Depth	166
VI-3	Logarithmic Relationship between Base Course Vertical Strain and Coverages	167
VI-4	Comparisons of Prediction Methods for Coverages to a 1-inch Rut Depth	168
VI-5	Flow Chart for Low-Volume Pavement Evaluation	169

LIST OF FIGURES
(Continued)

FIGURE	TITLE	PAGE
VI-6	ISM versus Allowable Coverages of an F-4 Aircraft for Low-Volume Flexible Pavements	170
B-1	Flow Chart for BISDEF Program	194

SECTION I
INTRODUCTION

A. BACKGROUND

The U. S. Air Force was tasked to consider options for constructing and maintaining pavements to support a limited number of aircraft operations in the European theater. With the development of hardened shelters for the protection of aircraft and support equipment during conventional air attacks, the weapon system vulnerability to conventional bombing shifts toward the mission-essential runway. To counteract this threat, the U. S. Air Force outlined a 9-year research program to provide the capability to launch and recover aircraft after an attack directed at runways and taxiways. One option is to construct and maintain Alternate Launch and Recovery Surfaces (ALRS). ALRS are relatively low-quality pavements constructed away from the main runway to effectively reduce the probability that all landing and takeoff areas would be destroyed in a given attack. The ALRS must (1) be relatively inexpensive in comparison to permanent pavements, (2) support the imposed loads with high reliability, (3) be easily maintained, and (4) provide an adequate surface for a limited number of sorties of the design aircraft.

Research on ALRS has been reported by several investigators (References 1-11). These research efforts were directed toward the design of the pavements for structural support requirements and to minimize the effects of environmental deterioration. Two pavement systems were selected on the basis of cost and performance requirements from these efforts: (1) a conventional asphalt/crushed stone pavement with a minimum thickness of

asphaltic concrete (AC) and (2) a pavement constructed with stabilized-material layers.

ALRS pavements for the Western European area will be subjected to 300-325 freezing degree-days, 25-30 inches of rainfall and 14-36 inches of snowfall per year (Reference 5). These environmental conditions may contribute to structural deterioration of the pavement layers through such phenomena as AC thermal cracking and cyclic freeze-thaw conditions. Freeze-thaw will saturate the subgrade and other frost-susceptible layers, and extreme temperatures may cause cracking of the AC which will allow water infiltration into the base and subgrade.

ALRS pavements are designed to support 150 passes of a fighter aircraft such as the F-4 which has a single main gear with a maximum load of 27,000 pounds and a 100-square inch contact area.

Normally, pavements are subjected to periodic traffic. If the pavement is not structurally adequate, distresses such as rutting or cracking appear, indicating a need for strengthening. Distresses may be localized where corrections can be accomplished with patching, or they may cover the entire pavement feature where the loads exceed the design aircraft load or material properties have changed due to environmental effects. ALRS pavements will not be subjected to traffic except in contingency situations. If there is a change in the pavement condition, there will be no preliminary indicator and failure could occur when the feature is critically needed. Therefore, ALRS pavements will require periodic monitoring to ensure that structural integrity is maintained and the ALRS retains high reliability.

The use of nondestructive testing (NDT) devices for evaluating the load-carrying capability of both airport and highway pavements has been widely accepted throughout the pavements field (References 12-18). The procedures for determining the allowable load or allowable passes have been derived by:

1. Correlating the NDT measurement to the allowable load determined by sampling the pavement structure and using a conventional design procedure (Reference 13).
2. Back calculating the pavement layer moduli and using a layered elastic model to calculate limiting stresses or strains (References 12, 14, 15, 17, and 18).

Both methods have been "calibrated" and apparently produce reasonable results though they have not been verified by actual performance data. In general, the methods have been verified only by laboratory or in situ materials tests.

Two research studies have been completed at the Waterways Experiment Station (WES) on the design of ALRS (References 6 and 10). Eleven pavement test sections were trafficked to failure with an F-4 load cart. Nondestructive falling weight deflectometer (FWD) data were collected on these sections before, during, and after traffic. These data provide an excellent source for use in establishing failure mode and pattern and predicting the performance of low-volume traffic pavements.

B. PURPOSE

The purpose of this study was to develop an FWD-based evaluation procedure to predict the allowable F-4 aircraft load and the allowable aircraft passes for marginal flexible pavements. Structural models for describing

the pavement system response will be evaluated and the model that produces responses that most accurately correlate to pavement performance will be selected. The method developed will be applicable to pavements for which very little structural information is known.

C. SCOPE

The nondestructive evaluation procedure developed in this study will be for flexible pavements with an AC surface and an unbound granular layer. Allowable load/passes will be predicted for aircraft with a tricycle gear having a single wheel main gear. The procedure will be developed based on data obtained from using a load cart simulating an F-4 aircraft having a 27,000-pound single-wheel load and a tire contact area of 100 square inches. Data collected during the aforementioned studies will be used to predict the expected life in terms of number of passes to produce failure as determined by rutting. The method will use only nondestructive data when thickness and type of the pavement layers are known. When thickness and types of layers are not known, coring will be required to determine these parameters.

D. THESIS FORMAT

Section II contains a description of the failure mechanisms for flexible pavements with thin AC surfaces and granular bases. Methods for evaluating the performance of flexible pavements are presented with the method selected for evaluating the data presented herein.

A description of the traffic tests is presented in Section III. Pavement properties and performance evaluation measurements are described.

An analysis of nondestructive data collected with the FWD and factors which influence FWD data is contained in Section IV.

Traffic test section data are analyzed in Section V. The performance of each traffic test section is compared to estimates of performance using the CBR design/evaluation procedure and layered elastic procedures.

Section VI contains the models developed to predict performance. The best estimator of performance is presented. A procedure for evaluating traffic volume for pavements is outlined.

Section VII presents conclusions and recommendations for evaluation of low traffic volume pavements and future research for flexible pavements containing granular base courses.

SECTION II

PERFORMANCE PREDICTION

A structural model must be selected to predict pavement responses such as stress or strain to loading. The model should be capable of utilizing the properties of the pavement layers such as modulus and strength. Responses computed from the structural model and computed from material properties can be used to predict pavement performance. For ALRS evaluations the structural model should not require the use of a main frame computer since an evaluation of an airfield in an underdeveloped country may require an immediate answer.

The pavement evaluation methods that were considered are the California Bearing Ratio (CBR) design procedure, multilayer linear elastic model, multilayer nonlinear elastic models, and rut depth prediction. Each system will be described in the following sections.

A. PAVEMENT PROPERTIES AFFECTING PERFORMANCE

1. Distresses

An ALRS pavement structure will consist of a thin AC layer (3 inches or less), an unbound granular layer, and a subgrade. Structural distress in pavements of this type are cracking of the AC layer and permanent deformation (rutting).

Cracking may be the initial distress, particularly for older pavements when the AC surface course has oxidized and lost its flexibility. Cracking of the AC surface influences rut depth accumulation. A cracked surface course does not provide the required confinement for the base course which leads to loss of strength. Shear stress in the granular base is

increased below a cracked surface course. Both decreased confinement and increased shear stress increase rutting accumulation once loading begins.

Aircraft operations on ALRS will occur in a short time interval (probably less than 24 hours). Cracking is a primary pavement distress. Surface cracking allows water to infiltrate into the base course and subgrade, weakening these layers and increasing rutting potential. Severe AC cracking can lead to spalling of the surface course and foreign object damage (FOD) to the aircraft engines. Due to the short time use (less than 24 hours) of ALRS pavements, water infiltration will not present a problem. FOD damage could be a problem for ALRS users, but most likely will not since operations will be occurring during battle. Also, although cracking may occur, 100 to 200 aircraft passes probably will not break the surface into pieces small enough to be dislodged.

Therefore, the primary load associated distress in ALRS pavements of concern is permanent deformation (rutting). Permanent or plastic deformation can occur in the AC layer, the granular layer, and the subgrade. Deformations within the AC layer will be small in comparison to those in the base and subgrade since the surface AC layer is relatively thin (3 inches or less). Therefore, rutting distress will be associated with the granular and subgrade layers for low traffic volume ALRS pavements.

2. Granular Layers

Thompson (Reference 19) described permanent strain accumulation in flexible pavements as two cases, "stable" or "unstable" (Figure II-1). "Stable" behavior occurs when the permanent strain accumulates at a fairly constant rate. "Unstable" behavior is the very rapid increasing accumulation of permanent strain at some time during the service life of the

pavement. The permanent strain accumulation for most ALRS pavements will be in the "unstable" category due to the design for a limited number of load applications and the high stress state imposed on the base and subgrade.

Walker et al. (Reference 20) showed that by limiting the stress ratio (repeated stress/strength) to less than approximately 70 per cent, stable behavior could be expected.

Accumulation of permanent strain in granular materials has been described (Reference 19) with the general form equation:

$$\epsilon_p = a + b \log N \quad (1)$$

where

ϵ_p - Permanent strain

N - Number of load repetitions

a,b - Experimentally derived factors from repeated load testing

Factors that affect the rate of permanent strain accumulation, the b term of the above equation, include increasing the compacted density, which leads to increased shear strength and therefore, a decreased rate of strain accumulation.

Barksdale reported in a detailed laboratory analysis of rutting in base course materials (Reference 21), that the type and amount of fines also significantly affect the accumulation of permanent strain. He further stated for crushed stone bases, only enough fines should be used to permit proper compaction if the amount of rutting in the base is to be minimized. Increase in the deviator stress ratio significantly increases the accumulation of permanent axial strain. The deviator stress ratio is given as:

$$\frac{\sigma_1 - \sigma_3}{\sigma_3} \quad (2)$$

Increasing the degree of saturation also was found to significantly increase the tendency to rut in the base (Reference 21).

A hyperbolic plastic stress-strain relationship has been proposed by Kondner (Reference 22) and used extensively by Duncan (Reference 23) for description of axial plastic strain as follows:

$$\epsilon_a = \frac{(\sigma_1 - \sigma_3) / (K \sigma_3^n)}{1 - \frac{(\sigma_1 - \sigma_3) R_f (1 - \sin \Phi)}{2 c \cos \Phi + \sigma_3 \sin \Phi}} \quad (3)$$

where

ϵ_a - Axial strain

$K \sigma_3^n$ - Relationship defining the initial tangent modulus as a function of confining pressure (K and n are constants)

c - Cohesion

Φ - Angle of internal friction

R_f - A constant relating compressive strength to an asymptotic stress difference

Barksdale (Reference 21) found that the above equation can fit the plastic stress-strain curves obtained from repeated load triaxial test results for 100,000 load repetitions. In order to use this relationship for a practical estimate of rut depth, an extensive testing program would be needed to calculate constants in the equations for various numbers of load repetitions since the above equation does not apply for repetitions in the range expected for ALRS pavements.

Khedr (Reference 24) in a study on the deformation characteristics of granular bases, developed a relationship for permanent strain for laboratory samples as follows:

$$\epsilon_p/N = A N^{-m} \quad (4)$$

where m is a material parameter and A is a material and stress state parameter.

Roberts et al. (Reference 25) presented a method for predicting permanent deformations in terms of three parameters, ϵ_0 , β , and ρ . The parameters were developed from the relationships of permanent strains to load cycles (Figure II-2). The curve was represented by

$$\epsilon_a = \epsilon_0 + \left(\frac{\rho}{N}\right)^\beta \quad (5)$$

in which

ϵ_a - Permanent strain

N - Cycles of load

ϵ_0 , β , and ρ - Material parameters

Methods were presented to determine the three parameters ϵ_0 , β , and ρ and were found to be related by

$$\rho = \left(\frac{10^c}{\beta}\right) 1/\beta \quad (6)$$

where β and c , a constant, could be obtained by plotting either known deformation data or laboratory determined data as shown in Figure II-3. The relationship presented in Figure II-3 is normalized for the number of cycles N as Khedr presented in Equation 4. ϵ_0 is determined by averaging the values of permanent strain against cycles of load.

The total deformation was obtained by integrating the derivative of ϵ_a over the thickness of each pavement layer. It was assumed in the development of this method that ϵ_r , the resilient strain, was large in comparison to the increase of the permanent strain with each load repetition. This assumption is not valid for ALRS pavements when 1-inch of rutting occurs in 100 to 150 coverages.

3. Subgrades

For fine grained soils, permanent strain is generally described by the following general equation.

$$\epsilon_p = A N^b \quad (7)$$

where

ϵ_p - Permanent strain

N - Number of load repetitions

A, b - Experimentally derived factors from repeated load material testing data

Factors that influence the permanent deformation characteristics of fine grained soils include the applied stress, the moisture content, and the degree of compaction (Reference 19). An increase in moisture content or a decrease in the compactive effort lead to decreased shear strength which contributes to increased rutting potential.

Lentz and Baladi (Reference 26) found that for sand subgrade materials, the permanent deformation could best be described with a semi-log relationship as:

$$\epsilon_p = a + b \ln N \quad (8)$$

where

ϵ_p - Accumulated permanent strain

N - Number of load repetitions

a and b - Regression constants

The constant, a , represents the plastic strain during the first cycle, and b is the slope of the plastic strain versus $\ln N$ curve.

Lentz and Baladi normalized the constants, a and b , (Reference 27) by using data from the static stress-strain curves. The resulting equation is:

$$\epsilon_p = \epsilon_{0.955S_d} \left[\ln \left(1 - \frac{\sigma_d}{S_d} \right)^{-0.15} \right] + \frac{\frac{d}{S_d} n}{\left[1 - m \left(\frac{\sigma_d}{S_d} \right) \right] \ln N} \quad (9)$$

where

ϵ_p - Accumulated permanent strain

$\epsilon_{0.955S_d}$ - A reference strain selected at 95 percent of static strength

S_d - Static strength

σ_d - Cyclic principal stress difference

N - Number of repetitions

m and n - Regression constants

Baladi, Vallejo, and Goitom (Reference 28) selected a model of similar form using the following hyperbolic equation:

$$\frac{\epsilon_p}{\epsilon_{0.95S_d}} = \frac{n}{\frac{S_d}{\sigma_d} - m} \quad (10)$$

The regression parameters, n and m , were determined for different materials using the functional relationship of the following form.

$$n = A_{ni} + b_{ni} \ln N \quad (11)$$

$$m = A_{mi} + b_{mi} \ln N \quad (12)$$

Regression constants, A_{ni} , b_{ni} , A_{mi} and b_{mi} , were determined for five materials ranging from ballast size aggregate to clay. Permanent strain of the test materials were found to be a function of:

- (a) stress level
- (b) stress path
- (c) consolidation
- (d) confining pressure
- (e) moisture content
- (f) density

Baladi et al. concluded that the normalized stress-strain model, Equation (10), was independent of the above variables but dependent on the number of load repetition and soil type.

Brabston reported in a study of deformation characteristics of subgrade soils (Reference 29) that the permanent axial strain response increases exponentially with load repetitions to a point and then increases linearly thereafter at a much reduced rate. The amount of rutting is significantly greater during the initial load applications. The rate of strain increase in both regions is a function of soil water content, density, and resistance to compaction as manifested by the slope of a plot of maximum density versus compaction energy and the ratio of repeated axial stress to failure deviator stress.

For flexible airfield pavements, a design procedure was developed using a layered elastic model to calculate the responses to applied multiple wheel loadings (Reference 30). The CHEVRON program was used to develop the limiting vertical strain criteria (Figure II-4). The vertical strain is computed at the top of the subgrade and is related not only to the number of repetitions of load but also to the strength properties of the subgrade material.

4. Summary

Rutting will be the primary cause of functional failure of ALRS pavements. Rutting can occur in either the granular base layer or in the subgrade. For "stable" cases, where rut depth accumulation has been shown to be a function of the compacted density, the applied stress, the amount of fines in the base course, and the moisture content (degree of saturation), methods for prediction have been presented that can reasonably estimate rutting accumulation. Prediction of rutting magnitude is difficult for pavements that are "unstable" where stress ratio's are greater than approximately 70 per cent in the base course. ALRS pavements, designed for minimum costs, can be expected to perform in the "unstable" case in most conditions. Therefore, estimating the performance of ALRS pavement will present a complicated task.

B. DESTRUCTIVE EVALUATION METHODS

1. California Bearing Ratio (CBR)

The CBR flexible pavement design/evaluation procedure is used by the Department of Defense (Army, Navy, and Air Force) (Reference 31) and the Federal Aviation Administration (Reference 32). It has also been selected as the basis for standardizing the ratio of classification number (which is

a standardized single-wheel load) and equivalent aircraft gross weight for a pavement type and subgrade class for the flexible pavement Aircraft Classification Number/Pavement Classification Number (ACN/PCN) by the International Civil Aviation Organization (ICAO) (Reference 33). The CBR system is the most universally used design/evaluation procedure for flexible airport pavements.

CBR is defined as the bearing ratio of a soil determined by comparing the resistance of that soil to penetration of a 3-square-inch circular piston of the soil with that of a standard material (Reference 34). The method covers evaluation of the relative quality of subgrade soils but is applicable to subbase and some base course materials.

The concept of the CBR design method is to provide layers of required quality and thickness to prevent shear deformation in the subgrade. The method has been calibrated over the years with actual performance data and covers a wide range of pavement designs for most of the aircraft that are presently using airfields.

To evaluate a pavement using the CBR procedure, a test pit must be opened in the runway. The facility may be closed for a period of 1 to 3 days. CBR is measured on each pavement layer in the pit, and bulk samples are collected for laboratory testing. It is important to note that usually only one or two pits are constructed in a given runway or taxiway. Despite the limited number of test pits, the data obtained are extrapolated for up to 10,000 lineal feet of pavement. ALRS pavements will vary in strength over these distances. Since periodic aircraft traffic will not necessarily locate "weak areas," additional data are necessary in order to more

accurately characterize in situ pavement material characteristics and to locate potential problem areas.

A Small Aperture Evaluation Procedure (Reference 35) has been developed that requires less downtime than the test pit method. CBR tests are conducted on the base course and subgrade layers through a 6-inch-diameter core hole. The depth into the pavement structure in which an accurate CBR test can be conducted is limited to depth that can be leveled by hand at the bottom of the hole (i.e., the length of a person's arm). With the small aperture procedure, pavement layer interfaces are difficult to locate for testing because the auguring operation may extend past the depth of interest unnoticed. Therefore, the CBR test may be conducted at some distance below the actual pavement layer interface.

The small aperture procedure offers a significant time savings over the test pit method, but to adequately sample a runway will require closure for a period of at least 1 day.

2. Rut Depth Prediction

Barber et al. (Reference 36) developed the following statistical regression model for rut depth prediction for two-layer flexible pavement systems with an AC surface course over a granular base:

$$RD = 1.9431 \frac{P_K^{1.3127} \tau_p^{0.0499} R^{0.3249}}{\log(1.25T_{ac} + T_{base})^{3.4202} C_1^{1.6877} C_2^{0.1156}} \quad (13)$$

Standard Error = 0.411 inches

$$r = 0.8779$$

where

RD - Rut depth, inches

P_k - Equivalent single-wheel load (ESWL), kips

t_p - Tire pressure, psi

Tac - Thickness of AC, inches

Tbase - Thickness of base, inches

C_1 - CBR on top of base

C_2 - CBR on top of subgrade

R - Repetitions of load or passes

Destructive testing is required to obtain the CBR parameters for use in this model. This model will be used to evaluate the data generated in this study.

Barker (Reference 37) presented the following rut depth prediction model based on the relationship between resilient strain and permanent strain in the subgrade:

$$\frac{\epsilon_P}{\epsilon_R} = 0.14 \left[\frac{70800}{M_R} \right]^A \quad (14)$$

where

$$A = 0.4 (\text{Stress Repetitions})^{0.12}$$

$$M_R = \frac{\sigma_d}{\epsilon_R}, \text{ ksi}$$

σ_d - Repeated deviator stress in laboratory triaxial test, ksi

ϵ_R - Measured resilient strain in laboratory triaxial test, inches/inches

ϵ_P - Measured permanent strain (deformation) in laboratory triaxial test, inches/inches

This model is applicable to permanent airfield pavements and assumes that most of the permanent deformation will occur in the subgrade. For ALRS pavements with a thin AC surface layer, rutting may also occur in the granular layer due to the high stress state in the granular base course.

C. NONDESTRUCTIVE EVALUATION METHODS

Nondestructive testing offers many advantages over conventional pavement evaluation testing. The major advantage is the ability to collect data at many locations on a runway or taxiway in a very short time. At least 20 tests can be conducted in 1 hour as compared to the day or more required for the construction and repair of one test pit.

Over the past 20 years several types of NDT equipment have been developed for the evaluation of roads and airfields. Most equipment applies either a vibratory or an impulse load to the pavement and measures the resulting pavement surface deflection. Deflection is obtained with most devices by integrating the surface velocity measured with velocity transducers. The force generators for the vibratory devices are either counter-rotating masses or electrohydraulic systems that produce a sinusoidal loading. The impulse load devices utilize a falling weight dropped on a set of cushions to dampen the impulse to produce a loading time to simulate a moving wheel. The magnitude of the load is measured on some devices and calculated on others.

1. DSM Procedure

A nondestructive pavement evaluation procedure for airfield pavements was developed at WES utilizing data collected with the WES 16-kip vibrator (Reference 13) for use with the CBR design method. The WES 16-kip vibrator is an electrohydraulic actuated device that applies a sinusoidal loading of up to 30,000 pounds (peak-to-peak). The load is applied through an 18-inch-diameter plate. The system is contained in a tractor-trailer unit.

Dynamic Stiffness Modulus (DSM) is defined as the slope of the upper third portion of the load/deflection relationship that is obtained when the sinusoidal dynamic loading is swept from 0 to 30,000 pounds (peak-to-peak). DSM from the WES 16-kip vibrator was correlated with the allowable single-wheel load (ASWL) for 24,000 total departures of a single-wheel aircraft as determined from destructive evaluation methods. Once the ASWL is determined and layer thickness data are obtained, the CBR of the subgrade can be back calculated. Using the CBR procedure with the derived subgrade CBR, allowable load for any aircraft can be determined.

Because it is an empirical correlation, the DSM procedure is valid only for the WES 16-kip vibrator. This device cannot be air transported, except on the C5A, and, therefore, could not be efficiently used in a worldwide testing program.

2. Wave Propagation Methods

Techniques for determining the modulus of pavement layers through the analysis of surface waves traveling through the pavement system have

been proposed by University of New Mexico and University of Texas researchers (References 38 and 39).

Both methods use an impact load from a falling weight device to induce a range of frequencies into the pavement structure. Wave velocities are monitored with accelerometers or velocity transducers located on the pavement surface. By describing the wave signals with Fourier series to give the amplitude and phase angle of each frequency, the signals between two accelerometers are analyzed to estimate the difference in phase angle. Differences in phase angle are used to calculate the wave velocity for each frequency. The wavelength of each frequency is estimated by multiplying the velocity by the frequency.

The wave velocity varies with the stiffness of the layers within the pavement system. A plot of velocity against wavelength is called a dispersion curve. The University of New Mexico procedure, developed for the U. S. Air Force, relates the wavelength to a depth within the pavement structure. The University of Texas procedure uses an inversion process to determine the propagation velocities at different depths. The wave velocity is then converted to shear modulus for each of the pavement layers.

These methods have not been developed for production testing on a large scale as would be required for ALRS type pavements. Analysis of the dispersion curve is difficult for untrained personnel.

3. Deflection Basin Methods

The deflection basin from an applied load offers a method to evaluate the stability of the layers within a pavement structure. Optimally, each layer modulus can be quantified if the thickness is known.

Several methods have been applied to airfield pavement structures and are summarized in several reports (References 15, 16, and 18). Most methods match surface deflections to deflections from layered elastic (linear and nonlinear) or finite element (linear and nonlinear) models.

a. Surface/Base Curvature Index Methods

Peterson (Reference 40) presented a method using the deflection basin data obtained from the Dynaflect device. Problem areas of the pavement structure were identified as shown in Figure II-5

where

Surface Curvature Index (SCI) - The difference between the deflections (mils) measured by the first and second sensors (D0-D12).

Base Curvature Index (BCI) - The difference between the deflections (mils) measured by the fourth and fifth sensor located 36 inches and 48 inches from the center of the loaded area, respectively (D36-D48).

Spreadability (SPR) - Determined from the equation:

$$SPR = \frac{D0 + D12 + D24 + D36 + D48}{5(D0)} \quad (15)$$

This method of analyzing the deflection basin is applicable to the rapid field evaluation of ALRS pavements. To use the values given in Figure II-5, deflections must be converted to equivalent Dynaflect deflections or new criteria developed for the selected NDT device.

b. Area/DO Concepts

Hoffman and Thompson (Reference 12) presented a pavement evaluation method that used the FWD deflection at the center of the load (DO) normalized to 9,000 pounds and the normalized cross-sectional area (AREA) of

the deflection basin out to the sensor at a 36-inch distance from the center of the applied load (Figure II-6). Algorithms and nomographs were developed to determine the modulus of the subgrade (E_{RI}) (See Figure II-7) from the ILLIPAVE finite element model (Reference 41).

c. Back Calculation Methods

Lytton et al. (Reference 18) summarized nine methods for matching deflection basins. Typically, methods have been developed to calculate moduli for up to five layers. Most methods do not handle nonlinear stress-strain effects and most can be operated on either a microcomputer or main frame.

A nondestructive evaluation procedure using a layered elastic method of analysis has been developed by WES for light aircraft pavements (Reference 14). In this method a computer program, CHEVDEF, was developed to back calculate the modulus of the pavement layers from the measured deflection basin. In CHEVDEF, the Chevron layered elastic program is used to calculate the deflections.

The Chevron program was replaced with BISAR (Reference 42) to allow for varying interface conditions between the pavement layers. The revised version, BISDEF, reported in References 15 and 17, is described in Appendix B.

Chua and Lytton (Reference 43) presented a method for predicting rut depth accumulation using NDT data from the Dynaflect or from an FWD. The method utilized the deflection basin to characterize the base and subgrade properties. The ILLIPAVE nonlinear structural model was used to describe the pavement. If traffic loadings and rutting had been observed, the number of passes to a given limiting rut depth or the rutting for a given

amount of traffic could be calculated. Rutting data will not be available for ALRS pavement since operations will occur in a 24-hour period.

D. METHODS SELECTED

1. Field Procedure

The FWD was selected as the testing apparatus for this study. The FWD offers distinct advantages over vibratory equipment for testing airport pavements all over the world. With an FWD a force output in the range of loading expected for the design aircraft can be developed with a relatively light test apparatus. The FWD weighs about 1,800 pounds and can be transported on most cargo aircraft. A maximum force output of approximately 25,000 pounds can be generated. In comparison the WES 16-kip vibrator places a 30,000 pound peak-to-peak loading and weighs 70,000 pounds. A Road Rater Model 2008 weighs approximately 8,000 pounds and outputs a 7,000 pound peak-to peak load.

2. Mechanistic Analysis

A layered elastic model was selected for analysis of the traffic test section data. The assumptions of linear elastic, homogeneous isotropic material properties do not give a good representation of true behavior, particularly after traffic is initiated. Due to the high stress state in the granular base layer and the subgrade, permanent deformation is likely to occur during initial traffic. Material responses are nonlinear when significant permanent deformations occur. However, this model was selected since it has been used previously for airfield pavements (Reference 14 and 30) and since it involves a manageable number of parameters for ALRS.

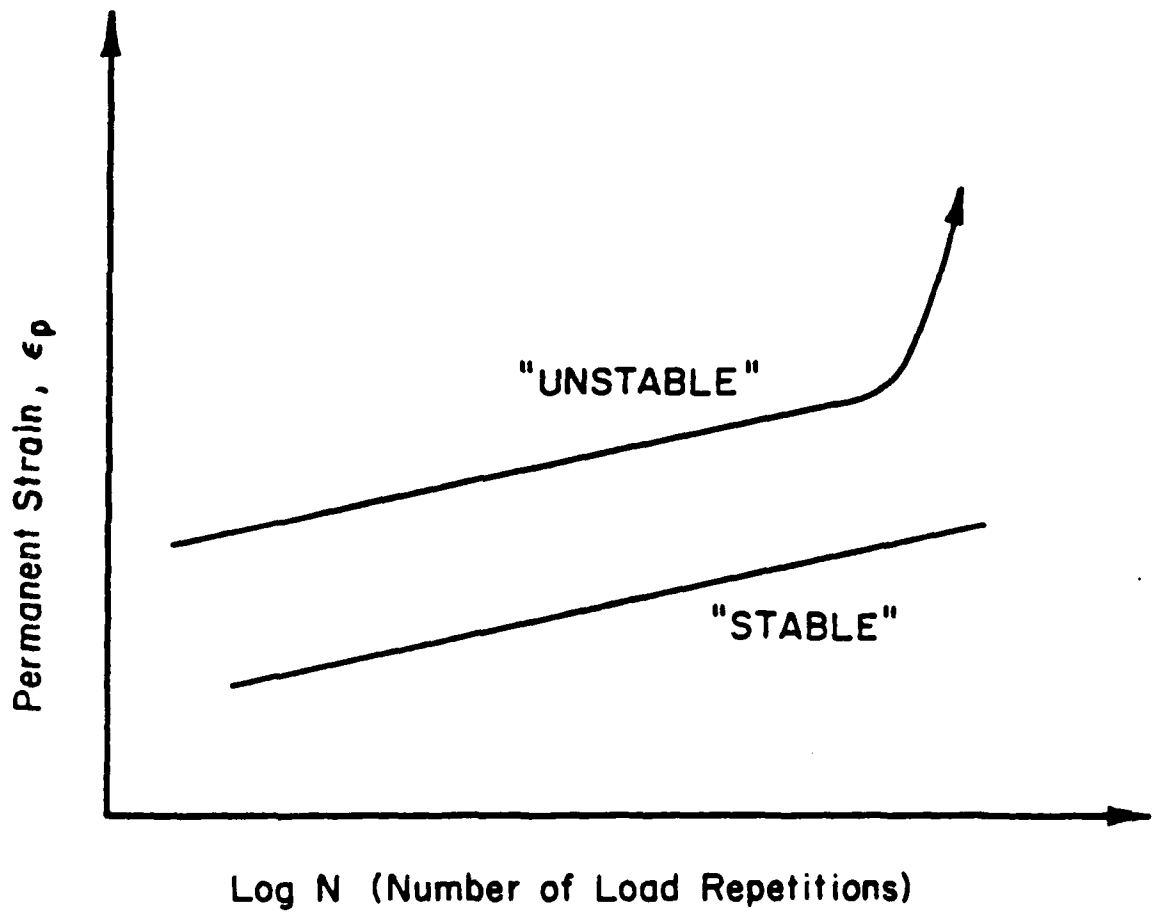


Figure II-1. Stable versus Unstable Behavior (Reference 19).

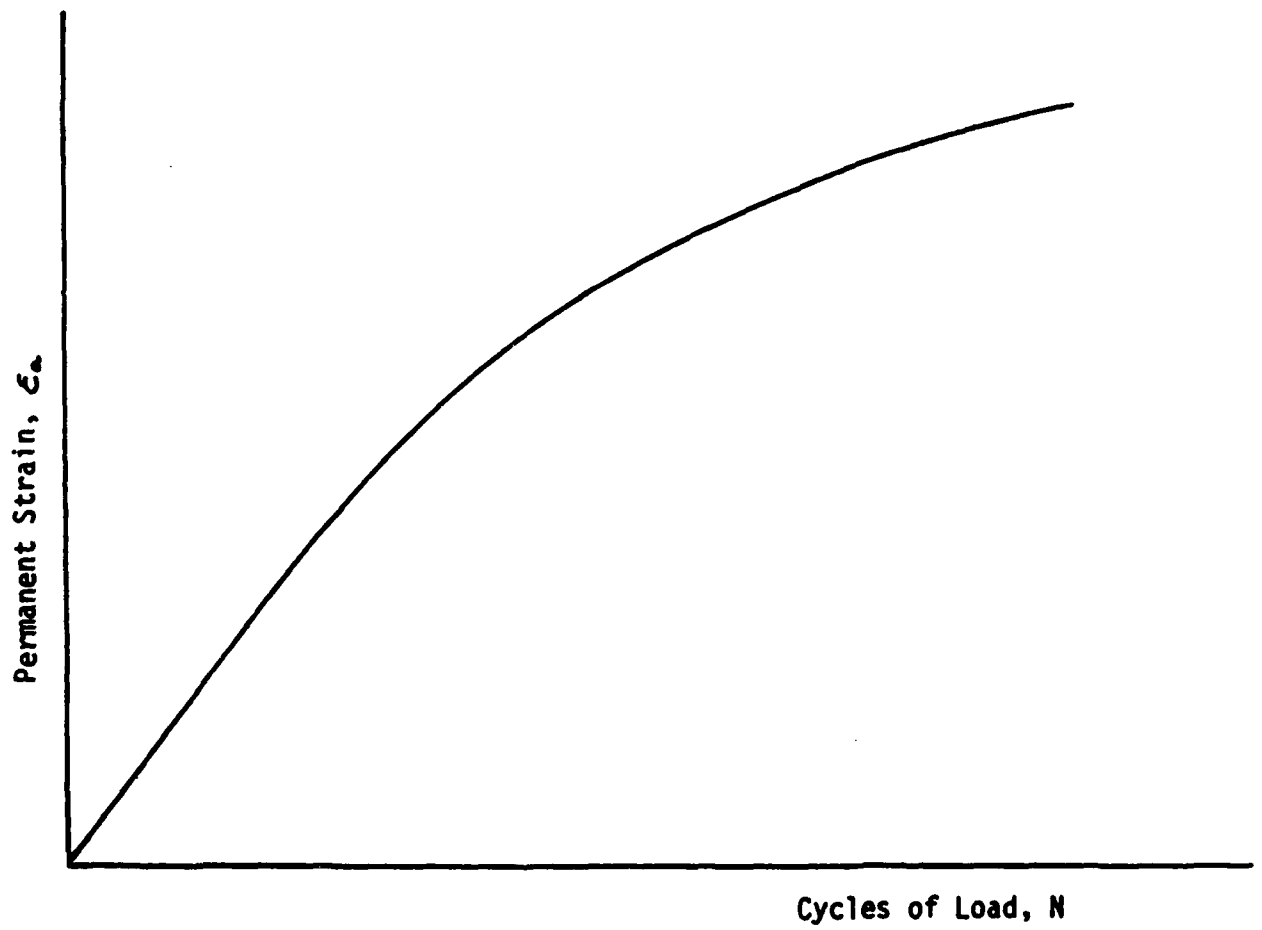


Figure II-2. Relationship Between Permanent Strain versus Cycles of Load (Reference 25).

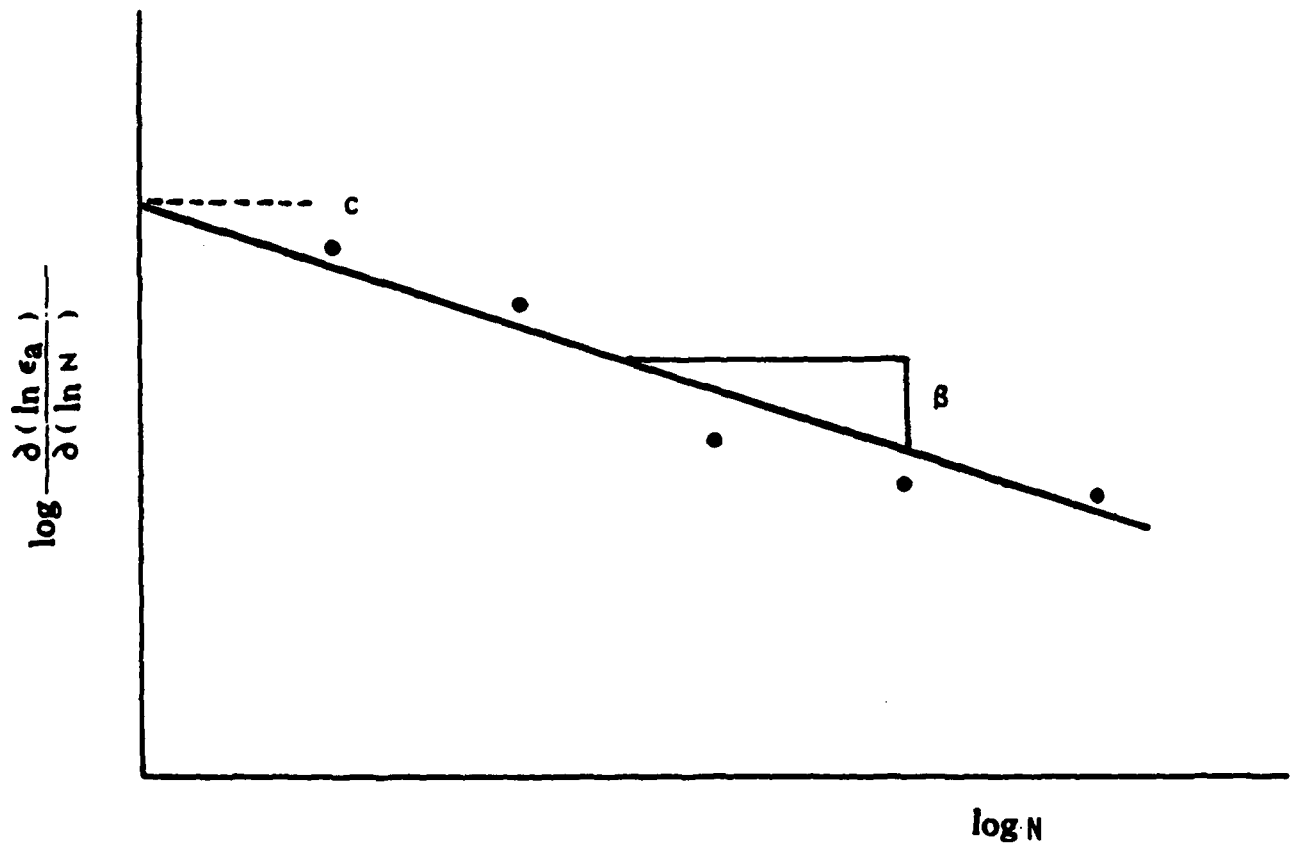


Figure II-3. Logarithmic Relationships of Permanent Strain and Cycles (Reference 25).

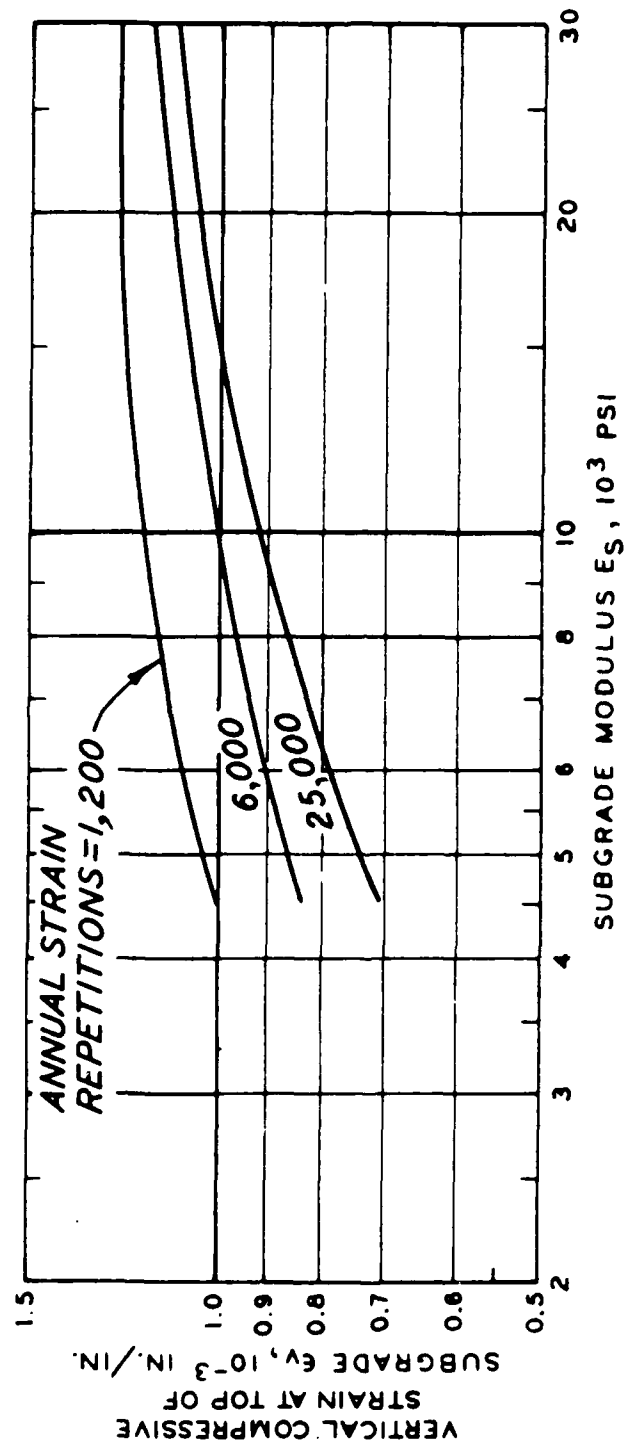
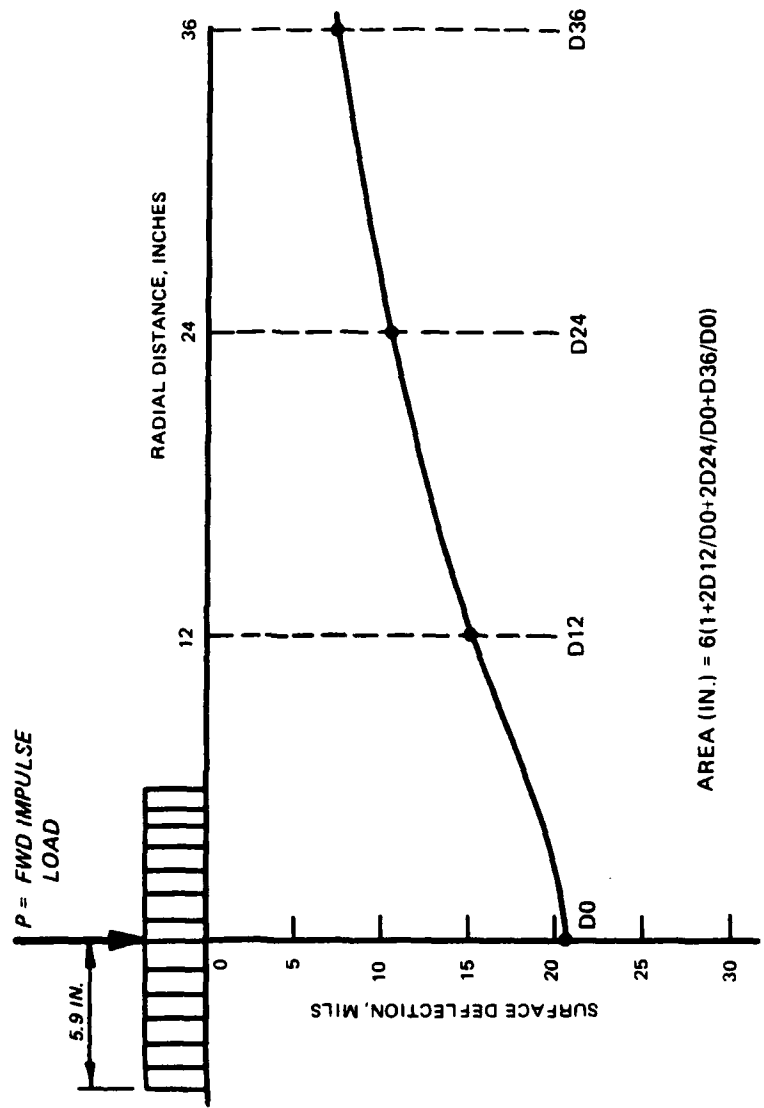


Figure II-4. Limiting Subgrade Strain Criteria for Conventional Flexible Pavements with a 20 Year Life (Reference 30).

MAXIMUM (DMD) DEFLECTION (MILS)	SURFACE CURVATURE INDEX (MILS)	BASE CURVATURE INDEX (MILS)	CONDITION OF PAVEMENT STRUCTURE
GT 1.25	GT 0.48	GT 0.11	PAVEMENT AND SUBGRADE WEAK
		LE 0.11	SUBGRADE STRONG, PAVEMENT WEAK
LE 1.25	LE 0.48	GT 0.11	SUBGRADE WEAK, PAVEMENT MARGINAL
		LE 0.11	DMD HIGH, STRUCTURE OK
GT 0.48	GT 0.48	GT 0.11	STRUCTURE MARGINAL, DMD OK
		LE 0.11	PAVEMENT WEAK, DMD OK
LE 0.48	GT 0.48	GT 0.11	SUBGRADE WEAK, DMD OK
		LE 0.11	PAVEMENT AND SUBGRADE STRONG

GT = GREATER THAN
 LE = LESS THAN OR EQUAL TO

Figure II-5. Use of Deflection Basin Parameters to Analyze Pavement Structural Layers (Reference 40).



$$\text{AREA (IN.)} = 6(1+2D12/D0+2D24/D0+D36/D0)$$

Figure II-6. Area of Deflection Basin (Reference 12).

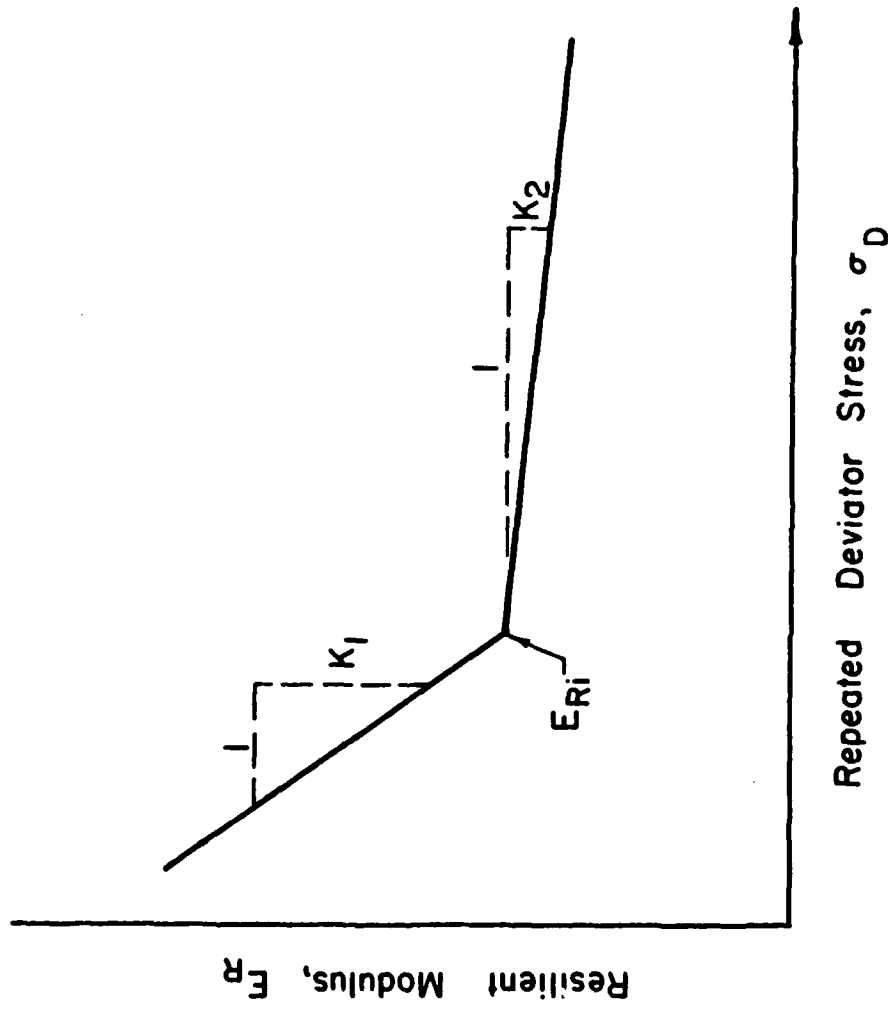


Figure II-7. Typical Resilient Modulus - Repeated Deviator Stress Relation (Reference 12).

SECTION III

FIELD TESTS

A. INTRODUCTION

To develop and verify a pavement design procedure for ALRS pavements, four bituminous surface over granular base pavement test sections were constructed (References 6 and 10) and trafficked with a load cart simulating F-4 loading. Three items were built at WES and one was built at North Field, South Carolina. Seven existing pavement sections, located in non-traffic areas such as shoulders or overruns, were also trafficked to failure (Reference 6). Four were at Wright-Patterson Air Force Base (AFB), Ohio, and three at Whiteman AFB, Missouri. The major purpose of trafficking all test sections was to evaluate whether the AC surface thickness could be reduced from the current required 3 inches (Reference 31) to minimize the cost of the ALRS pavements. The purpose of trafficking the existing pavements was to evaluate the effect of environmental aging of the asphalt surface due to oxidation and the effects of aging on the properties of the base and subgrade layers when the pavements were in nontraffic areas.

FWD data were acquired on each section. These data will be used to develop a prediction model for evaluation purposes. These pavements provide a range of age and condition data for establishing an evaluation procedure that is comparable to those pavements to be evaluated. The objectives of these research efforts were to develop and verify design for low-volume airfield pavements. CBR, water content, and density data were collected on these pavements. Samples were collected and returned for laboratory classification tests and for compaction tests to compare the laboratory density to

that density obtained in the field. Funding was not available for resilient modulus testing, except for one test section at North Field.

B. PAVEMENT CHARACTERISTICS

1. WES Test Items

Three test items were constructed at WES to simulate the strength conditions that were expected for ALRS pavements. The primary purpose of these tests was to evaluate surface thicknesses of less than 3 inches. The subgrade of the test section was constructed for a 6 CBR \pm 1. The strength was selected to represent soil at U. S. airbases in the Federal Republic of Germany (Reference 5). Using the flexible pavement design procedure (Reference 31), a total pavement thickness of 12 inches is required for a light duty airfield with a design aircraft gross weight of 60 kips and 150 aircraft passes over a subgrade strength of 5 CBR. Three wearing surfaces, a double-bituminous surface treatment (DBST), a 1-inch AC surface, and a 2-inch AC surface were selected for evaluation. The layout of the test items is shown in Figure III-1.

The materials used to construct the WES test items were selected to meet the requirements specified in Reference 31. The subgrade soil was a CH material, according to the Unified Soil Classification System (USCS). It is commonly called "Vicksburg buckshot clay" and is frequently used in constructing test sections at the WES because of its high plasticity and low permeability. This clay will maintain nearly the same strength over the duration of traffic testing. The material used for the base course of the ALRS test section was a crushed limestone. Classification data for the limestone and CH material are shown in Figure III-2. Laboratory compaction and CBR data, as-molded conditions, for the clay subgrade and base course

are shown in Figures III-3 and III-4. The materials were compacted at three compactive efforts, CE-12 (standard), CE-26, and CE-55 (modified) (Reference 44). The crushed limestone base course showed very little strength loss with increased water content (Figure III-4).

The double-bituminous surface treatment (DBST) was constructed using a CRS-2 emulsified asphalt as the binder. The AC surface mix was designed in accordance with the 75-blow Marshall mix design method given in MIL-STD-620 (Reference 45). Aggregates selected were a crushed limestone of coarse and fine gradations and a local concrete sand. For identification the items will be designated as WES1 for 2-inch AC, WES2 for 1-inch AC, and WES3 for the DBST.

A summary of pre-traffic and post-traffic CBR, density, and water contents of the WES test section is shown in Table III-1. In-place density of the granular base material was determined using a nuclear density gage (Reference 46) and the water balloon method (Reference 47). Densities of the clay subgrade were obtained using the drive cylinder method (Reference 38). The density of the base course increased with traffic, but there was no significant change in the subgrade properties. As-built thickness data for the WES test items are shown in Table III-2. These data were determined from rod and level cross sections taken after each layer was completed. Therefore, the averages are from a large number of readings. These average thicknesses will be used for analysis.

2. Wright-Patterson and Whiteman Test Items

The design freezing index was used as the basis for selection of continental United States test pavements that had been environmentally aged under conditions similar to those in Germany, where ALRS pavements are to be built. Wright-Patterson AFB, Ohio, and Whiteman AFB, Missouri, were selected, based on the design freezing index and because more pavement areas were available in fewer locations minimizing transportation costs. The design freezing indexes for Wright-Patterson AFB and Whiteman AFB were 892 and 686 freezing degree-days, respectively.

The areas selected for traffic test at both Wright-Patterson AFB and Whiteman AFB were taxiway and apron shoulder pavement, runway overrun, and a parking pad for fire equipment. All of the traffic test features except one were constructed with an AC surface course. One feature was constructed with a DBST surface. An airfield pavement layout and the location of the test features are shown in Figures III-5 and III-6. From each feature a section 10 feet by 30 feet was selected for traffic testing. A list of pertinent data including construction and maintenance dates are shown in Table III-3. The pavements ranged in age from 9 to 30 years at the time of testing. The surface thickness varied from 1 inch for the DBST to 3 inches for the AC. The base course thickness varied from 6 to 47 inches. The pavement structure with measured CBR values within the structure is shown in Figure III-7. Designations for these pavements are also shown and will be used herein.

Gradations for base and subgrade materials are shown in Figures III-8 and III-9. The dashed lines are limits for base course materials as specified by the Department of Defense in Reference 31. The base courses are

relatively close to those limits but are 1 to 2 percent higher on the fines passing the No. 200 sieve. Laboratory CE-55 compaction and CBR test results for the Wright-Patterson AFB and Whiteman AFB base courses are shown in Figures III-10 through III-16. These results are presented to show the effect of higher water contents on the CBR of the material. From the compaction results (Figures III-10 through III-16), one concludes the strengths of these base course materials are highly susceptible to moisture content. The field measured CBR's, densities, and water contents are presented in Table III-4. Densities of granular bases were obtained with a nuclear gage (Reference 46). Densities of subgrade material were obtained using the drive cylinder method (Reference 44). The base course densities met specifications at the top of the layer but were significantly low from 6 to 10 inches into the layer. The subgrade layer was not reached on items WP-2 and W-1. The water table was reached at a significant depth into the pavement structure as indicated in Figure III-7. The sides of the pit became unstable and excavation was stopped.

3. North Field Test Section

To verify test results from the WES test sections and the environmentally aged pavements at Wright-Patterson and Whiteman AFB's, a test section was constructed at North Field, South Carolina, and subjected to F-4 aircraft traffic operating at maximum load. After aircraft trafficking was completed, the test section was trafficked to failure with load carts simulating maximum loaded F-4 and F-15 aircraft. A layout of the airfield with the location of the test area is shown in Figure III-17. The pavement structure at North Field was designed to support 150 passes of the

F-4 aircraft. The subgrade soil at North Field was a sand with a strength of more than 20 CBR measured before construction. The total thickness of granular base and AC above this subgrade was less than the minimum required base thickness as specified in the Tri-Service Manual (Reference 31). Therefore, the pavement was constructed with 2 inches of AC over 6 inches of crushed granite base, the minimum requirement for base thickness and the recommended thickness of surfacing for ALRS pavements.

The base course material used in the North Field test section was well-graded crushed granite with the gradation shown in Figure III-18. Compaction test results for the base are shown in Figure III-19. The gradation for the subgrade material is shown in Figure III-18. Compaction tests were conducted at two efforts (CE-12 and CE-55) for the subgrade. Results are presented in Figure III-20. The before and after traffic soils data are presented in Table III-5. Density data were obtained using a nuclear gage on the granular base material (Reference 46) and the drive cylinder method on the sand subgrade (Reference 44).

C. TEST CONDITIONS AND PROCEDURES

1. Instrumentation

The North Field test item was instrumented with linear variable differential transformer (LVDT) displacement transducers to measure vertical surface deflections. The LVDT produced DC output voltages directly proportional to the movement of the sensing unit. The transducer consisted of a main body, which housed the sensing coil and its associated electronics, and a movable core through the center of the sensing coil to transfer the mechanical movement of the core to a change in an electrical signal in the coil. The LVDT transducers were mounted on reference rods that extended to

reference flanges located approximately 6 feet below the bottom of the test bed. The reference rods were cased with 2-inch PVC pipe attached to the gage housing with flexible hose. The construction and details of the deflection gage are given in References 6, 10, and 48.

Pressure gages were also installed in the North Field test item. Construction of the WES soil pressure cells is described in several publications (References 49-51). WES soil pressure cells are designed to average vertical stress components applied across a 6-inch-diameter faceplate. The soil stress acts on the faceplate, which reacts on an internal mercury chamber. Pressure in the mercury chamber is an accurate analog of the average stress applied to the faceplate. The mercury chamber pressure is measured by a strain-gaged diaphragm, which completes the transduction mechanism. The cells were calibrated to either 50 or 100 psi. Two sets of gages were placed in the item so that they would be under the main gears of the F-4 aircraft when the aircraft was centered on the test item. A set of gages consisted of one deflection gage mounted at the surface, one 100-psi pressure gage mounted at the subgrade surface, and a 50-psi gage mounted 12 inches from the top of the subgrade. A layout of the instrumentation at North Field is shown in Figure III-21.

2. Nondestructive Testing

An FWD was used to determine the pavement deflections before, during, and after traffic tests on each of the test items. Two models of an FWD manufactured by Dynatest Consulting were used in this study. The model used on the WES test items and the environmentally aged pavements at Wright-Patterson and Whiteman AFB's had a 440-pound drop weight, which applied a

dynamic force of up to 15,000 pounds through an 11.8-inch-diameter plate on the pavement surface. The applied force and pavement deflections were measured with load cells and velocity transducers. On subgrades a 17.7-inch plate was used to reduce the magnitude of the deflection to within the range of the velocity transducers (0.080 inches maximum). The data acquisition equipment displays the resulting pressure in kilopascals and the maximum peak displacement in micrometers. Only three displacement transducers are provided with this model. Therefore, to obtain five deflections to describe the deflection basin, tests were conducted with the sensors at 0, 12, and 36 inches from the center of the load. Two sensors were repositioned to 24 and 48 inches from the center of the load and testing was repeated.

The model used for the North Field testing operated with the same configuration as described above but was controlled by a microcomputer. A total of seven deflections were recorded with each drop. The force output can range from 1,500 to 24,000 pounds by varying the mass level from 110 to 660 pounds and the drop height from 0.8 to 15.0 inches.

Nondestructive tests were conducted with the FWD at quarter points of the WES test items and at one-third points on the Wright-Patterson, Whiteman, and North Field items. Testing was conducted before, during, and after traffic. Tests were conducted at force levels of approximately 9,000 and 15,000 pounds. Deflections in many tests at the 15,000-pound force level exceeded the 80-mil limit of the velocity transducers.

3. F-4 Load Cart

Traffic tests were performed on each test item using a specially constructed load cart to simulate a fully loaded F-4 aircraft. The cart was loaded to 27,000 pounds and used a 30 x 11.5-14.5, 24-ply rated tire inflated to 265 psi. A tire contact area of 102 square inches was measured by placing the loaded tire on a plank of landing mat and painting the outline with spray paint. The outline was traced on a sheet of paper and the area was then measured with a planimeter.

4. Traffic Pattern

Each of the test items was trafficked with a distributed pattern simulating the expected wander width (70 inches) of the F-4 aircraft on runway ends and taxiways. The traffic distribution pattern is shown in Figure III-22. To apply the traffic, the test cart was driven backward and forward along the same path, then shifted laterally the distance of one tire width (10 inches) and the process repeated. The interior 40 inches received 100 percent of the maximum number of passes in any wheel path and the exterior portions of the lane received 67 and 33 percent.

Traffic will be described in terms of coverages. Based on traffic distribution studies, the number of passes required to produce one coverage is computed for the distribution of traffic over the width of the pavement area (runway, taxiway, or apron). For a single-wheel aircraft such as the F-4, the distribution is computed for one main gear. The F-4 aircraft pass to coverage ratio is 8.58. The pass to coverage ratio for the distribution pattern used in this study was 7 (Figure III-22). Therefore, predictions will be presented in terms of coverages herein.

5. Failure Criteria

The failure criteria initially proposed by the Air Force Engineering and Services Center for ALRS pavements are:

- a. Base course aggregate exposure sufficient to pose a foreign object damage (FOD) potential;
- b. AC disintegration sufficient to present FOD potential;
- c. A rut depth in excess of 3 inches;
- d. Other conditions, as determined by the project engineer, that cause the pavement to be nonserviceable.

Whenever one of these failure criteria was reached on a given item under testing, the traffic was discontinued and final data were recorded.

The CBR design procedure failure criteria (Reference 34) for flexible pavements designed as permanent structures based on accelerated traffic test data are:

- a. Surface upheaval of the pavement adjacent to the traffic lane of 1-inch or more;
- b. Surface cracking to the point that the pavement was no longer waterproof.

This criteria distinguishes between settlement due to traffic compaction and distortion due to shear deformation. Settlement, which is the result of densification of the base and subbase under accelerated traffic, is expected because of problems of obtaining density in thin pavement layers on a weak subgrade.

For the purpose of this investigation both the ALRS criteria and the permanent pavement criteria were evaluated. Rut depth was measured using a 10-foot straightedge. A 10-foot beam was placed across the traffic lane,

and the depth of rut was measured vertically to the lowest point within the traffic lane.

6. Other Data

Rod and level cross section data were collected at quarter points on the WES items and at one-third points on the remainder of the items. Data were collected prior to, during, and after traffic. AC surface cracking was monitored throughout the traffic testing. The distressed area was measured and recorded as a percent of the total area of the traffic test section.

TABLE III-1. SUMMARY OF CBR, DENSITY, AND WATER CONTENT DATA FOR SUBGRADE AND BASE ON WES TEST ITEMS.

Item	Pre-Traffic				After Traffic			
	Depth in.	Water Content, % Dry Weight	Density pcf	CBR	Depth in.	Water Content, % Dry Weight	Density pcf	CBR
	BASE COURSE							
1	2	2.2	144.9	91	2	1.9	148.0	110
2	1	2.7	144.4	85	1	2.2	148.8	107
3	1	2.3	144.1	96	1	2.1	145.3	103
	SUBGRADE							
1	12	26.2	93.4	6.3	12	26.5	92.8	7.0
	18	27.9	89.7	5.5	18	26.3	93.0	8.0
	24	26.6	92.9	6.9	24	25.9	93.3	6.0
	AVG	26.9	92.0	6.2	AVG	26.2	93.0	7.0
2	12	26.9	92.6	5.6	12	27.2	92.6	6.0
	18	27.7	91.2	7.0	18	27.5	91.9	6.7
	24	27.7	90.3	6.7	24	27.2	91.7	6.3
	AVG	27.4	90.4	6.4	AVG	27.3	91.1	6.3
3	12	26.8	92.1	6.7	12	26.7	91.9	7.3
	18	28.2	90.1	5.3	18	26.7	90.2	6.0
	24	27.7	91.0	5.6	24	28.7	90.5	5.0
	AVG	27.6	91.1	5.9	AVG	27.4	90.9	6.1

TABLE III-2. AS-BUILT LAYER THICKNESS FOR WES TEST ITEMS

<u>Item Number</u>	<u>Layer</u>	<u>Average Thickness in.</u>	<u>Standard Deviation in.</u>
1	Asphalt	1.7	0.6
1	Base	8.2	0.6
2	Asphalt	1.4	0.3
2	Base	9.0	0.4
3	DBST	0.5	0.2
3	Base	9.4	0.5

TABLE III-3. PAVEMENT CONSTRUCTION HISTORY.

Feature	Location	Pavement	Base		Subgrade		Constr. Date	Maintenance
			Type	Thickness	Type	In-place CBR		
<u>Wright-Patterson AFB, Ohio</u>								
WP-1	Fire Equip. Parking Pad	3 in. AC	Gravel (GW)	6 in.	12	---	1961	----
WP-2	Shoulder Pavement T/W-17	1 in. AC over 2 in. AC	Clayey Gravel (GP-GC)	47 in.	33	---	1959	Overlay, 1971 Rejuvenator, 1979
WP-3	Apron D	2 in. AC	Gravel (GP)	12 in.	33	Clayey Sand (SC)	1974	Excavated 2-in. base MC-30 prime coat 2 in. AC, 1974
WP-4	Shoulder Pavement T/W-5	2 in. AC	Silty Gravel (GW-GM)	12 in.	72	Clayey Sand (SC)	1962	Rejuvenator, 1974
<u>Whiteman AFB, Missouri</u>								
W-1	North Overrun R/W-01-09	1 in. DBST	Sandy Clayey Gravel (GC)	29 in.	33	---	1961	Seal coat, 1979
W-2	Shoulder Pavement T/W-9B	2.5 in. AC	(GC)	12 in.	102	Clay (CH)	1953	Slurry Seal, 1966
W-3	Blast Pavement Alert Apron	2.5 in. AC	(GC)	16 in.	37	Clay (CL)	1959	Slurry Seal, 1966

TABLE III-4. BASE COURSE AND SUBGRADE PROPERTIES FOR WRIGHT-PATTERSON AFB AND WHITEMAN AFB ITEMS.

Feature	Depth in.	Material	CBR	Water Content	Dry Density - PCF		Percent CE55 Density
					In-Place (A)	CE55* (B)	
WP-1	3.0	Base (GW)	12	4.3	143.3	141.3	101
	9.0	Base (GW)	13	11.8	119.0	---	---
WP-2	3.0	Base (GP-GC)	33	5.4	145.3	143.1	102
	16.0	Base (GP-GC)	35	15.3	117.0	---	---
WP-3	2.0	Base (GP)	33	5.3	135.3	140.1	97
	14.0	Subg. (SC)	7	11.7	112.3	129.2	87
WP-4	2.0	Base (GW-GM)	72	3.6	138.7	143.3	97
	14.0	Subg.	8	20.6	100.8	---	---
W-1	1.0	Base (GC)	33	5.6	132.1	137.2	96
W-2	2.5	Base (GC)	102	4.5	140.3	137.5	102
	15.0	Subg. (CH)	4.2	24.1	97.4	120.1	81
W-3	2.5	Base (GC)	37	4.7	135.1	139.8	97
	19.0	Subg. (CL)	4.2	25.2	94.3	113.5	83

* Laboratory densities shown in this column are the CE55 maximum densities at optimum water content.

Table III-5. SUMMARY OF CBR, DENSITY, AND WATER CONTENT
FOR NORTH FIELD TEST ITEM

<u>Station</u>	<u>Material</u>	<u>Depth in.</u>	<u>CBR</u>	<u>Modulus of Subgrade Reaction, k pci</u>	<u>Water Content percent</u>	<u>Dry Density pcf</u>	<u>Percent of CE-55 Density</u>
<u>BEFORE TRAFFIC</u>							
25	Subgrade	0	16		6.4	111.3	92
		6	44		4.8	115.2	95
		12	45		5.0	114.1	94
50			444				
75		0	27		5.2	115.4	95
		6	26		5.2	115.6	96
		12	25		6.7	116.2	96
25	Base	0	52		5.2	143.2	106
40		0	96		5.2	143.2	106
50			526				
75		0	69		5.2	143.2	106
<u>AFTER TRAFFIC</u>							
35	Subgrade	0	63		3.8	112.7	93
		6	79		3.5	111.5	92
		12	53		3.4	110.0	91
35	Base	0	100+		4.1	147.2	109

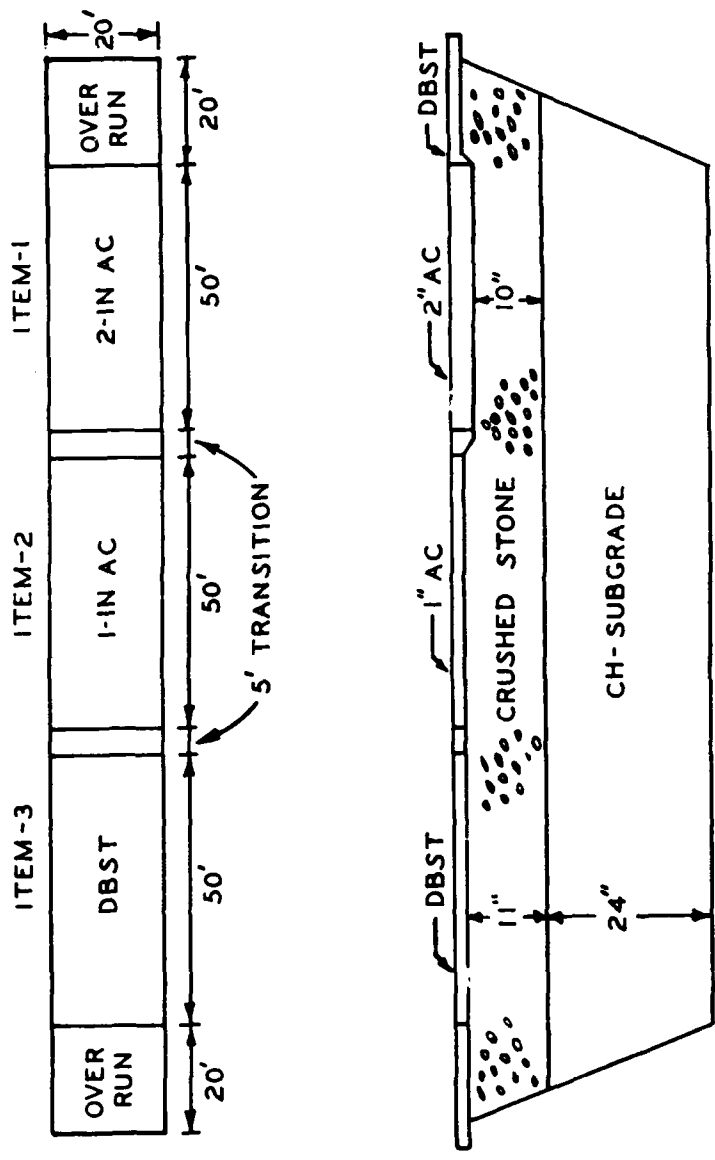
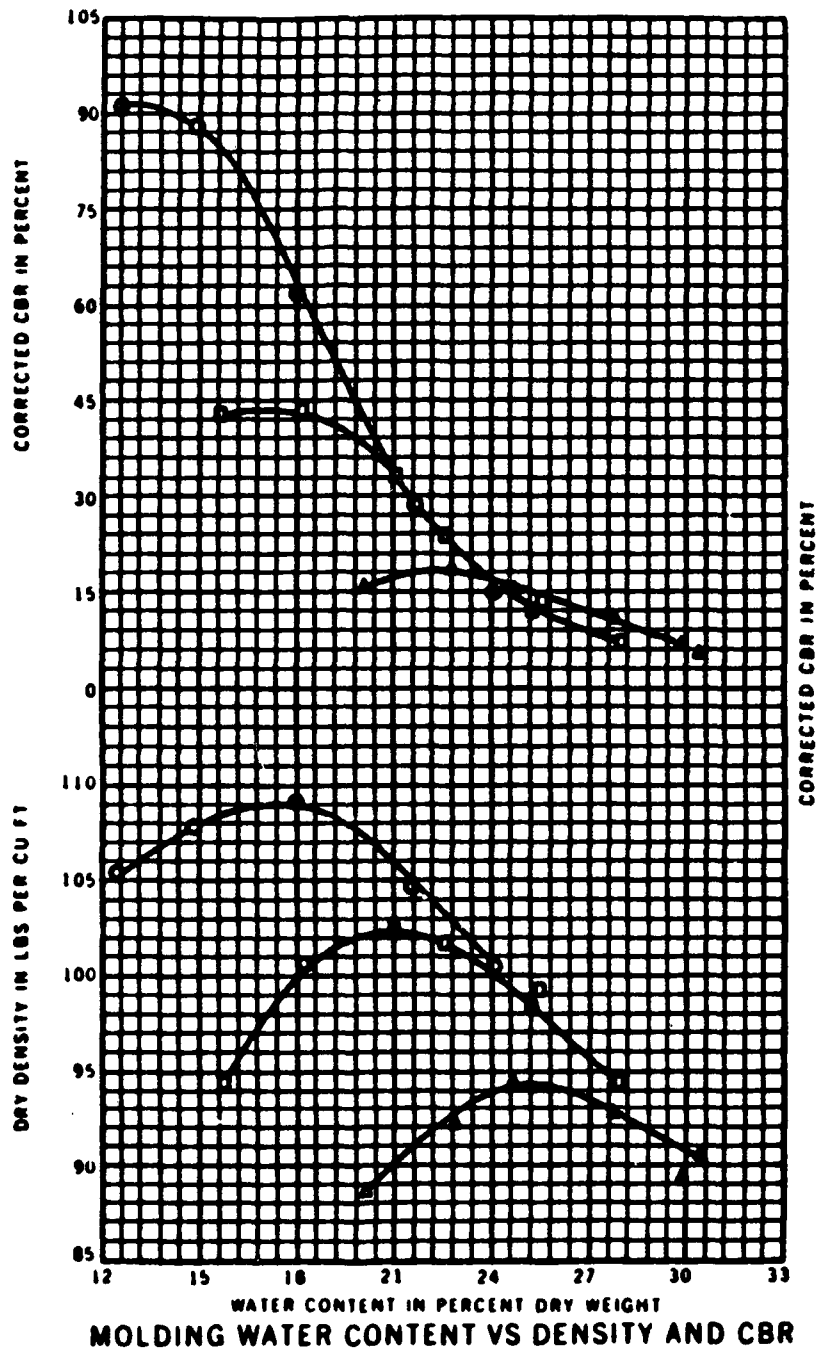


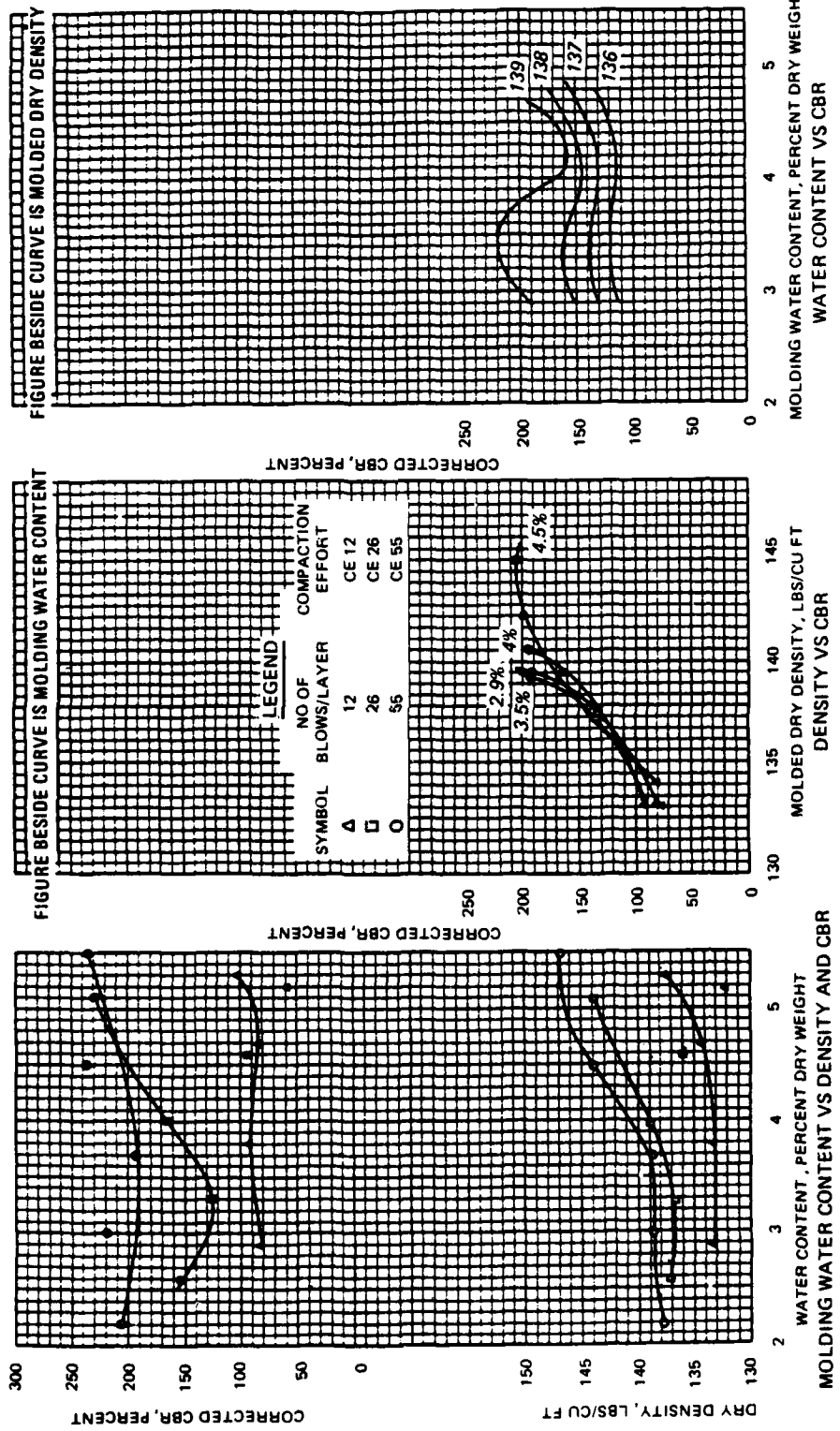
Figure III-1. Layout of WES Test Item.



LEGEND

SYMBOL	NO OF BLOWS/LAYER	COMPACTION EFFORT
Δ	12	CE 12
◻	26	CE 26
○	55	CE 55

Figure III-3. Laboratory Compaction and CBR's for WES Test Item Subgrade.



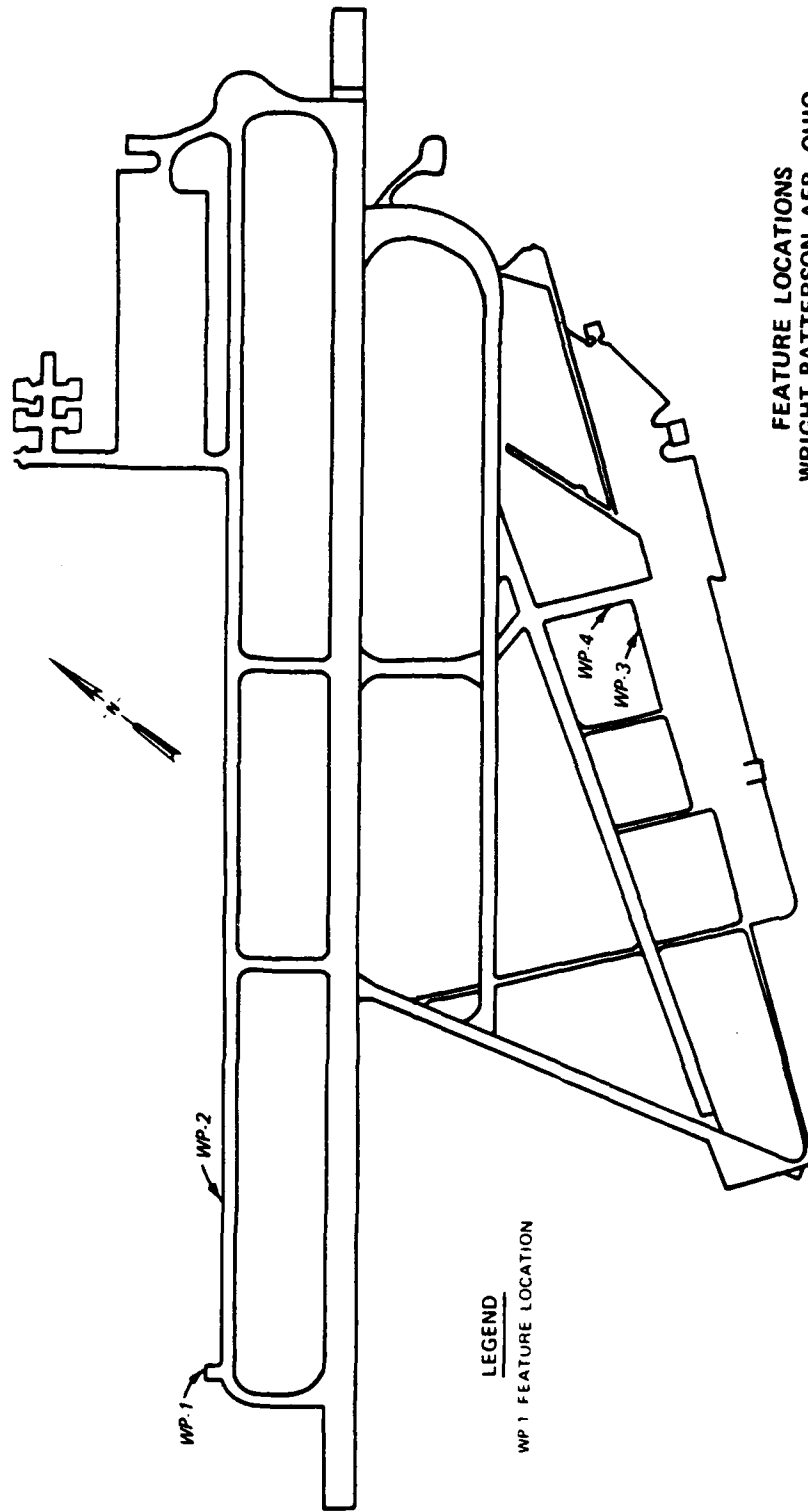
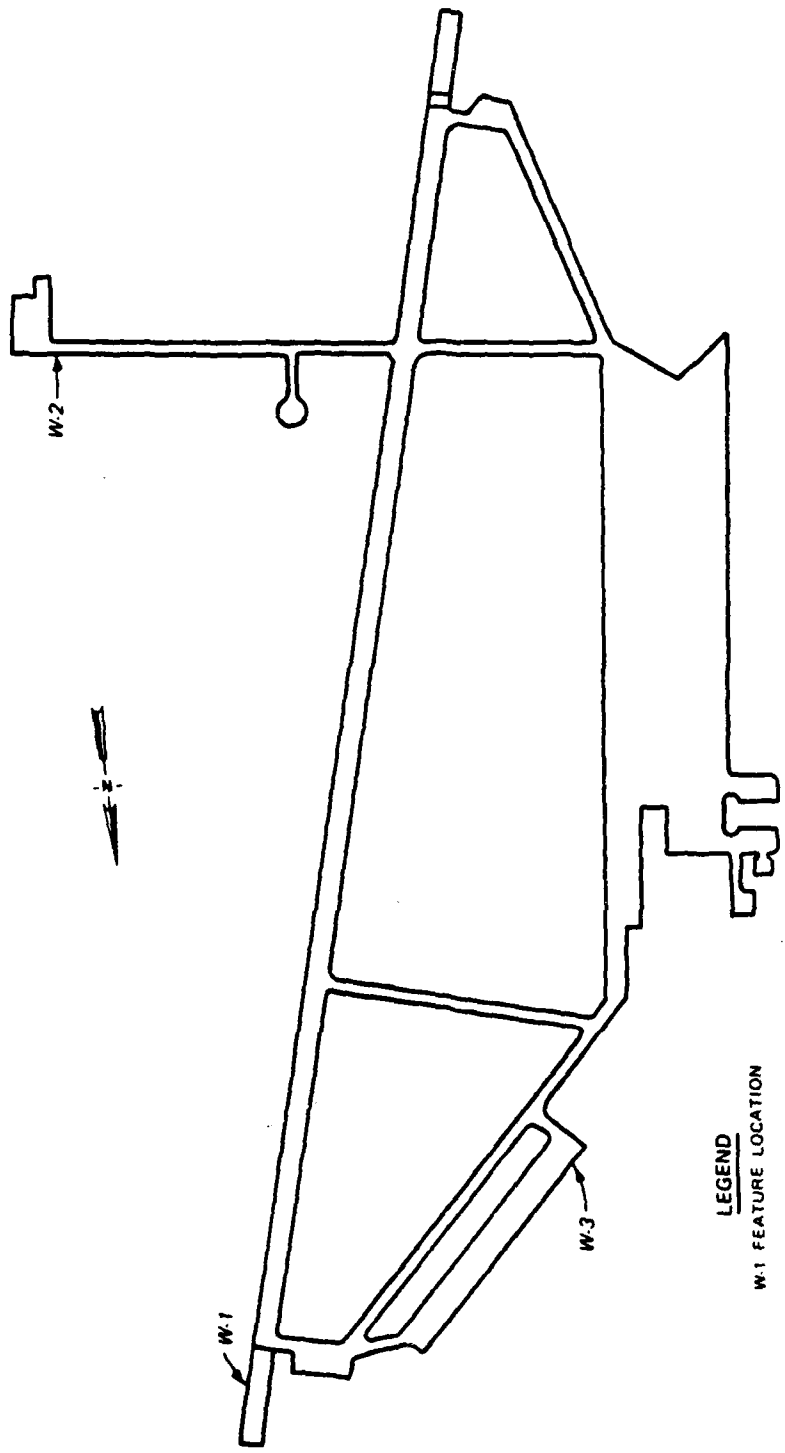


Figure III-5. Layout of Airfield Pavements Showing Location of Test Items, Wright-Patterson AFB, Ohio.

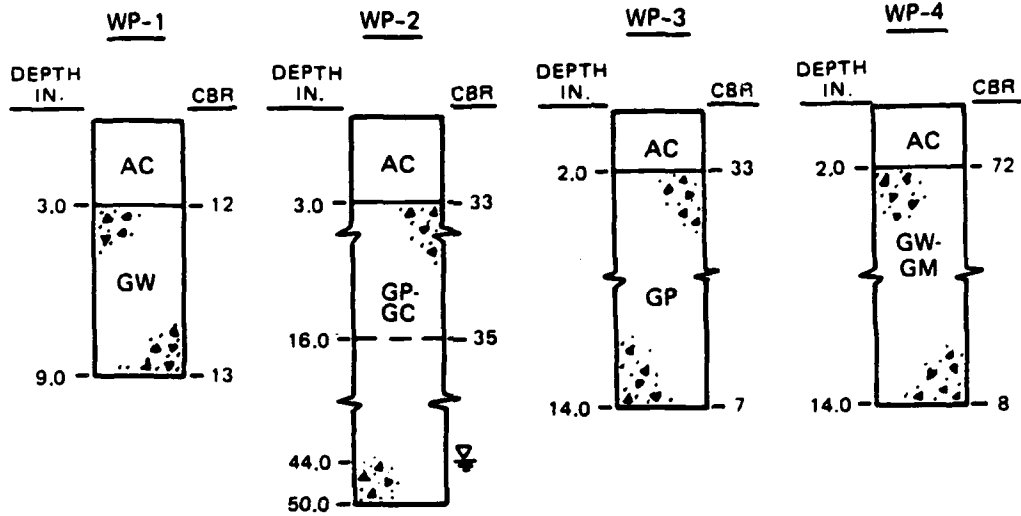


LEGEND
 W-1 FEATURE LOCATION

FEATURE LOCATIONS
 WHITEMAN AFB, MISSOURI

Figure III-6. Layout of Airfield Pavements Showing Location of Test Items, Whiteman AFB, Missouri.

WRIGHT - PATTERSON AFB, OHIO



WHITEMAN AFB, MO.

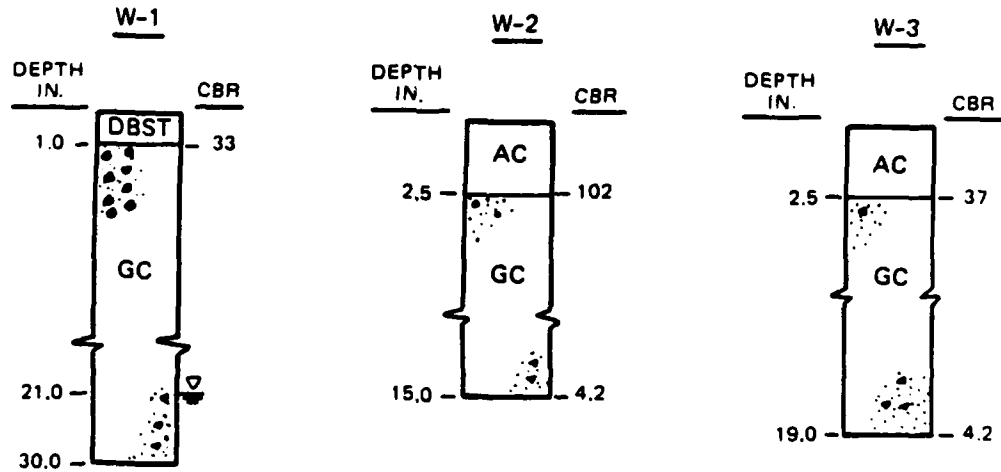
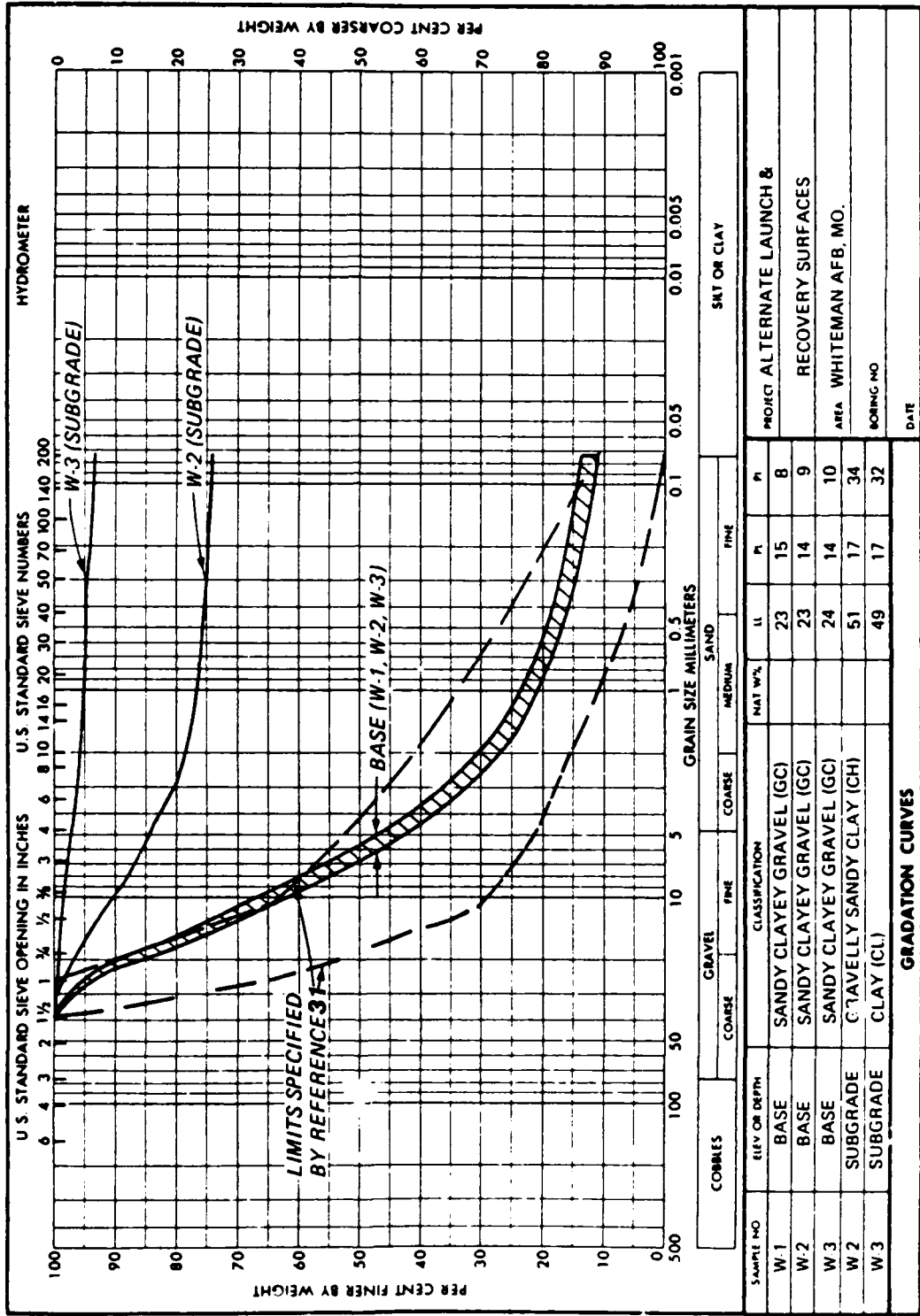


Figure III-7. Structure of Wright-Patterson and Whiteman AFB Test Items.



ENG FORM 2 (1977) REPLACES WES FORM NO 1271, SEP 1952, WHICH IS OBSOLETE
1 MAY 63

U.S. GOVERNMENT PRINTING OFFICE: 1961 O - 780,118

Figure III-9. Gradation Curves for Whiteman AFB Materials.

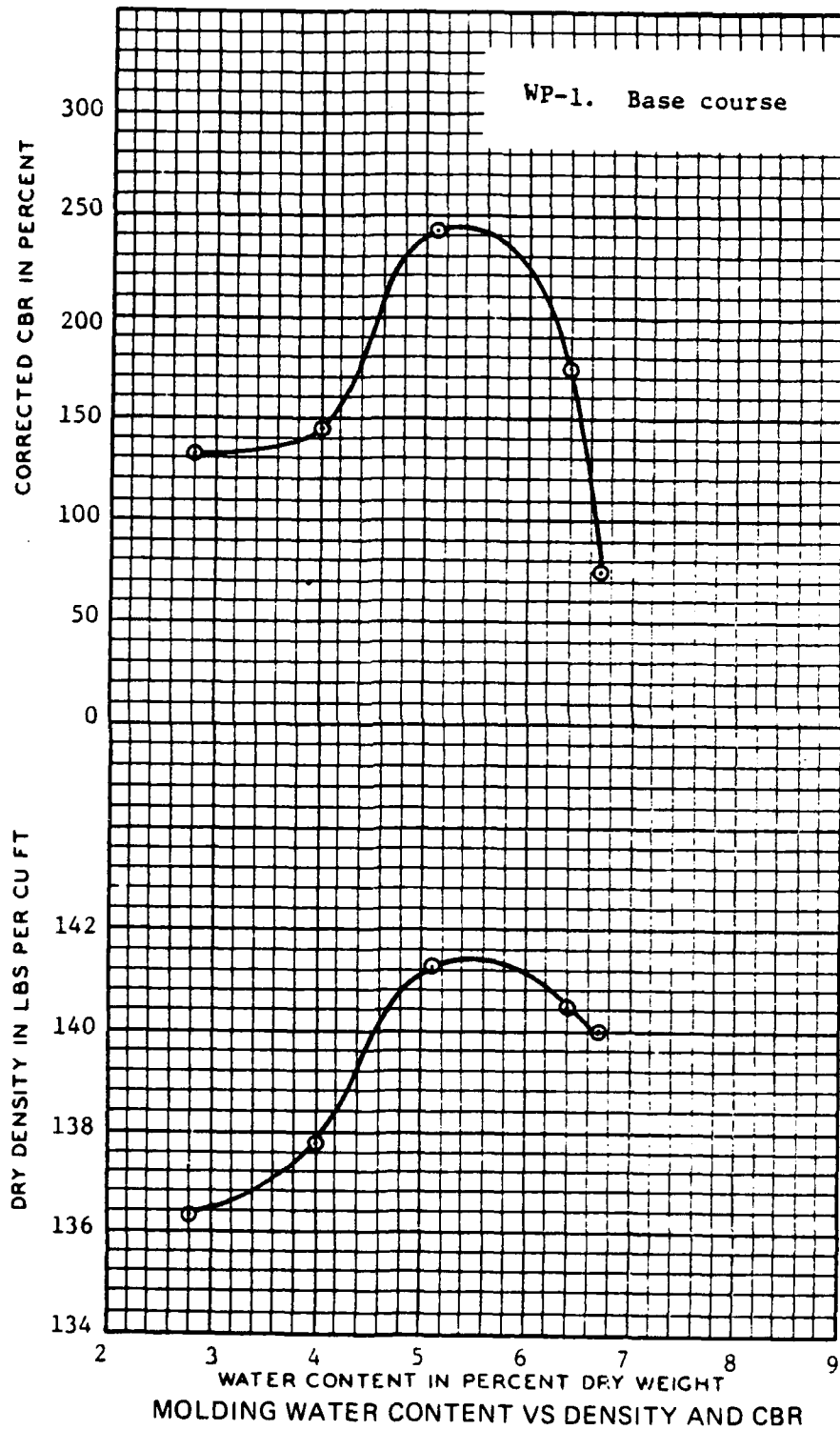


Figure III-10. Laboratory CE55 Compaction and Unsoaked CBR's for WP-1 Base Course.

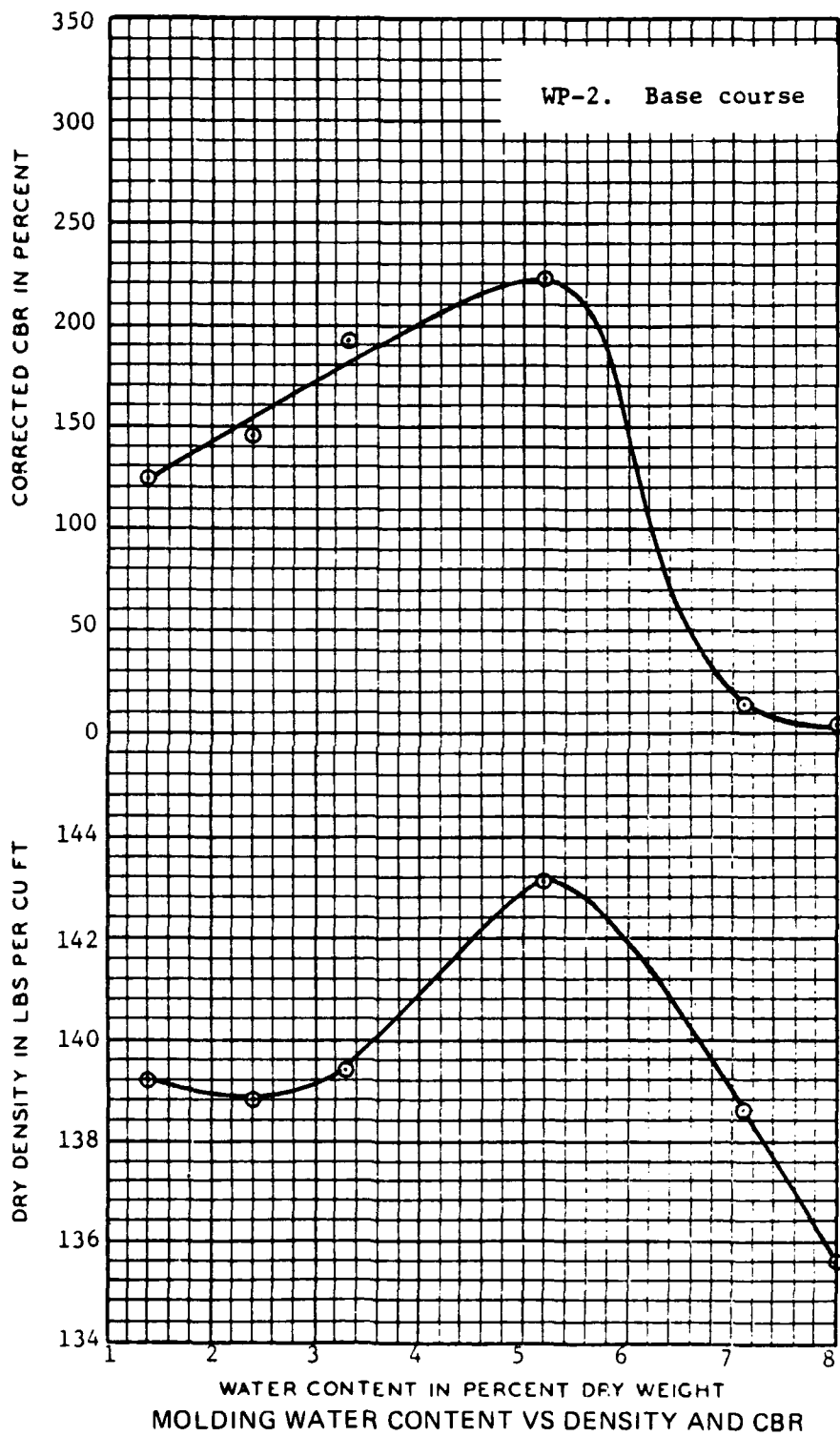


Figure III-11. Laboratory CE55 Compaction and Unsoaked CBR's for WP-2 Base Course.

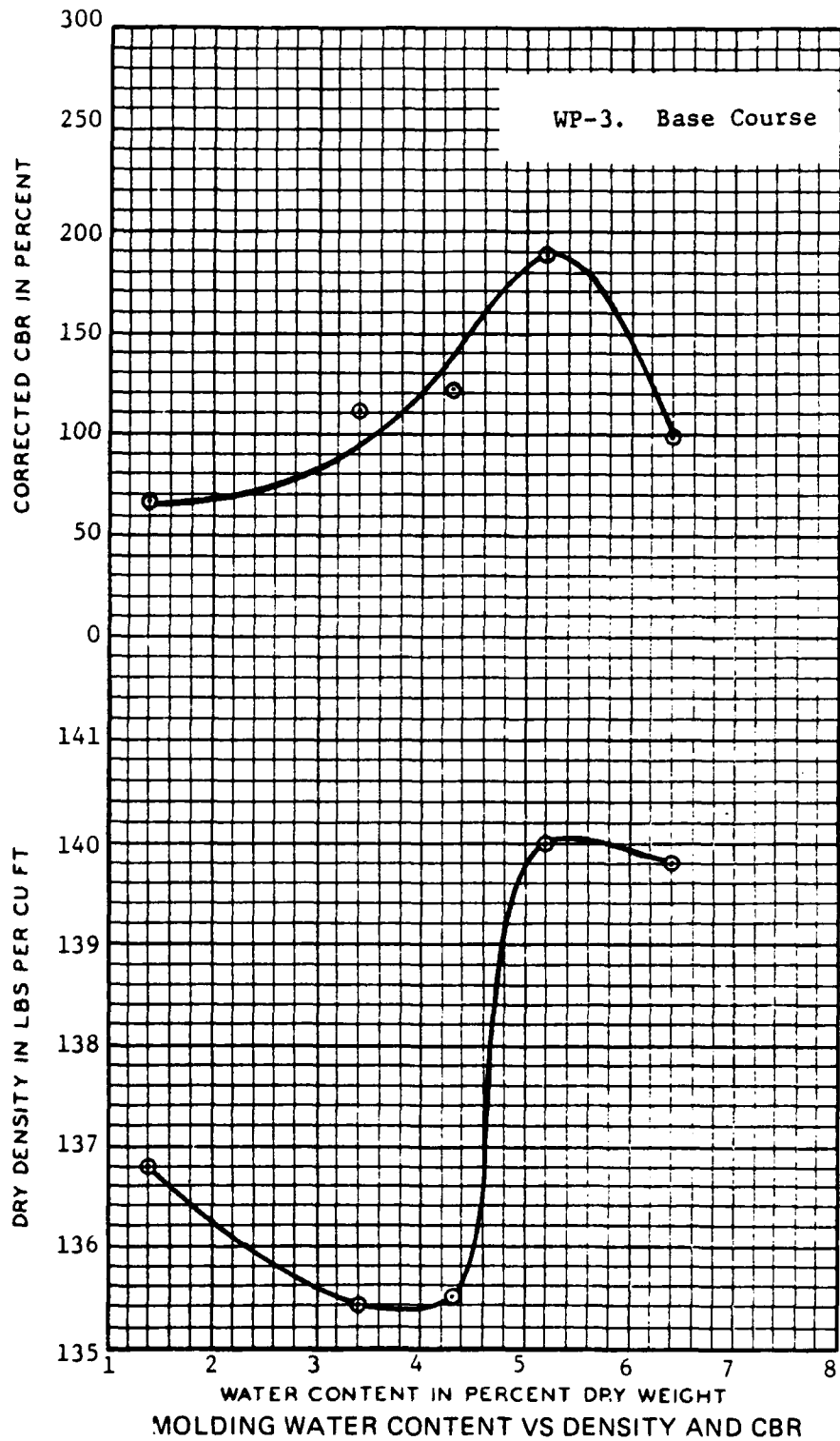


Figure III-12. Laboratory CE55 Compaction and Unsoaked CBR's for WP-3 Base Course.

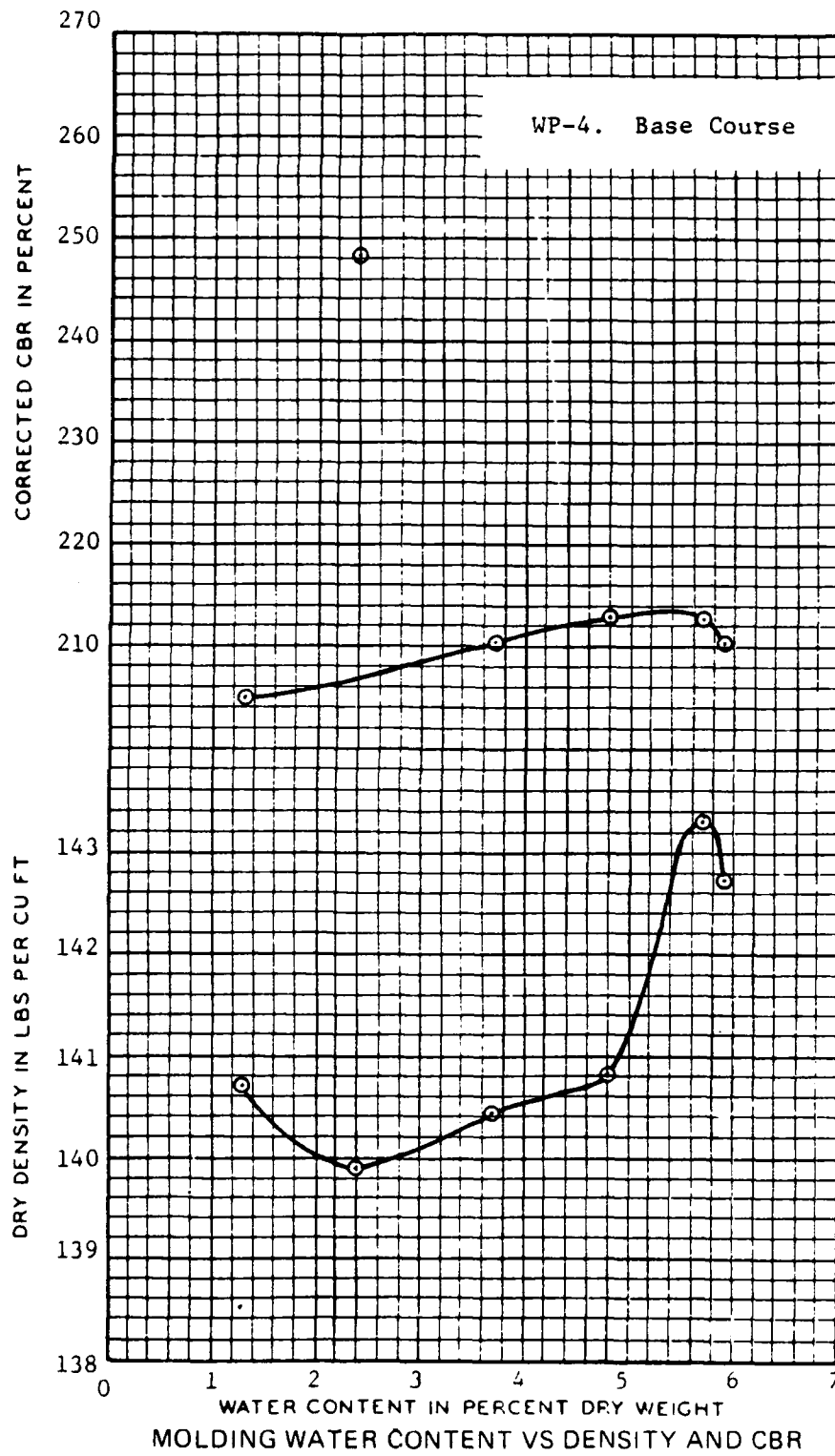


Figure III-13. Laboratory CE55 Compaction and Unsoaked CBR's for WP-4 Base Course.

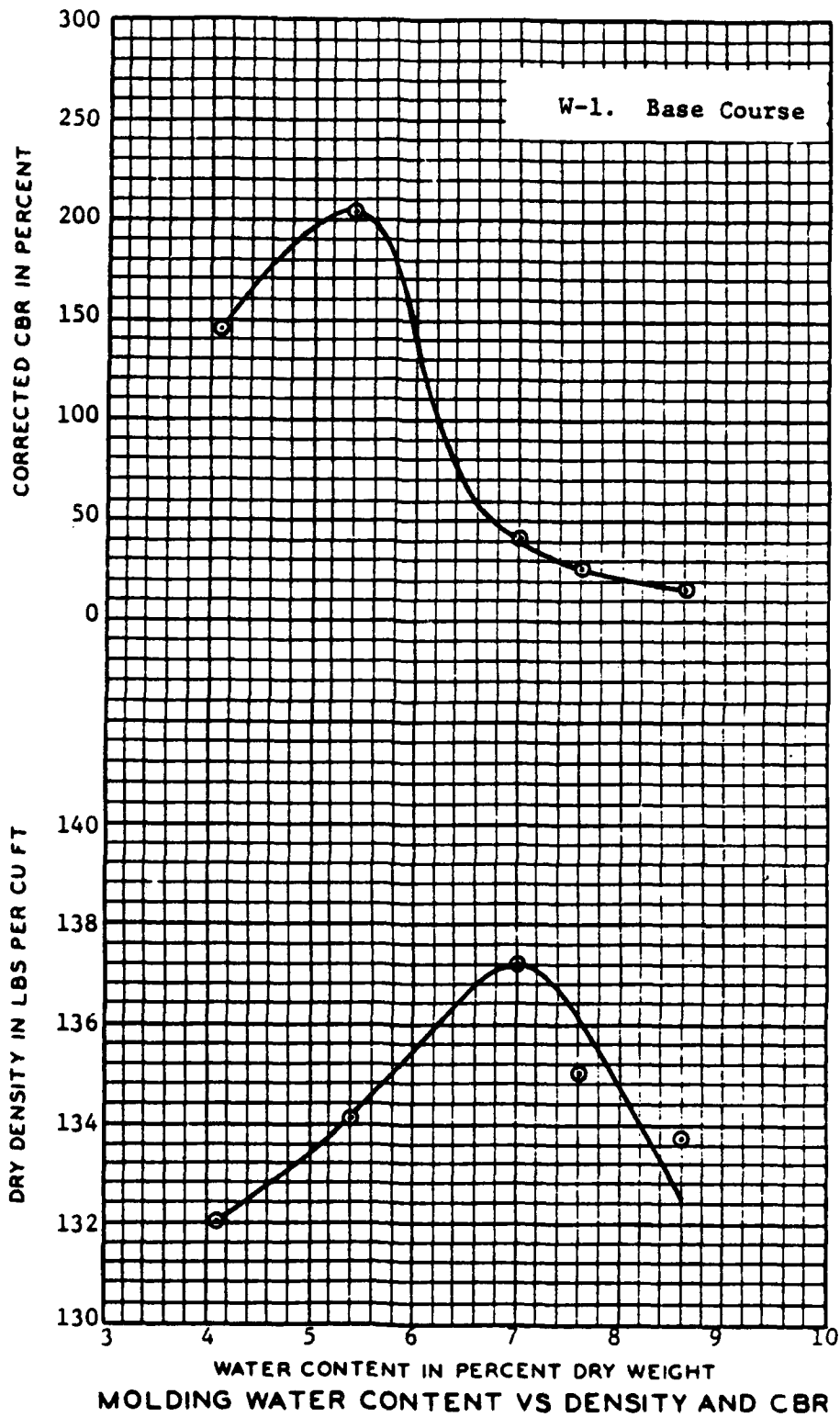


Figure III-14. Laboratory CE55 Compaction and Unsoaked CBR's for W-1 Base Course.

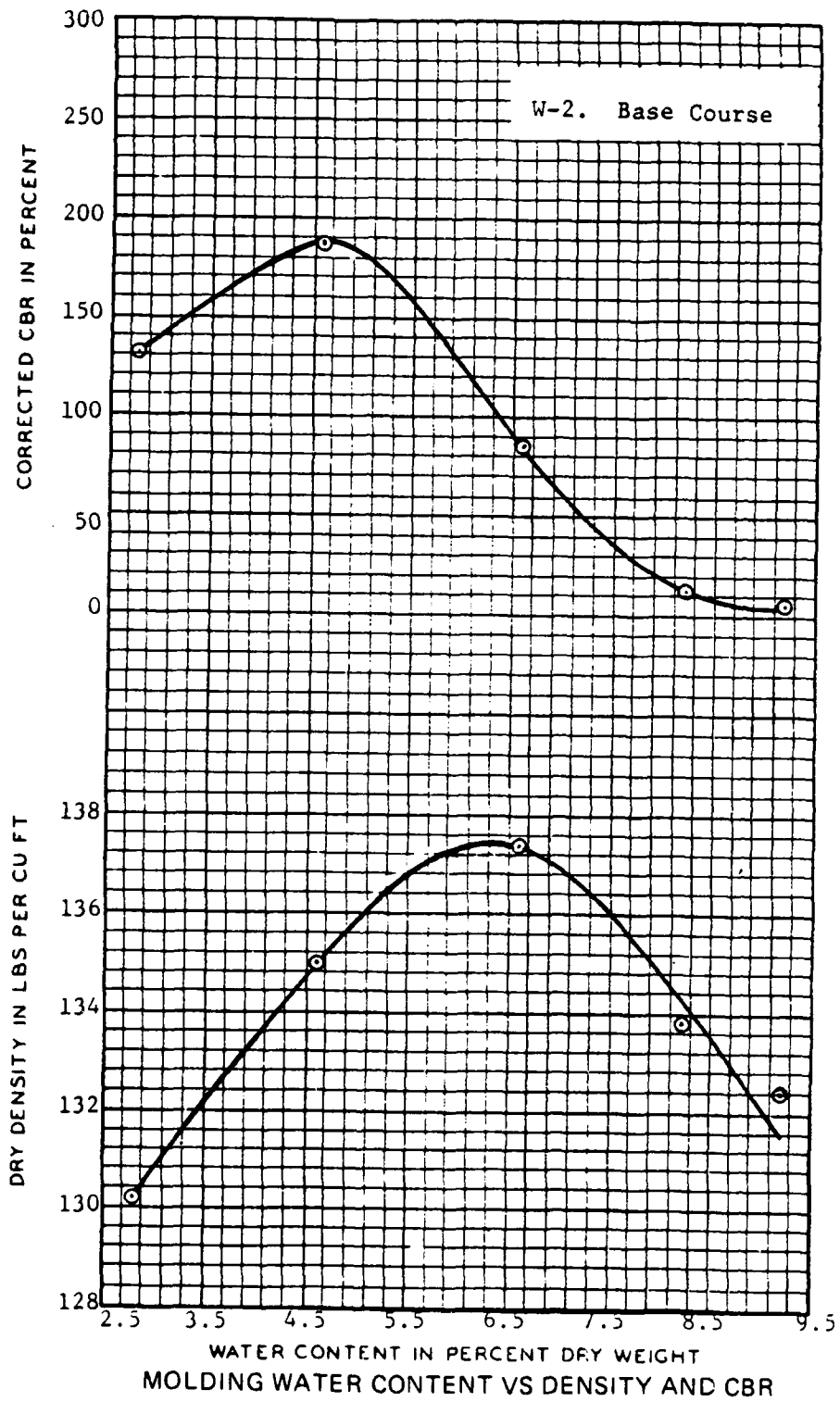


Figure III-15. Laboratory CE55 Compaction and Unsoaked CBR's for W-2 Base Course.

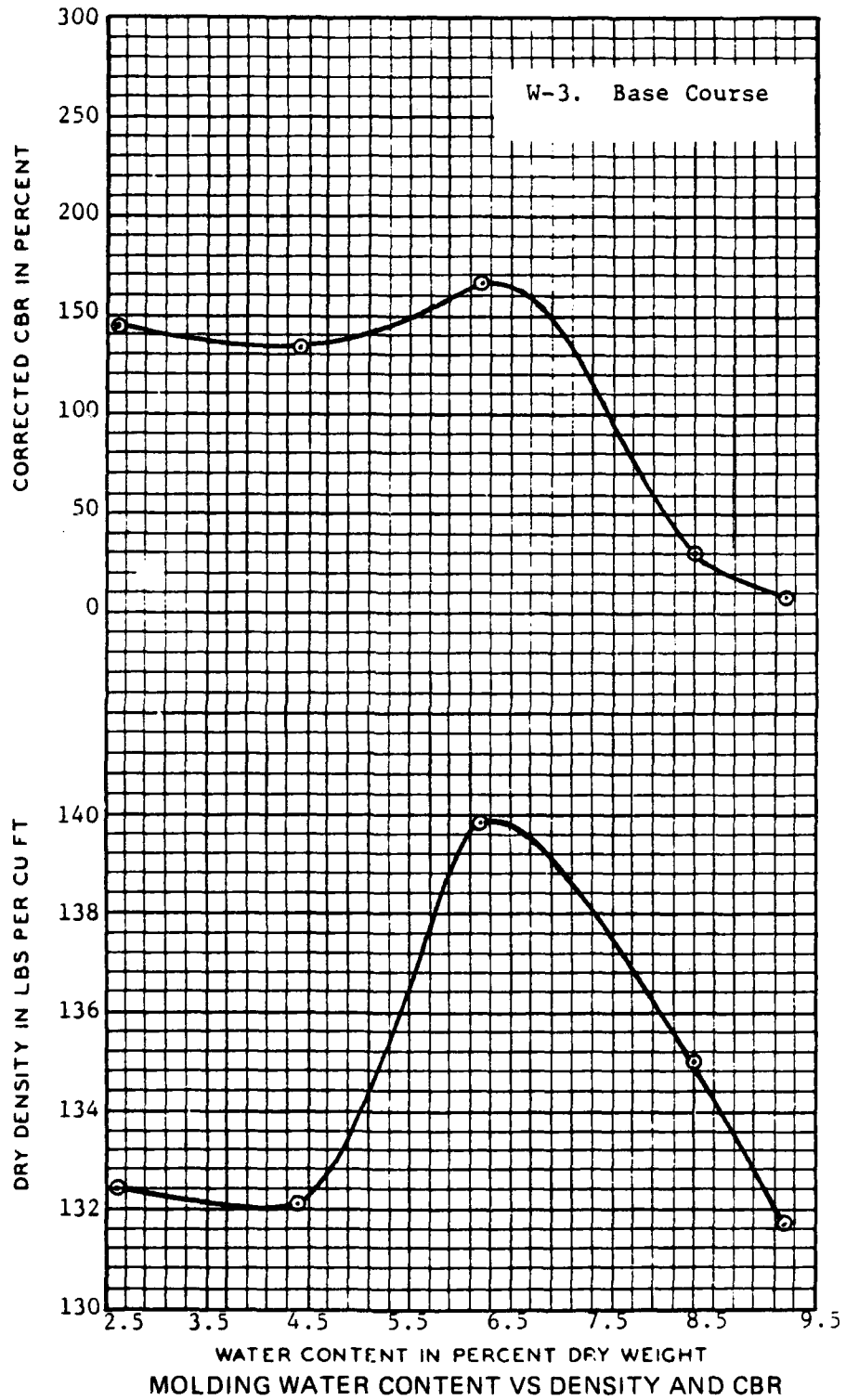


Figure III-16. Laboratory CE55 Compaction and Unsoaked CBR's for W-3 Base Course.

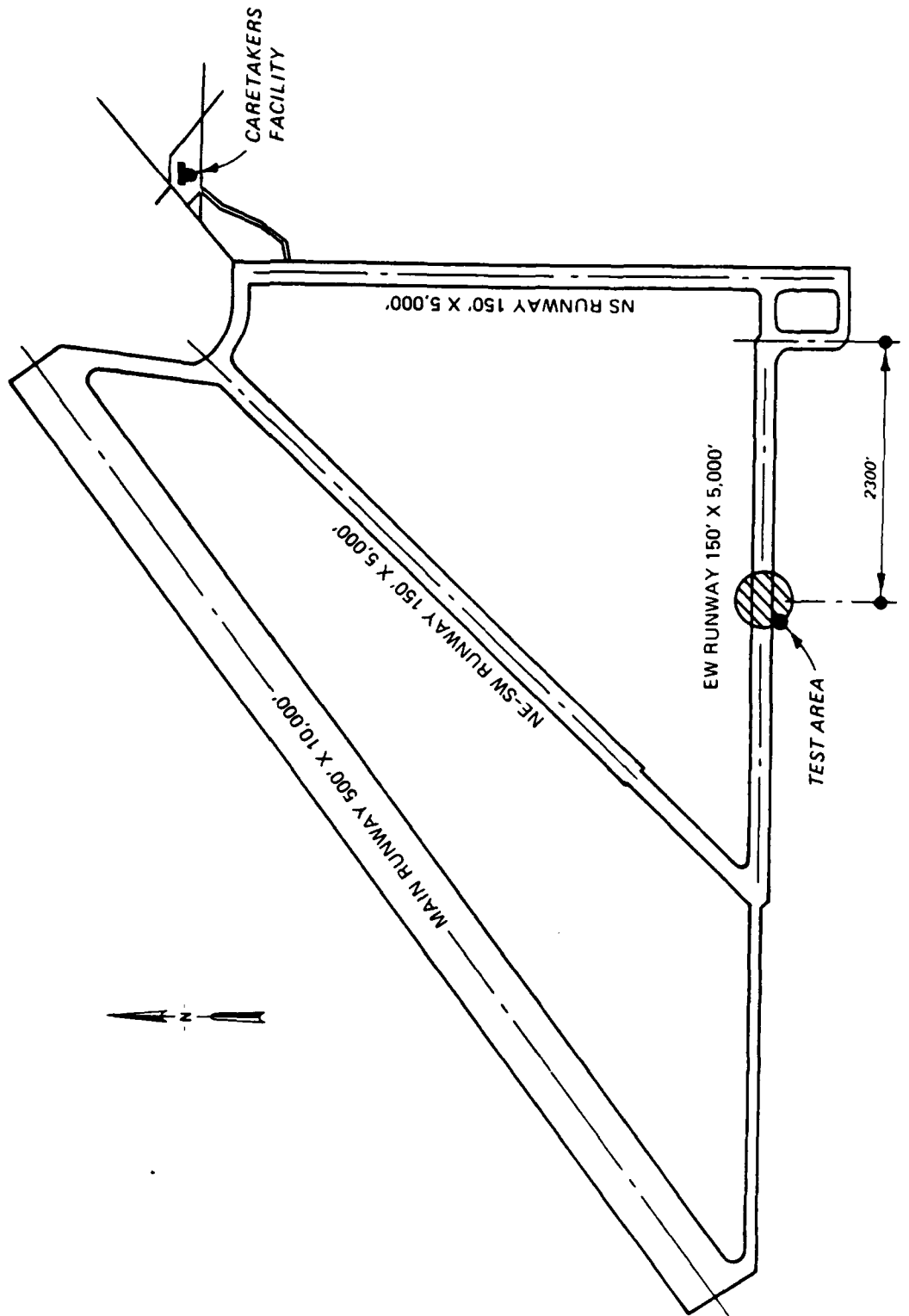
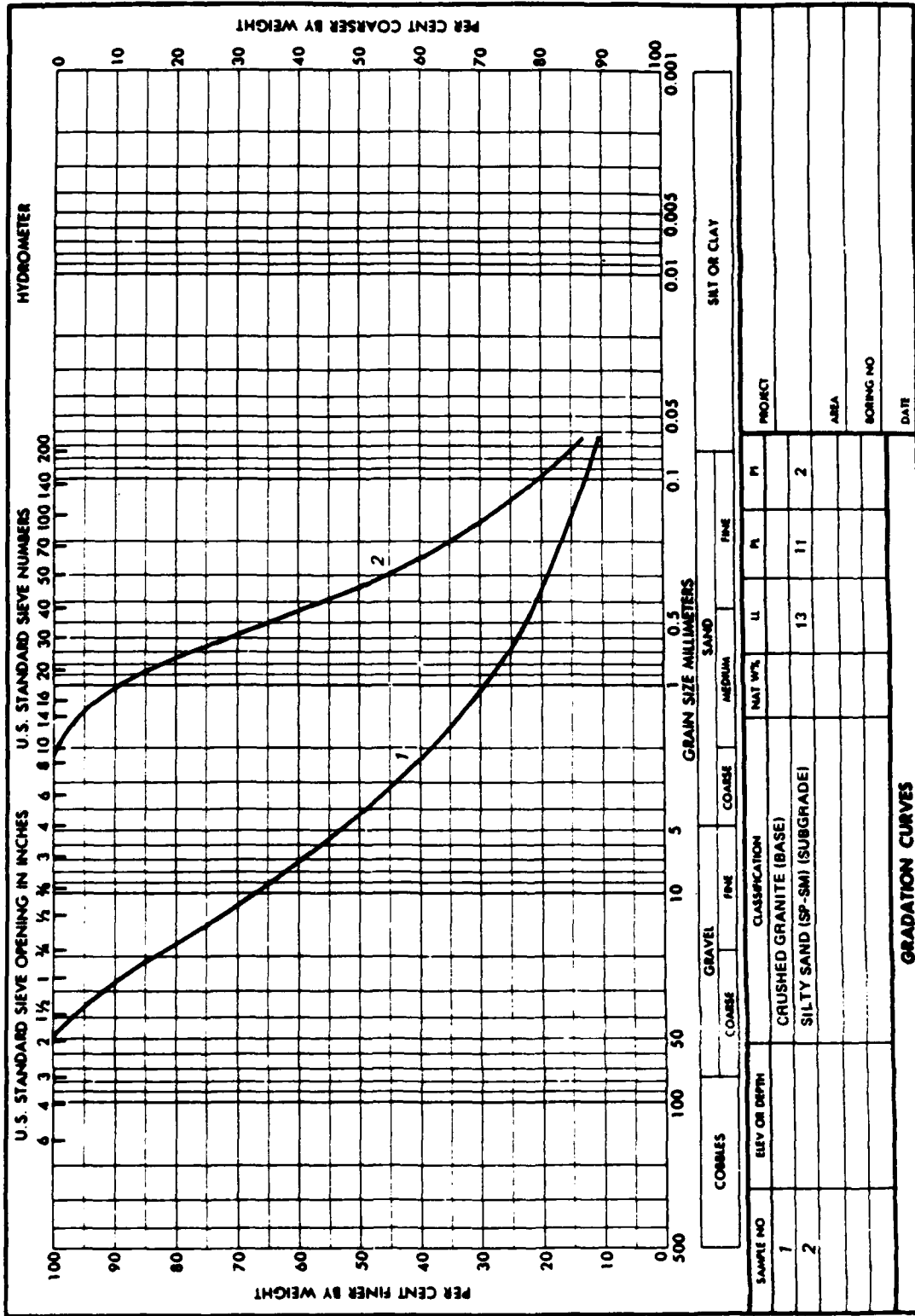


Figure III-47



U. S. GOVERNMENT PRINTING OFFICE 1963 O7 - NO. 118

REPLACES WIS FORM NO 1241, SEP 1962, WHICH IS OBSOLETE.

ENG FORM 2087
1 MAY 63

Figure III-18. Grain Size Distribution of North Field Base and Subgrade Material.

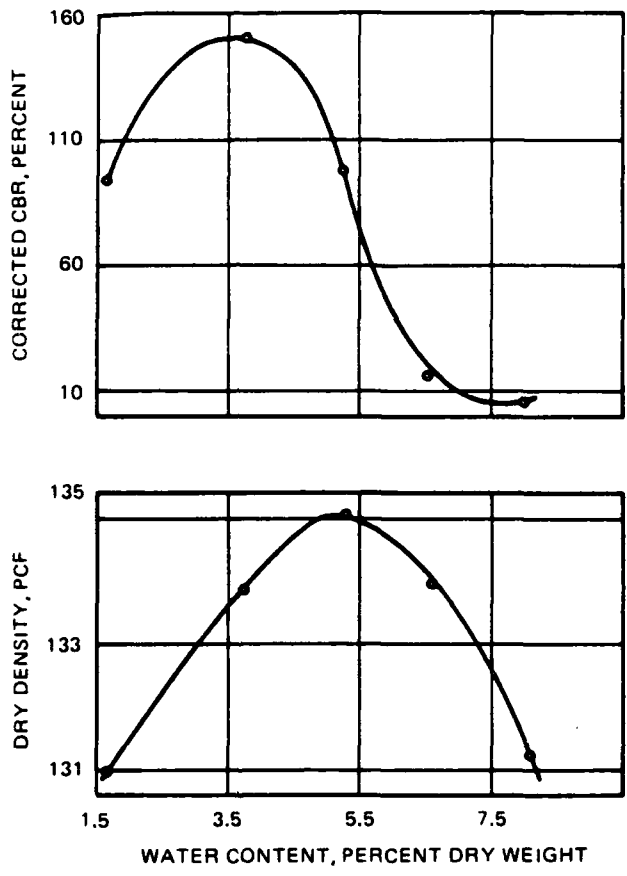


Figure III-19. Laboratory CE55 Compaction Results for North Field Base Course Material.

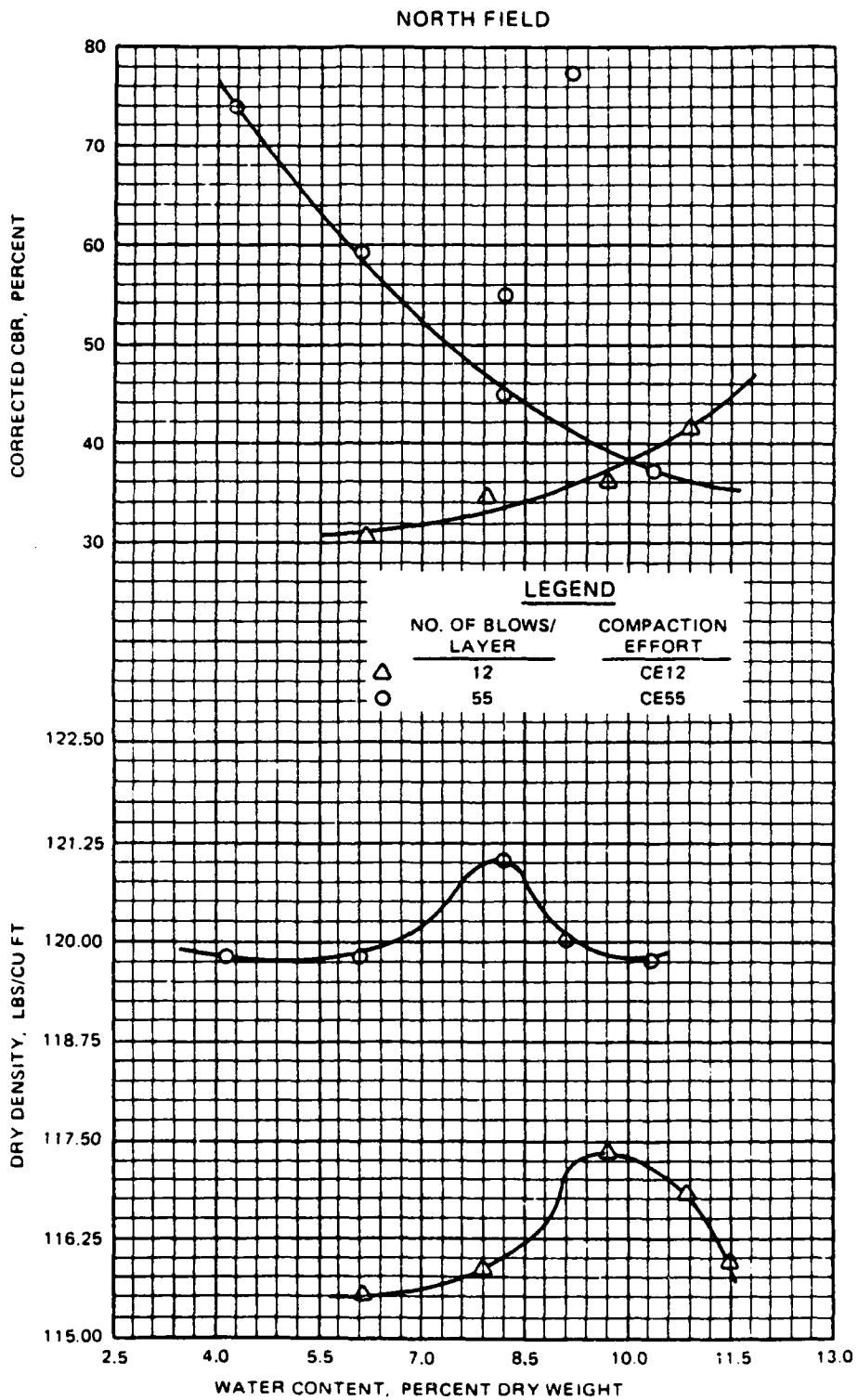
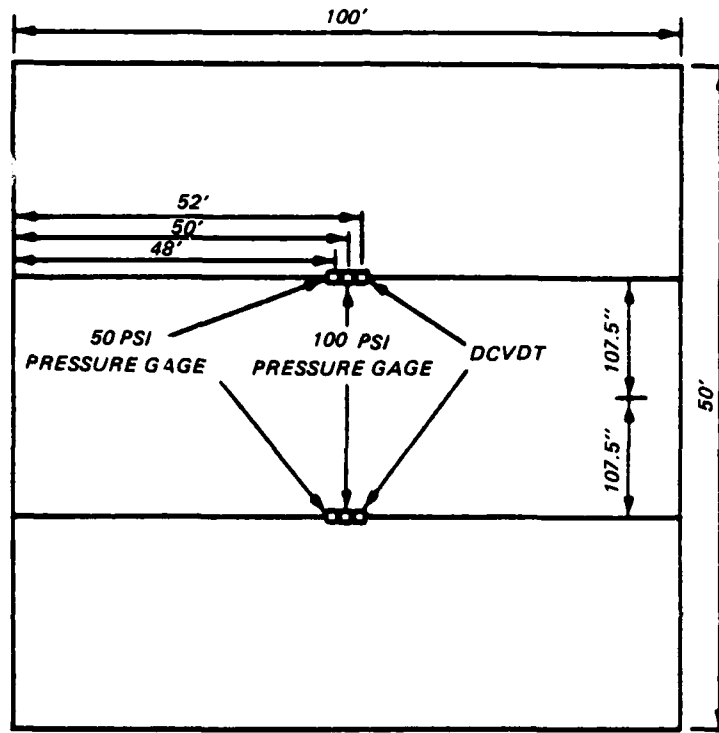
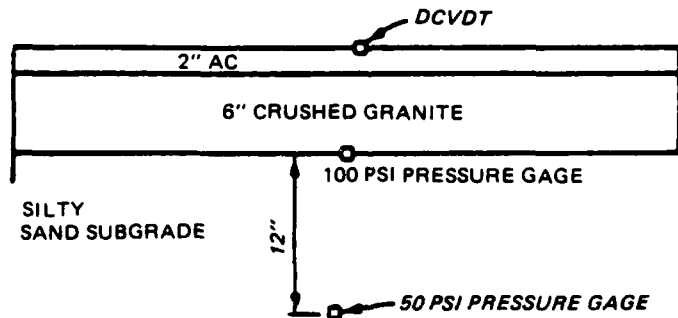


Figure III-20. Laboratory Compaction Results for North Field Subgrade.



PLAN



PROFILE

Figure III-21. North Field Instrumentation Layout.

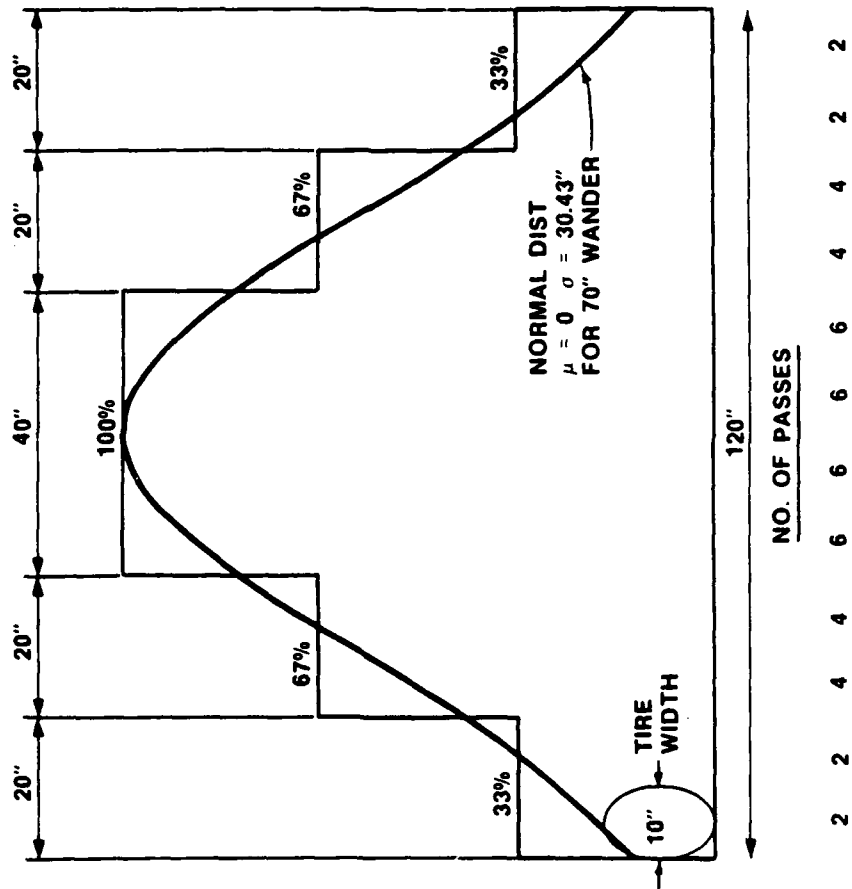


Figure III-22. Traffic Distribution Pattern.

SECTION IV
ANALYSIS OF DATA

To extract as much information as possible from the FWD data, several analyses were performed. Load deflection response was analyzed to illustrate the effects of higher load levels and ascertain if higher loads are required to adequately characterize the pavement response/performance. Surface deflections from the FWD were verified in the instrumented test section at North Field. The effects of asphalt concrete temperature were studied and will be presented.

A. FALLING WEIGHT DEFLECTOMETER

1. Verification of Deflections

The FWD applies an impulse load to the pavement surface. The resulting deflection is measured with a velocity transducer. The velocity time response resulting from an impulse load is contained in a frequency spectrum from about 1 to 70 hertz in the signal. Velocity transducers used on the FWD are nonlinear below about 5 hertz. Therefore, calibration cannot be accomplished with an instrumented "shake table." A typical response from an FWD transducer placed on a "shake table" is shown in Figure IV-1. A correction for the nonlinearity is made by the FWD's registration equipment. A typical time history output from the FWD's load and velocity transducers is shown in Figure IV-2. Phase shift between the force signal and the velocity cannot be measured from this figure since the output from the velocity transducers contain a phase shift caused by the difference between the time the surface wave arrives at the transducer and when the signal is transmitted. Since there is a nonlinear response from the velocity

transducer, the deflections were verified by comparing the deflections to those of the deflection gages at North Field as described in Section IIIC. The FWD load plate was placed directly over the gages. The resulting outputs are shown below.

<u>FWD Load</u> lbs	<u>FWD Deflection</u> mils	<u>LVDT Deflection</u> mils	<u>Difference</u> percent
9,064	37.9	38.0	-0.2
14,232	55.9	57.5	-3.0
13,874	65.2	64.0	2.0

The differences are considered reasonable considering the accuracy of both measuring systems. Based on the above measurements, the FWD deflections are assumed to be valid over a range from 1 to 80 mils (0.001 to 0.080 inches). The maximum displacement for the FWD velocity transducers is 80 mils. Readings greater than 80 mils should be discarded. Results from FWD tests on the 11 test items exceeded this 80 mil limit at load levels above 9,000 pounds in most cases after traffic was initiated.

2. Effects of Force Level

To evaluate the effects of different loads on ALRS type pavements, a test was conducted with the FWD 25,000-pound model over the full range of loads. Tests were conducted on a road section at WES. The pavement structure was 2 inches of AC over 6 inches of granular base over a CL subgrade. All loading weights were installed on the device and a test was conducted at the maximum drop height, two intermediate drop heights, and the lowest drop height. Two weights were then removed and the process repeated. At each successive weight configuration, the manufacturer's recommended configuration of rubber cushions was adopted. The process was repeated until all weights were removed, and only the loading frame was dropped. The

results of this test are presented in Figure IV-3. A minimum force of 2,000 pounds was obtained with all weights removed and the apparatus dropped at a minimum drop height. The results are nonlinear below 6,000 pounds force and nearly linear above 6,000 pounds force. Slight variations that occur at similar loads are the result of one test being at an intermediate or lower drop height and greater weight configuration compared to a high drop, lower weight configuration test. Variations could be due to different load pulse widths or slight variation in deflection or load accuracy.

The force output from the FWD varies with temperature pavement stiffness for a particular load configuration and drop height. Foxworthy (Reference 52) reported a variation from 23,532 pounds at 61° F to 28,318 at 36° F measured at the center of a 21-inch-thick portland cement concrete (PCC) slab. Alexander et al. (Reference 11) reported the following results on asphalt pavements.

<u>Thickness, in.</u>		<u>Pavement Temperature degrees F</u>	<u>Force lbs</u>	<u>Deflection, D0 mils</u>
<u>AC Surface</u>	<u>Granular Base</u>			
3.5	20.5	55	24,560	68.9
		83	22,960	72.2
3.0	10.0	38	28,304	17.1
		66	24,624	22.6
		75	23,608	23.3

From the above results the following differences in force output of the FWD for the same drop height were observed.

- a. 5,344 pounds or 23 percent on two different pavement sections;
- b. 4,696 pounds or 20 percent on the same pavement section.

These results emphasize the need for a load cell to record the load applied to the pavement.

To illustrate the effects of different FWD force levels on ALRS pavements, the impulse stiffness modulus (ISM) was calculated for the different tests on each of the test items. The ISM (secant modulus) is defined as:

$$\text{ISM, } \frac{\text{KIPS}}{\text{in.}} = \frac{\text{FWD FORCE}}{\text{FWD DEFLECTION}} \quad (16)$$

ISM was selected over deflection because the FWD load varies as a function of the magnitude of deflection and ambient temperature.

Results for the three WES test items and the North Field test item are shown in Figure IV-4. Generally, the ISM value is constant for the range of loadings from 5,000 to 14,000 pounds. Results from the Wright-Patterson and Whiteman AFB items are shown in Figure IV-5. There is an ISM increase for items WP-2 and W-1. These pavements had large granular base course thicknesses (47 and 29 inches, respectively). The granular base material stiffened with increased load and consequently increased confining stress and the sum of principal stresses (θ).

To examine the effects of stress-dependent materials on FWD response, tests were conducted on the subgrade, base, and pavement during the construction of the WES and North Field test items. The load deflection response on the CH subgrade material used in the WES test items is shown in Figure IV-6. The deflection at the center of the plate exceeded the 80-mil limit for the FWD; therefore, the deflection at 12 inches is shown. The material exhibits the expected stress-softening effect as would be expected for the clay material. Figure IV-7 shows the response at the same location

after the base course has been placed and compacted. The stress-softening effect is somewhat reduced from that shown by the clay as would be expected since quality granular materials do not show stress-softening. The load deflection response at the same location on item WES1 on the pavement surface is shown in Figure IV-8. The response is very linear on the surface, as shown in Figures IV-3 and IV-4. Figure IV-9 shows the results on the subgrade, base, and pavement and the decrease in nonlinearity.

Results from similar tests at North field are shown in Figure IV-10. The subgrade exhibits a nonlinearity, whereas the pavement and base are nearly linear.

3. Effects of Temperature

The stiffness of pavements containing AC layers is related to the temperature of the asphalt layer. During the development of the dynamic stiffness modulus (DSM) evaluation procedure (Reference 13), it was realized that the stiffness of a pavement must be corrected in order to obtain a consistent evaluation of AC pavements tested at varying temperatures. A temperature test section was constructed, and tests were conducted at different temperatures. From these results a set of correction curves was developed.

These curves were later modified (Reference 53) using a mechanistic analysis. The pavements were modeled using the BISAR program to calculate deflections. A nominal load of 7,000 pounds on a 9-inch radius circular area was used. The modulus-temperature relationship developed by Kingham and Kallas (Reference 54) was selected (Figure IV-11). Results of this analysis were selected for the DSM temperature correction procedure.

For ALRS pavements the effect of temperature on the measured deflections must be considered. Since the FWD has an 11.8-inch-diameter plate and the WES 16-kip vibrator has an 18-inch plate, the correction procedure was not applicable. A similar study was conducted with the FWD. Nine pavements were selected at WES for testing over a range of temperatures. Thicknesses and structure of the nine sites are shown in Figure IV-12. FWD testing was conducted between January and June 1986 to cover a wide range of pavement temperatures.

The mean pavement temperature was selected as the temperature to use for calculations. The mean pavement temperature is defined as the average temperature of the AC layer from a depth of one inch below the surface to one inch above the bottom of the layer. During this study the method of measuring the pavement surface temperature with an infrared gun was evaluated. At each test site a 1-inch-diameter core was drilled into the pavement to a depth greater than half the thickness of the AC layer. The hole was filled with oil, and a thermistor was placed at a depth of one half the thickness of the AC layer. The temperature was allowed to stabilize. The temperature measured with this gage was assumed to be the mean pavement temperature.

The surface temperature was measured with an infrared gun and with a thermistor taped to the pavement surface. For calculation of the mean pavement temperature, the method developed by H. F. Southgate, Kentucky Department of Highways and presented in Reference 55 was selected. The method correlated the pavement surface temperature added to the previous

5-day mean air temperature to the temperature measured at a depth in an asphalt surfacing.

A comparison of measured to predicted center pavement temperature determined by measuring the surface temperature with both the infrared gun and a thermistor and using the Kentucky procedure with the previous 5-day mean air temperature is shown in Figure IV-13. The infrared gun measurements produce as good or better results than the thermistor. This may be due to the fact that the gun measures an average over an area from 2 to 6 square inches whereas the thermistor is only a point measurement.

The ISM values obtained on the nine sites are shown in Figures IV-14 through IV-22. For the pavements with 3 inches or more AC surface thickness there is a definite decrease in stiffness with an increase in mean pavement temperature (Sites 1, 6, 7, 8, and 9). Other variables such as moisture conditions and accuracy of the FWD load and deflections appear to have a greater influence than temperature on deflections in pavements with less than 3 inches of AC than temperature. Therefore, a temperature correction factor will not be applied to the results obtained from those pavements.

To develop correction factors for pavements with 3 inches or more of AC, the procedure described above using modulus values from Figure IV-11 and the FWD loading configuration was selected. These relationships are presented in Figure IV-23.

For Sites 1, 6, 7, and 8, the ISM value at a mean pavement temperature of 70° F was selected from polynomial regression of the ISM values. This value was divided by the ISM at all other temperatures for

normalization. These values are shown in Figures IV-24 through IV-27. Also shown are the curves from Figure IV-23 for the corresponding thickness.

Since the measured data fits the curves, the relationships shown in Figure IV-23 can be used to select ISM correction factors. For a mean pavement temperature, the factor is multiplied by ISM to give an ISM corrected to 70° F. These factors can also be applied to the deflection measured at the center of the applied load by dividing the measured ISM by the correction factor. The relationships do not apply to deflections measured away from the load.

4. Effects of Traffic on ISM and Deflection Basin Descriptors

The WES1 and NFF4 items were the only items where the FWD data were collected throughout traffic without overranging the velocity transducers. For those items, relationships of ISM, BCI, SCI, area, and spreadability will be presented. WES1 was constructed over a clay subgrade whereas NFF4 had a sand subgrade. ISM relationships are presented in Figures IV-28 and IV-29. ISM for the WES1 item dropped rapidly during initial trafficking and remained relatively constant throughout the remainder of traffic testing. The stiffness of the NFF4 items decreased throughout traffic.

The load-normalized deflection basin area is shown in Figures IV-30 and IV-31. The change in area with traffic is different for the two items. NFF4 is constant for the first 20 coverages then decreases with traffic. The area for WES1 drops rapidly then increases. The magnitude of the change in area is small.

The surface curvature index (SCI) relationships are shown in Figures IV-32 and IV-33. The contrast between SCI change for the two items

is similar to ISM but inverted. There is a large change in magnitude for SCI values with traffic.

Base curvature index (BCI) change for the two items is shown in Figures IV-34 and IV-35. Except for Station 50, the BCI for NFF4 changed very little whereas WES1 increased with traffic.

Spreadability for each item is shown in Figures IV-36 and IV-37. Spreadability change for the items follows the change in ISM almost exactly. The magnitude of the change is very small.

B. USE OF DEFLECTION BASIN DESCRIPTORS

1. Surface/Base Curvature

In an effort to identify failure locations within each pavement from the FWD data using the procedure shown in Figure II-1, the FWD deflections were converted to Dynaflect deflections using the following (from Reference 18):

$$\text{Dynaflect Deflection} = (\text{FWD Deflection @ 9,000-pound load} + 7.24472) / 29.6906 \quad (17)$$

The SCI, BCI, and DO values were compared to the relationships in Figure II-5. From these results all pavements except WP2 and NFF4 were classified as subgrade strong, pavement weak. The NFF4 and WP2 gave a condition of the pavement structure as pavement weak and DMD as okay.

2. Nonlinear Subgrade Modulus

The E_{RI} (Figure II-7) values for each test item were calculated using the ILLIPAVE algorithm (Reference 56):

$$E_{RI} = 24.06 - 5.08(D36) + 0.28(D36)^2 \quad (18)$$

where

E_{RI} - modulus, ksi

D36 - deflection 36 inches from an applied 9000-pound load,
mils

The above algorithm is valid for cohesive soils and for D36 values less than 9 mils.

E_{RI} values and the modulus values from BISDEF are presented in Figure IV-38. As expected, the E_{RI} values are slightly lower but follow the same pattern as the BISDEF subgrade modulus values.

E_{RI} was calculated for the WES1 item from FWD deflection data collected before, during, and after traffic. Results are presented in Figure IV-39. The change in E_{RI} with traffic is very similar to the change in subgrade modulus from BISDEF as shown in Figure IV-43.

C. RESULTS FROM BACK CALCULATION PROCEDURE

Results from FWD tests on all pavement items during construction, before, during, and after traffic are given in Appendix A. For determination of layer moduli values, the BISDEF program was used. A description of BISDEF is given in Appendix B. Each pavement was treated as a three-layer system with an AC surface, base, and subgrade. A stiff layer ($E = 1,000,000$ psi) was placed at a depth of 20 feet from the pavement surface. For most pavements the base course and subgrade layers were allowed to vary in the program. The modulus of the AC surface course was estimated from surface temperatures at the time of testing. Layer modulus values for all items back calculated from the before traffic FWD data are

given in Table IV-1. Moduli values for the base course were lower than subgrade moduli values for all Wright-Patterson pavements.

1. Verification of Modulus Values and Resulting Stress Calculations

Laboratory tests were conducted on the North Field subgrade material to determine the resilient modulus properties of the sand at different confining pressures and normal stresses. Results of these tests are presented in Figure IV-40. The BISAR computer program was used to calculate the bulk stress ($\sigma_1 + \sigma_2 + \sigma_3$ or $\sigma_1 + 2\sigma_3$) at the top of the subgrade for the modulus values for Station 25 of NFF4 given in Table IV-1. For a 9,000-pound FWD load the bulk stress at the top of the subgrade was 131 psi. From Figure IV-40 the modulus would be approximately 35,000 psi. This is within 2000 psi of the average of the subgrade values for NFF4 in Table IV-1.

The use of a layered elastic model offers a method to compare stresses measured with pressure gages under an F-4 loading. A comparison of calculated stresses and measured pressures is shown in Figure IV-41. Measured and computed stresses are closer when the Boussinesq stress distribution is assumed.

Stresses and strains were calculated with the BISAR program using modulus values from Table IV-1 for the F-4 loading at points in each pavement structure as shown in Figure IV-42. Values are shown in Table IV-2. These values will be used to predict performance.

Costigan and Thompson (Reference 57) reported laboratory resilient modulus results on the "Vicksburg buckshot" material used in the subgrade construction of a stabilized soil test section. The material is the same type of subgrade used in the WES test items in this study. Comparisons

of pertinent material properties are shown below. The E_{RI} value (see Figure II-3) was determined at a deviator stress of 6 psi.

	<u>Stabilized Soil</u> <u>Test Section</u>	<u>WES ALRS</u> <u>Test Items</u>
Water content, %	30.1	27.3
Dry density, pcf	92.8	91.5
CBR	6.8	6.1
E_{RI} , ksi	7.1	--
Range	(3.1-10.4)	
M_R , ksi	--	8.0
Range		(5.8-11.0)

2. Effects of Traffic on Modulus Values

As in the comparison of basin parameters, items WES1 and NFF4 are the only test items with data within the range of the FWD transducers over all traffic applications. Changes in subgrade modulus with traffic, as back calculated from BISDEF, for items WES1 and NFF4 are shown in Figures IV-43 and IV-44. After the initial 10 coverages on each item, both plastic and elastic deformation probably occurred under the FWD impulse loading. Deflections from the FWD include both plastic or permanent deformation and elastic deformations and are not identified separately. The elastic layer model is not applicable when plastic deformation occurs.

Kelly (Reference 58) reported the difficulty with analyzing deflections that were composed of both resilient and permanent components. For ALRS pavements, particularly after traffic has been initiated, considerable permanent deformation is expected.

Base course modulus change for the two items is shown in Figures IV-45 and IV-46. The base course modulus is reduced significantly with

traffic and the change mirrors the change in ISM with coverages as shown in Figures IV-28 and IV-29.

Table IV-1. LAYER MODULUS VALUES BACK CALCULATED FROM FWD 9-KIP DATA USING BISDEF

ITEM	STATION FT	BACK CALCULATED MODULUS, PSI			AVG % DIFF. FROM MEASURED DEFLECTIONS
		SURFACE*	BASE	SUBGRADE	
WES1	10	300000	17666	11047	6.8
	20	300000	17000	9228	8.6
	30	300000	21170	10120	7.0
	40	100000	22116	8849	11.4
WES2	10	300000	12164	7447	11.8
	20	300000	13598	7467	11.6
	30	300000	12308	7103	16.8
	40	100000	20959	7927	12.0
WES3	10	300000	12970	6469	11.6
	20	300000	14003	5791	14.8
	30	300000	16188	6175	9.0
	40	300000	15199	7973	5.0
WP1	5	500000	770	29334	25.8
	15	500000	1284	26617	14.4
	25	500000	974	25152	18.2
WP2	5	424269	22653	32000	11.6
	15	363214	17166	30000	11.6
	25	381722	18213	30000	6.8
WP3	5	300000	9739	14221	17.4
	15	300000	9385	16979	16.0
	25	300000	9000	13871	26.6
WP4	5	300000	14131	18554	33.2
	15	300000	16958	23044	22.0
	25	300000	16652	23008	9.6
W1	5	300000	20082	16471	12.6
	15	300000	16930	16972	13.6
	25	300000	22035	17536	19.4
W2	5	300000	10135	8213	6.4
	15	300000	12012	8125	7.4
	25	300000	10710	9177	6.8

* Surface modulus values were allowed to vary between 100,000 and 300,000 psi except when testing was conducted at lower temperatures. Then, the upper limit was set at 500,000 psi.

Table IV-1. LAYER MODULUS VALUES BACK CALCULATED
FROM FWD 9-KIP DATA USING BISDEF (CONCLUDED)

<u>ITEM</u>	<u>STATION FT</u>	<u>BACK CALCULATED MODULUS, PSI</u>			<u>AVG % DIFF. FROM MEASURED DEFLECTIONS</u>
		<u>SURFACE*</u>	<u>BASE</u>	<u>SUBGRADE</u>	
W3	5	100673	12467	11556	3.4
	15	300000	10963	11375	3.2
	25	288293	10742	12527	0.4
NFF4	25	125898	18177	35548	3.0
	50	142322	17283	30126	4.4
	75	190633	18189	33612	4.0

* Surface modulus values were allowed to vary between 100,000 and 300,000 psi except when testing was conducted at lower temperatures. Then, the upper limit was set at 500,000 psi.

Table IV-2. STRESSES AND STRAINS FOR F-4 LOADING

ITEM	STATION FT	ASPHALT STRAIN 10E-06 IN	BASE COURSE		BASE COURSE		BASE COURSE		BASE COURSE		SUBGRADE	
			VERT STRESS PSI	VERT STRAIN 10E-06 IN	SHEAR STRESS PSI	TENSILE STRESS 10E-06 IN/IN	VERT STRESS PSI	TENSILE STRESS 10E-06 IN/IN	VERT STRESS PSI	VERT STRAIN 10E-06 IN/IN		
WES1	10	1860	223	9860	58.2	26.9	63.9	5710				
	20	1940	220	10200	58.9	34.8	60.2	6480				
	30	1580	228	8420	63.6	43.5	58.7	5780				
	40	1120	254	8370	80.0	59.3	61.2	6840				
WES2	10	2390	234	14600	57.8	27.2	59.6	7970				
	20	2150	238	13200	60.4	33.5	57.8	7730				
	30	2370	235	14400	58.4	30.5	58.4	8190				
	40	7260	263	8610	82.2	60.1	56.3	7050				
WES3	10	126	271	12900	80.9	45.3	65.4	10100				
	20	244	270	11800	83.2	57.9	60.7	10500				
	30	354	270	9990	85.1	63.6	59.0	9560				
	40	207	270	10800	81.9	41.9	67.2	8390				
WP1	5	2810	39	27500	0.3	22.9	34.6	719				
	15	2550	48	21000	0.9	27.0	41.2	1000				
	25	2700	43	24200	0.6	24.6	37.3	932				
WP2	5	1290	135	5100	32.8	0.5	4.9	154				
	15	1610	129	6410	30.8	1.0	5.2	170				
	25	1520	129	6070	31.0	1.0	5.1	169				
WP3	5	2880	173	14200	37.5	6.8	45.8	3090				
	15	2940	172	14600	36.3	11.1	47.9	2670				
	25	3020	169	15000	36.0	7.9	45.9	3160				
WP4	5	2230	192	10900	44.1	4.5	46.7	2440				
	15	1950	201	9480	47.0	5.4	48.1	2020				
	25	1980	200	9620	46.6	5.8	48.2	2030				

Table IV-2. STRESSES AND STRAINS FOR F-4 LOADING (CONCLUDED)

ITEM	STATION FT	ASPHALT STRAIN 10E-06 IN	BASE COURSE		BASE COURSE		BASE COURSE		SUBGRADE	
			VERT STRESS PSI	VERT STRAIN 10E-06 IN	SHEAR STRESS PSI	TENSILE STRESS 10E-06 IN/IN	VERT STRESS PSI	VERT STRAIN 10E-06 IN/IN		
W1	5	870	272	9370	68.5	2.7	11.7	720		
	15	1120	271	11200	66.4	1.1	12.4	737		
	25	755	272	8510	69.7	3.0	11.6	672		
W2	5	2620	138	11300	32.4	6.6	32.3	3890		
	15	2380	146	10200	35.7	11.5	31.1	3820		
	25	2530	141	10900	33.1	5.4	33.2	3570		
W3	5	3120	203	13500	53.7	3.5	27.3	2360		
	15	2480	143	10800	33.0	1.1	25.0	2180		
	25	2550	144	11100	33.1	-0.6	25.9	2040		
NFF4	25	2010	237	10300	54.6	-33.6	115.0	3160		
	50	2090	231	10600	52.9	-29.5	111.0	3510		
	75	1930	222	9690	48.8	-31.1	109.0	3080		

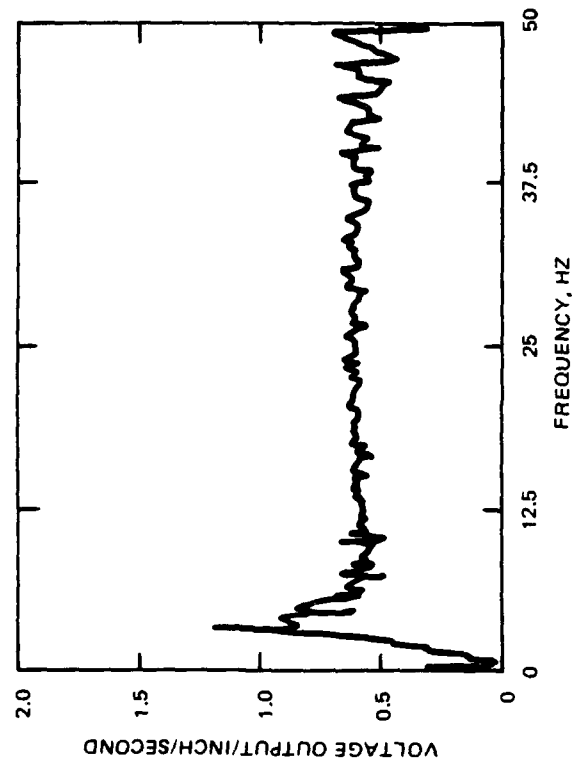


Figure IV-1. FWD Velocity Transducer Response.

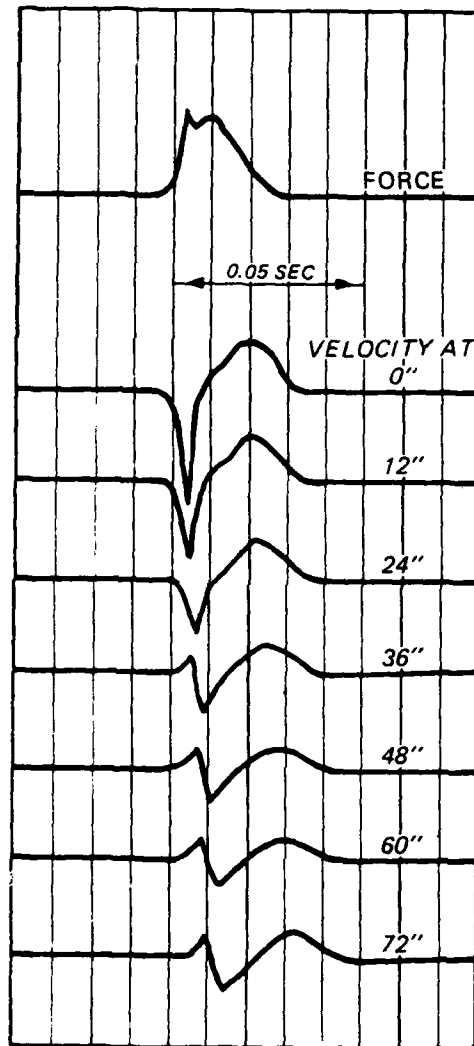


Figure IV-2. Time History Output from FWD Load Cell and Velocity Transducers.

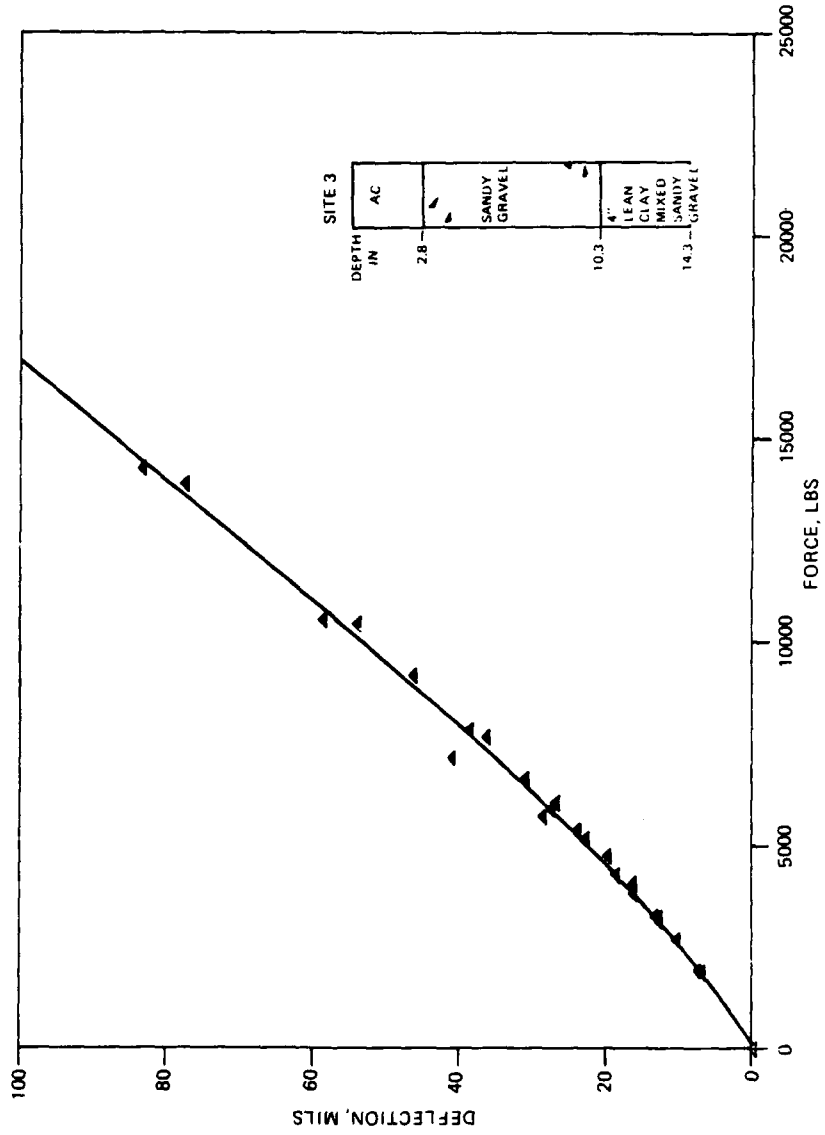


Figure IV-3. Load-Deflection Response of FWD Over Full Range of Deflections.

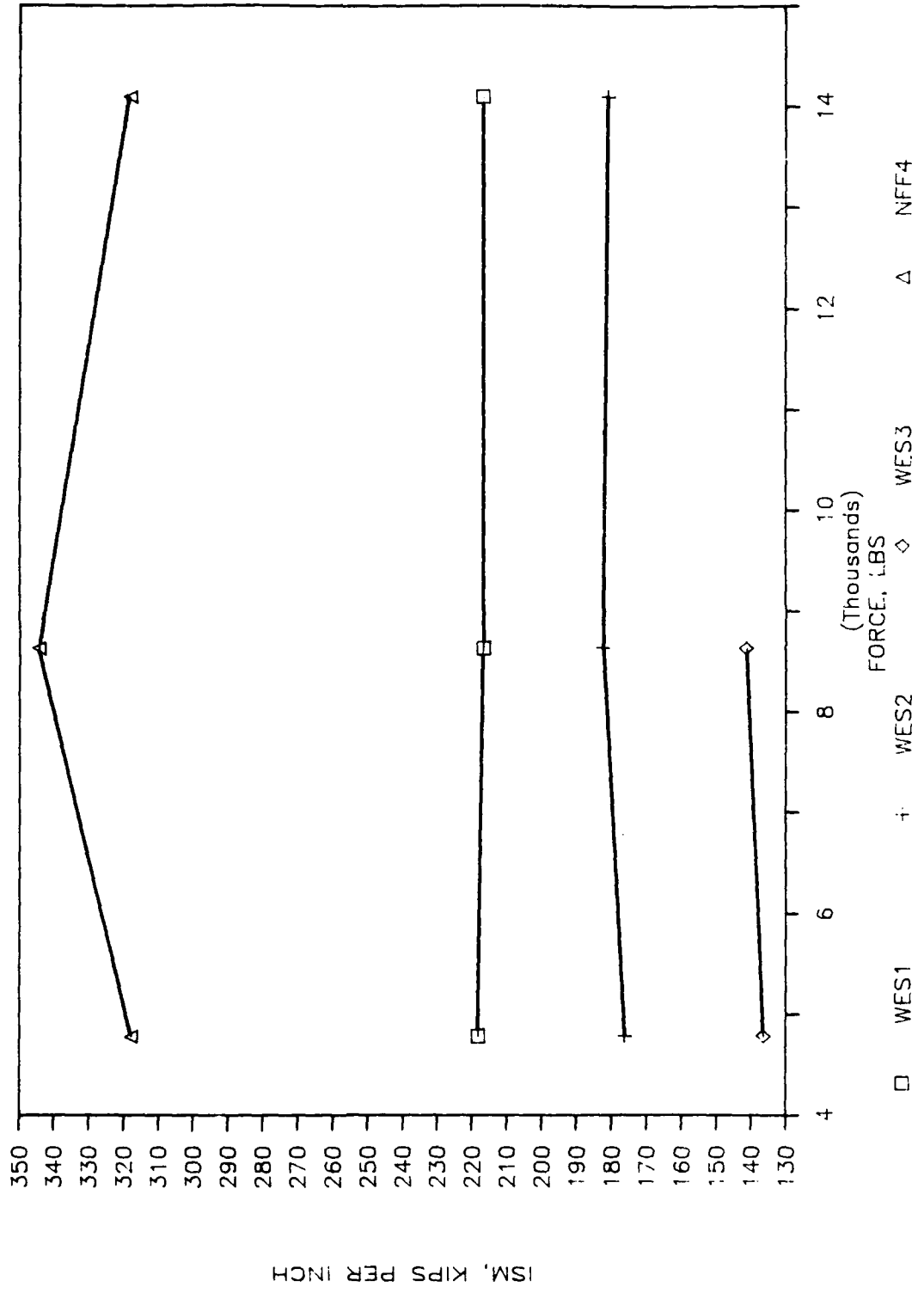


Figure IV-4. ISM/Force Relationship on WES and NFF4 Items.

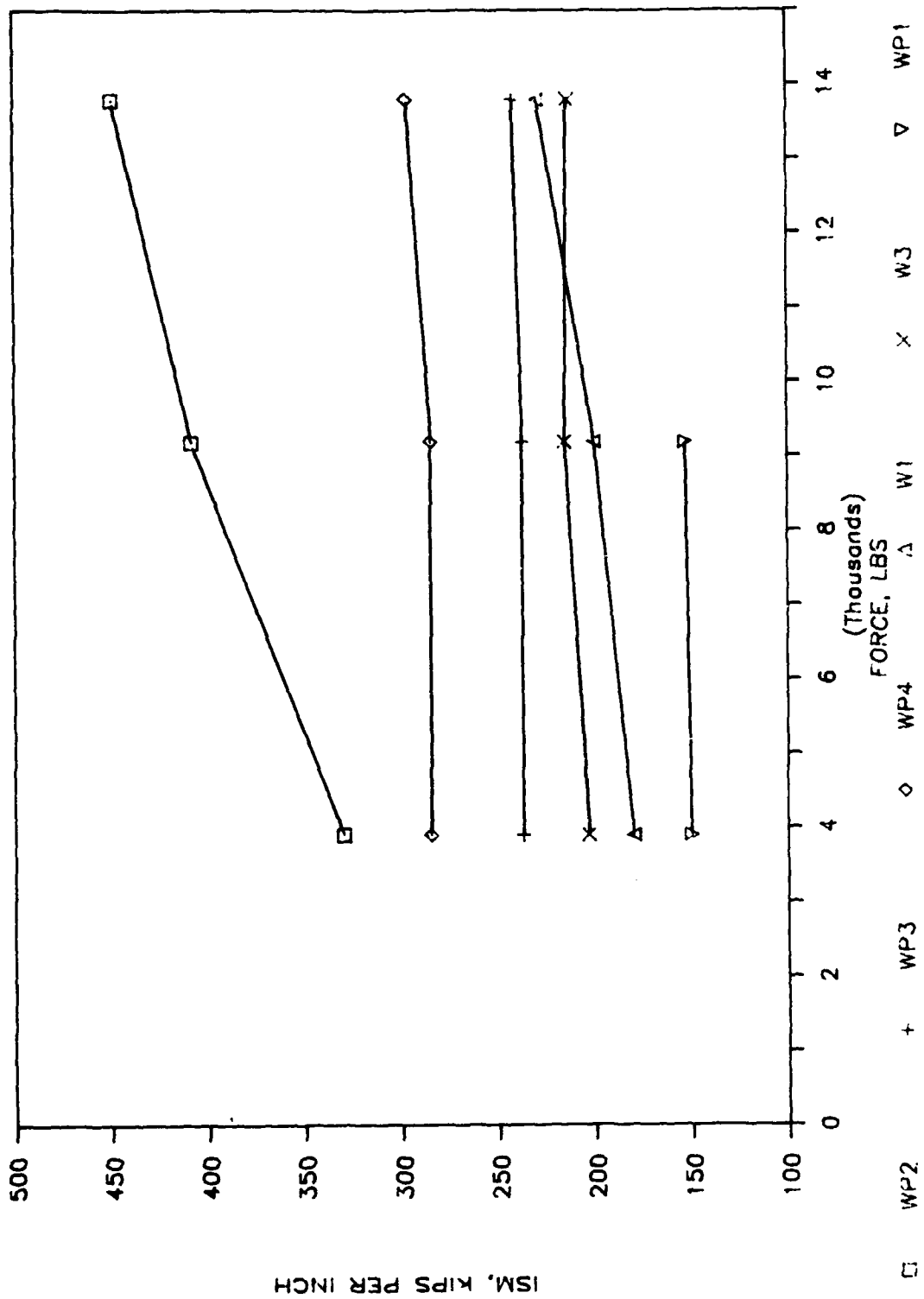


Figure IV-5. ISM/Force Relationship on Wright-Patterson and Whiteman AFB Items.

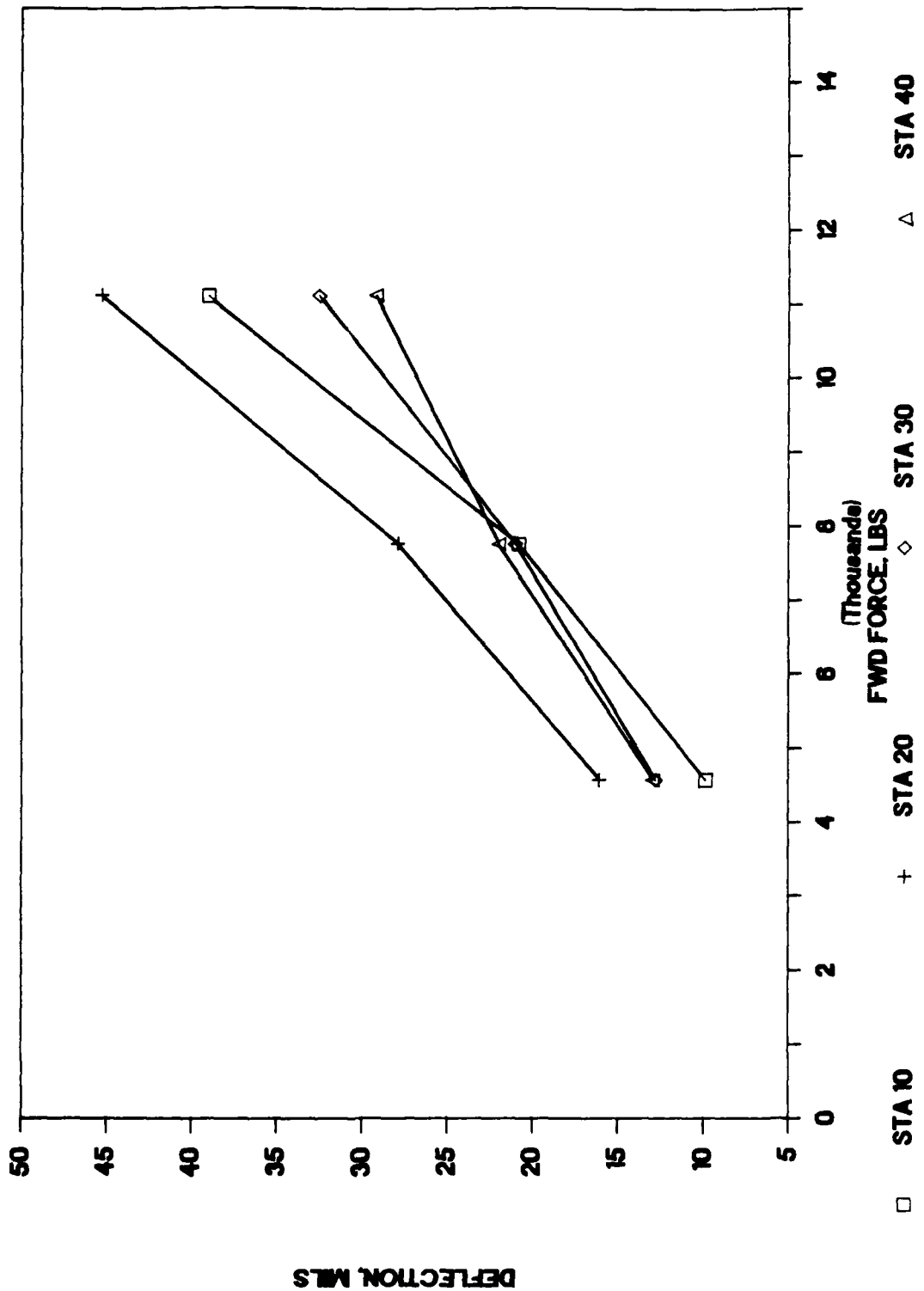


Figure IV-6. Load/Deflection Response on WES Test Item Clay Subgrade.

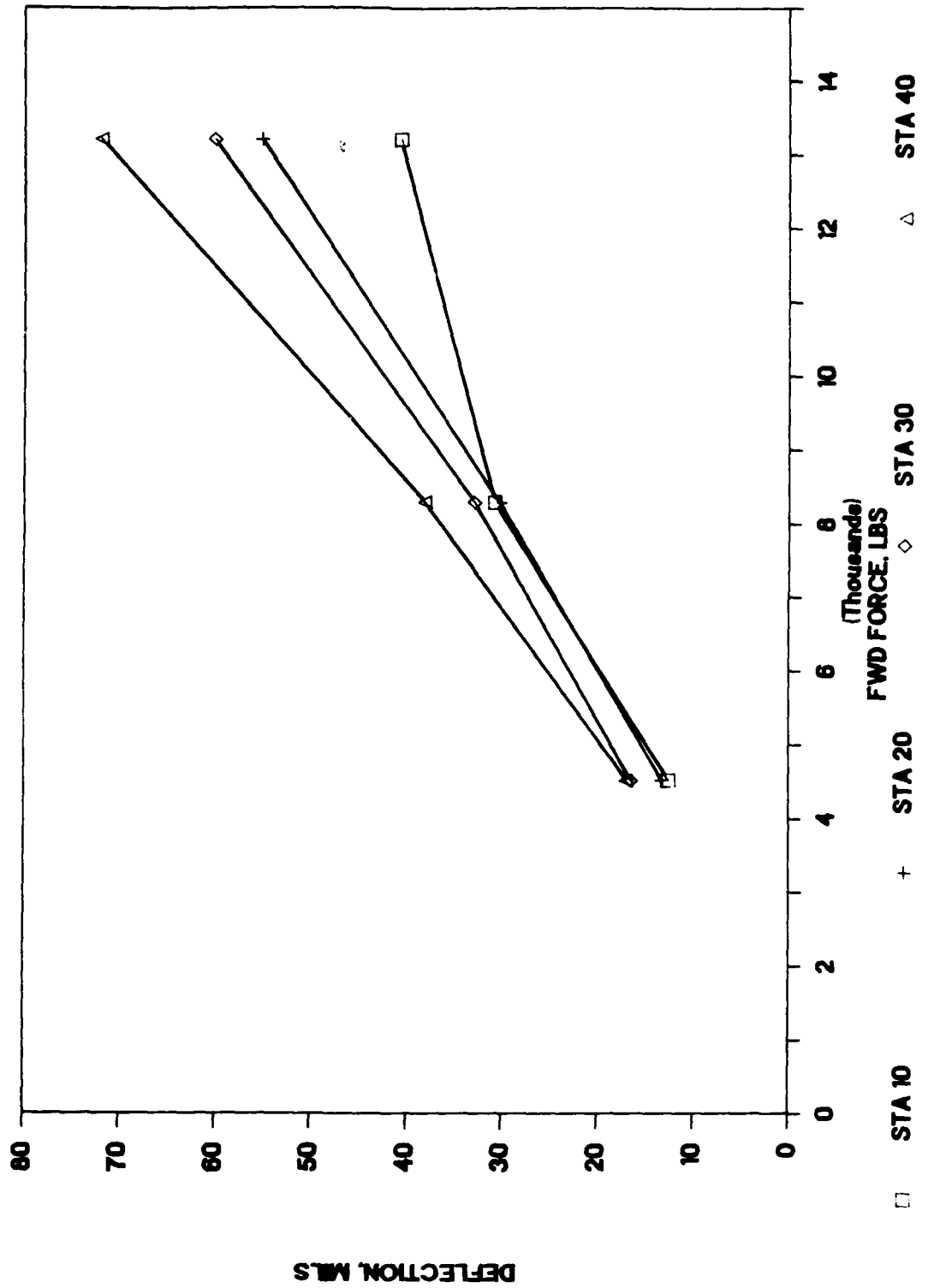


Figure IV-7. Load/Deflection Response on WES Test Item Base Course.

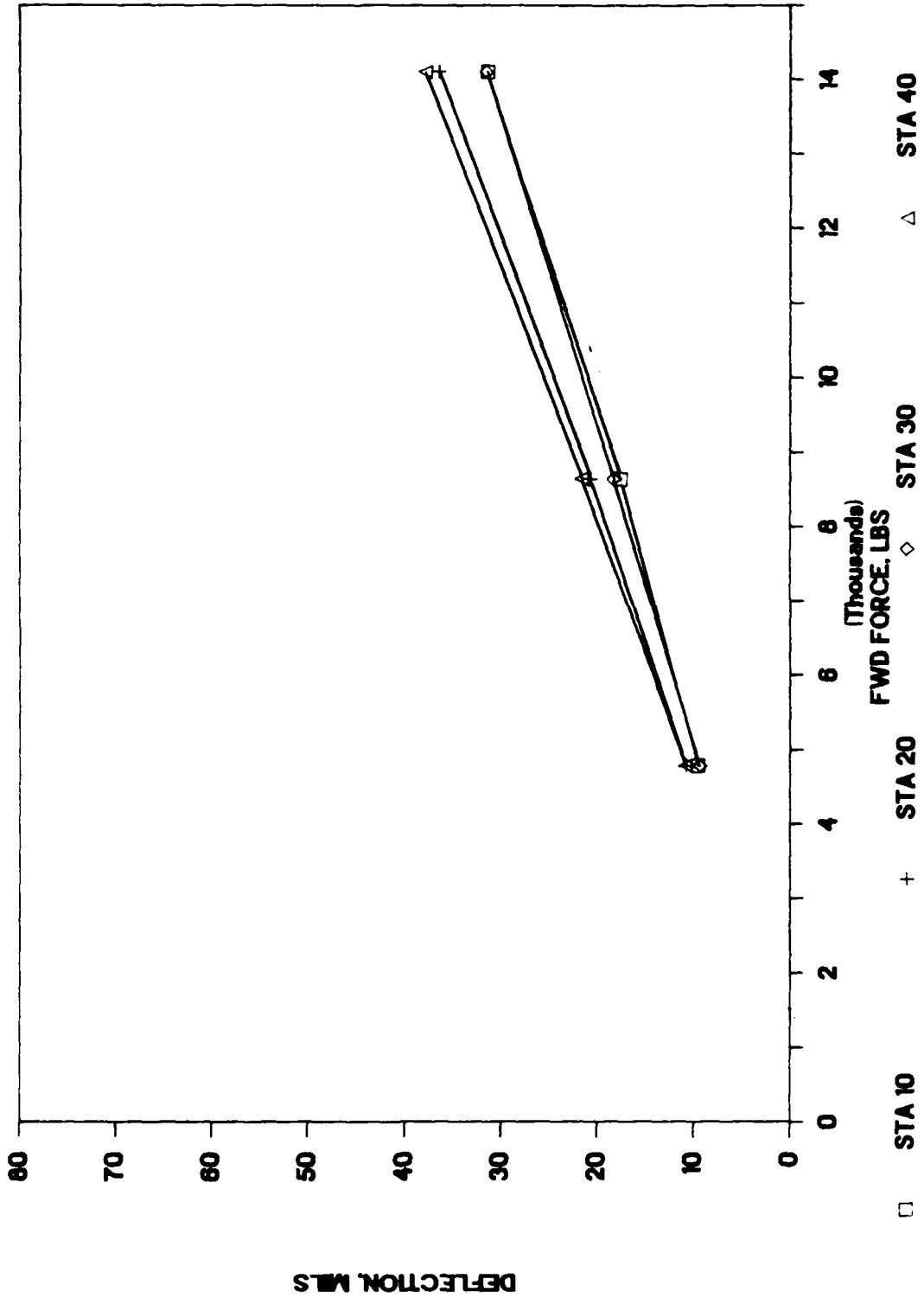


Figure IV-8. Load/Deflection Response on WES 1 Pavement.

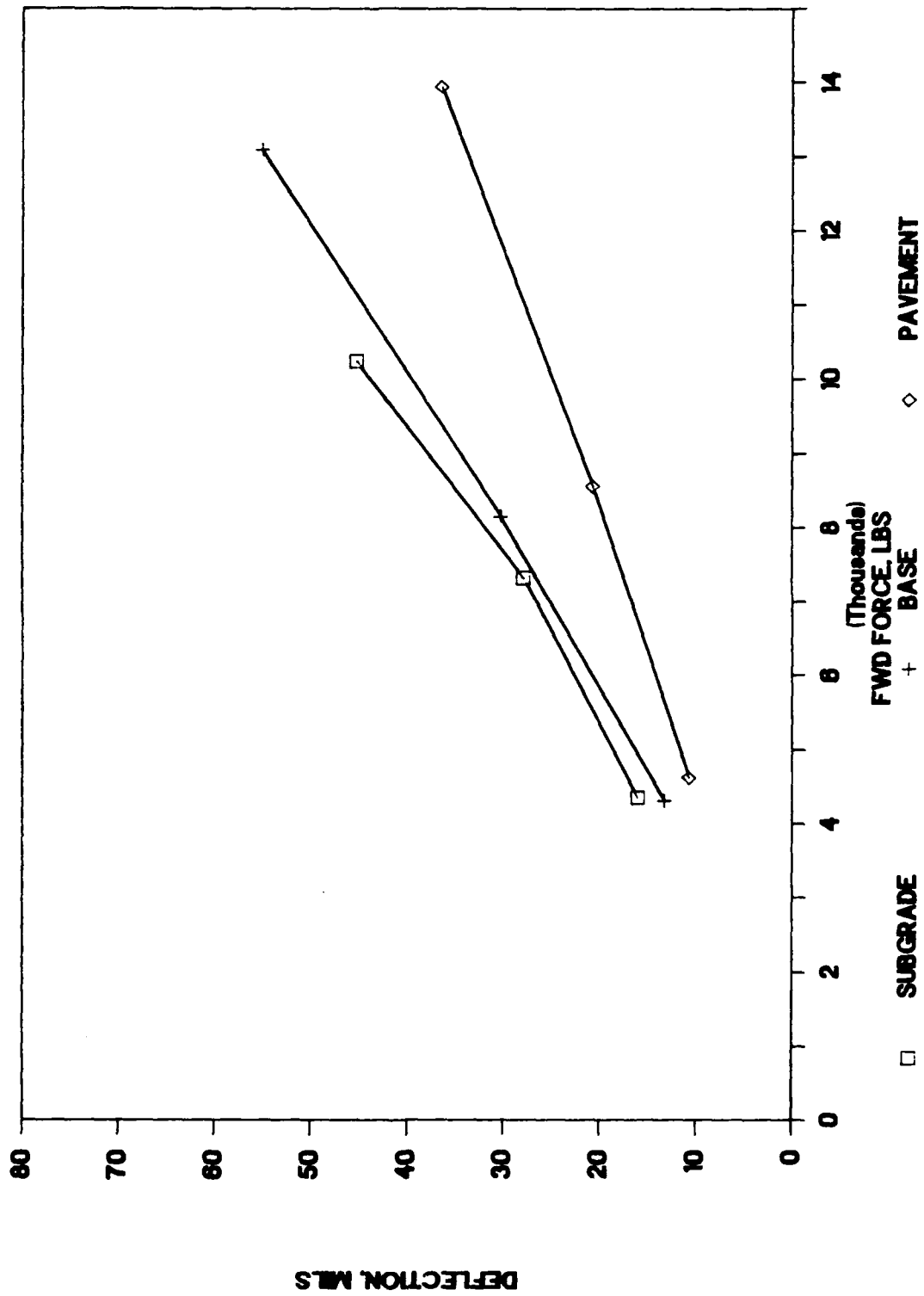


Figure IV-9. Response on WES1 from Subgrade, Base, and Pavement.

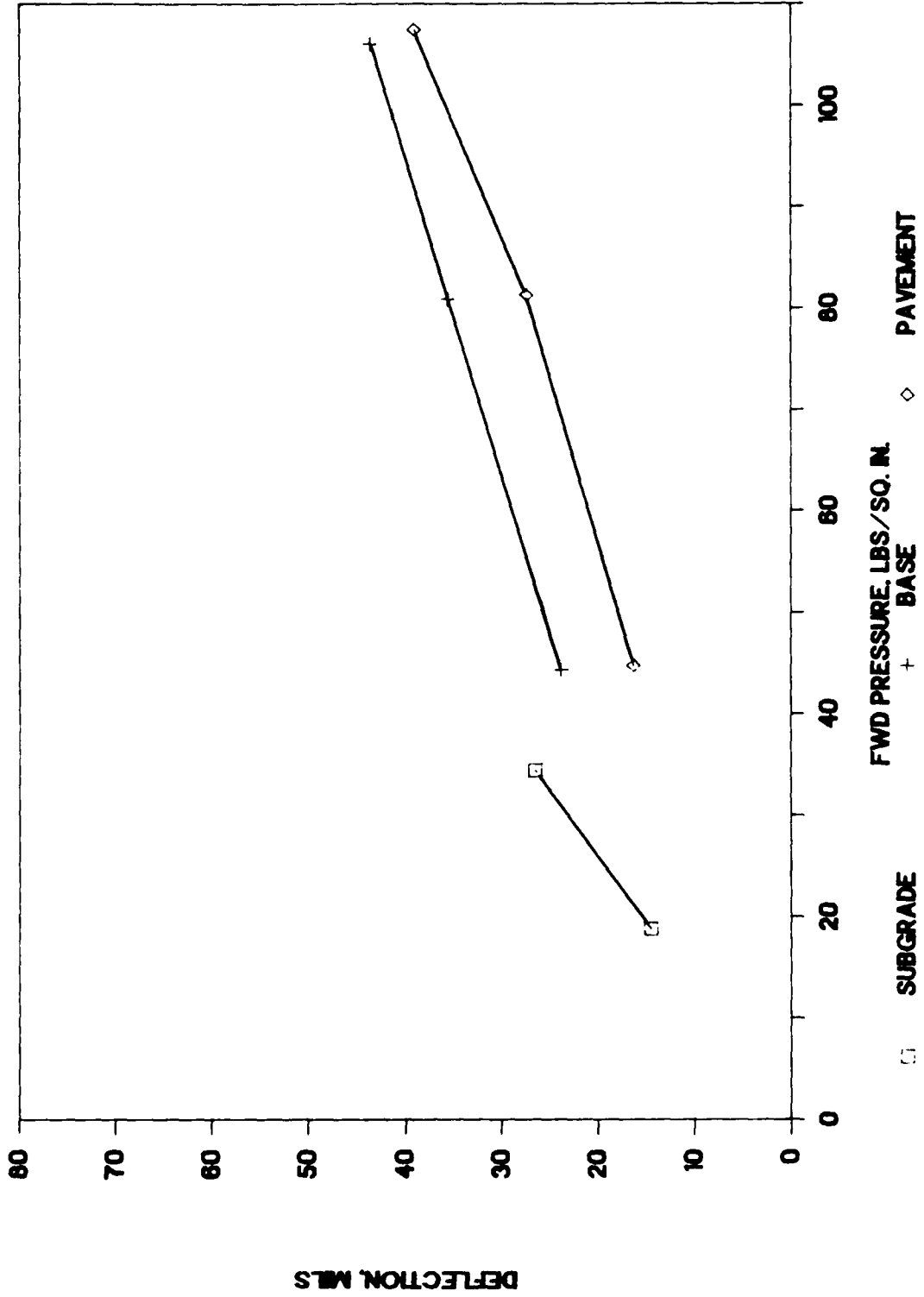


Figure IV-10. Response on NFF4 from Subgrade, Base, and Pavement.

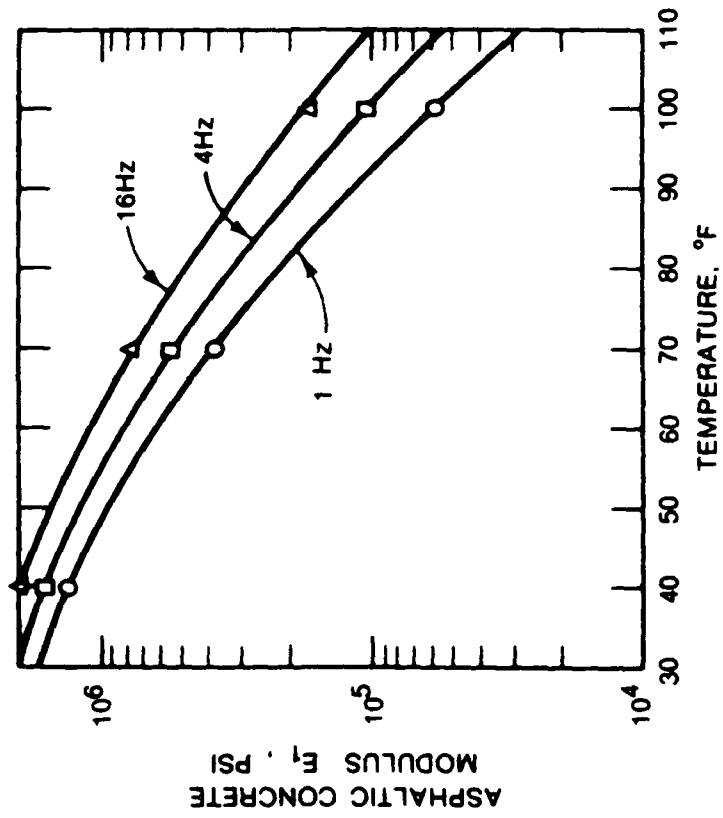


Figure IV-11. Modulus-Temperature Relationships for Asphaltic Concrete (Reference 54).

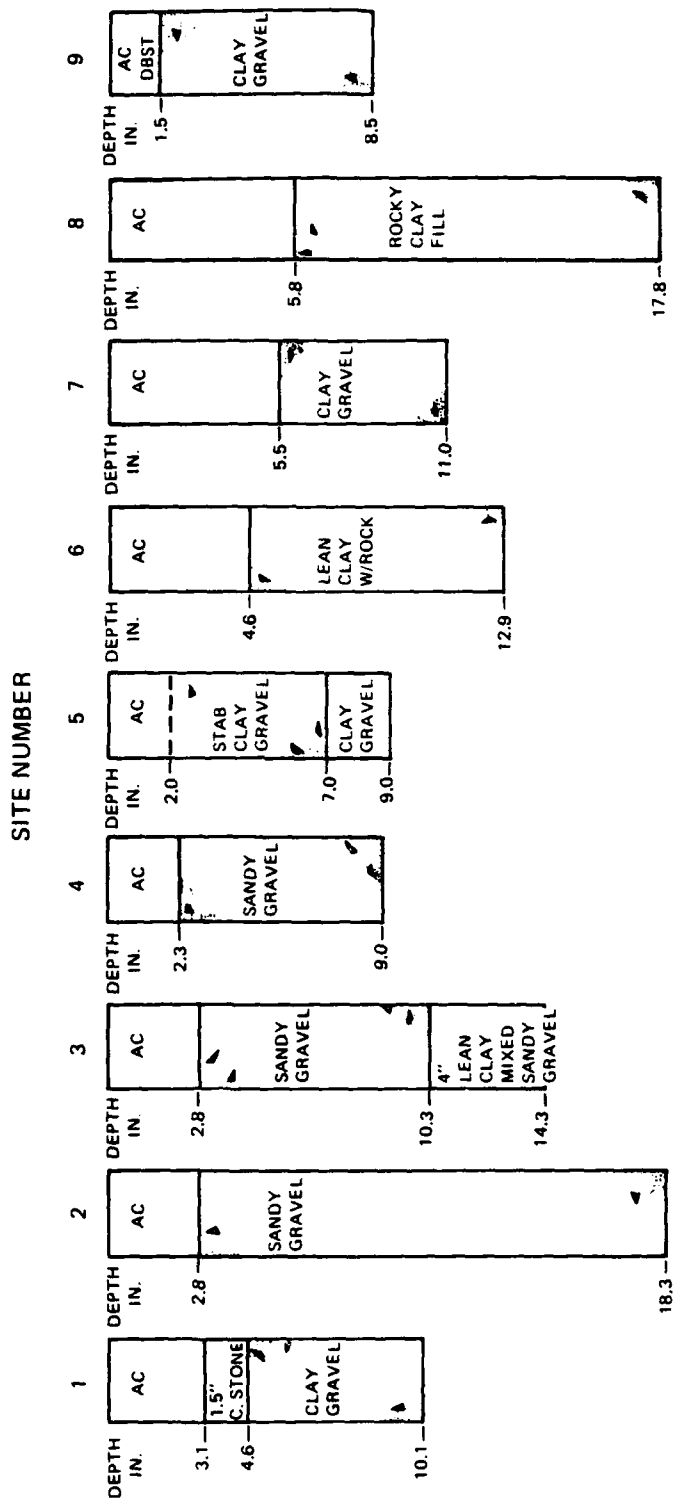


Figure IV-12. Structure of Temperature Test Site.

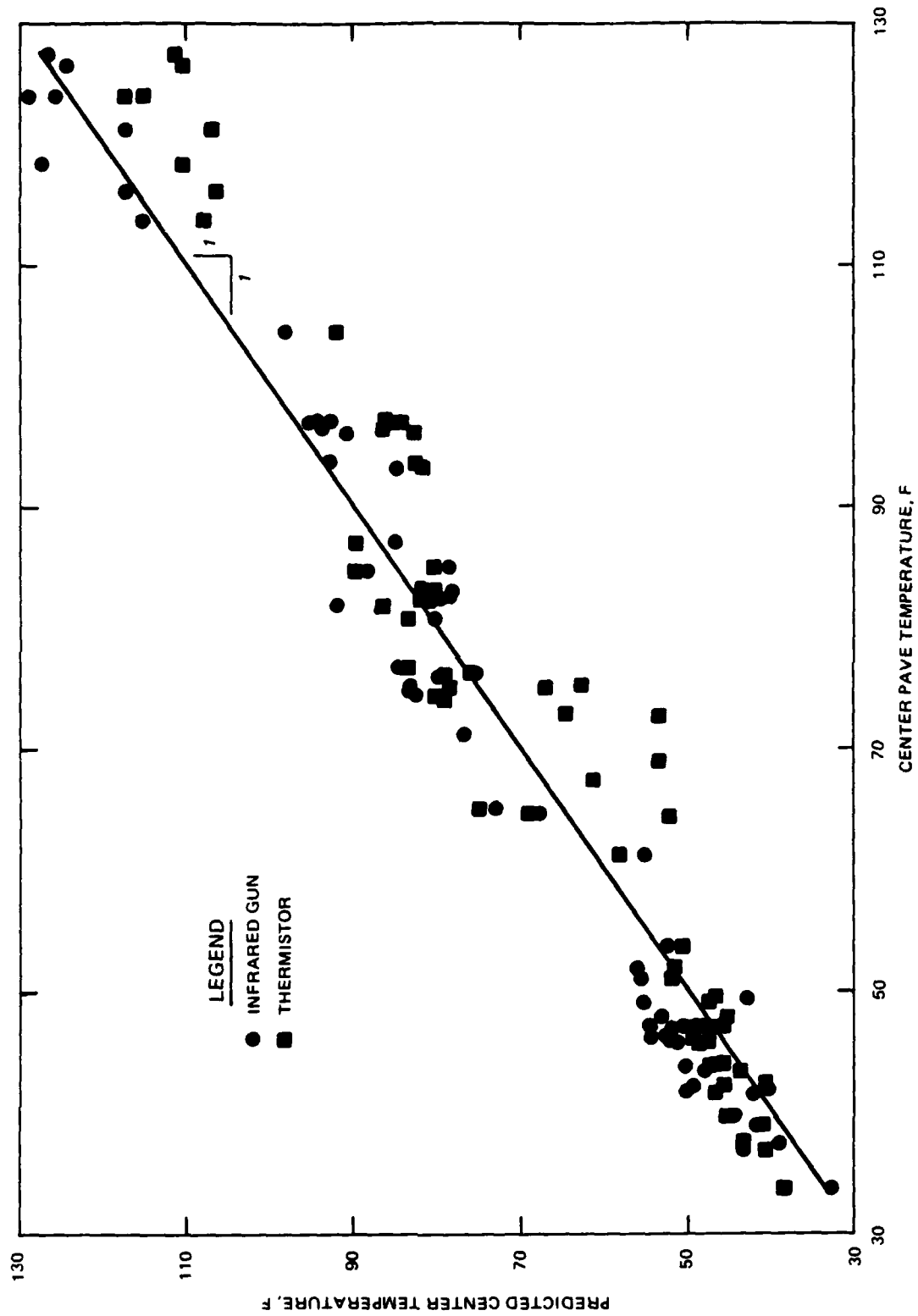


Figure IV-13. Comparison of Predicted to Measured Mean Pavement Temperature.

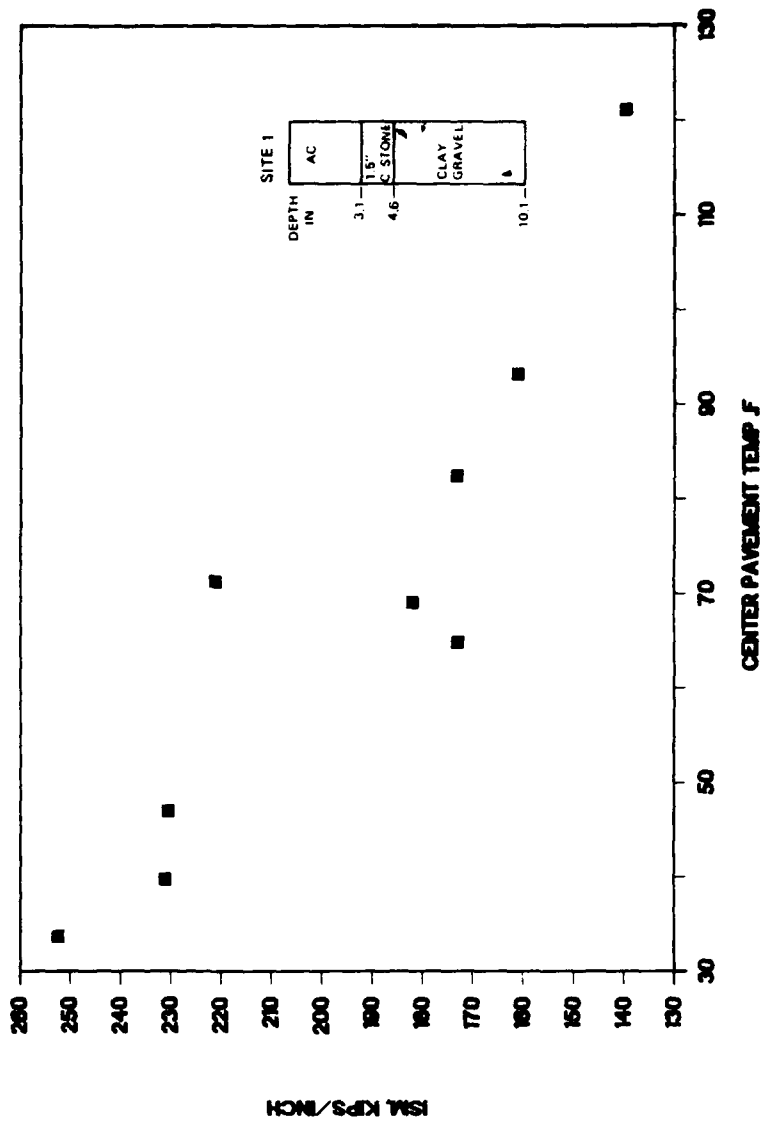


Figure IV-14. Stiffness Values for Temperature Site 1.

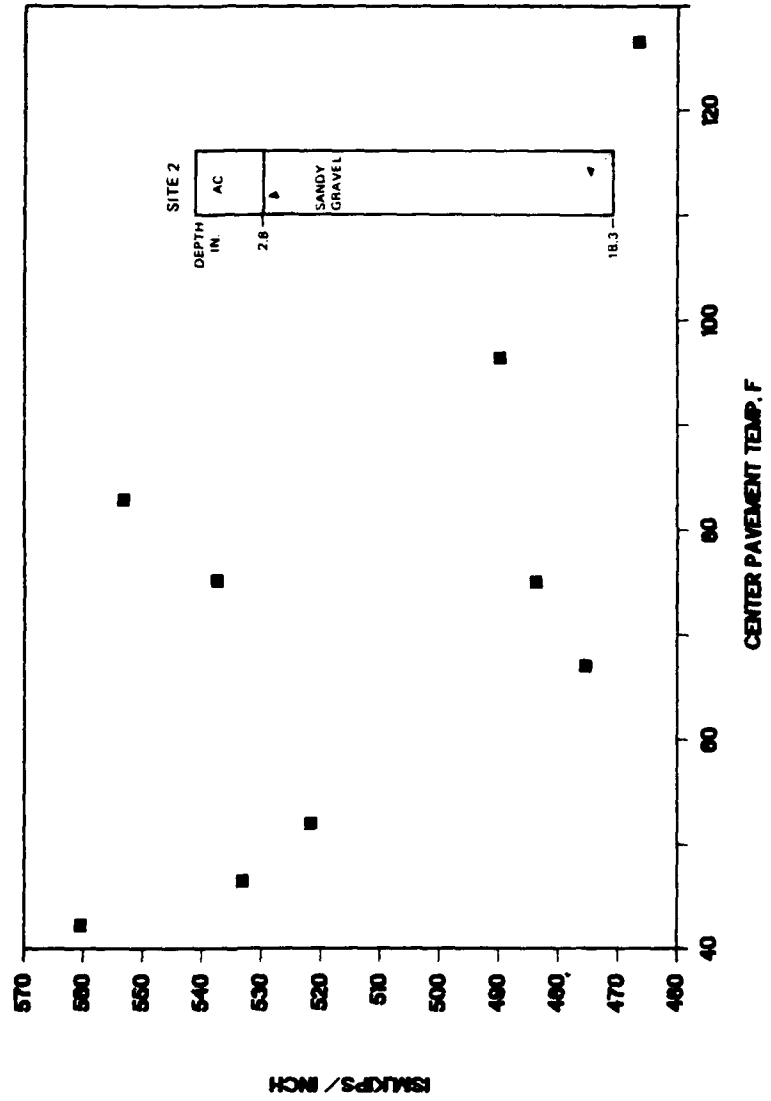


Figure IV-15. Stiffness Values for Temperature Site 2.

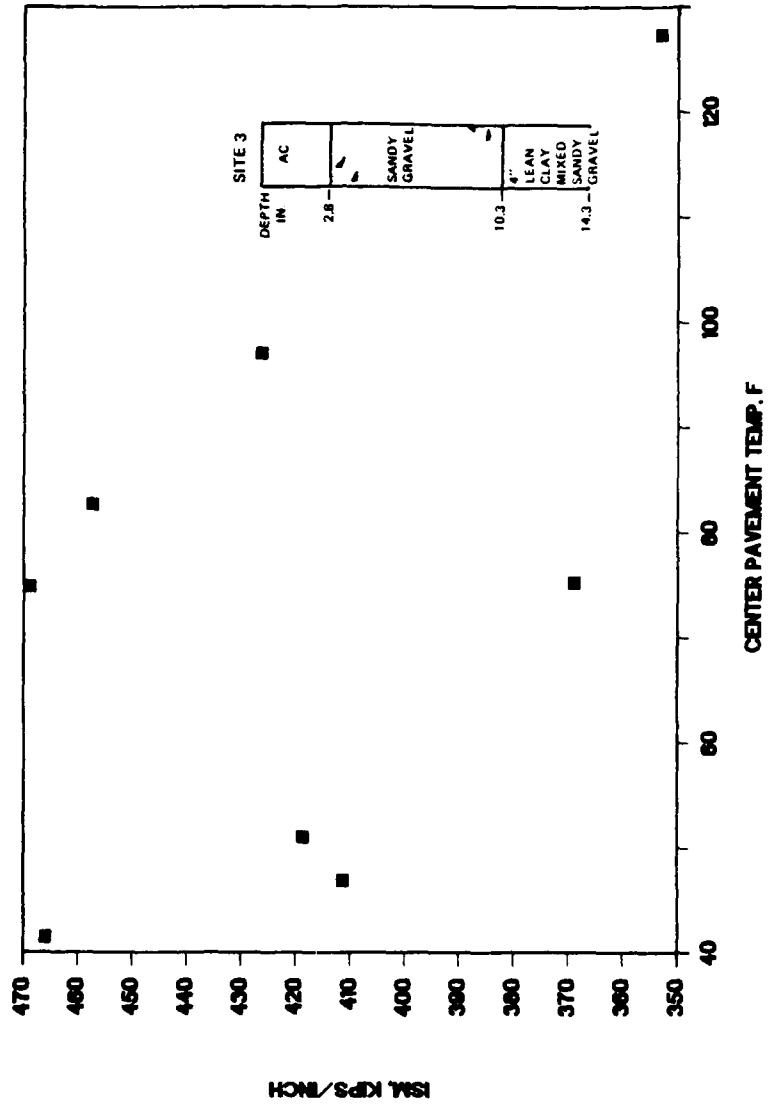


Figure IV-16. Stiffness Values for Temperature Site 3.

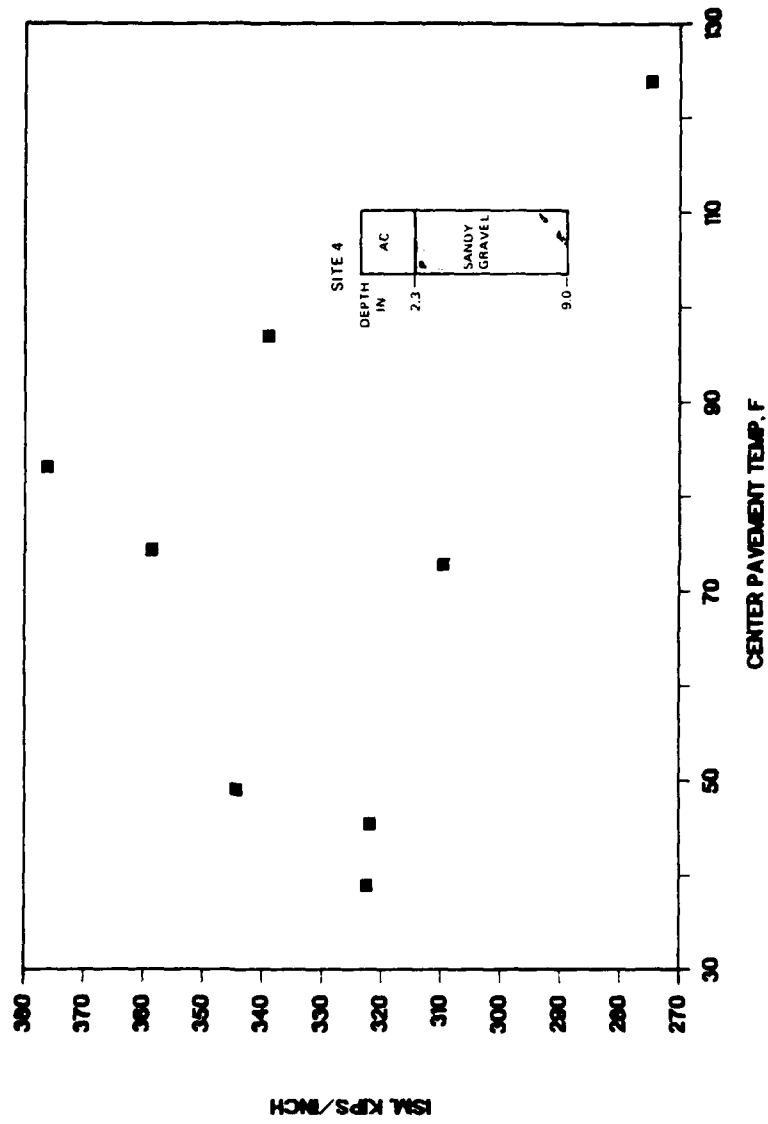


Figure IV-17. Stiffness Values for Temperature Site 4.

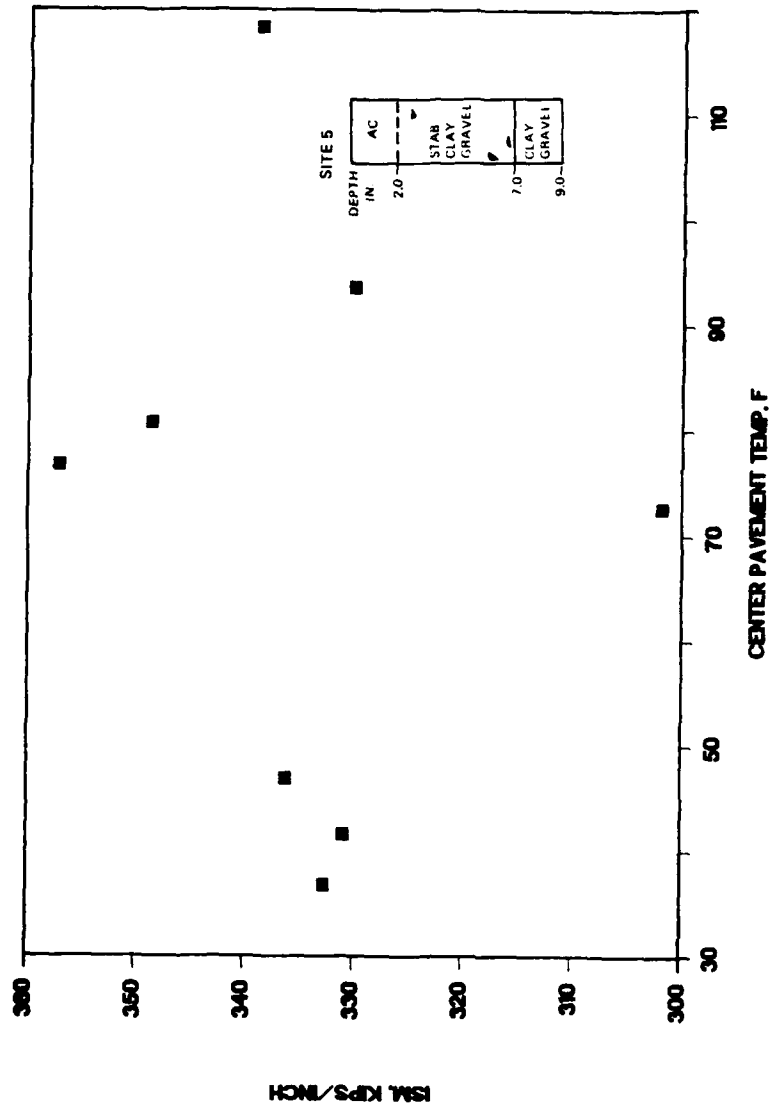


Figure IV-18. Stiffness Values for Temperature Site 5.

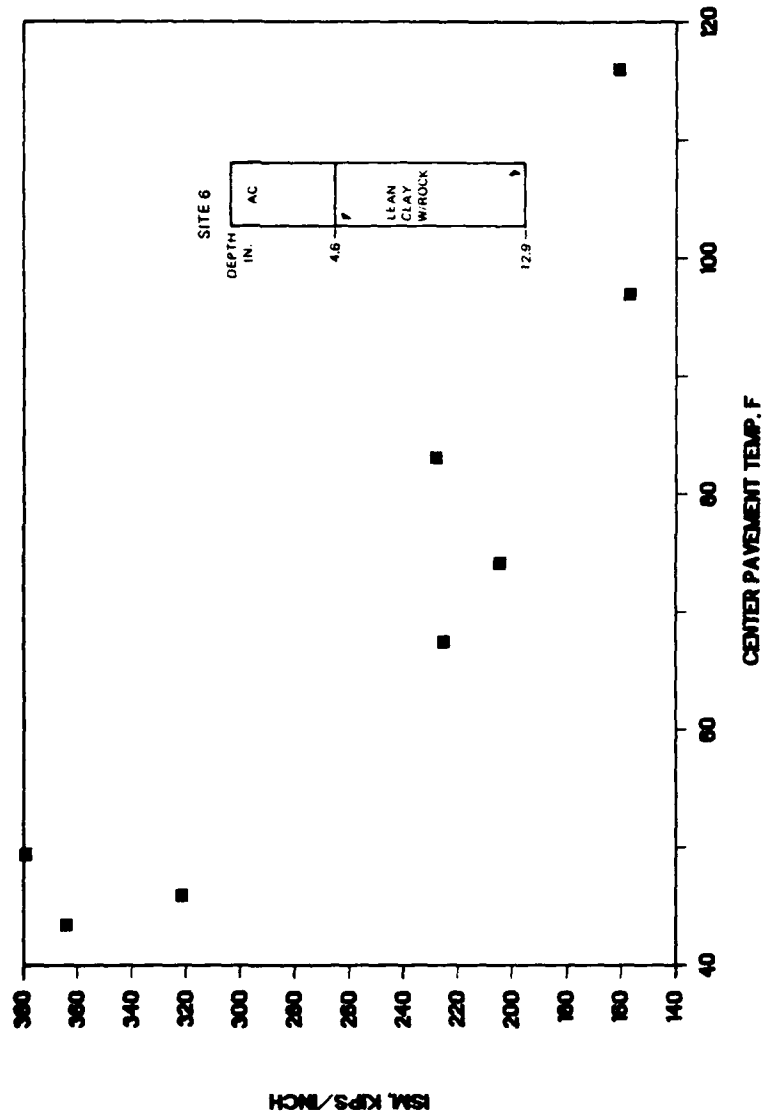


Figure IV-19. Stiffness Values for Temperature Site 6.

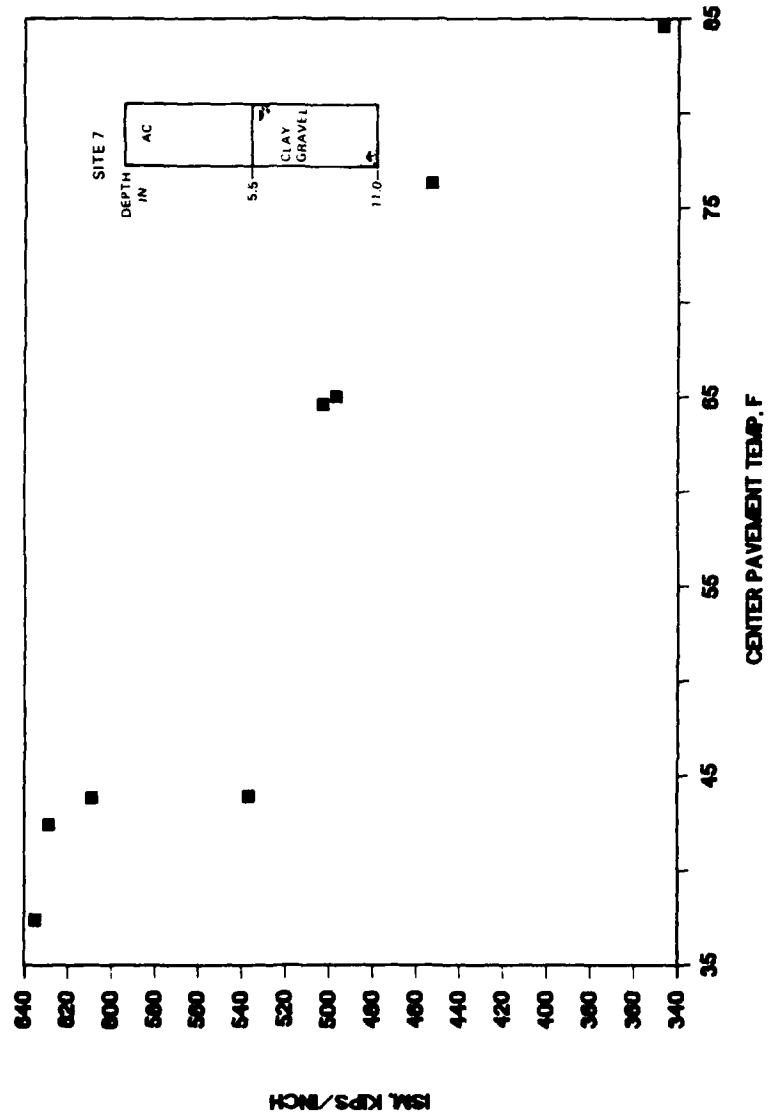


Figure IV-20. Stiffness Values for Temperature Site 7.

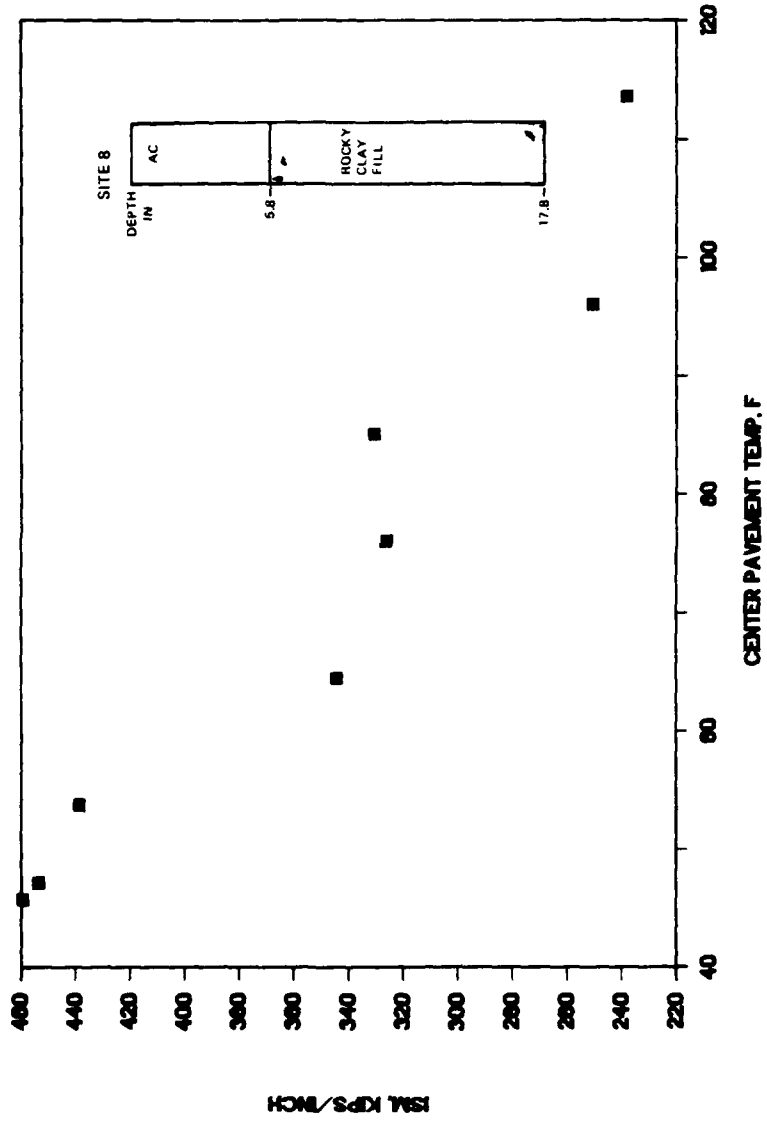


Figure IV-21. Stiffness Values for Temperature Site 8.

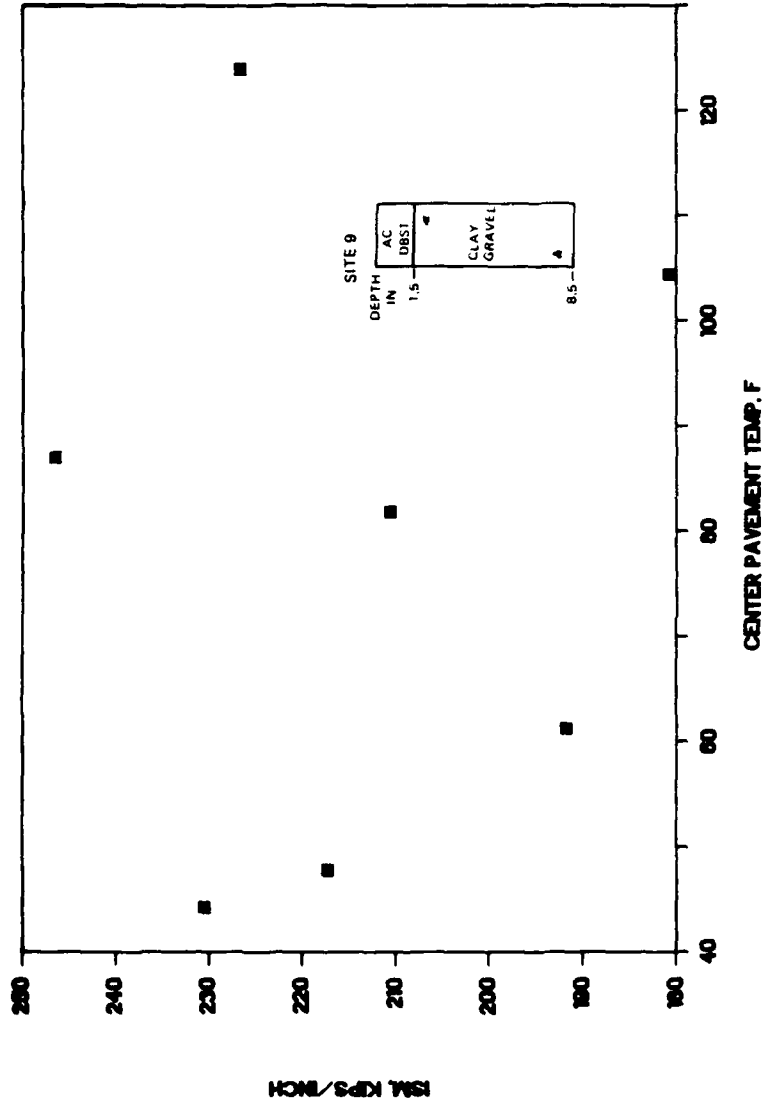


Figure IV-22. Stiffness Values for Temperature Site 9.

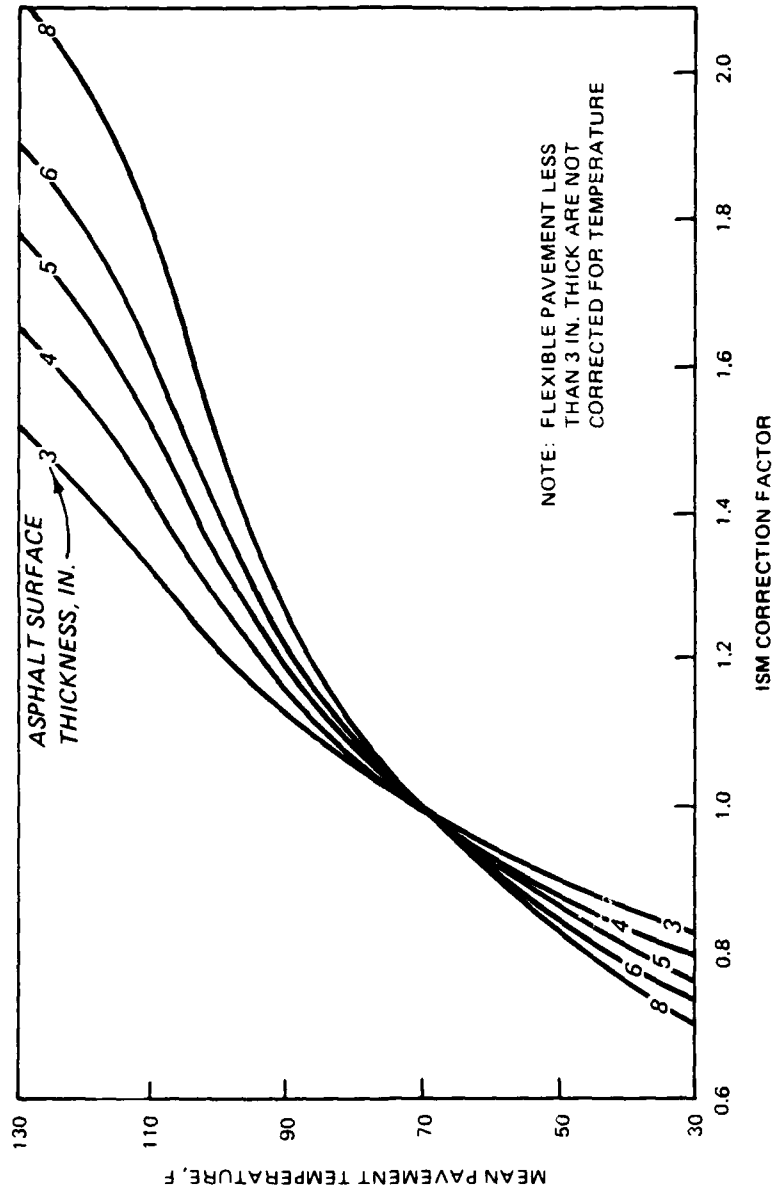


Figure IV-23. Falling Weight Deflectometer ISM Temperature Correction Factors.

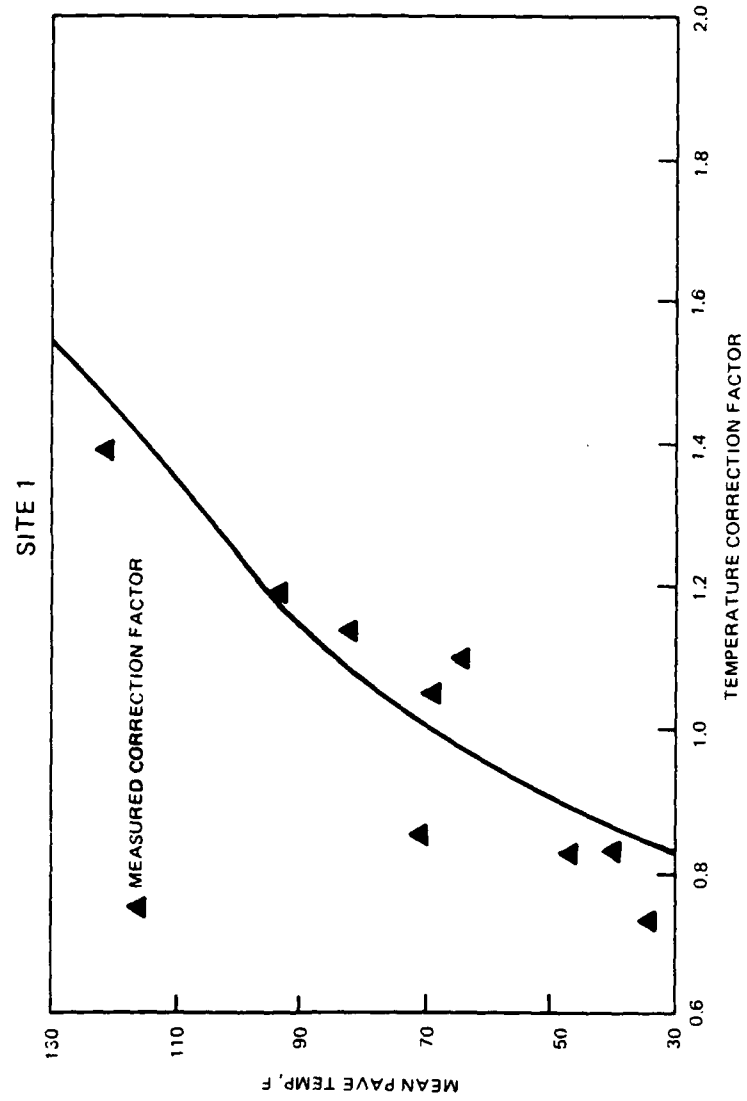


Figure IV-24. Temperature Factors for Site 1.

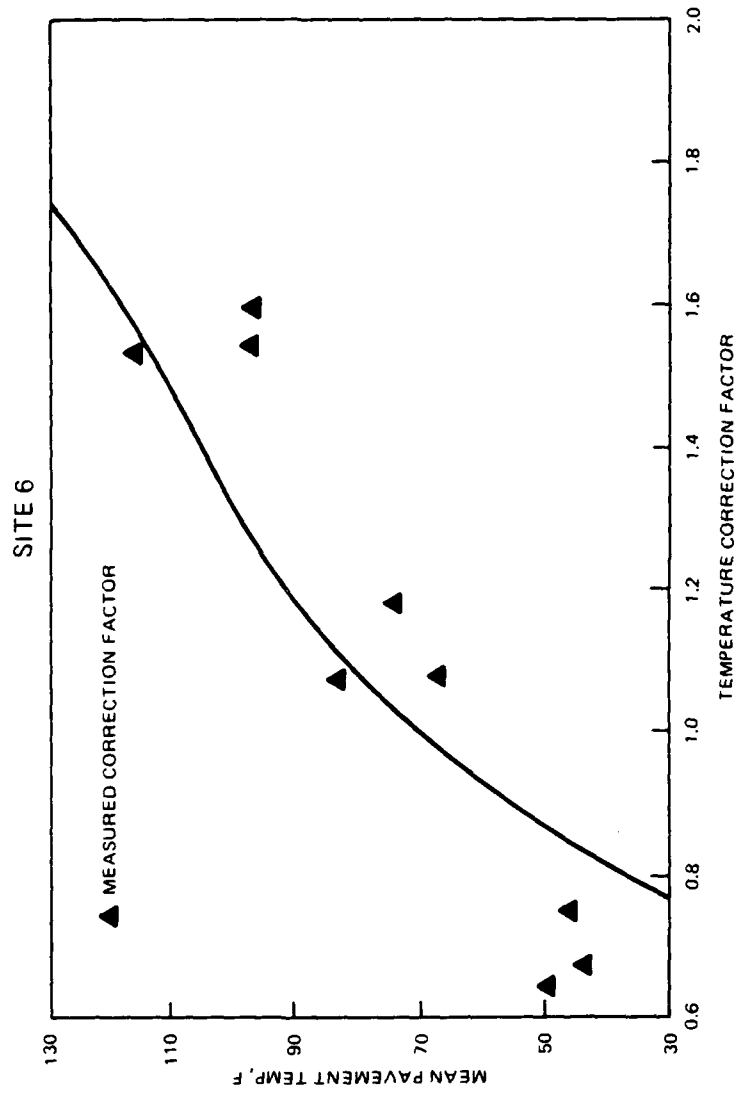


Figure IV-25. Temperature Factors for Site 6.

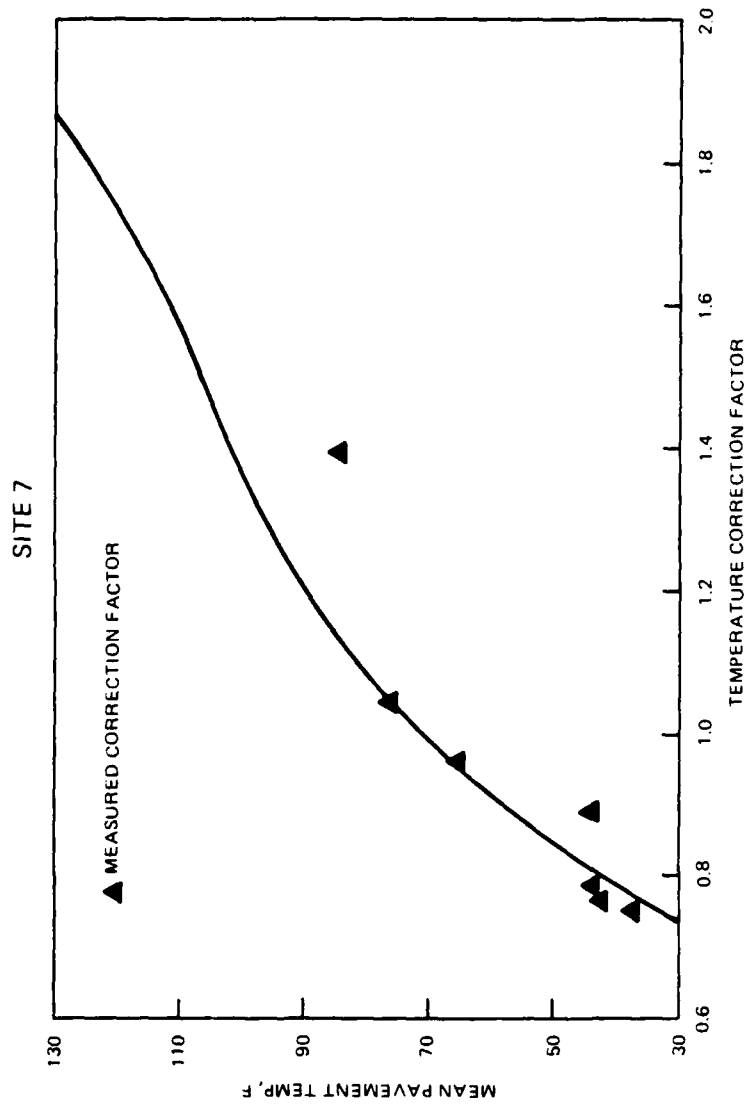


Figure IV-26. Temperature Factors for Site 7.

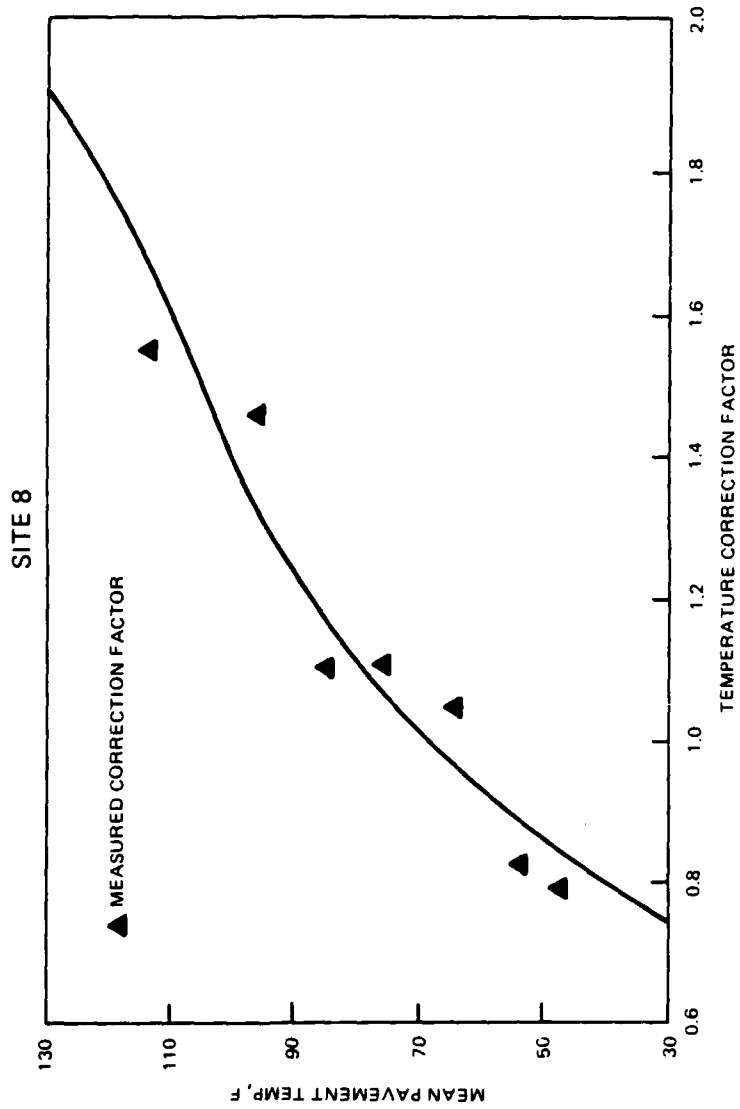


Figure IV-27. Temperature Factors for Site 8.

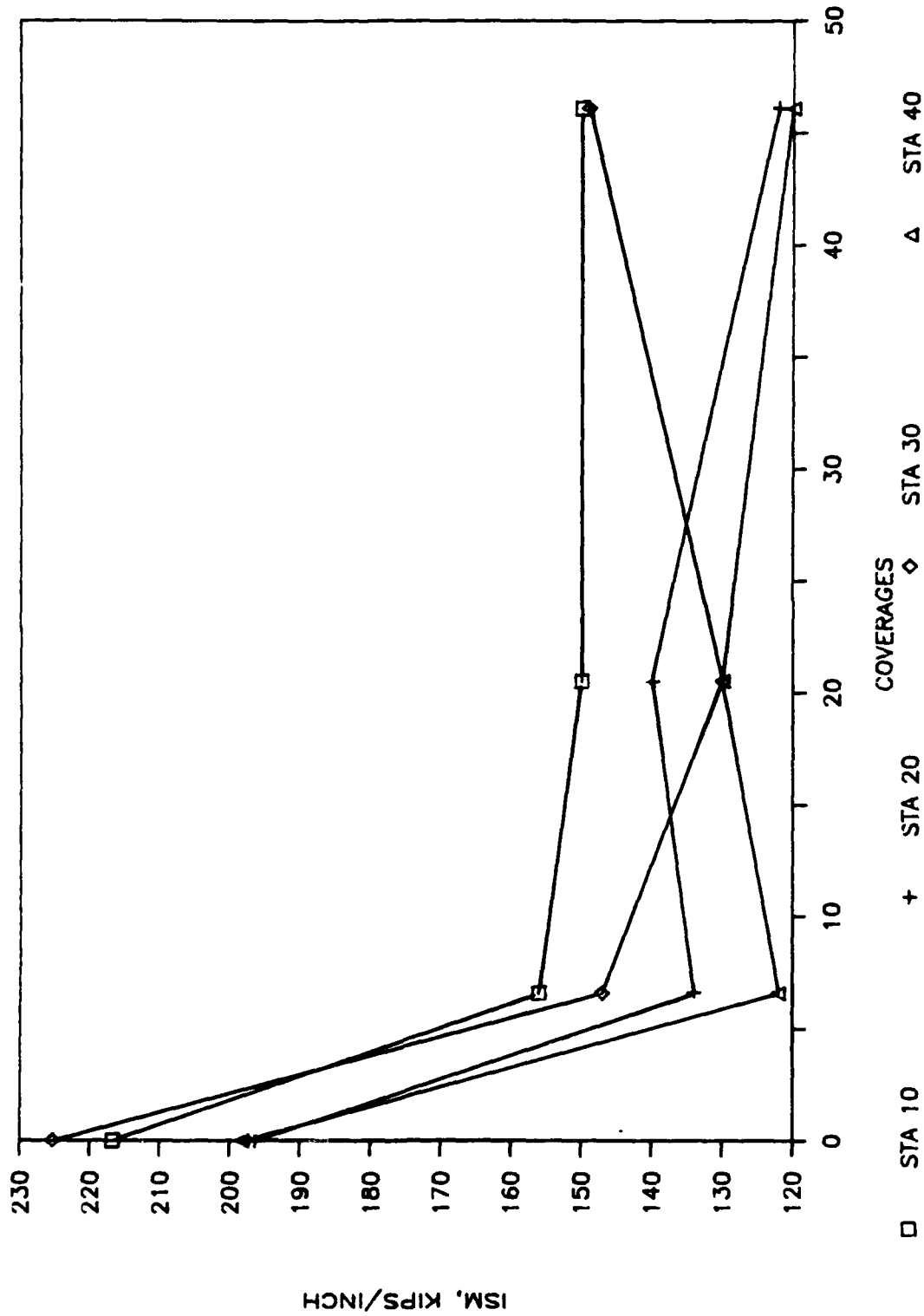


Figure IV-28. ISM versus Coverages for WES1 Item.

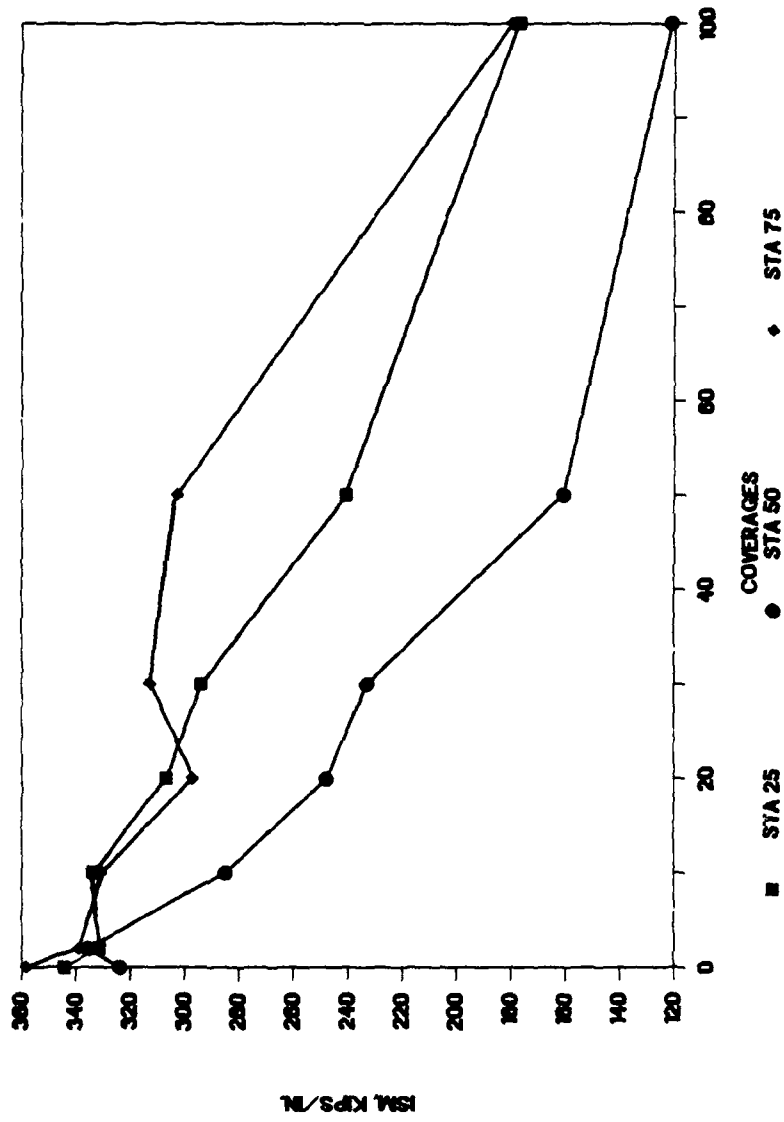


Figure IV-29. ISM versus Coverages for NFF4 Item.

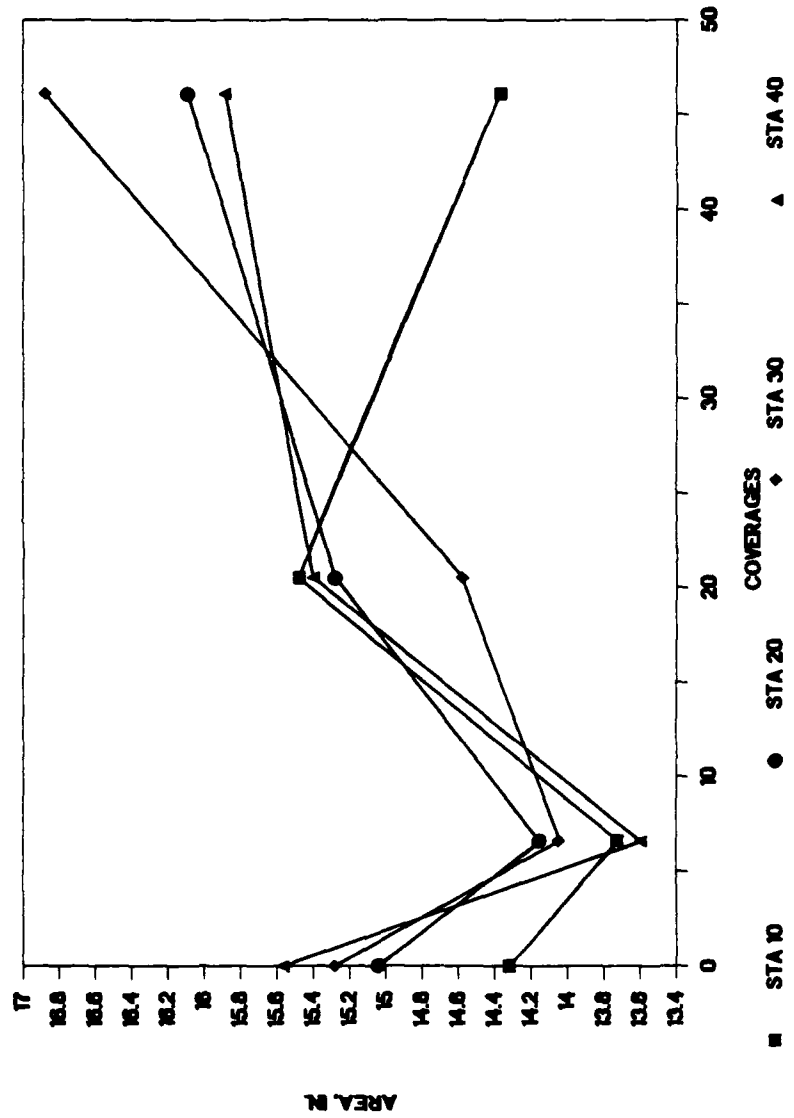


Figure IV-30. Area versus Coverages for WES1 Item.

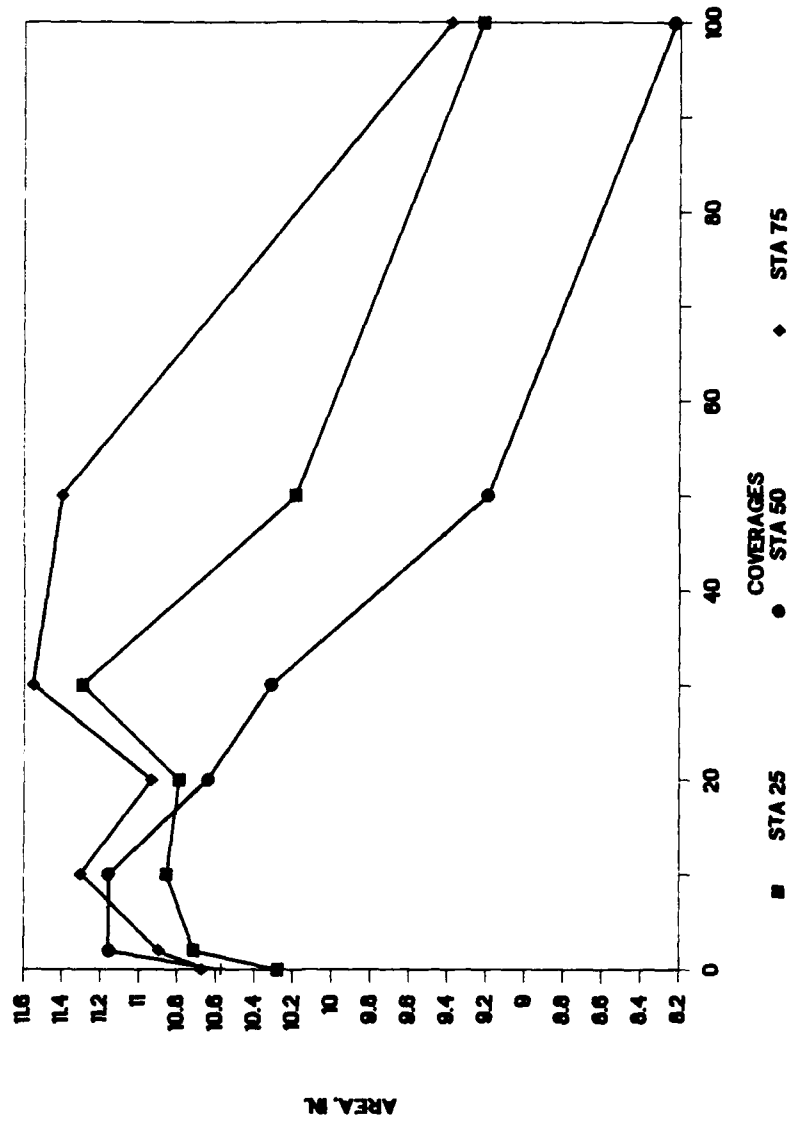


Figure IV-31. Area versus Coverages for NFF4 Item.

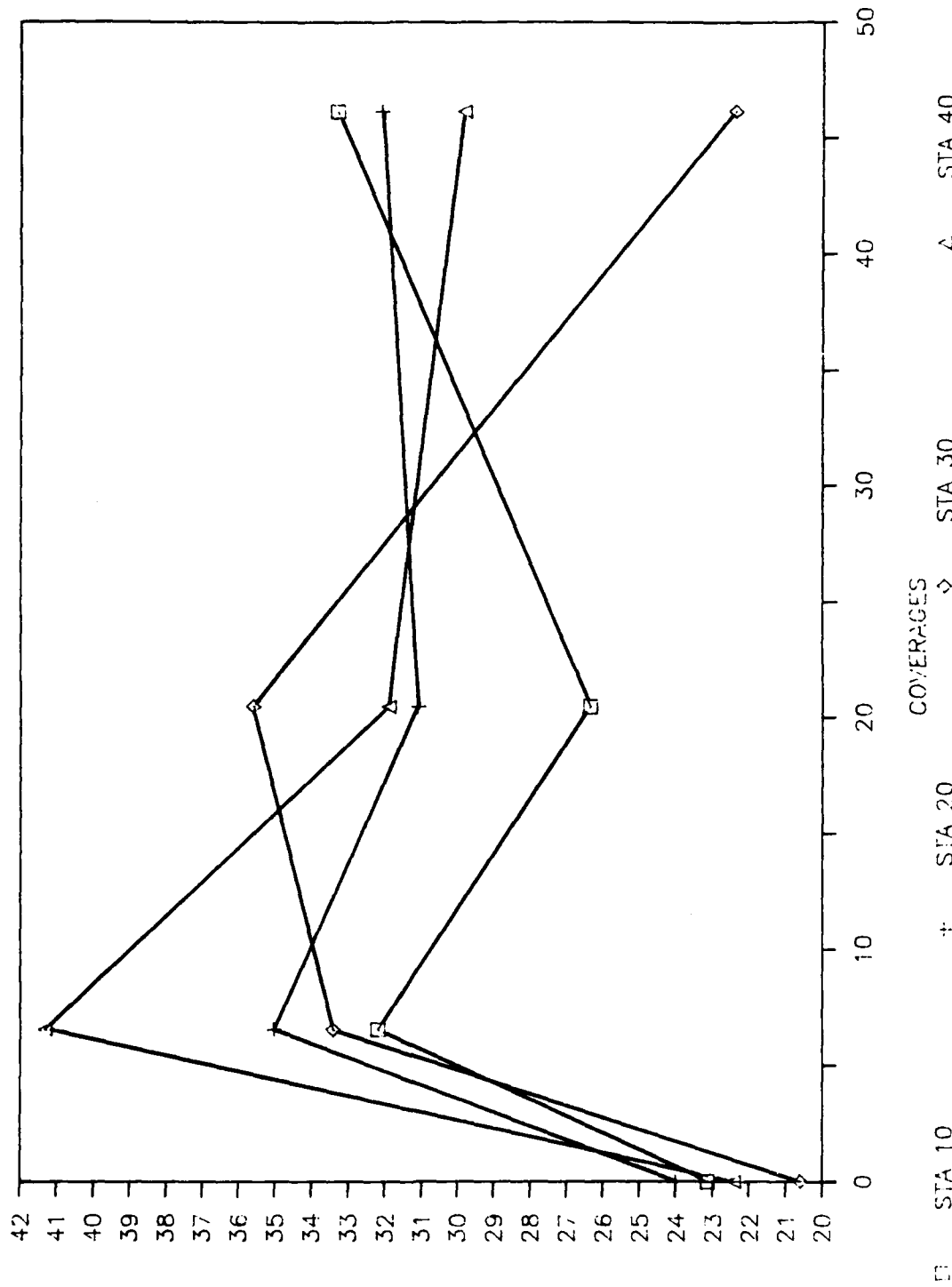


Figure IV-32. Surface Curvature Index versus Coverages for WES1 Item.

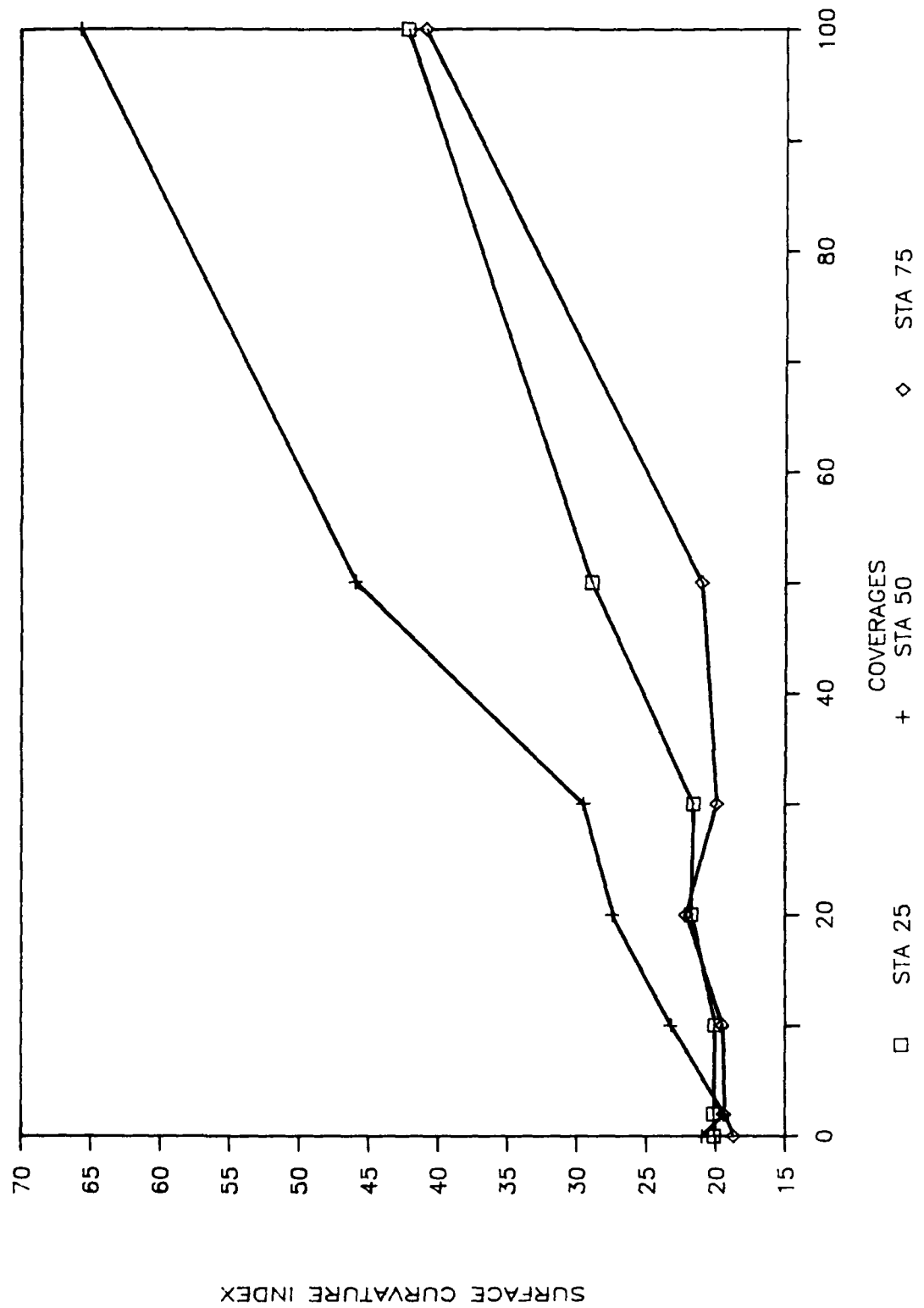


Figure IV-33. Surface Curvature Index versus Coverages for NFF4 Item.

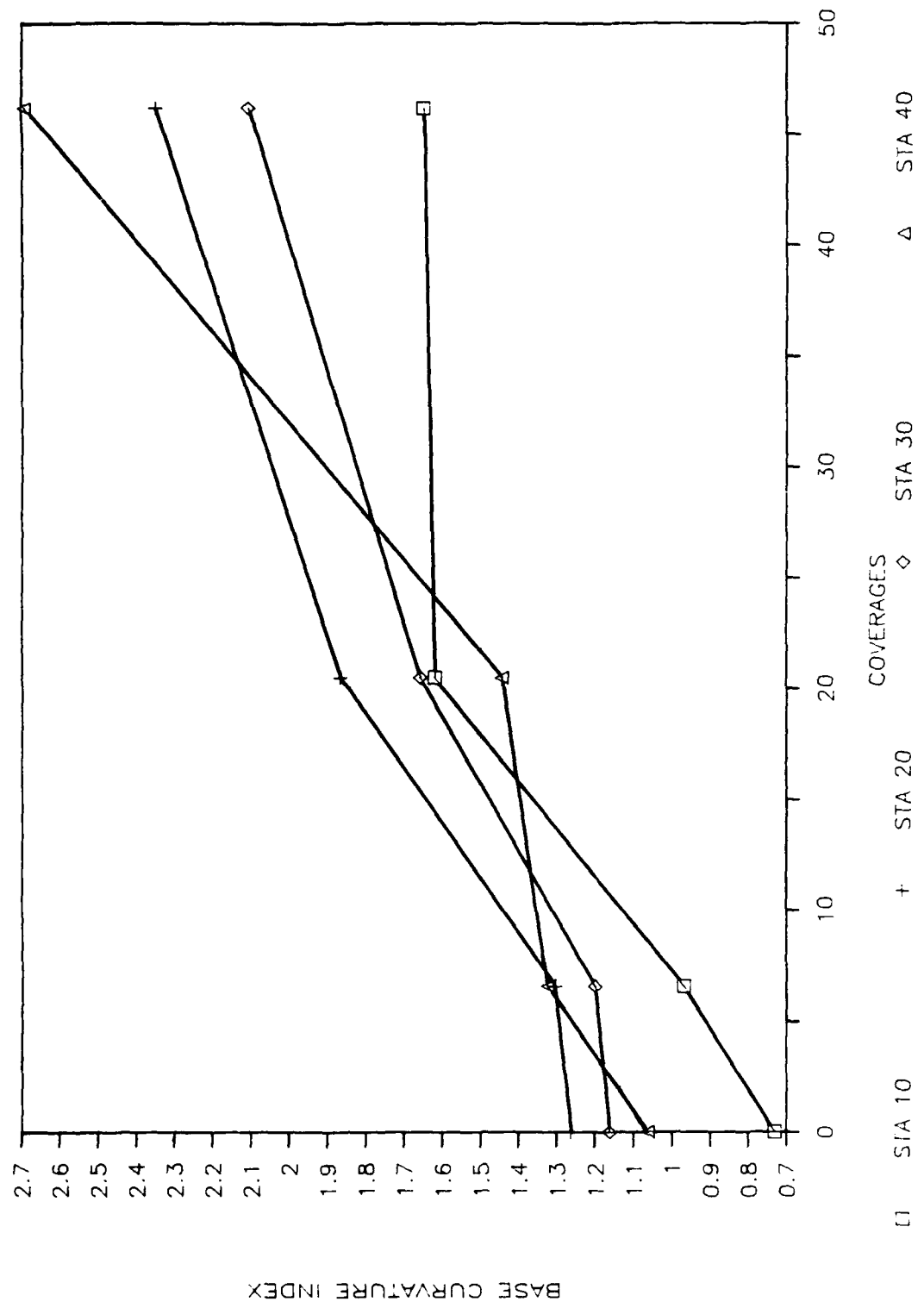


Figure IV-34. Base Curvature Index versus Coverages for WES1 Item.

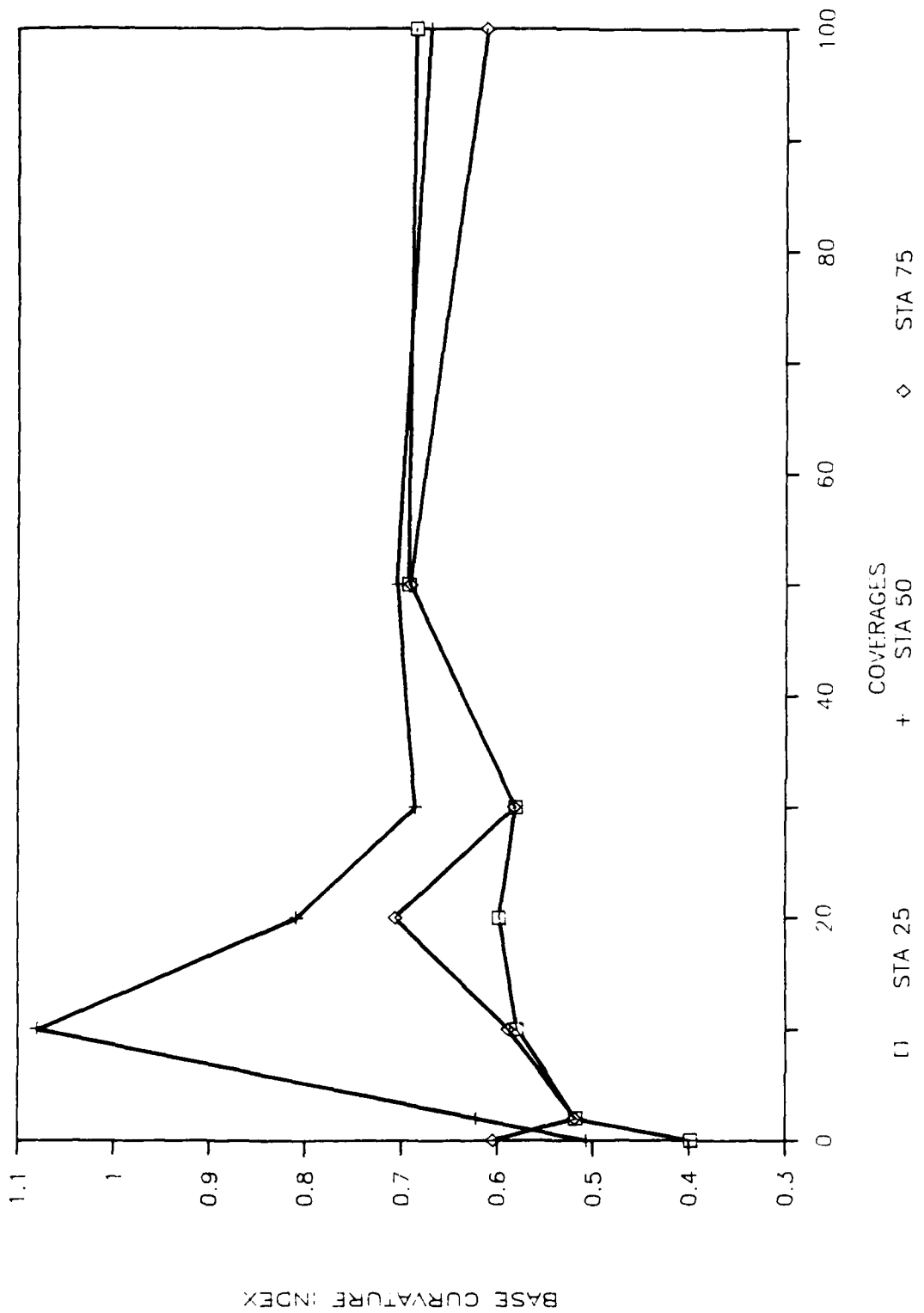


Figure IV-35. Base Curvature Index versus Coverages for NFF4 Item.

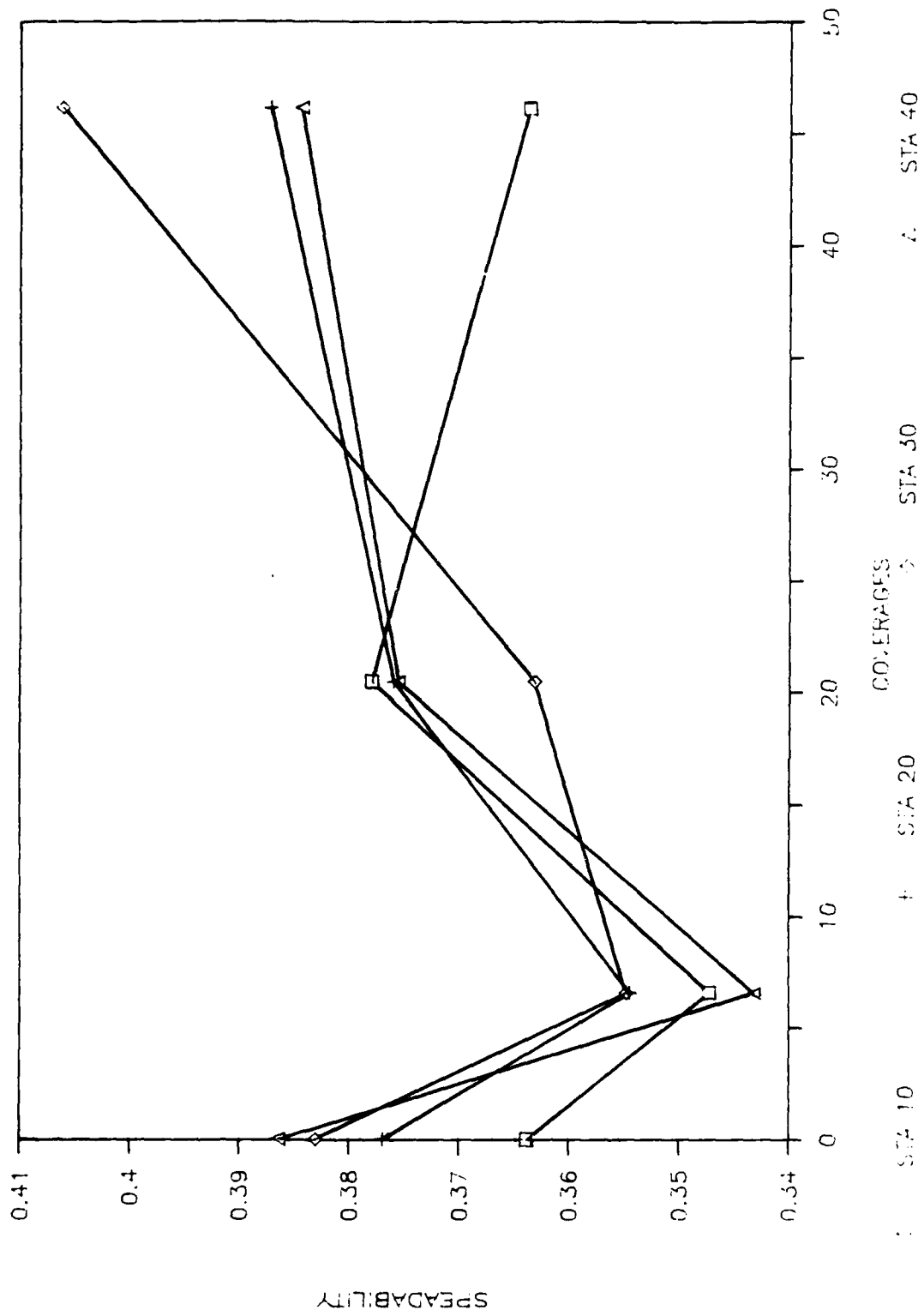


Figure IV-36. Spreadability versus Coverages for WES1 Item.

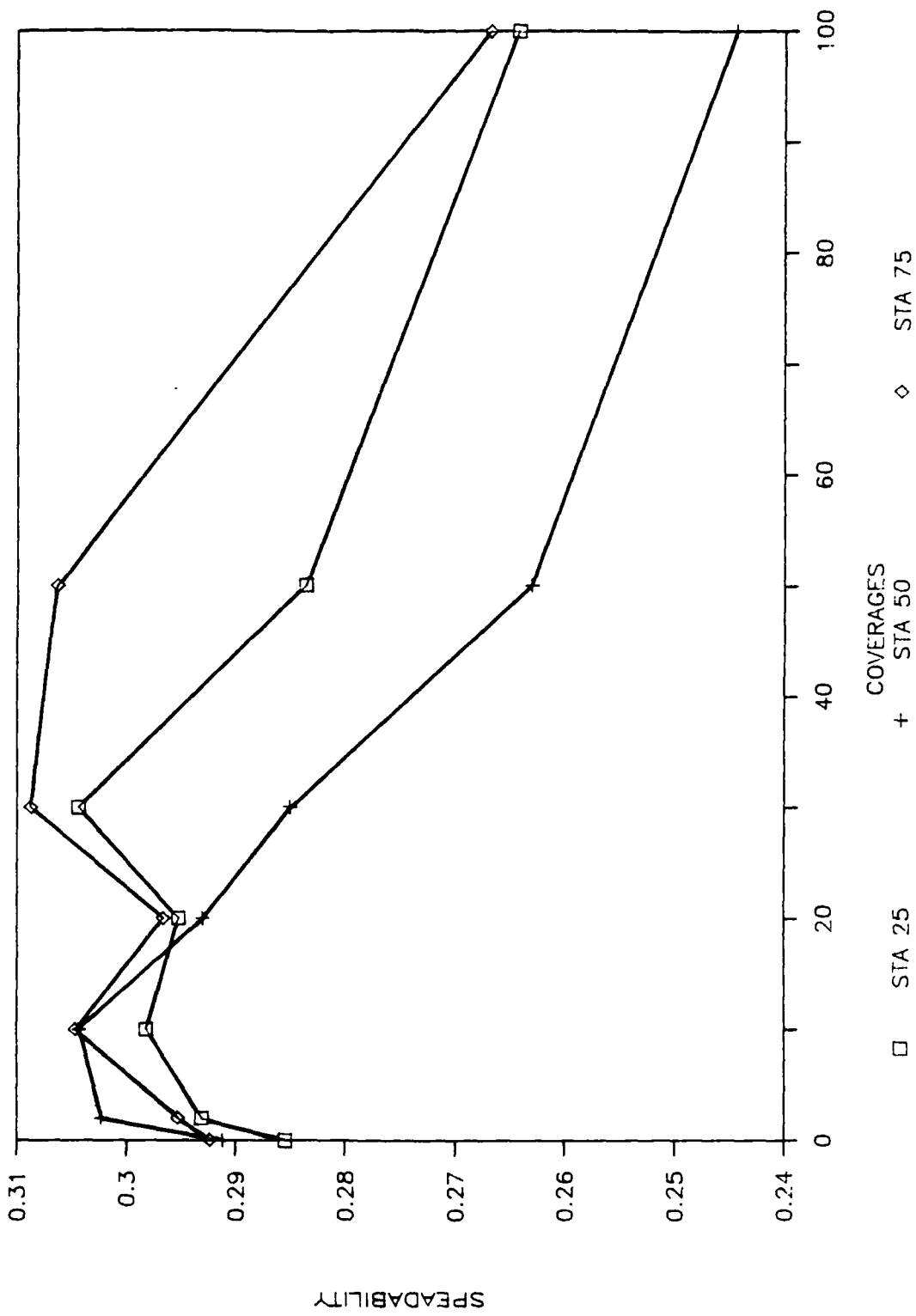


Figure IV-37. Spreadability versus Coverages for NFF4 Item.

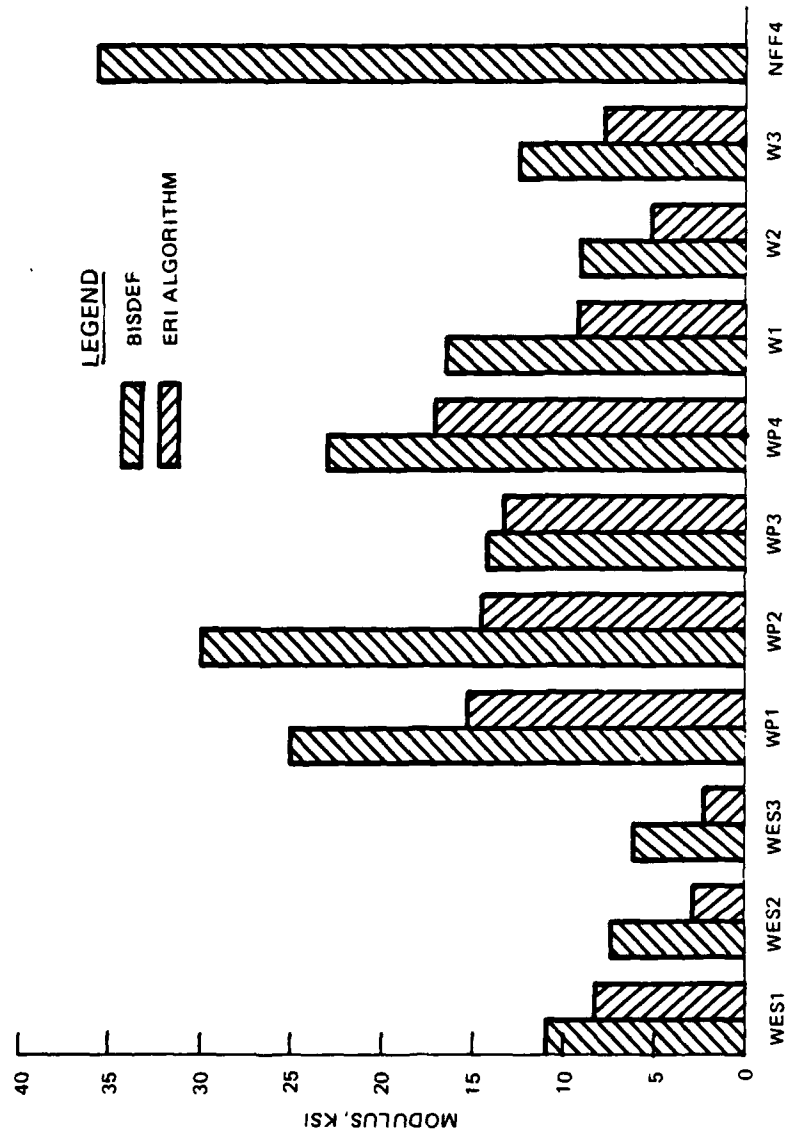


Figure IV-38. Comparison of ERI and BISDEF Subgrade Modulus Values.

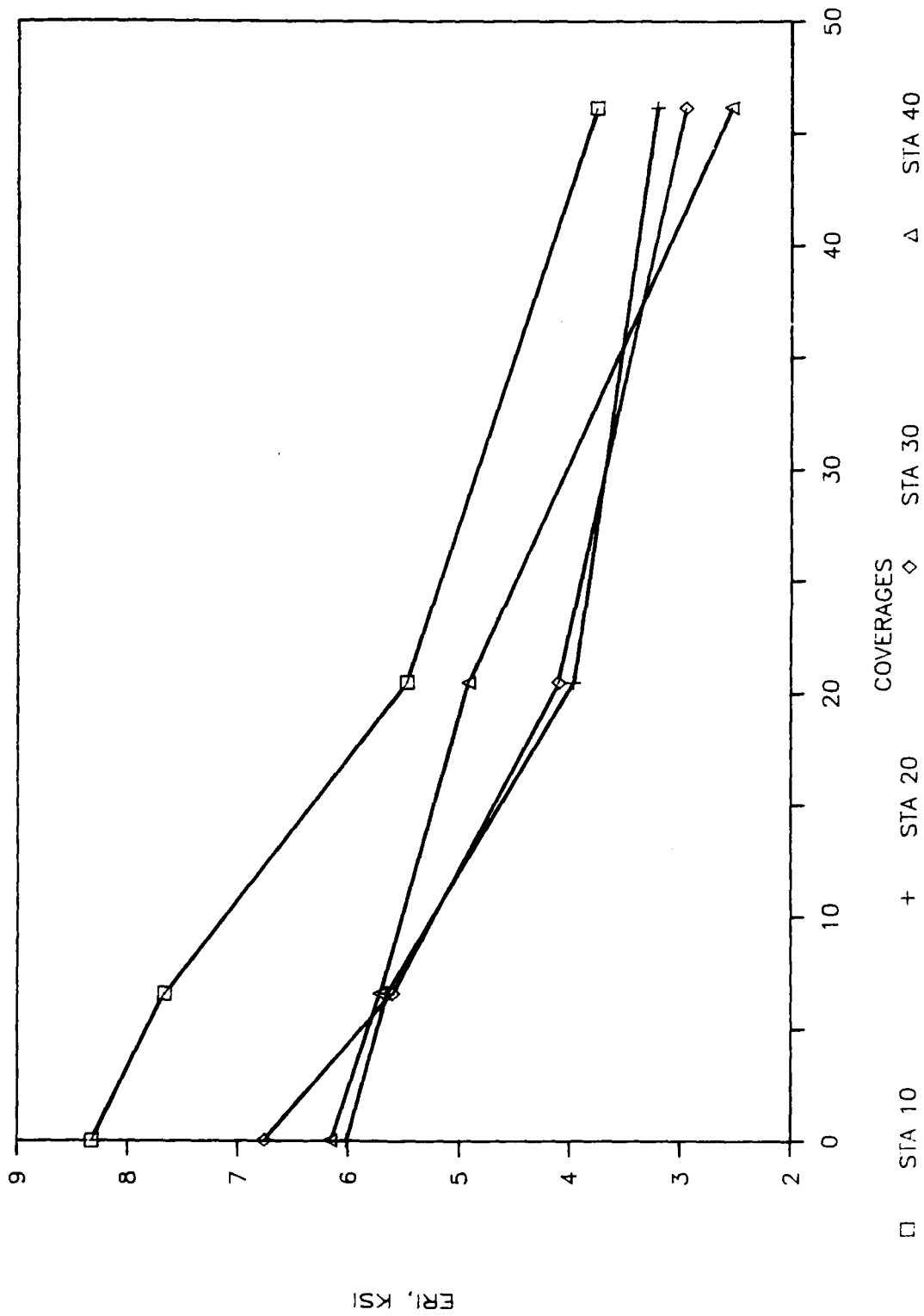


Figure IV-39. ERI versus Coverages for WES1 Item.

ERI, KSI

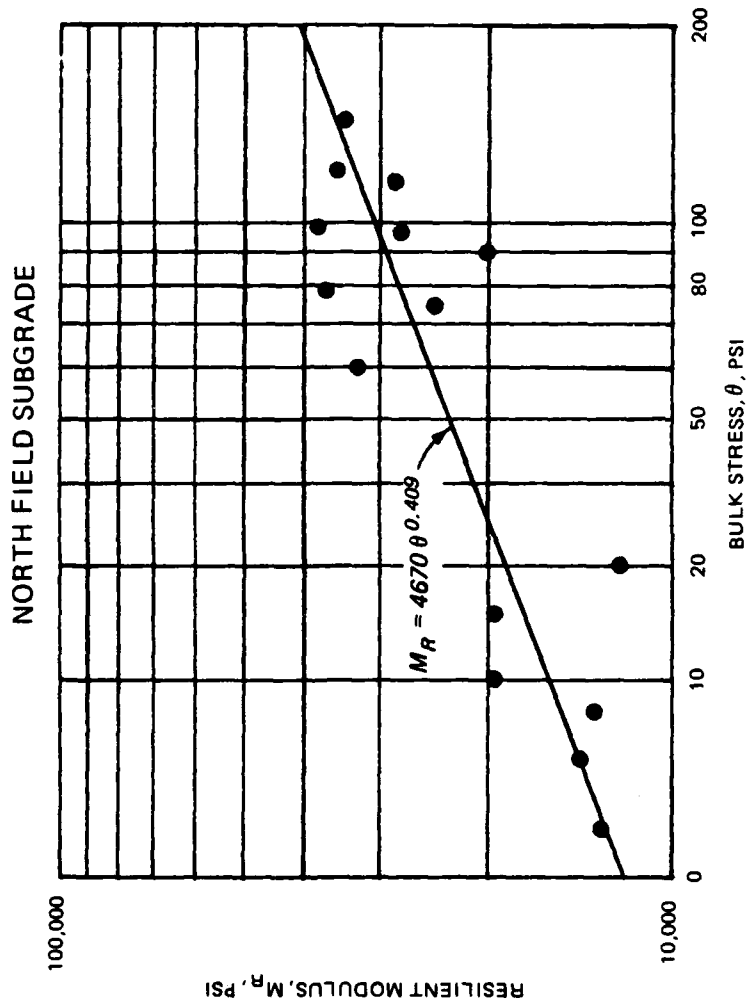


Figure IV-40. Laboratory Resilient Modulus Test Results on NFF4 Subgrade.

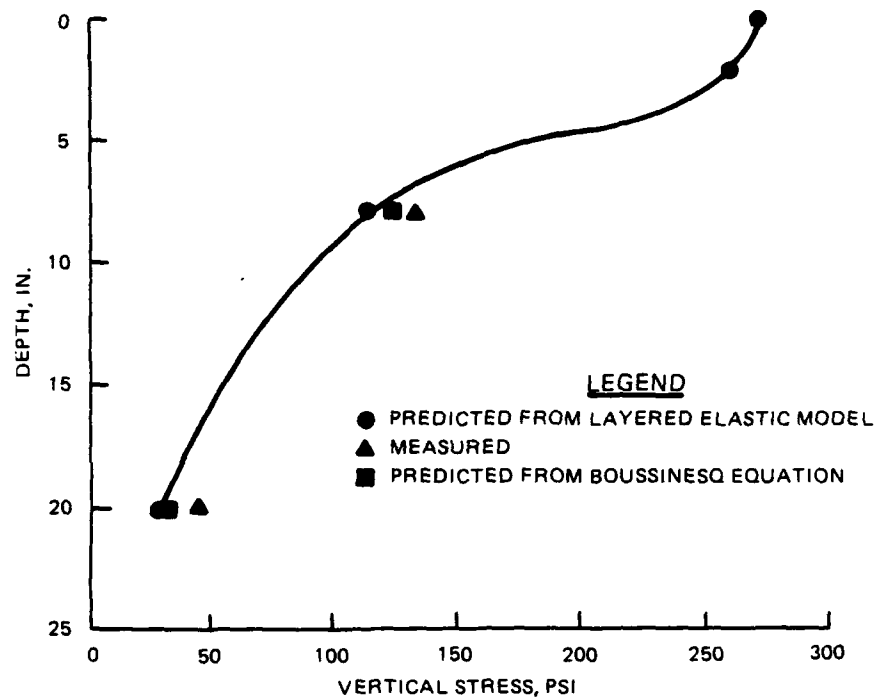
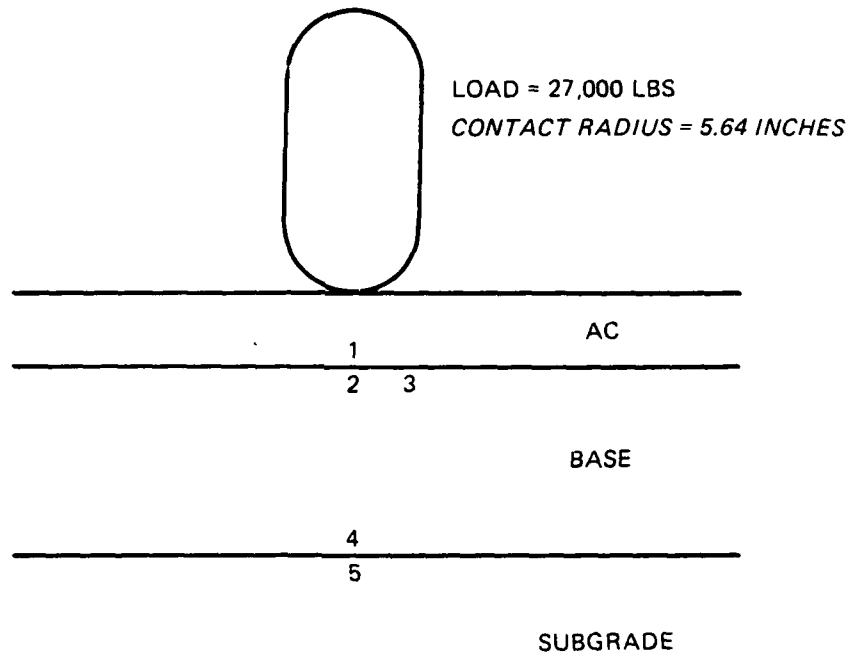


Figure IV-41. Measured and Predicted Stresses on NFF4 Items for F-4 Loading.



LOCATION PARAMETER

- 1 TENSILE STRAIN IN AC
- 2 VERTICAL STRESS AND STRAIN IN BASE
- 3 SHEAR STRESS IN BASE
- 4 TENSILES STRAIN IN BASE
- 5 VERTICAL STRESS AND STRAIN IN SUBGRADE

Figure IV-42. Location of Stress and Strain Calculation Points.

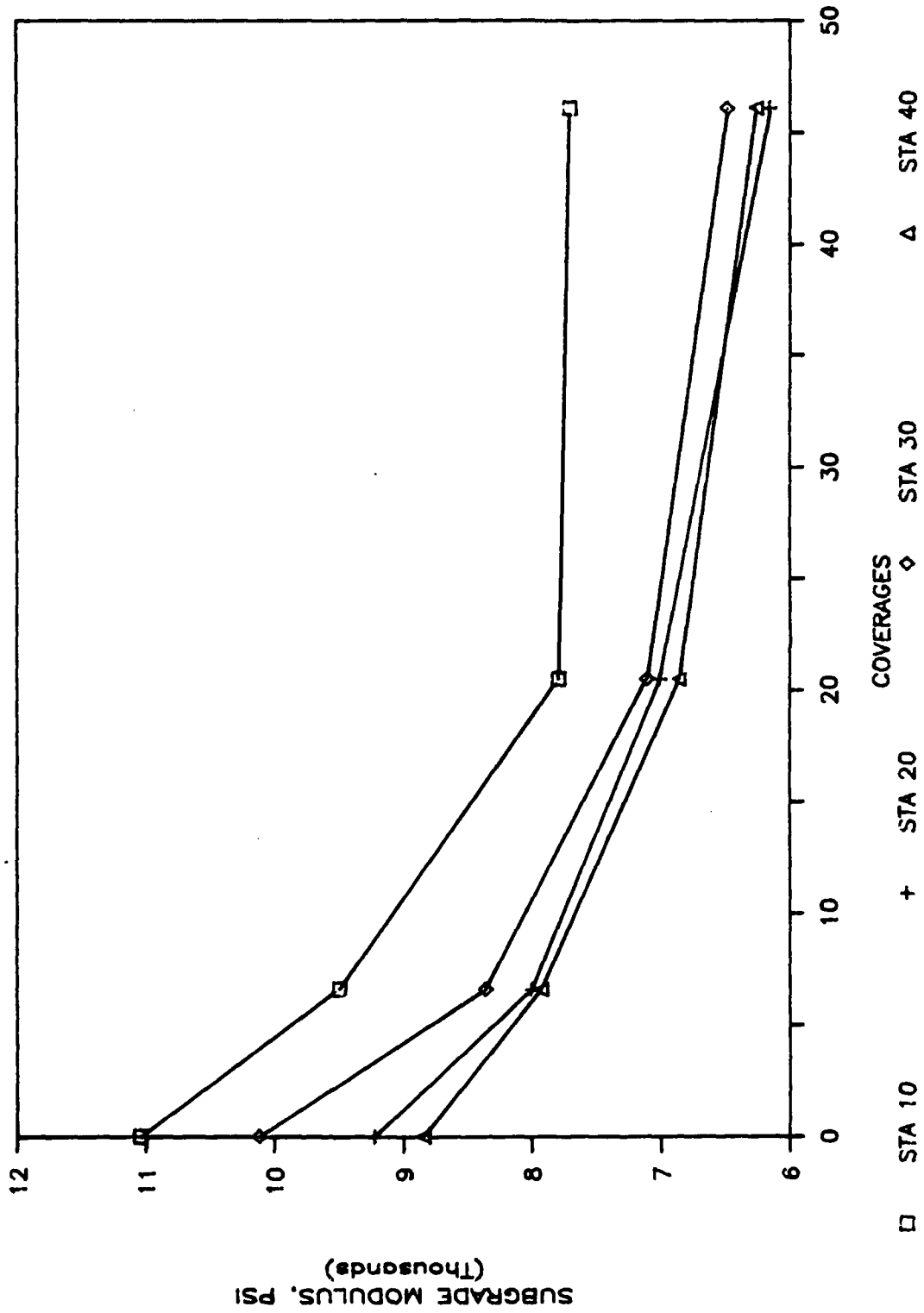


Figure IV-43. Subgrade Modulus versus Coverages for WES1 Item.

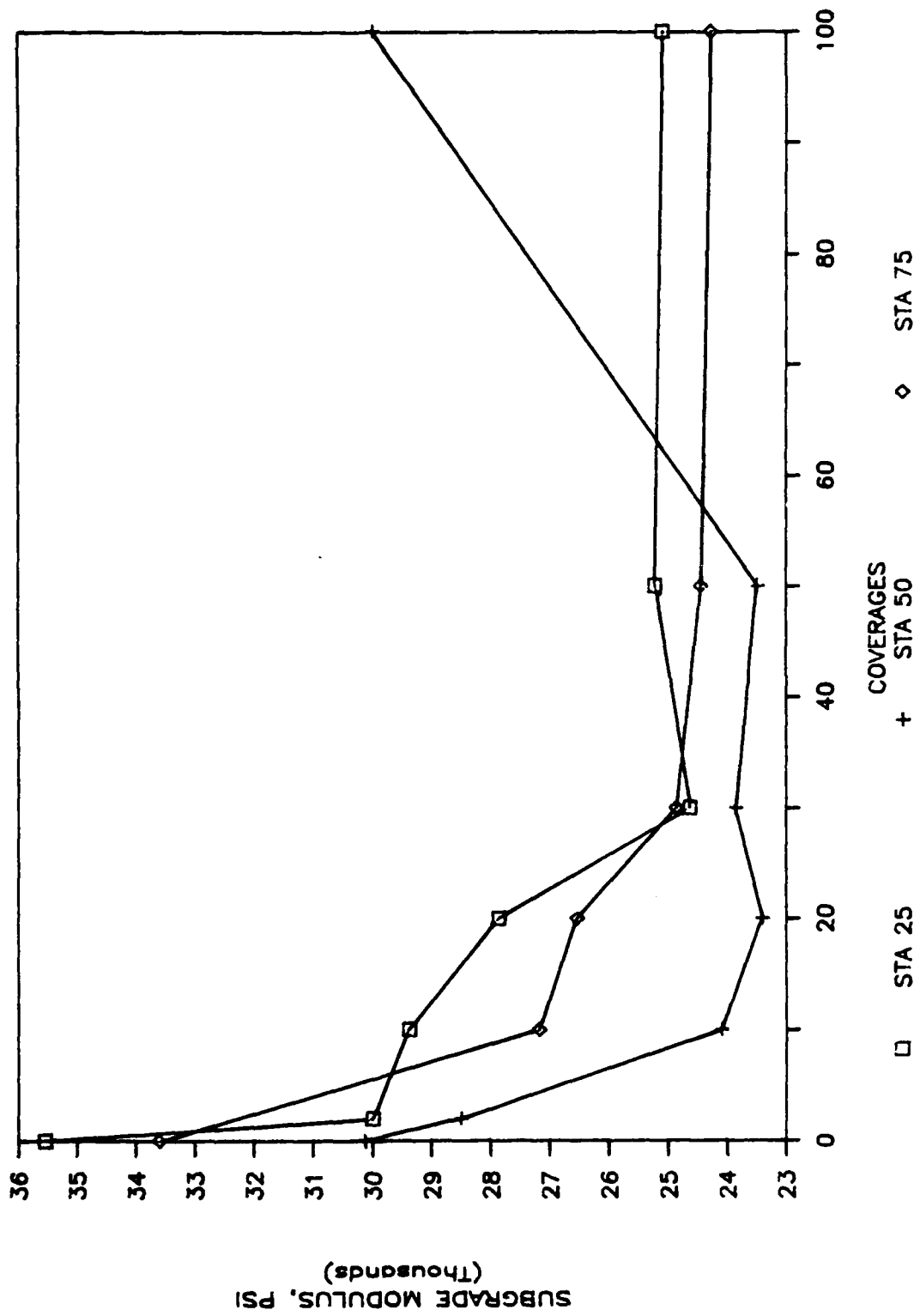


Figure IV-44. Subgrade Modulus versus Coverages for NFF4 Item.

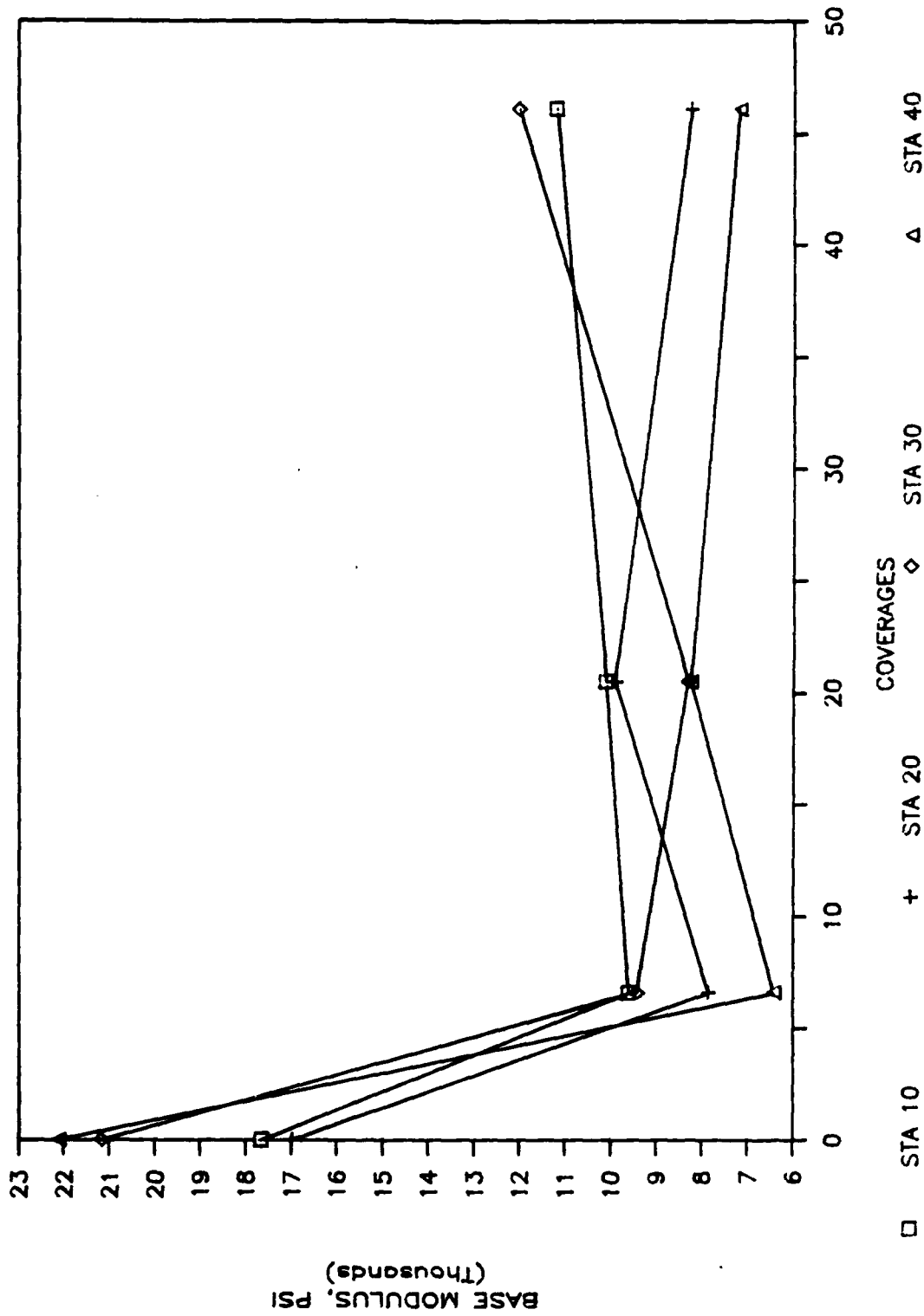


Figure IV-45. Base Modulus versus Coverages for WES1 Item.

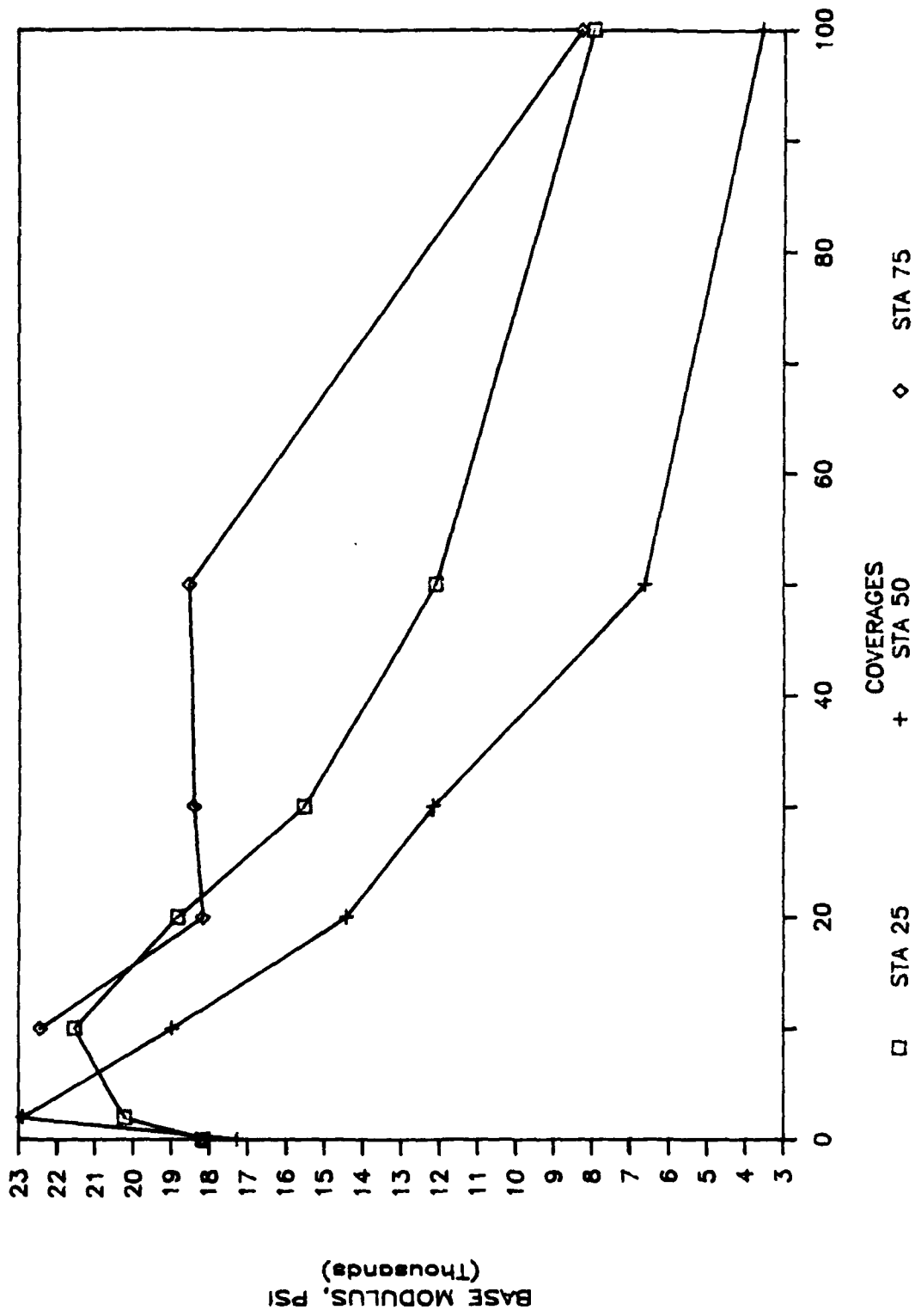


Figure IV-46. Base Modulus versus Coverages for NFF4 Item.

SECTION V

ANALYSIS OF PERFORMANCE OF TRAFFIC TEST ITEMS

A. PERFORMANCE OF TRAFFIC TEST SECTIONS

Development of distress in the traffic test items can be characterized by cracking of the AC surface course followed by rapid increase in rut depth. The two surface treatment items (WES3 and W-1) exhibited shallow rutting directly under the F-4 wheel indicating failure occurred in the base course rather than the subgrade. WES1 and WES2 exhibited rutting that was wider than the tire over the four center traffic lanes indicating deformation lower in the pavement subgrade. A comparison of the two types of rutting is shown in Figure V-1. The other items showed cracking in the surface, which led to increased stress on the surface of the base and failure could be attributed to base course. Performance details are given in References 6 and 10.

Three of the eleven test items (WES1, NFF4, and WP-2) exceeded 150 passes to a 1-inch rut depth. Seven test items exceeded 150 passes to a 3-inch rut depth.

1. Cracking

The progression of cracking with coverages for each item is shown in Table V-1. The DBST item (W-1) cracked early. Generally, at 1-inch rutting the cracking was less than 10 percent of the area. Three-inch rutting occurred generally when more than 50 percent of the area contained alligator cracking.

2. Rutting

The maximum rut depth measured within each test item is shown in Figures V-2 through V-11. Generally, those items with rut depth/time curves which flatten out, such as NFF4 and WP-2, indicate the surface had failed as shown in Figure V-1; but since the base course thickness was large, compaction was occurring in the lower portion of the layer prior to failure. Item WP-1 had a failure where the load cart punched through the asphalt surface.

B. ESTIMATE OF PERFORMANCE USING CBR PROCEDURE

The CBR procedure is the most extensively used procedure for the design and evaluation of airfield pavements. An assessment of its efficiency in predicting the performance of low-volume pavements will be presented. Coverages to a 1-inch rut depth will be used for comparison.

The base course strengths of the Wright-Patterson and Whiteman pavements were under 80 CBR. Data on the test items are summarized in Table V-2. Gradation curves (Figures III-8 and III-9) for these base courses and densities measured in place indicate that the design specifications were probably met. Therefore, if the measured CBR of the subgrade is used for the evaluation, regardless of the measured base course CBR, expected coverages to failure are as shown in Figure V-12. Also presented are the predicted coverages from the evaluation where the base course CBR was considered (i.e., the minimum coverages were selected based on the thickness above each measured CBR). These compare to the actual coverages to failure much closer than the designer would estimate based on subgrade

CBR's only. The constructed test sections (NFF4, WES1, WES2, and WES3) also compared to the actual coverages to failure.

Base course failure occurred in six of the eleven test items as analyzed with the CBR procedure (WP-1, WP-2, WP-3, WP-4, W-1, and W-3). These failures can be attributed to loss of base course strength due to increased moisture content, loss of compaction, or loss of confining stress. Water infiltration through a cracked surface layer or freeze-thaw action contributed to the increased moisture content. Freeze-thaw action may have contributed to a decrease in density, and the cracking of the surface layer contributed to the loss of confining stress. Each of the above factors emphasize the need for monitoring ALRS pavements.

C. LAYERED ELASTIC ESTIMATE OF PERFORMANCE

1. Subgrade Vertical Strain

The most common parameter used in design and evaluation of pavements with layered elastic and finite element methods is vertical strain in the subgrade. However, many of the test items failed due to low base course strength as indicated in the CBR procedure analysis.

Chou et al. (Reference 59) presented relationships between vertical strain at the subgrade surface and coverages to failure for single-wheel aircraft (Figure V-13). It should be noted that all failures that occurred before 100 coverages were classified as "subgrade not critical before initial failure" in Figure V-13.

Vertical subgrade strain for the test items, as calculated from F-4 loading and modulus values (Table IV-1) back-calculated from FWD results, are presented for comparison in Figure V-14. This figure indicates subgrade strain is not a good predictor of coverages to failure for the test items

evaluated in this study since base course failure occurred in most cases. The relationship indicated was selected for analysis. The relationship fits the present data better than the Chou et al. relationship and allows some conservatism. The relationship is an extension of the Barker criteria (Reference 30) for a subgrade modulus of 4,600 psi. The variation in the data indicates that other criteria must be considered for a better prediction of coverages to failure for low-volume pavements.

2. Base Course Vertical Strain

Base course vertical strain was investigated as a possible parameter for prediction since the failures for most of these pavements occurred in the base course. Using the back calculated modulus values and the F-4 loading, the vertical strain in the base course was computed with the BISAR model. A relationship is shown in Figure V-15. The equation for the relationship is as follows.

$$\epsilon_{\text{base}} = \frac{15.46}{\text{COV}^{0.14458}}, 10^{-3} \text{ in./in.} \quad (19)$$

where

$$\begin{aligned} R^2 &= 0.20 \\ \text{Standard error} &= 1.69, 10^{-3} \text{ in./in.} \end{aligned}$$

This relationship is a better predictor of performance than subgrade strain for low-volume pavements.

D. RUT DEPTH PREDICTIONS

Using the pavement thickness data and CBR data presented in Table V-2 and the Barber equations presented in Section II-B-2, an attempt was made to evaluate the rut depth prediction model. Results are presented in Figure V-16. The model consistently predicted smaller rut depths than were measured and with a large amount of scatter. An attempt was made to use

the form of the equation to develop new coefficients for low-volume pavements for the data base developed during this study.

The results of the analysis are:

Dependent Variable - Log (Rut Depth)	
Independent Variables	Coefficients
Log COV	0.73058
Log C ₂	-0.81735
Log[Log(1.25 Tac + Tbase)]	-3.15362
Log C ₁	-0.57708
R ²	= 0.49
Standard error	= 0.2567
Number of cases	= 47

The form as presented in Reference 36 is:

$$RD = 0.151 \frac{P_k^{1.3127} t_p^{0.0499} COV^{0.731}}{\log(1.25 Tac + Tbase)^{3.15} C_1^{0.577} C_2^{0.817}} \quad (20)$$

Standard error = 0.91; R² = 0.38; Number of cases = 47

where

RD - Rut depth in inches

P_k - Single-wheel load, kips

t_p - Tire pressure, psi

COV - Coverages

Tac - Thickness of asphalt surface, inches

Tbase - Thickness of base course, inches

C_1 - CBR of base course

C_2 - CBR of subgrade

This model was dismissed because of the low R^2 (0.38) and high standard error (0.91 inches).

TABLE V-1. RUTTING AND CRACKING PROGRESSION OF TEST ITEMS

<u>ITEM</u>	<u>COV</u>	<u>MAXIMUM RUT DEPTH, IN.</u>	<u>% OF AREA CRACKING</u>
WES1	13.1	0.50	--
	16.4	0.75	5.0
	18.6	1.00	21.0
	20.5	1.25	28.0
	22.9	1.50	48.0
	26.2	1.75	72.0
	29.5	2.00	80.0
	32.7	2.00	95.0
	36.0	2.25	95.0
	39.3	2.25	95.0
	42.6	2.50	95.0
	45.8	2.50	95.0
	46.1	3.75	95.0
WES2	6.6	0.25	--
	13.1	0.50	7.0
	16.4	2.00	14.0
	18.6	2.00	57.0
	19.7	2.25	57.0
	20.5	3.00	--
WES3	6.5	3.00	100.0
WP1	--	--	--
	6.0	--	6.0

TABLE V-1. RUTTING AND CRACKING PROGRESSION OF TEST ITEMS (CONTINUED)

<u>ITEM</u>	<u>COV</u>	<u>MAXIMUM RUT DEPTH, IN.</u>	<u>% OF AREA CRACKING</u>
WP2	--	--	--
	7.0	0.25	0.6
	33.0	0.50	4.0
	46.0	1.50	15.0
	66.0	2.00	17.8
	72.0	2.75	--
WP3	88.0	3.50	51.0
	0.0	--	--
	7.0	1.125	--
	8.0	1.25	0.6
	12.0	3.50	52.0
WP4	7.0	--	3.3
	16.0	--	19.5
	20.0	2.25	--
	22.0	3.50	65.0
W1	7.0	--	4.5
	14.0	1.75	100.0
	17.0	2.00	--
	20.0	--	--
	30.0	2.50	--
	34.0	2.75	--
	38.0	3.00	--

TABLE V-1. RUTTING AND CRACKING PROGRESSION OF TEST ITEMS (CONTINUED)

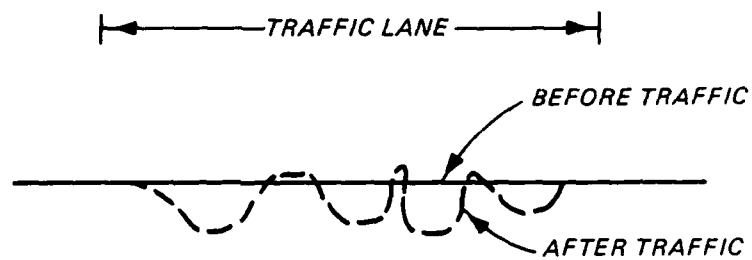
<u>ITEM</u>	<u>COV</u>	<u>MAXIMUM RUT DEPTH, IN.</u>	<u>% OF AREA CRACKING</u>
W2	7.0	--	3.0
	14.0	1.75	27.0
	18.0	3.75	100.0
W3	0.0	--	--
	7.0	2.25	70.0
	12.0	3.50	75.0
NFF4	10.0	0.75	2.8
	20.0	0.75	6.0
	30.0	1.00	6.9
	40.0	1.25	7.0
	50.0	2.25	16.4
	60.0	2.50	36.0
	80.0	2.75	--
	90.0	2.937	69.0
	100.0	4.00	78.0

TABLE V-2. SUMMARY OF CHARACTERISTICS OF TRAFFIC TEST ITEMS

Item	Surface		Base		Subgrade		Total Thickness inches	Maximum			
	Type ^a	Thickness inches	Type ^b	Thickness inches	Type ^b	CBR		1-inch rut Passes	3-inch rut Coverages		
WES-1	AC	1.7	GW	8.2	CH	100	6.6	150	20.5	338	46.1
WES-2	AC	1.4	GW	9.0	CH	100	6.3	120	16.3	150	20.5
WES-3	DBST	0.5	GW	9.4	CH	100	6.0	12	1.6	48	6.5
WP-1	AC	3.0	GW	6.0	--	12	---	39	5.3	44	6.0
WP-2	AC	3.0	GP-GC	47.0	--	33	---	400	54.5	643	87.7
WP-3	AC	2.0	GC	12.0	SC	33	7.0	60	8.2	90	12.3
WP-4	AC	2.0	GW-GM	12.0	SC	72	8.0	100	13.6	162	22.1
W-1	DBST	1.0	GC	29.0	--	33	---	105	14.3	280	38.2
W-2	AC	2.5	GC	12.0	CH	102	4.2	25	3.4	132	18.0
W-3	AC	2.5	GC	16.0	CL	37	4.2	33	4.5	86	11.7
NFF4	AC	2.1	GM	6.3	SP-SM	100	20.0	220	30.0	682	93.0

^aAC = asphaltic concrete; DBST = double bituminous surface treatment.

^bClassified according to the Unified Soil Classification System.



DEFORMATION IN SURFACE
AND BASE COURSE LAYERS



DEFORMATION IN SUBGRADE

Figure V-1. Rutting Types Indicating Failure Location.

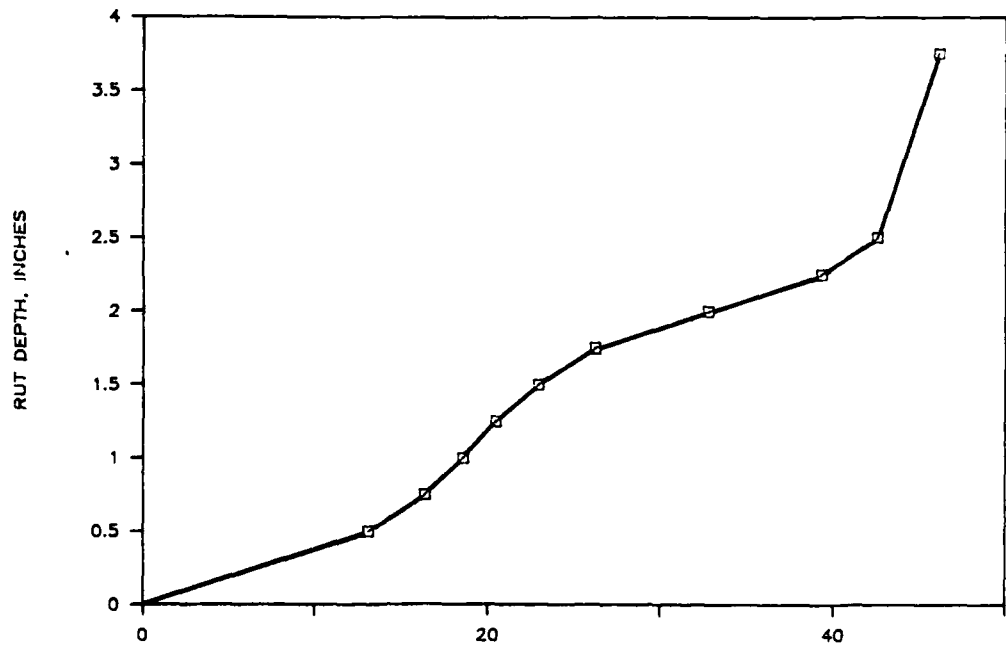


Figure V-2. Rut Depth Progression of WES1.

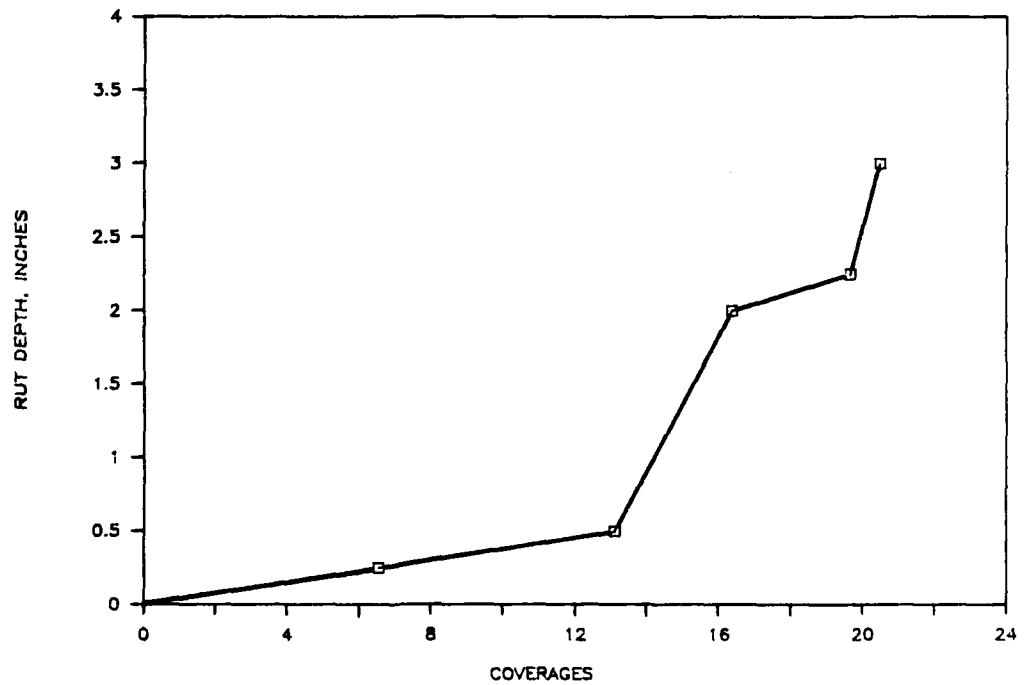


Figure V-3. Rut Depth Progression of WES2.

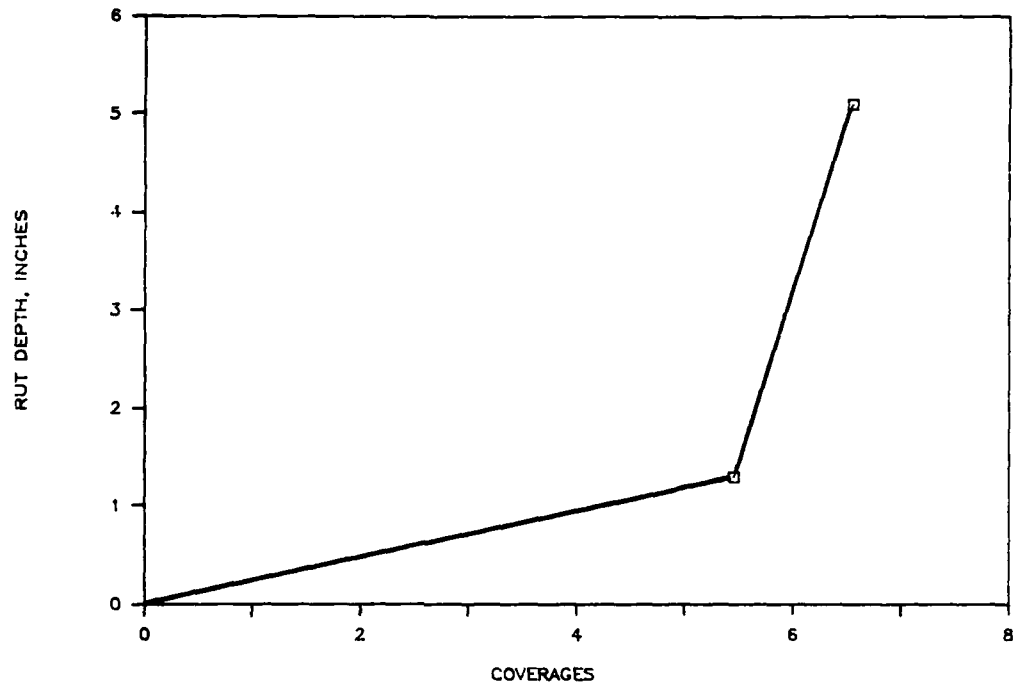


Figure V-4. Rut Depth Progression of WP-1.

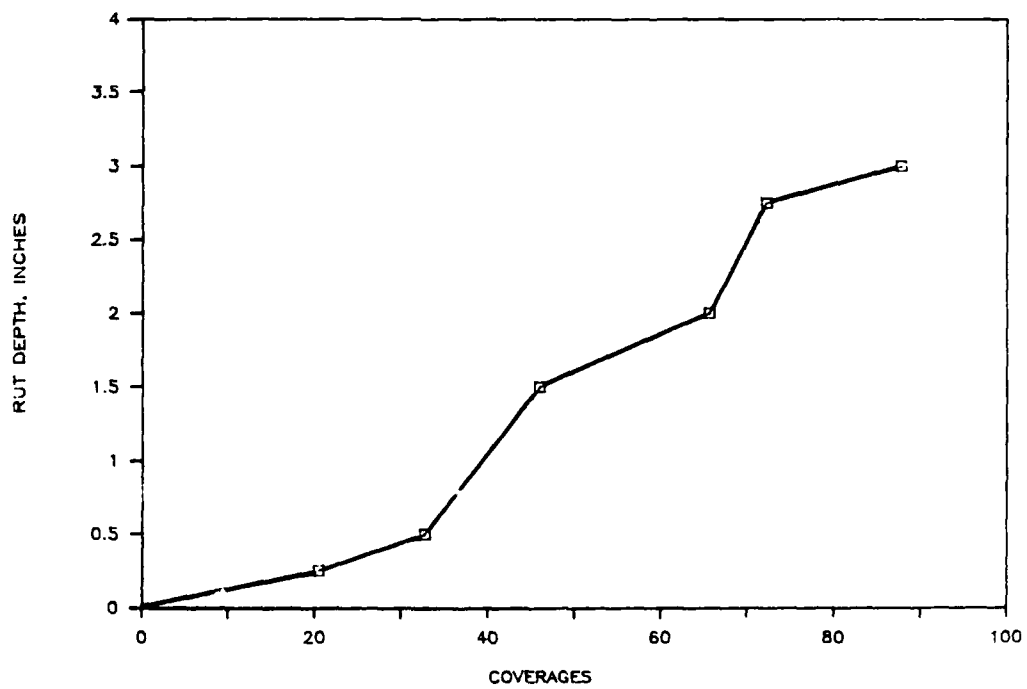


Figure V-5. Rut Depth Progression of WP-2.

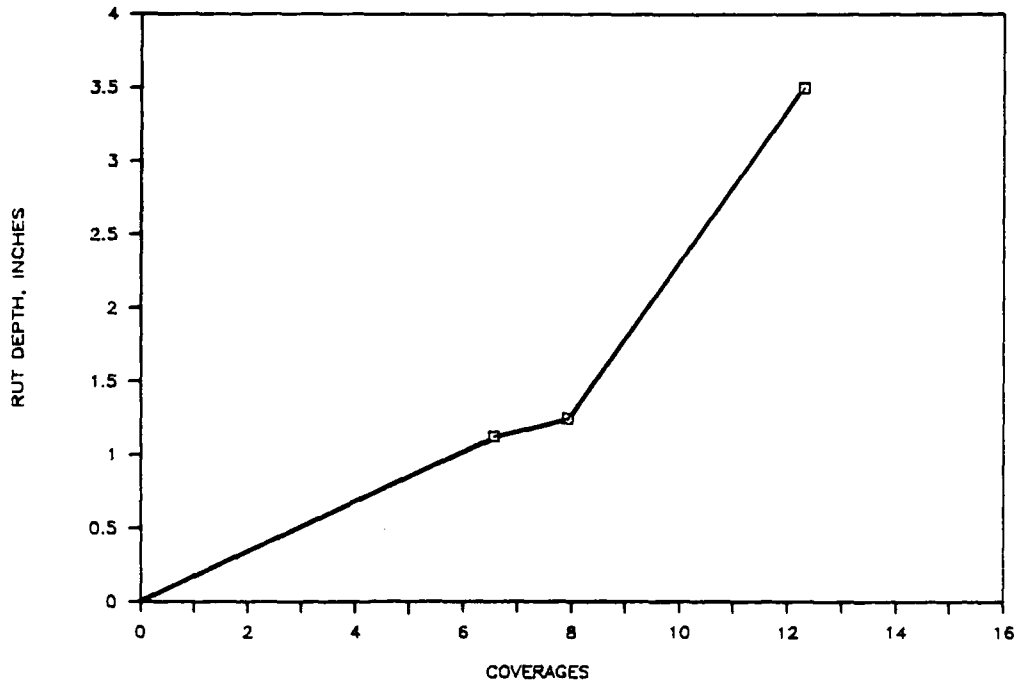


Figure V-6. Rut Depth Progression of WP-3.

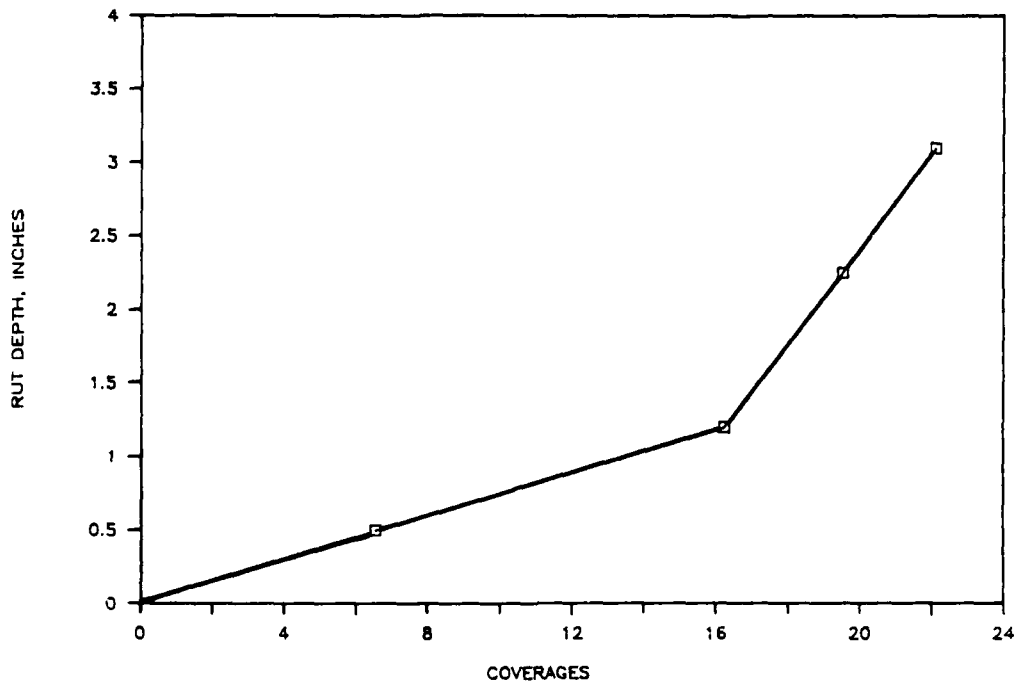


Figure V-7. Rut Depth Progression of WP-4.

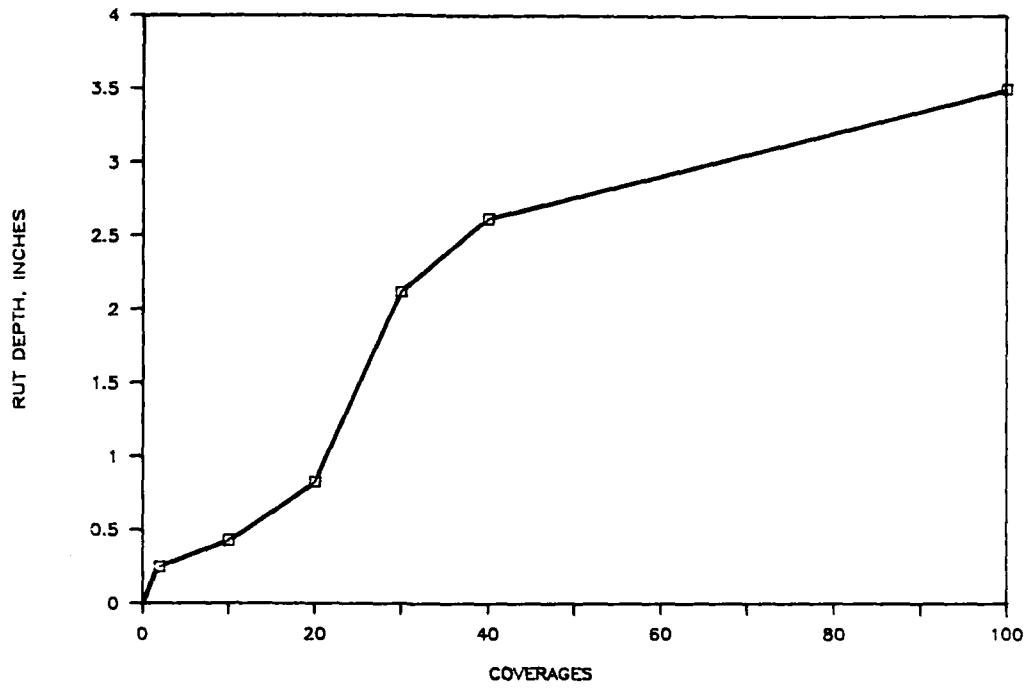


Figure V-8. Rut Depth Progression of NFF4.

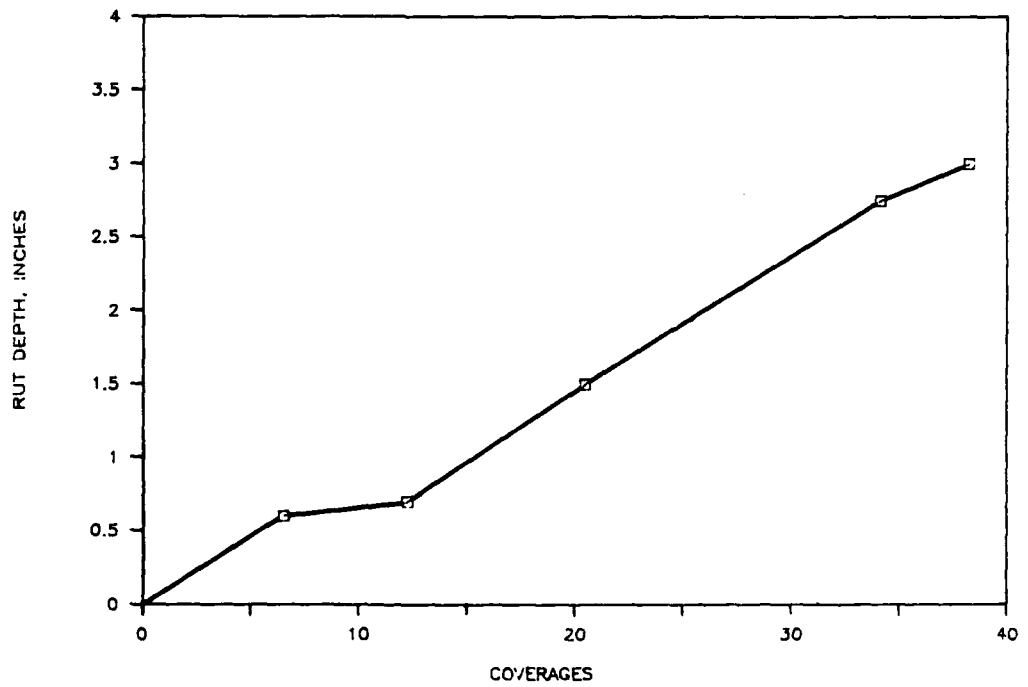


Figure V-9. Rut Depth Progression of W1.

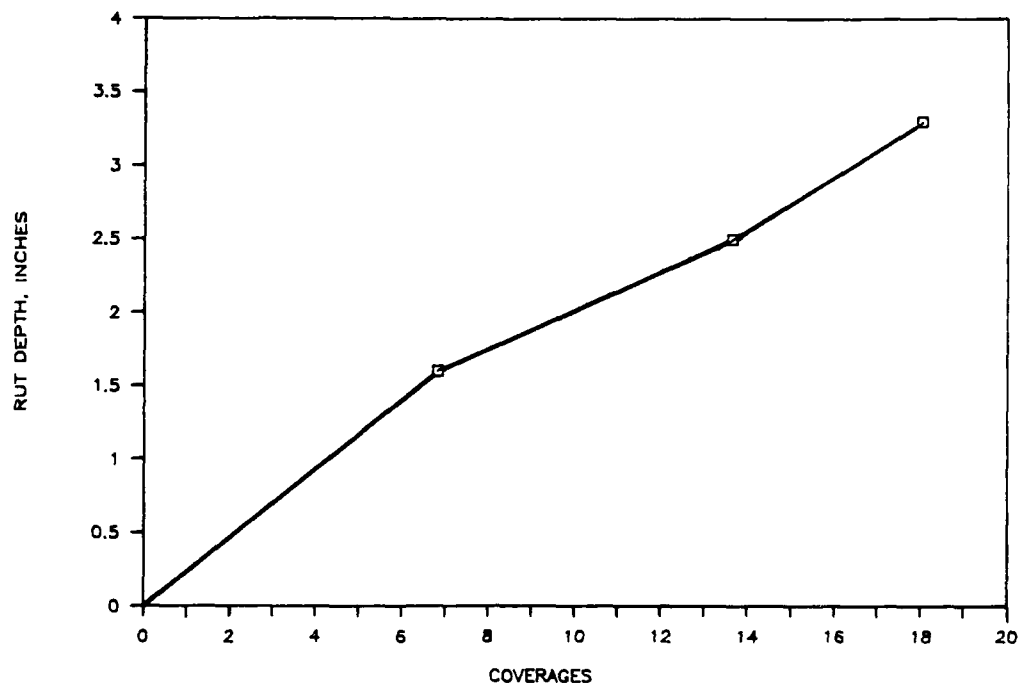


Figure V-10. Rut Depth Progression of W2.

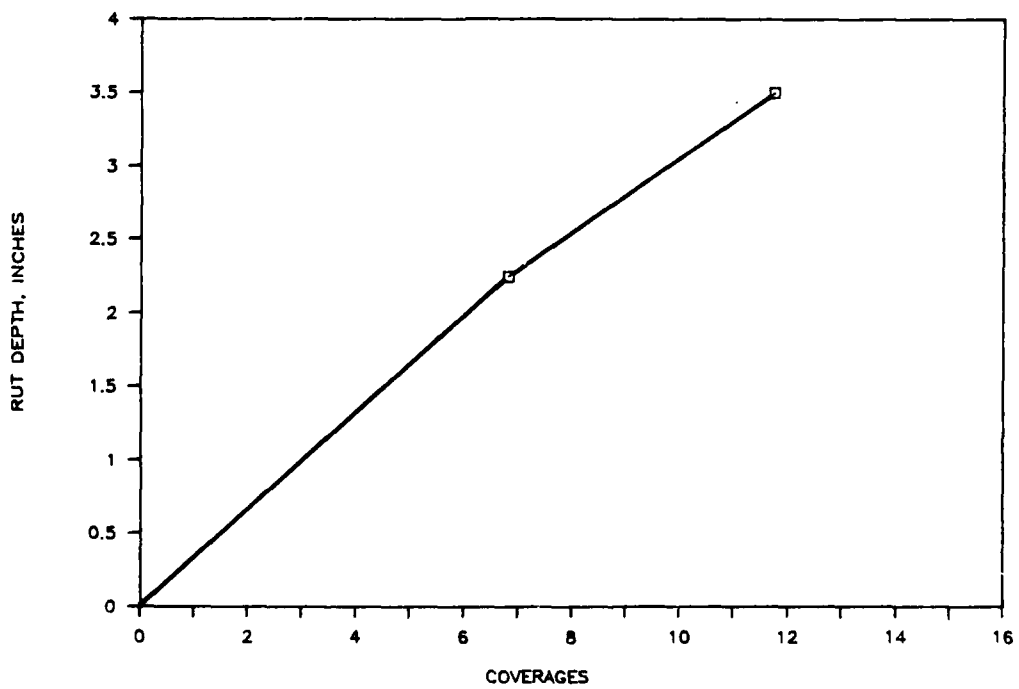


Figure V-11. Rut Depth Progression of W3.

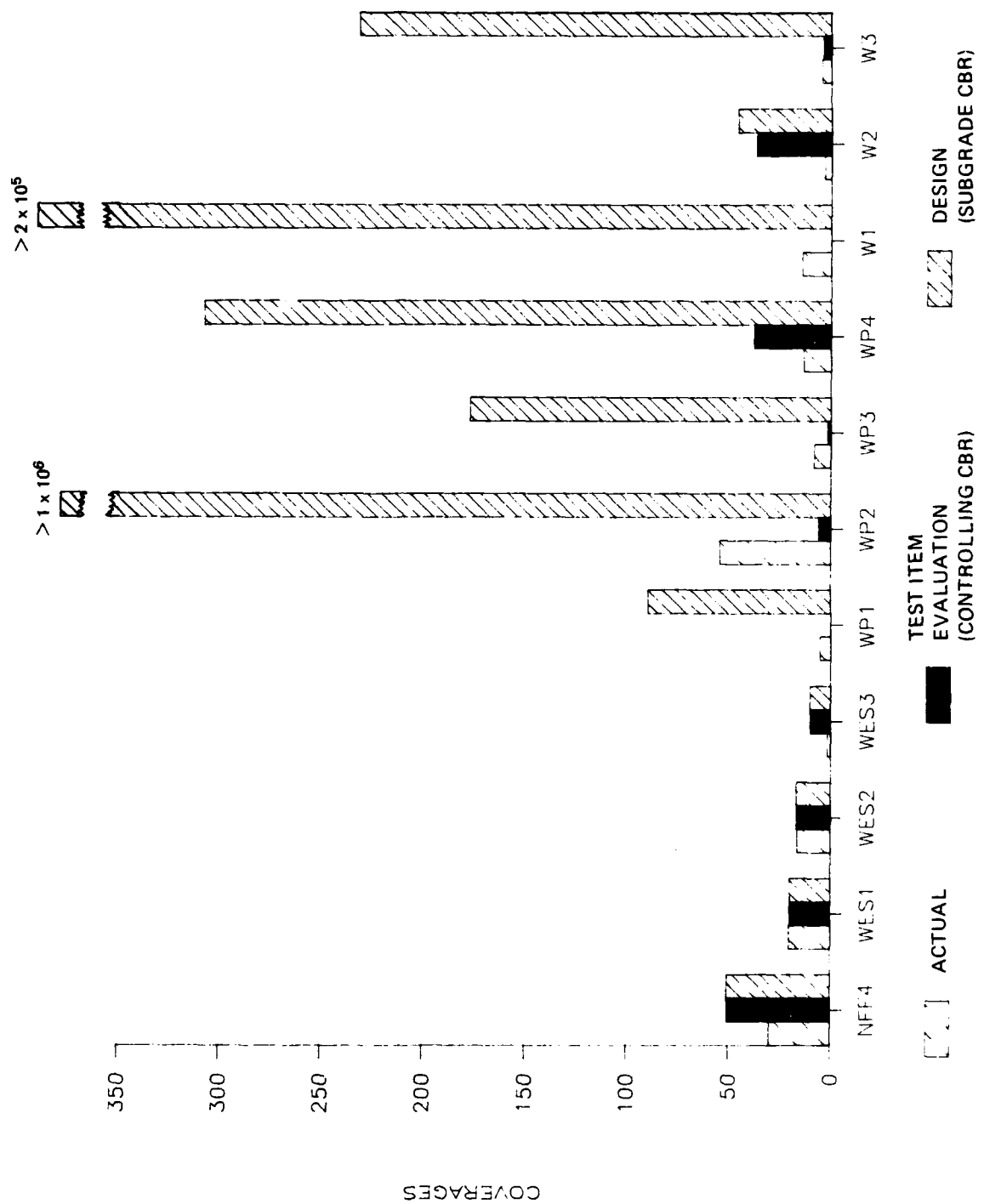


Figure V-12. Comparison of Predictions with CBR Procedure.

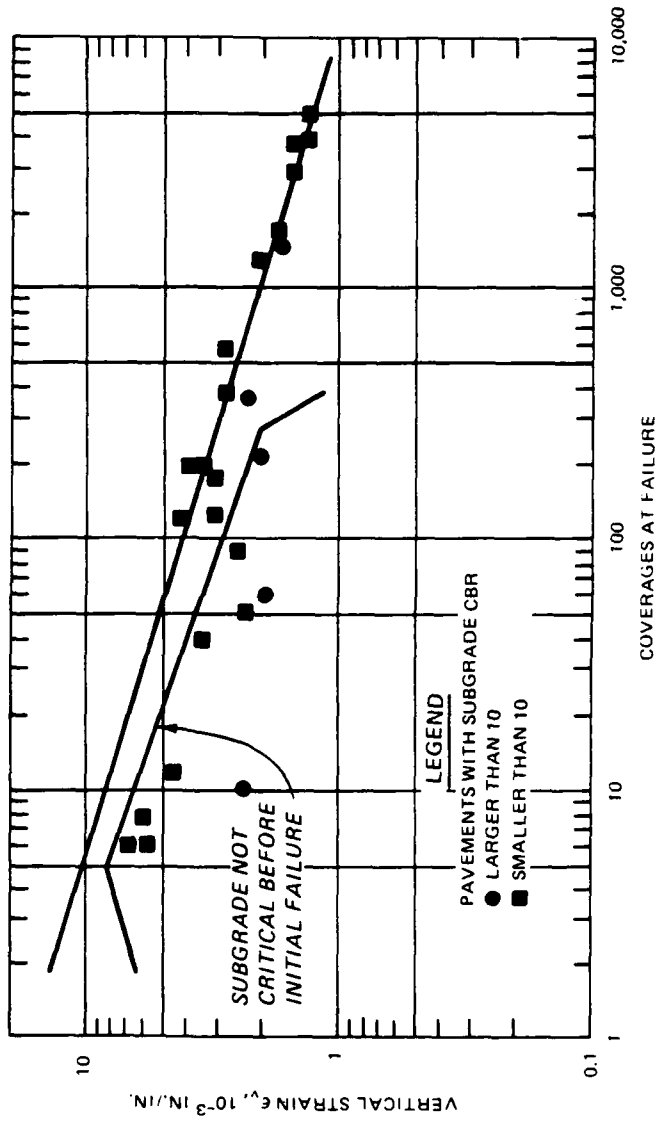


Figure V-13. Relationship Between Vertical Strain at Subgrade Surface and Performance of Pavement Under Single-Wheel Loads (Reference 59).

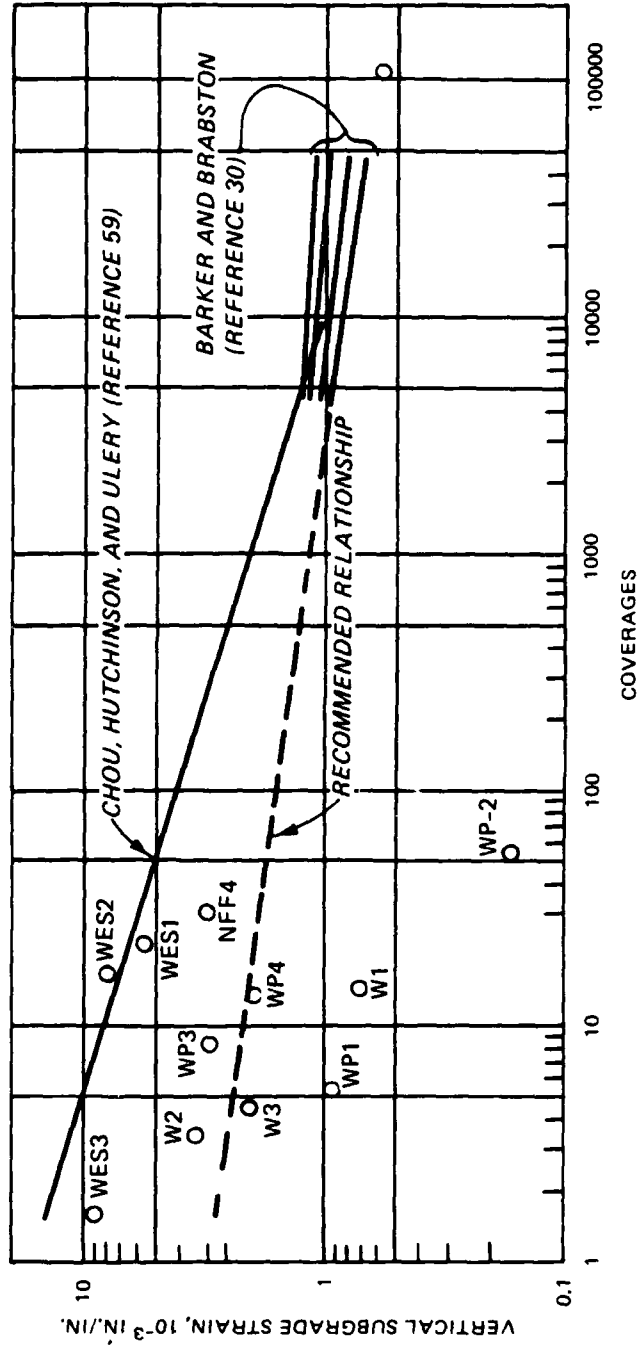


Figure V-14. Relationship Between Vertical Strain at Subgrade Surface and Performance of Pavements.

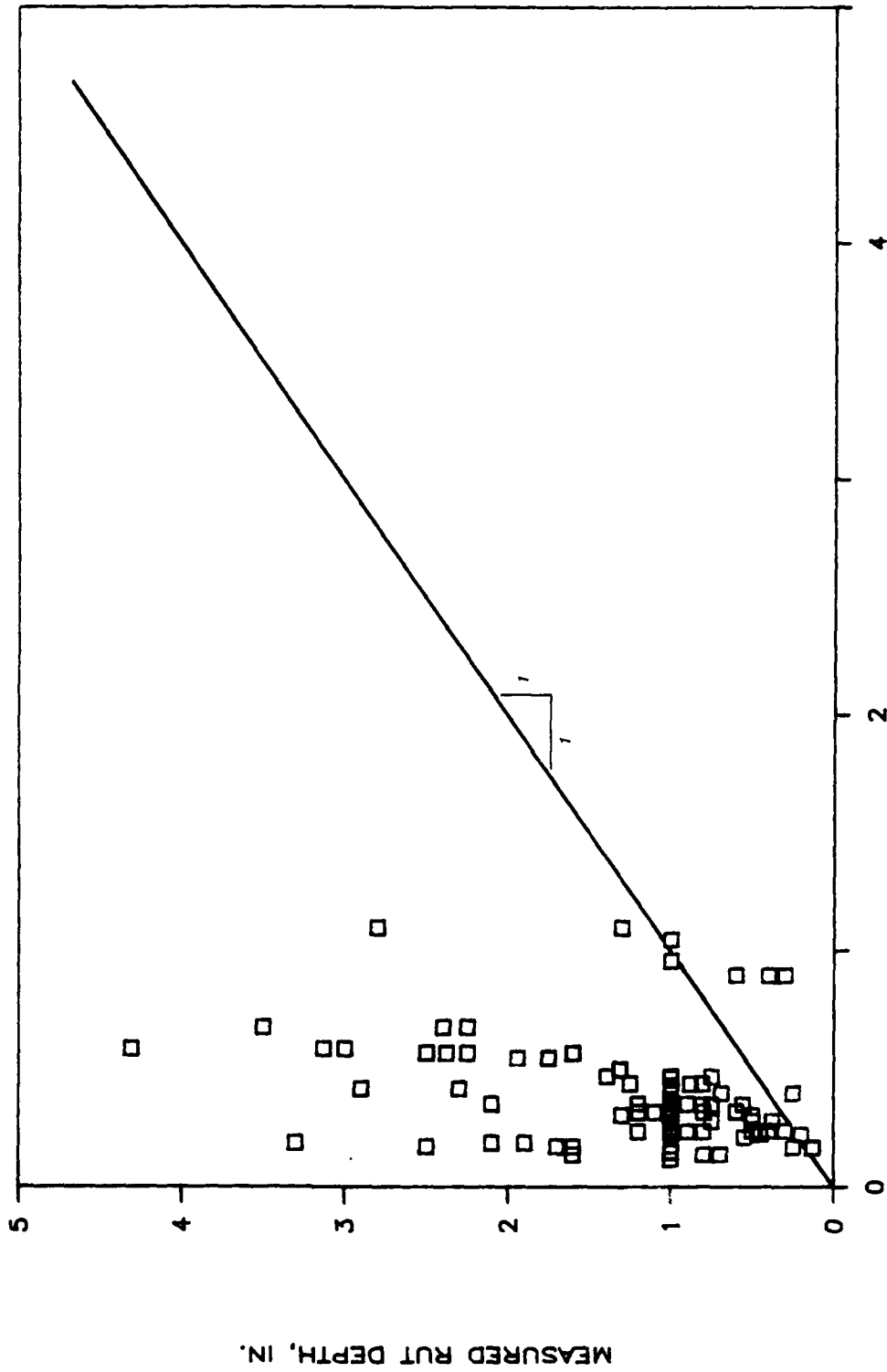


Figure V-16. Comparison of Measured Rut Depth to Predicted Rut Depth Using Barber Model.

SECTION VI

NEW PREDICTION MODELS

A. ESTIMATES OF PERFORMANCE

Prediction of rut depth and number of coverages to both 1- and 3-inch rut depths will be presented. To develop models, initially a stepwise regression method was applied to all data presented in Table VI-1. Many attempts were made in an effort to obtain meaningful models. Variables that showed strong correlation were selected from these attempts and are used in the models presented herein.

1. Rut Depth

For prediction of rut depth the following model was developed. Log coverages were entered into each variable since coverages is dominant, and at small coverage levels the rut depth values will approach zero as expected.

$$\text{Dependent Variable} = [(\text{Independent variables} \times \text{Coefficient}) + \text{Constant}$$

$$\text{Dependent Variable} = \text{Log (rut depth)}$$

Independent Variables	Coefficient
Log Cov * Base vertical strain, (10^{-6} in./in.)	-0.00001
Log Cov * AGE	0.04586
Log Cov * Subgrade vertical strain, (10^{-6} in./in.)	0.00029
Log Cov * Thickness of base, (in.)	0.01304
Log Cov * Base curvature index, (mils)	-0.75268
Log Cov * Surface curvature index deflections at "0" offset, (mils)	0.00194
Log Cov * Thickness of asphalt surface, (in.)	0.78863
Log Cov * Basin area, (in.)	-0.18625
Log Cov * Base tensile strain, (10^{-6} in./in.)	-0.00783
Log Cov * Impulse stiffness modulus, (kips/in.)-	-0.00179
Constant	-1.27505

R^2 - 0.792
Standard error - 0.177
Number of cases - 47

The above model can be discredited since many of the variables are adding to rut depth when there should be a decrease. For example, thickness of base and thickness of AC both have positive coefficients indicating that their increase would increase rut depth. For a pavement with an AC surface over a granular base, if the thickness of the AC was increased while the thickness and quality of the base and the strength of the subgrade remained constant, the magnitude of the rut depth should decrease. Likewise, if the thickness of the base was increased with the other parameters remaining constant, the rut depth should decrease. Therefore, this model is not valid.

Using a similar relationship as presented by Khedr (Reference 24), a regression analysis was performed on the rut depth data base. The following results were obtained and are shown in Figure VI-1.

Dependent Variable - Log (Rut Depth/Cov)

Independent Variable	Coefficient
Log Cov	-0.6579
Constant	-0.4357

R^2 - 0.508
Standard Error - 0.277
No. of Cases - 106

It should be noted that when the rut depth equals 1-inch, the relationship falls on a negative-sloped 45 degree line since $\log(1/\text{Cov})$ is plotted against $\log(\text{Cov})$.

2. Coverages to a 3-inch Rut Depth

ISM proved highly significant using stepwise regression analysis in predicting both rut depth and coverages to a selected rut depth where all variables were considered. Therefore, since the data base is rather small, regression was attempted using ISM and one other variable. For predicting coverages to a 3-inch rut depth, models were developed for new pavements and aged pavements as shown in Figure VI-2. The data base for developing the coverage level models is shown in Table VI-2. Relationships are as follows:

Three-inch Rut Depth

Coverages - $.530264(\text{ISM}) - 64.54$ for new pavements (21)

R^2 - 0.99
Standard error - 0.52
Number of cases - 4
Range of ISM - 141 to 344
Range of coverages - 6.5 to 93

Coverages - $.358388(\text{ISM}) - 57.62$ for aged pavements (22)

R^2 - .90
Standard error - 9.65
Number of cases - 7
Range of ISM - 187 to 382 kips per inch
Range of coverages - 6 to 87.7

By using the variable, $\text{Log}(\text{Age} + 1)$, to account for the difference in the above relationships, the following model was developed using the entire data base.

$$\text{Coverages} = -23.41(\text{Log (Age+1)}) + 0.4386(\text{ISM}) - 45.7 \quad (23)$$

R^2 - .927
 Standard error - 10.86
 Number of cases - 11
 Range of age - 0 to 30 years
 Range of ISM - 141 to 382 kips per inch

Characteristics of AC that change with age are the stiffness and ductility of the asphalt binder. Penetration of the extracted binder is an indicator of these properties. Hence, a regression model was developed for prediction of coverages to a 3-inch rut using penetration of the extracted AC binder. Results are as follows:

Dependent Variable - Cov to 3-inch rut

Independent Variables	Coefficients
ISM	0.4156
Penetration	0.4320
Constant	-76.45

R^2 - 0.907
 Standard error - 12.3
 Number of cases - 11

This model showed no improvement over the use of ISM and Age, which can be determined without destructive testing.

Another variable that is highly significant in predicting performance is the SCI multiplied by the deflection measured at the center of the applied load (DO). The deflections were normalized to 9,000 pounds to allow for load variations. The models developed are as follows:

Dependent Variable - Log coverages to 3-inch rut

For new test items:

Independent Variables	Coefficients
SCI * DO	-0.00070
Constant	2.350642

R^2 - 0.99
 Standard error - 0.055
 Number of cases - 4

For the aged test items:

Dependent Variable - Log coverages to 3-inch rut

Independent Variables	Coefficients
SCI * DO	-0.00099
Constant	2.128

R^2 - 0.65
Standard error - 0.000326

By including age the results are:

Dependent Variable - Log coverages to 3-inch rut

Independent Variables	Coefficients
SCI * DO	-0.00077
Log (Age + 1)	-0.35667

R^2 - 0.76
Standard error - 0.22

3. Coverages to 1-inch Rut Depth

For prediction of traffic levels to a 1-inch rut depth, several methods were evaluated. Prediction models using FWD data are given as follows:

One-inch Rut Depth

Coverages = .164(ISM) - 22.267 (24)

R^2 - .726
Standard error - 8.32
Number of cases - 11
Range of ISM - 141 to 382 kips per inch
Range of coverages - 1.6 to 54.5

Coverages = .1722(ISM) - 4.54(Log (Age + 1)) - 20.32 (25)

R^2 - .766
Standard error - 8.17
Number of cases - 11
Range of age - 0 to 30 years
Range of ISM - 141 to 382 kips per inch
Range of coverages - 1.6 to 54.5

$$\text{Log Coverages} = -0.344(\text{Log (Age+1)}) + 0.004518(\text{ISM}) + 0.00247(\text{Penetration}) \quad (26)$$

R^2 = 0.659
 Standard error = 0.307
 Number of cases = 11
 Range of ISM = 141 to 382 kips per inch
 Range of age = 0 to 30 years
 Range of penetration = 10 to 85

New Pavements:

$$\text{Log Coverages} = -0.00072 (\text{SCI})(\text{DO}) + 1.996 \quad (27)$$

R^2 = 0.794
 Standard error = 0.320
 Number of cases = 4

Aged Pavements:

$$\text{Log Coverages} = -0.00102 (\text{SCI})(\text{DO}) + 1.839 \quad (28)$$

R^2 = 0.598
 Standard error = 0.284
 Number of cases = 7

By combining and using Age:

$$\text{Log Coverages} = -0.00082 (\text{SCI})(\text{DO}) - 0.34279(\text{Log(Age+1)}) + 2.123 \quad (29)$$

R^2 = 0.693
 Standard error = 0.278
 Number of cases = 11

Using the relationship shown by Khedr (Reference 24), a similar form was developed for the base course vertical strain calculated for the F-4 loadings with the modulus values back calculated from the before-traffic FWD data. The results are shown in Figure VI-3 and the regression results are as follows:

$$\text{Log Cov} = 3.496 - 0.8197 (\text{Log Base Vert Strain/Coverages}) \quad (30)$$

R^2 = 0.938
 Standard error = 0.118
 Number of cases = 11
 Range of Base Vertical Strain = 6070 to 24200 10^{-6} in./in.
 Range of Coverages = 1.6 to 54.5

B. SELECTION OF BEST ESTIMATOR OF PERFORMANCE

The investigations described above were developed based on destructive test data (CBR), layered elastic methods (Base Vertical Strain) and the ISM. Figure VI-4 presents a comparison of the different methods.

The CBR predictions are based on the measured field CBR at the controlling layer. Hence, low base course strengths are considered. The base strain is based on the maximum vertical strain at the top of the base course. The ISM estimation is based on the model given as:

$$\text{COV} = 0.172 (\text{ISM}) - 4.54 (\text{Log}(\text{Age} + 1)) - 20.32 \quad (31)$$

The average difference in actual and predicted for the 11 items for each method is given below:

<u>Prediction</u>	<u>Average Difference for Actual Coverages</u>
CBR	1.13
Base Vertical Strain	15.3
Log(Base Vertical Strain/coverages)	2.44
ISM and Age	0.43

Considering all pavement test items, Equation 31 based on ISM and Age is the best predictor for this data base.

C. VALIDATION OF MODEL

In addition to traffic with the F-4 load cart at the North Field test site, traffic was applied with an F-15 load cart. The layer thicknesses were the same as for the F-4. The average ISM for the test item was 220 kips per inch. Using equation 31, the predicted F-4 coverages are 17.5.

Using the CBR evaluation procedure, a subgrade CBR of 9 with 2.1 inches of AC and 6.3 inches of base would produce 17.5 coverages of the F-4.

The F-15 evaluation would be as follows:

Design load - 68,000 pounds
Total thickness - 8.4 inches
CBR - 9
Allowable passes - 112
Pass to coverage ratio - 9.36
Estimated coverages - 11.9
Actual coverages from Reference 10 - 12.1

D. EVALUATION PROCEDURE

The evaluation procedure outlined herein is applicable only to flexible pavements containing unbound granular layers with ISMs less than 400 kips/inch. The procedure presented in this study is based on an ISM from a FWD loading of approximately 9000 lbs. applied through a 11.8-inch-diameter plate. FWD testing should be conducted at a loading as near as possible to the loading conditions of the evaluation aircraft. For pavements with ISMs greater than 400 kips/inch, a mechanistic procedure should be applied as described in Section V-C where the moduli are back calculated and limited vertical subgrade strain is calculated for the design aircraft.

The evaluation procedure is outlined in Figure VI-5. A program for correcting for temperature is given in Appendix C. The model for estimating coverages of an F-4 aircraft to a 1-inch rut is shown in Figure VI-6.

For determining the allowable passes for aircraft other than the F-4, the thickness of the layers is required. Using the allowable passes for the F-4, the load and contact area of the F-4, and the total pavement thickness above the subgrade, an "equivalent CBR" can be computed with the CBR design/evaluation procedure. With the equivalent CBR and thickness

data, allowable coverages for other aircraft can be calculated using the CBR procedure.

Layer thicknesses are also required for the mechanistic analysis. Coring will be required for determining thicknesses of the pavement layers when construction data are not available.

Table VI-1. DATA BASE FOR RUT DEPTH PREDICTION

ITEM	DEPTH IN.	COV	ISM K/IN	AGE YRS	FORCE LBS	D0 MILS	D12 MILS	D24 MILS	D36 MILS	D48 MILS	AREA IN	AC		BASE		BASE		SUBC		SURF		BASE		SUBC	
												STRAIN 10E-6	STRESS PSI	VERT STRAIN 10E-6	TENSILE STRESS PSI	VERT STRESS PSI	VERT STRAIN 10E-6	THICK IN.	CBR %	STRAIN 10E-6	STRESS PSI	THICK IN.	CBR %	STRAIN 10E-6	THICK IN.
NFF4	0.25	2.0	344	0	9024	26.2	6.0	2.6	1.5	1.1	10.28	2010	237	10300	54.6	-33.6	115.0	3160	2.1	6.3	100	20			
NFF4	0.43	10.0	344	0	9024	26.2	6.0	2.6	1.5	1.1	10.28	2010	237	10300	54.6	-33.6	115.0	3160	2.1	6.3	100	20			
NFF4	0.83	20.0	344	0	9024	26.2	6.0	2.6	1.5	1.1	10.28	2010	237	10300	54.6	-33.6	115.0	3160	2.1	6.3	100	20			
NFF4	2.12	30.0	344	0	9024	26.2	6.0	2.6	1.5	1.1	10.28	2010	237	10300	54.6	-33.6	115.0	3160	2.1	6.3	100	20			
NFF4	2.62	40.0	344	0	9024	26.2	6.0	2.6	1.5	1.1	10.28	2010	237	10300	54.6	-33.6	115.0	3160	2.1	6.3	100	20			
NFF4	3.50	100.0	344	0	9024	26.2	6.0	2.6	1.5	1.1	10.28	2010	237	10300	54.6	-33.6	115.0	3160	2.1	6.3	100	20			
WES1	0.50	13.1	217	0	8628	39.8	17.6	8.1	3.8	3.1	14.32	1860	223	9860	58.2	26.9	63.9	5710	1.7	8.2	100	7			
WES1	1.00	18.6	217	0	8628	39.8	17.6	8.1	3.8	3.1	14.32	1860	223	9860	58.2	26.9	63.9	5710	1.7	8.2	100	7			
WES1	1.25	20.5	217	0	8628	39.8	17.6	8.1	3.8	3.1	14.32	1860	223	9860	58.2	26.9	63.9	5710	1.7	8.2	100	7			
WES1	1.50	22.9	217	0	8628	39.8	17.6	8.1	3.8	3.1	14.32	1860	223	9860	58.2	26.9	63.9	5710	1.7	8.2	100	7			
WES1	1.75	26.2	217	0	8628	39.8	17.6	8.1	3.8	3.1	14.32	1860	223	9860	58.2	26.9	63.9	5710	1.7	8.2	100	7			
WES1	2.00	32.7	217	0	8628	39.8	17.6	8.1	3.8	3.1	14.32	1860	223	9860	58.2	26.9	63.9	5710	1.7	8.2	100	7			
WES1	2.25	39.3	217	0	8628	39.8	17.6	8.1	3.8	3.1	14.32	1860	223	9860	58.2	26.9	63.9	5710	1.7	8.2	100	7			
WES1	2.50	42.6	217	0	8628	39.8	17.6	8.1	3.8	3.1	14.32	1860	223	9860	58.2	26.9	63.9	5710	1.7	8.2	100	7			
WES1	3.75	46.1	217	0	8628	39.8	17.6	8.1	3.8	3.1	14.32	1860	223	9860	58.2	26.9	63.9	5710	1.7	8.2	100	7			
WES2	0.25	6.5	157	0	8323	53.0	27.6	10.0	6.0	3.8	15.19	2150	238	13200	60.4	33.5	57.8	7730	1.4	9.0	100	6			
WES2	0.50	13.1	157	0	8323	53.0	27.6	10.0	6.0	3.8	15.19	2150	238	13200	60.4	33.5	57.8	7730	1.4	9.0	100	6			
WES2	2.00	16.4	157	0	8323	53.0	27.6	10.0	6.0	3.8	15.19	2150	238	13200	60.4	33.5	57.8	7730	1.4	9.0	100	6			
WES2	2.25	19.6	157	0	8323	53.0	27.6	10.0	6.0	3.8	15.19	2150	238	13200	60.4	33.5	57.8	7730	1.4	9.0	100	6			
WES2	3.00	20.5	157	0	8323	53.0	27.6	10.0	6.0	3.8	15.19	2150	238	13200	60.4	33.5	57.8	7730	1.4	9.0	100	6			
WES3	3.00	6.5	141	0	8164	57.7	27.2	12.2	6.3	4.3	14.85	354	270	9990	85.1	63.6	59.0	9560	0.5	9.4	100	6			
WP1	1.30	5.5	187	22	8851	47.4	23.5	3.5	1.9	1.1	13.08	2700	43	24200	0.6	24.6	37.3	932	3.0	6.0	12	6			
WP1	5.10	6.5	187	22	8851	47.4	23.5	3.5	1.9	1.1	13.08	2700	43	24200	0.6	24.6	37.3	932	3.0	6.0	12	6			
WP2	0.25	20.5	382	24	8867	23.2	11.3	3.5	2.1	1.5	14.20	1520	129	6070	31.0	1.0	5.1	169	3.0	47.0	33	6			
WP2	0.50	32.7	382	24	8867	23.2	11.3	3.5	2.1	1.5	14.20	1520	129	6070	31.0	1.0	5.1	169	3.0	47.0	33	6			
WP2	1.50	46.0	382	24	8867	23.2	11.3	3.5	2.1	1.5	14.20	1520	129	6070	31.0	1.0	5.1	169	3.0	47.0	33	6			
WP2	2.00	65.6	382	24	8867	23.2	11.3	3.5	2.1	1.5	14.20	1520	129	6070	31.0	1.0	5.1	169	3.0	47.0	33	6			

Table VI-1. DATA BASE FOR RUT DEPTH PREDICTION (CONCLUDED)

ITEM	RUT DEPTH IN.	COV	ISM K/IN	AGE YRS	FORCE LBS	D0 MILS	D12 MILS	D24 MILS	D36 MILS	D48 MILS	AREA IN	AC STRAIN 10E-6		BASE VERT STRAIN 10E-6		BASE SHEAR STRESS		BASE TENSILE STRESS		SUBC VERT STRAIN 10E-6		SUBC TENSILE STRESS		SURF THICK IN.	BASE THICK IN.	BASE CBR %	SUBC CBR %
												IN/IN	PSI	IN/IN	PSI	IN/IN	PSI	IN/IN	PSI	IN/IN	PSI	IN/IN	PSI				
WP2	2.75	72.2	382	24	8867	23.2	11.3	3.5	2.1	1.5	14.20	1520	129	6070	31.0	1.0	5.1	169	3.0	47.0	33	6					
WP2	3.00	87.7	382	24	8867	23.2	11.3	3.5	2.1	1.5	14.20	1520	129	6070	31.0	1.0	5.1	169	3.0	47.0	33	6					
WP3	1.13	6.5	201	9	9200	45.7	23.6	6.3	2.5	2.4	14.18	2880	173	14200	37.5	6.8	45.8	3090	2.0	12.0	33	7					
WP3	1.25	7.9	201	9	9200	45.7	23.6	6.3	2.5	2.4	14.18	2880	173	14200	37.5	6.8	45.8	3090	2.0	12.0	33	7					
WP3	3.50	12.3	201	9	9200	45.7	23.6	6.3	2.5	2.4	14.18	2880	173	14200	37.5	6.8	45.8	3090	2.0	12.0	33	7					
WP4	0.50	6.5	280	21	9057	32.3	14.3	3.7	1.5	1.4	12.97	1980	200	9620	46.6	5.8	48.2	2030	2.0	12.0	72	8					
WP4	1.20	16.2	280	21	9057	32.3	14.3	3.7	1.5	1.4	12.97	1980	200	9620	46.6	5.8	48.2	2030	2.0	12.0	72	8					
WP4	2.25	19.5	280	21	9057	32.3	14.3	3.7	1.5	1.4	12.97	1980	200	9620	46.6	5.8	48.2	2030	2.0	12.0	72	8					
WP4	3.10	22.1	280	21	9057	32.3	14.3	3.7	1.5	1.4	12.97	1980	200	9620	46.6	5.8	48.2	2030	2.0	12.0	72	8					
W1	0.60	6.5	249	22	9081	36.5	8.5	5.1	3.7	2.9	11.08	870	272	9370	68.5	2.7	11.7	720	1.0	29.0	33	4					
W1	0.70	12.3	249	22	9081	36.5	8.5	5.1	3.7	2.9	11.08	870	272	9370	68.5	2.7	11.7	720	1.0	29.0	33	4					
W1	1.50	20.5	249	22	9081	36.5	8.5	5.1	3.7	2.9	11.08	870	272	9370	68.5	2.7	11.7	720	1.0	29.0	33	4					
W1	2.75	34.1	249	22	9081	36.5	8.5	5.1	3.7	2.9	11.08	870	272	9370	68.5	2.7	11.7	720	1.0	29.0	33	4					
W1	3.00	38.2	249	22	9081	36.5	8.5	5.1	3.7	2.9	11.08	870	272	9370	68.5	2.7	11.7	720	1.0	29.0	33	4					
W2	1.60	6.8	203	30	9149	45.0	25.9	9.7	5.3	3.8	16.20	2530	141	10900	33.1	5.4	33.2	3570	2.5	12.0	102	4					
W2	2.50	13.6	203	30	9149	45.0	25.9	9.7	5.3	3.8	16.20	2530	141	10900	33.1	5.4	33.2	3570	2.5	12.0	102	4					
W2	3.30	18.0	203	30	9149	45.0	25.9	9.7	5.3	3.8	16.20	2530	141	10900	33.1	5.4	33.2	3570	2.5	12.0	102	4					
W3	2.25	6.8	210	24	8875	42.2	18.4	7.1	4.1	2.8	13.83	2550	144	11100	33.1	-0.6	25.9	2040	2.5	16.0	37	4					
W3	3.50	11.7	210	24	8875	42.2	18.4	7.1	4.1	2.8	13.83	2550	144	11100	33.1	-0.6	25.9	2040	2.5	16.0	37	4					

Table VI-2. DATA BASE FOR PREDICTING COVERAGES

RUT ITEM DEPTH IN.	NORMALIZED BASINS FOR 9000 LBS FORCE														AC BINDER PENETRATION 0.1 mm							
	COVERAGES		D0	D12	D24	D36	D48	ISM	AREA	D0	D12	D24	D36	D48	SCI	BCI	SPR	ERI	SCI*DO	AGE		
	LBS	MILS	MILS	MILS	MILS	MILS	MILS	K/IN	IN	MILS	MILS	MILS	MILS	MILS	MILS	MILS	MILS	KSI	MILS*2	YEARS	0.1 mm	
NFF4	1	30.0	9024	26.2	6.0	2.6	1.5	1.1	344	10.28	26.1	6.0	2.6	1.5	1.1	20.1	0.399	0.285	17.1	526.4	0	80
WES1	1	20.5	8628	39.8	17.6	8.1	3.8	3.1	217	14.32	41.5	18.4	8.4	4.0	3.2	23.2	0.730	0.364	8.3	961.4	0	80
WES2	1	16.3	8323	53.0	27.6	10.0	6.0	3.8	157	15.19	57.3	29.8	10.8	6.5	4.1	27.5	2.379	0.379	2.9	1574.1	0	80
WES3	1	1.6	8164	57.7	27.2	12.2	6.3	4.3	141	14.85	63.6	30.0	13.4	6.9	4.7	33.6	2.205	0.373	2.3	2138.7	0	80
WP1	1	5.3	8851	47.4	23.5	3.5	1.9	1.1	187	13.08	48.2	23.9	3.6	1.9	1.1	24.3	0.813	0.327	15.3	1171.3	22	19
WP2	1	54.5	8867	23.2	11.3	3.5	2.1	1.5	382	14.20	23.5	11.5	3.6	2.1	1.5	12.1	0.609	0.359	14.5	284.4	24	24
WP3	1	8.2	9200	45.7	23.6	6.3	2.5	2.4	201	14.18	44.7	23.1	6.2	2.4	2.3	21.6	0.098	0.352	13.3	966.5	9	19
WP4	1	13.6	9057	32.3	14.3	3.7	1.5	1.4	280	12.97	32.1	14.2	3.7	1.5	1.4	17.9	0.099	0.329	17.1	574.1	21	20
W1	1	14.3	9081	36.5	8.5	5.1	3.7	2.9	249	11.08	36.2	8.4	5.1	3.7	2.9	27.8	0.793	0.311	9.2	1003.8	22	9
W2	1	3.4	9149	45.0	25.9	9.7	5.3	3.8	203	16.20	44.3	25.5	9.5	5.2	3.7	18.8	1.476	0.399	5.2	831.7	30	2
W3	1	4.5	8875	42.2	18.4	7.1	4.1	2.8	210	13.83	42.8	18.7	7.2	4.2	2.8	24.1	1.318	0.354	7.8	1032.9	24	5
NFF4	3	93.0	9024	26.2	6.0	2.6	1.5	1.1	344	10.28	26.1	6.0	2.6	1.5	1.1	20.1	0.399	0.285	17.1	526.4	0	80
WES1	3	46.1	8628	39.8	17.6	8.1	3.8	3.1	217	14.32	41.5	18.4	8.4	4.0	3.2	23.2	0.730	0.364	8.3	961.4	0	80
WES2	3	20.5	8323	53.0	27.6	10.0	6.0	3.8	157	15.19	57.3	29.8	10.8	6.5	4.1	27.5	2.379	0.379	2.9	1574.1	0	80
WES3	3	6.5	8164	57.7	27.2	12.2	6.3	4.3	141	14.85	63.6	30.0	13.4	6.9	4.7	33.6	2.205	0.373	2.3	2138.7	0	80
WP1	3	6.0	8851	47.4	23.5	3.5	1.9	1.1	187	13.08	48.2	23.9	3.6	1.9	1.1	24.3	0.813	0.327	15.3	1171.3	22	19
WP2	3	87.7	8867	23.2	11.3	3.5	2.1	1.5	382	14.20	23.5	11.5	3.6	2.1	1.5	12.1	0.609	0.359	14.5	284.4	24	24
WP3	3	12.3	9200	45.7	23.6	6.3	2.5	2.4	201	14.18	44.7	23.1	6.2	2.4	2.3	21.6	0.098	0.352	13.3	966.5	9	19
WP4	3	22.1	9057	32.3	14.3	3.7	1.5	1.4	280	12.97	32.1	14.2	3.7	1.5	1.4	17.9	0.099	0.329	17.1	574.1	21	20
W1	3	38.2	9081	36.5	8.5	5.1	3.7	2.9	249	11.08	36.2	8.4	5.1	3.7	2.9	27.8	0.793	0.311	9.2	1003.8	22	9
W2	3	18.0	9149	45.0	25.9	9.7	5.3	3.8	203	16.20	44.3	25.5	9.5	5.2	3.7	18.8	1.476	0.399	5.2	831.7	30	2
W3	3	11.7	8875	42.2	18.4	7.1	4.1	2.8	210	13.83	42.8	18.7	7.2	4.2	2.8	24.1	1.318	0.354	7.8	1032.9	24	5

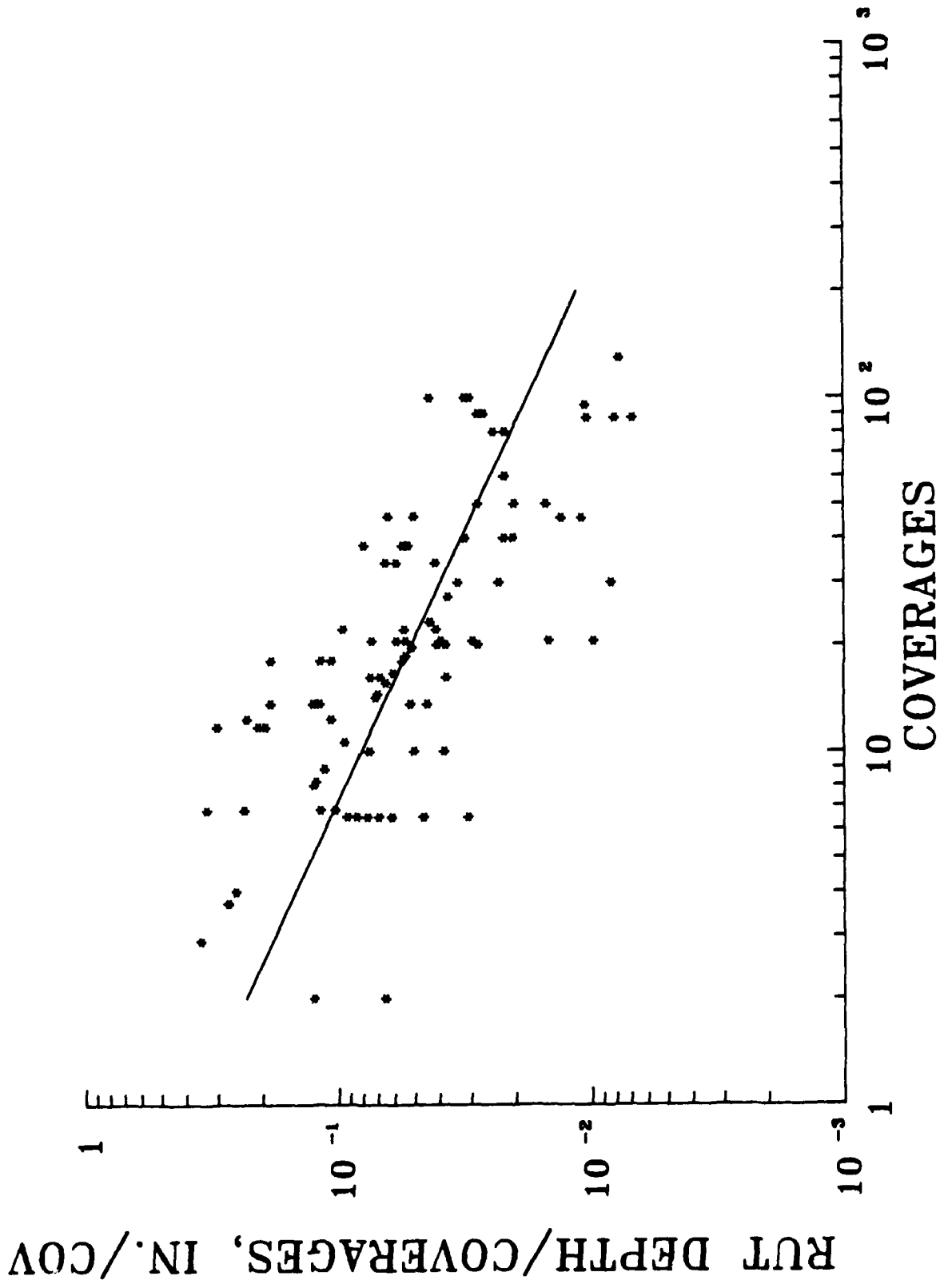


Figure VI-1. Logarithmic Relationship between Rut Depth and Coverages

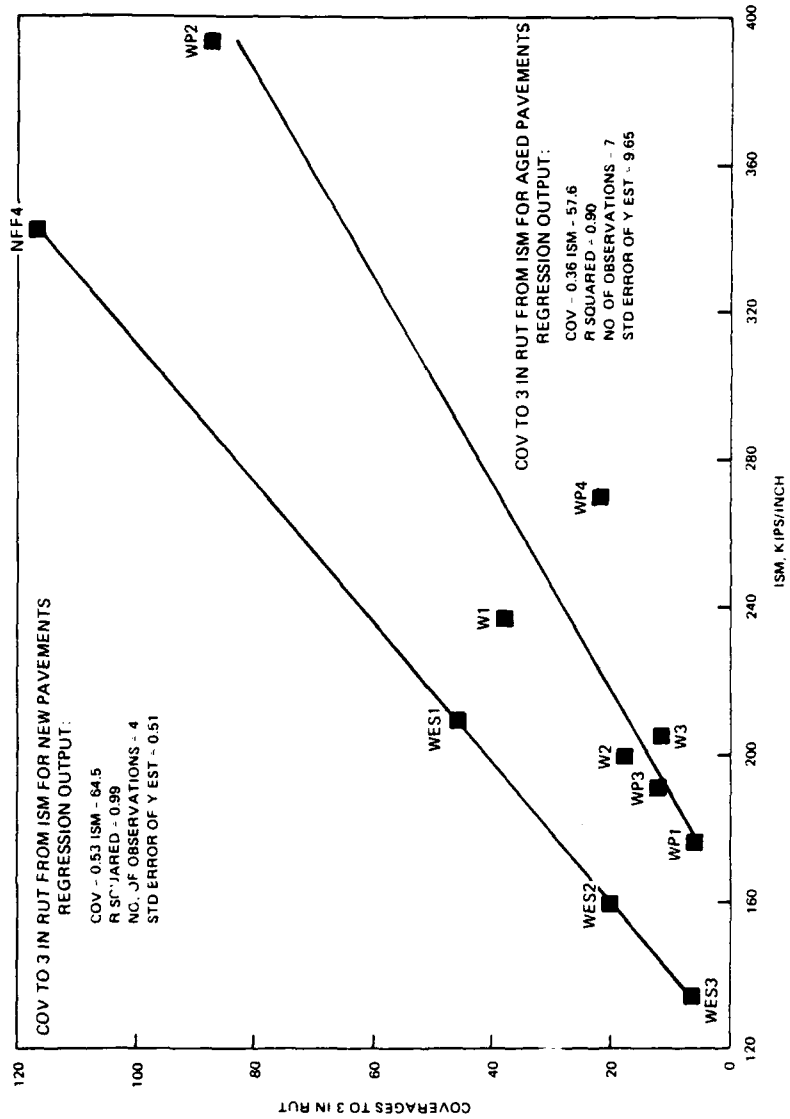


Figure VI-2. Estimates of Coverages to a 3-inch Rut Depth.

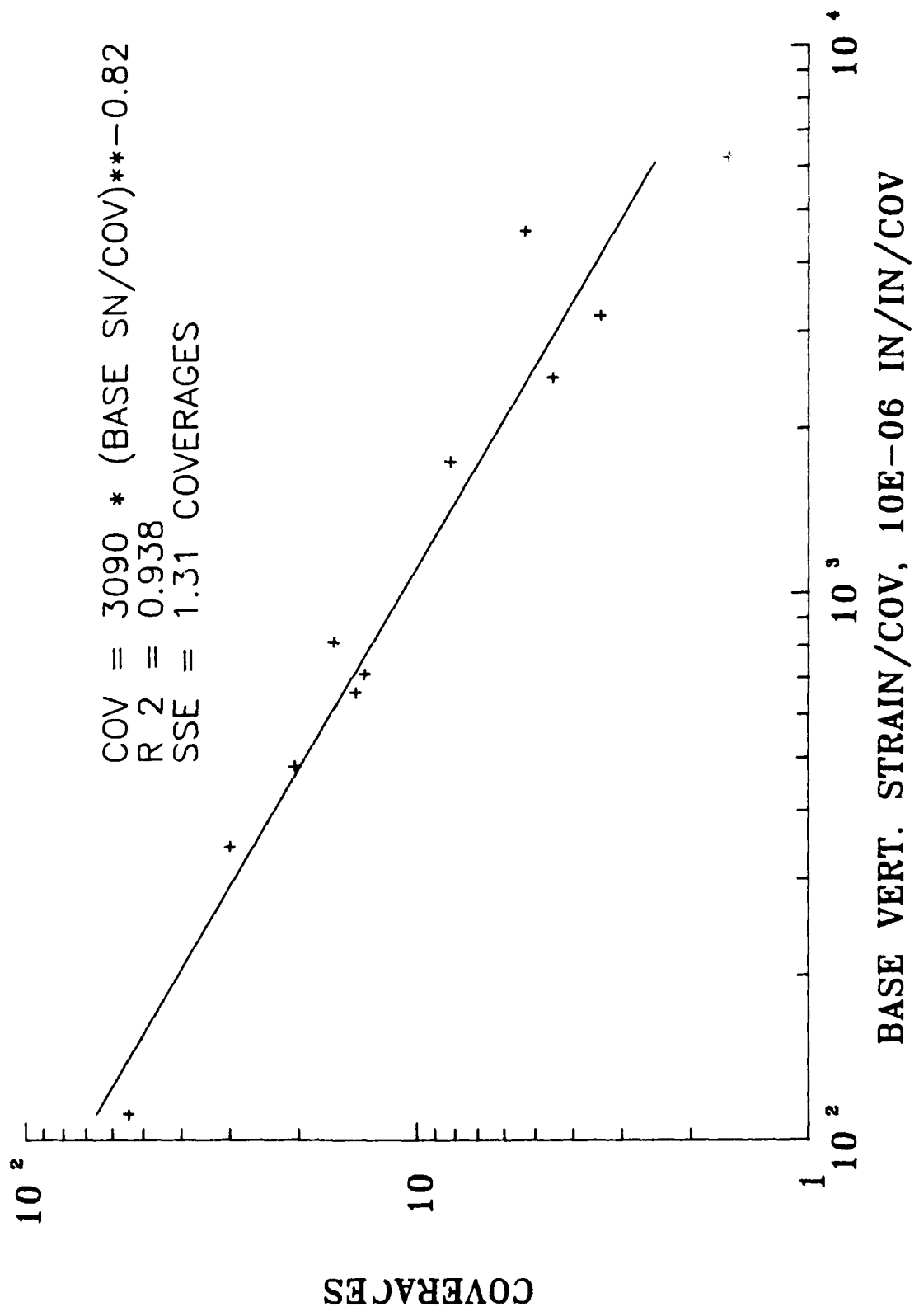


Figure VI-3. Logarithmic Relationship between Base Course Vertical

TO A ONE INCH RUT DEPTH

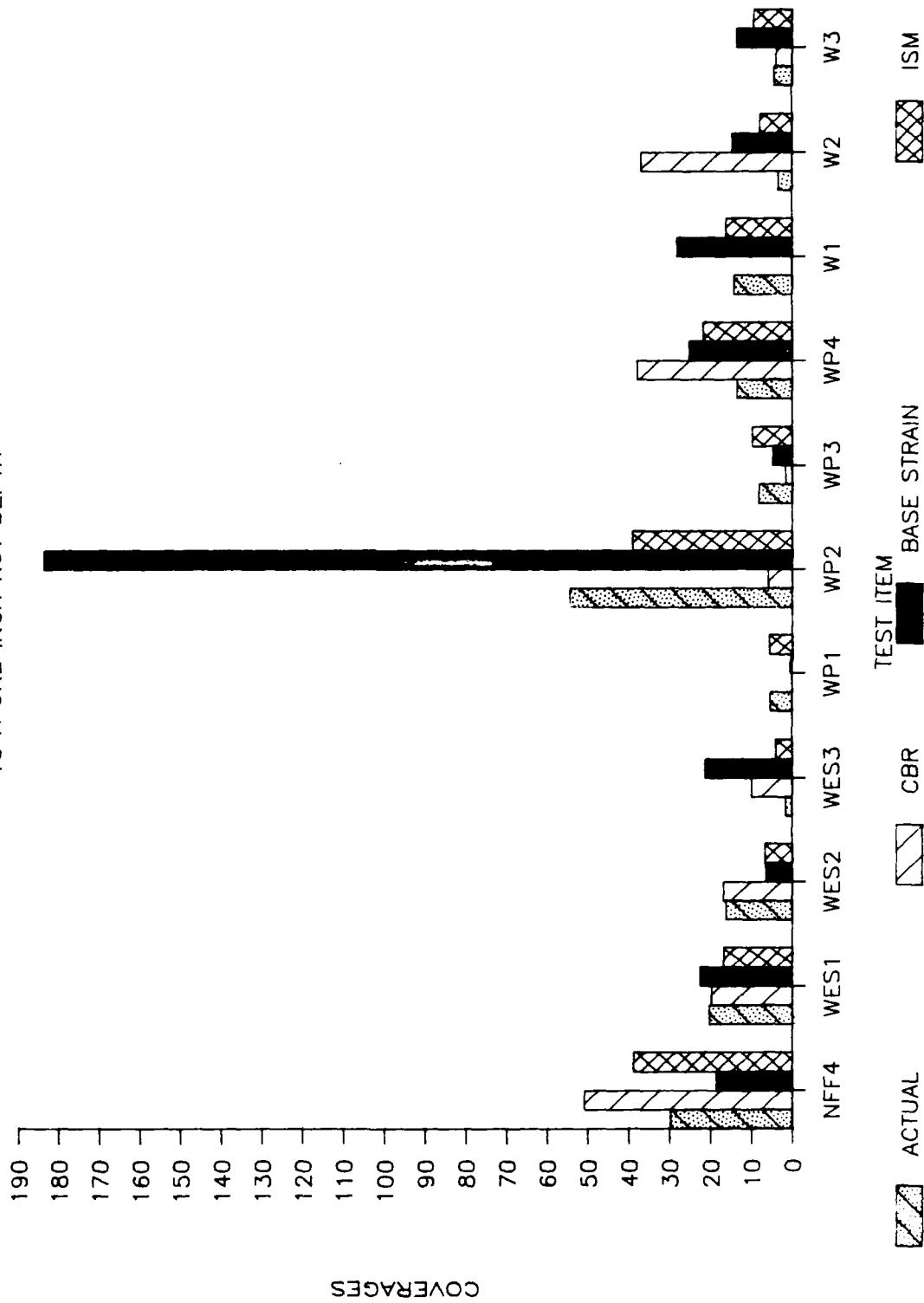


Figure VI-4. Comparisons of Prediction Methods for Coverages to a 1-inch Rut Depth.

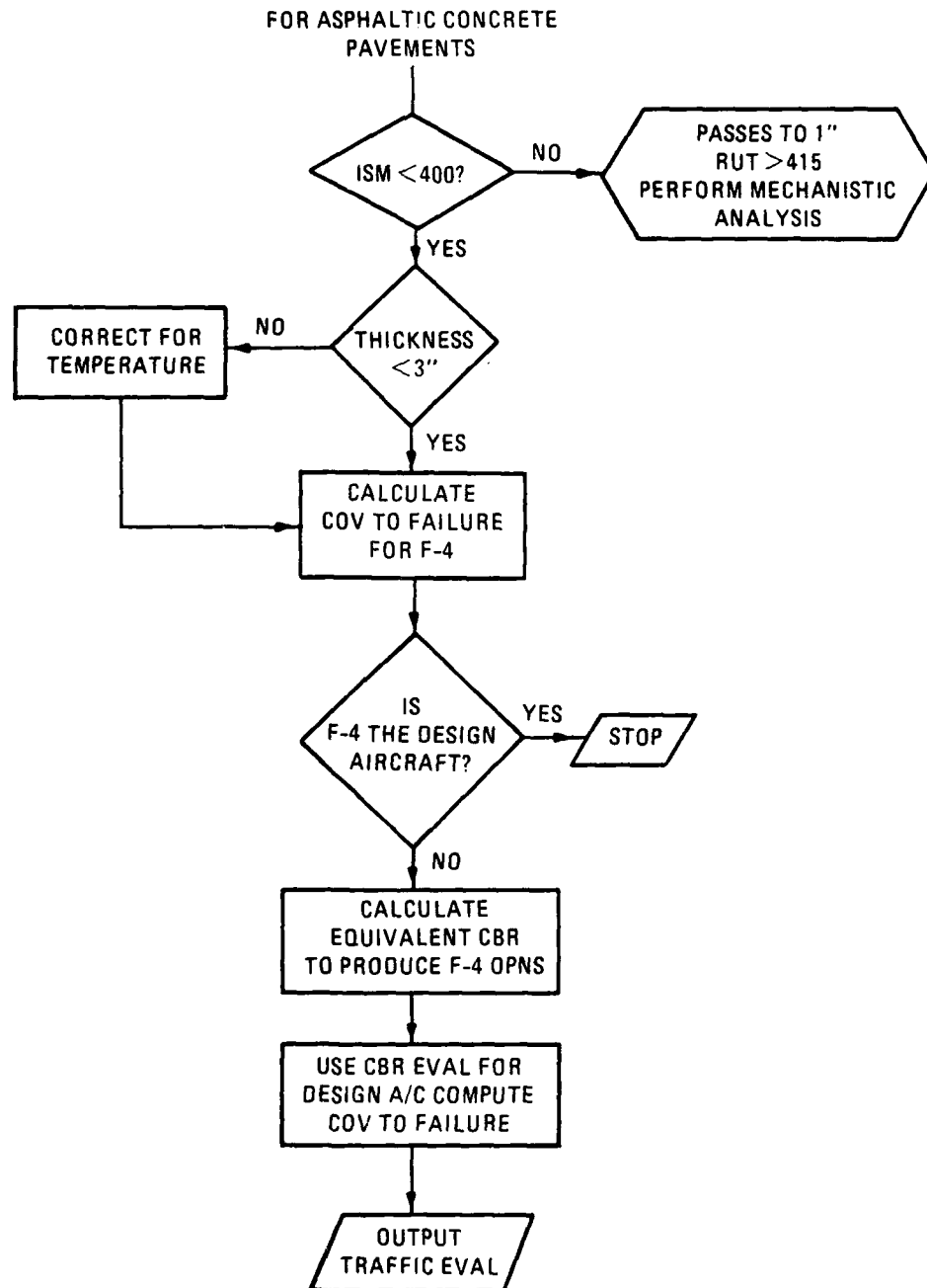


Figure VI-5. Flow Chart for Low-Volume Pavement Evaluation.

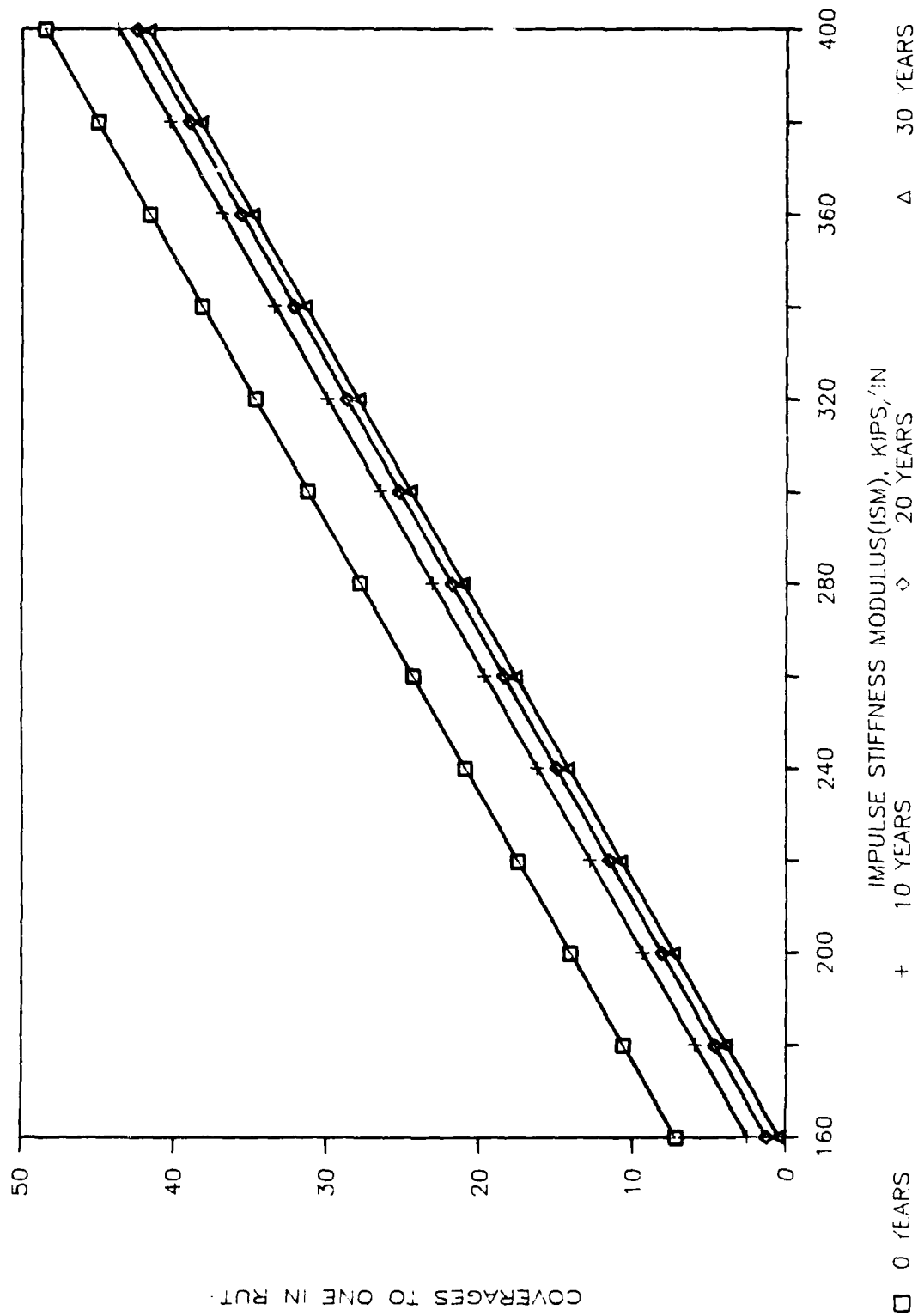


Figure VI-6. ISM versus Allowable Coverages of an F-4 Aircraft for Low-Volume Flexible Pavements.

SECTION VII

CONCLUSIONS AND RECOMMENDATIONS

The findings of this report are applicable to the evaluation of low traffic volume pavements containing AC or DBST surface courses over an unbound granular base/subbase layer. Potential ALRS pavements may be constructed at airfields or may be selected from existing facilities such as roads, streets, or major highways. The findings will apply to pavements (highway and airfield) with the above construction for the evaluation for fighter-type aircraft. An evaluation methodology was developed for low-volume pavements that accounts for age and temperature at the time of testing and utilizes data from an FWD nondestructive test device.

A. CONCLUSIONS

The following conclusions apply to low traffic volume pavements of asphalt and granular material construction.

1. Equation 31, which is a function of the ISM, is the best estimator of pavement performance for low-volume airfield pavements with the following constraints.

- a. ISM should be less than 400 kips/inch.
- b. ISM testing should be conducted at a loading as near as possible to the loading conditions of the evaluation aircraft.

2. For evaluation when CBRs are measured on all pavement layers, the CBR procedure is the next best estimator of performance of low-volume pavements.

3. Pavement age is significant in predicting coverages to both 1- and 3-inch rut depths.

4. Temperature did not cause a measurable change in deflections for pavements containing less than a 3-inch asphalt surface layer.

5. Base course failure (rutting) is a significant mode of failure for pavements with thin asphalt surfacing.

6. Base course modulus estimated from back calculation methods may be unreasonably low when the AC surface course contains cracks and does not behave as a continuum.

7. Mechanistic procedures must include consideration of potential base course layer failure as well as the subgrade.

8. Surface temperatures measured with an infrared gun provide excellent input for the estimation of mean pavement temperatures.

B. RECOMMENDATIONS

The following recommendations are presented as a result of the investigation reported herein.

1. The evaluation procedure using the FWD presented herein is recommended for monitoring the structural condition of ALRS pavements to ensure that the ALRS will support the required mission.

2. A detailed monitoring program for an existing ALRS is recommended to confirm the nondestructive evaluation procedure and to ascertain the time interval required for testing ALRS pavements to be constructed in the future. This program should include CBR tests and other measurements of strength (i.e., shear strength of granular layer) on pavement layers in areas of questionable strength. This program will also identify any change in strength properties due to environmental aging and changing moisture conditions.

3. Further investigations are recommended for determining a better procedure for modeling granular materials to describe the total pavement response and performance.

4. The base course materials selected for construction of ALRS pavements should have strength properties with minimum moisture and frost sensitivity.

5. For ALRS pavement evaluations where the FWD is not available, the CBR procedure is recommended where CBRs are obtained for all unbound pavement layers.

6. For testing pavements under *simulated service traffic*, a detailed laboratory investigation should be performed on the AC, base, and subgrade materials. The test program should include repeated load test to determine modulus and permanent deformation behavior for all materials and triaxial shear strength testing on unbound materials to establish shear strength parameters c and Φ .

APPENDIX A

FALLING WEIGHT DEFLECTOMETER DEFLECTION BASIN DATA

TABLE A-1. FALLING WEIGHT DEFLECTOMETER DEFLECTION BASIN DATA

Station No.	Force lbs.	Deflections				
		0-in. mils	12-in. mils	24-in. mils	36-in. mils	48-in. mils
<u>WES 1 (Clay Subgrade)^a</u>						
0+10	4,560	*	9.9	4.4	2.9	3.4
	7,749	*	20.8	7.2	10.0	3.3
	11,102	*	39.0	10.0	6.5	4.8
0+20	4,350	*	16.1	5.5	2.8	1.9
	7,309	*	27.9	9.6	4.8	3.0
	10,233	*	45.3	12.2	6.6	4.3
0+30	4,420	*	12.8	4.1	2.4	1.8
	7,325	*	21.0	6.8	4.0	2.9
	10,226	*	32.5	8.9	5.5	4.3
0+40	4,358	*	13.0	5.4	2.8	1.7
	7,266	*	22.0	9.8	4.4	2.6
	10,129	*	29.2	12.2	5.8	5.0
<u>WES 2 (Clay Subgrade)</u>						
0+10	4,258	*	18.8	6.8	18.1	18.1
	7,107	*	32.9	10.8	5.6	3.7
	9,902	*	45.7	14.0	6.4	4.2
0+20	4,001	*	17.5	7.4	3.5	1.8
	6,781	*	36.8	12.2	5.3	3.8
	9,403	*	51.1	15.4	7.0	5.3
0+30	4,172	*	17.2	6.3	3.1	2.0
	7,007	*	31.4	10.7	5.1	3.4
	9,721	*	7.5	14.7	7.3	4.8
0+40	4,366	*	15.2	5.9	3.0	2.0
	7,312	*	29.6	10.6	5.0	3.4
	10,115	*	45.6	14.8	7.7	4.8

^a 11.8-in.-diameter plate.

* Deflection exceeded range of velocity transducer.

TABLE A-1. FALLING WEIGHT DEFLECTOMETER DEFLECTION BASIN DATA
(CONTINUED)

Station No.	Force lbs.	Deflections				
		0-in. mils	12-in. mils	24-in. mils	36-in. mils	48-in. mils
<u>WES 3 (Clay Subgrade)</u>						
0+10	4,190	*	16.2	6.6	3.5	2.1
	7,091	*	30.5	11.4	5.3	3.3
	9,772	*	66.1	15.9	7.5	4.8
0+20	4,258	*	17.7	6.9	4.4	2.2
	7,147	*	33.0	12.8	6.4	3.8
	9,939	*	52.2	17.3	8.4	5.7
0+30	3,707	*	16.7	8.3	4.0	2.3
	6,225	*	36.4	13.6	6.5	4.0
	8,906	*	51.0	19.3	9.7	5.6
0+40	4,295	*	14.4	6.0	3.2	2.1
	7,334	*	30.5	10.5	5.5	3.5
	10,265	*	46.7	25.6	7.9	5.2
<u>WES South Overrun (Silt Subgrade)</u>						
	4,457	28.5	6.0	3.3	1.8	1.3
	8,485	49.1	12.2	5.3	3.4	2.6
	14,092	77.9	19.5	9.0	5.4	3.9
<u>WES-North Overrun (Silt Subgrade)</u>						
	4,488	32.3	6.9	4.7	1.8	1.1
	8,485	51.3	12.0	4.8	2.9	2.4
	14,067	*	20.7	7.3	4.7	3.5
<u>WES 1 (Base Course)</u>						
0+10	4,510	40.6	12.6	5.0	2.7	1.8
	8,279	76.6	30.8	9.4	4.8	3.6
	13,201	*	40.6	14.6	7.2	3.6

* Deflection exceeded range of velocity transducer.

TABLE A-1. FALLING WEIGHT DEFLECTOMETER DEFLECTION BASIN DATA
(CONTINUED)

Station No.	Force lbs.	Deflections				
		0-in. mils	12-in. mils	24-in. mils	36-in. mils	48-in. mils
<u>WES 1 (Base Course) Continued</u>						
0+20	4,303	38.1	13.3	5.3	3.1	2.0
	8,136	72.8	30.3	10.6	5.4	3.7
	13,085	*	55.1	17.7	9.1	5.7
0+30	4,338	42.4	16.5	6.3	3.5	2.4
	8,088	*	32.9	11.6	6.2	3.9
	12,982	*	60.0	18.9	9.4	6.2
0+40	4,288	46.1	17.0	6.0	3.1	2.0
	8,021	*	38.1	11.4	5.4	3.4
	12,796	*	71.9	19.7	8.7	5.6
<u>WES 2 (Base Course)</u>						
0+10	4,327	54.1	22.8	8.1	3.8	2.4
	7,870	*	47.6	14.6	6.6	4.3
	12,450	*	*	24.0	9.7	6.8
0+20	4,160	53.5	22.3	8.7	4.3	2.5
	7,818	*	46.5	16.1	7.4	4.7
	12,466	*	*	26.2	11.5	7.2
0+30	4,227	46.1	19.5	-	3.5	-
	7,894	*	42.1	12.8	6.3	3.8
	12,644	*	76.0	21.9	9.8	6.4
0+40	4,168	46.5	19.5	7.5	3.7	1.9
	7,894	*	39.4	13.4	6.5	4.3
	12,718	*	69.7	23.5	10.4	6.5
<u>WES 3 (Base Course)</u>						
0+10	4,259	41.1	19.5	7.5	3.9	2.4
	7,905	77.6	40.4	15.0	7.0	4.0
	12,788	*	73.8	25.2	11.4	6.5

* Deflection exceeded range of velocity transducer.

TABLE A-1. FALLING WEIGHT DEFLECTOMETER DEFLECTION BASIN DATA
(CONTINUED)

Station No.	Force lbs.	Deflections				
		0-in. mils	12-in. mils	24-in. mils	36-in. mils	48-in. mils
<u>WES 3 (Base Course) Continued</u>						
0+20	4,096	37.5	17.5	7.1	3.6	1.9
	7,918	77.3	38.4	13.8	6.9	4.2
	12,812	*	73.0	23.6	11.3	6.9
0+30	4,136	35.4	16.1	6.9	3.9	2.3
	7,926	69.1	35.4	13.8	7.1	4.2
	12,895	*	66.9	24.3	11.2	7.3
0+40	4,009	32.4	13.8	5.9	3.0	2.0
	7,910	64.0	30.3	11.8	6.3	3.8
	12,987	*	59.1	21.3	10.7	6.7
<u>WES 1 (0 Coverages)</u>						
0+10	8,628	39.8	17.6	8.1	3.8	3.1
	14,099	65.0	31.4	14.3	6.5	5.2
0+20	8,546	43.5	20.7	9.8	4.6	3.4
	13,952	72.6	36.5	17.3	7.7	5.6
0+30	8,517	37.8	18.3	8.8	4.3	3.2
	13,999	62.2	31.5	18.5	7.4	5.9
0+40	8,466	42.7	21.6	10.2	4.5	3.5
	13,840	70.1	37.9		8.1	
<u>WES 1 (6.5 Coverages)</u>						
0+10	8,358	53.5	23.6	8.9	3.9	3.0
	13,546	*	44.1	14.6	6.5	5.1
0+20	8,271	61.5	29.3	10.2	4.6	3.4
	13,305	*	45.1	17.7	7.3	5.6

* Deflection exceeded range of velocity transducer.

TABLE A-1. FALLING WEIGHT DEFLECTOMETER DEFLECTION BASIN DATA
(CONTINUED)

Station No.	Force lbs.	Deflections				
		0-in. mils	12-in. mils	24-in. mils	36-in. mils	48-in. mils
<u>WES 1 (6.5 Coverages) Continued</u>						
0+30	8,239	56.2	25.6	9.8	4.6	3.5
	13,435	*	45.3	17.1	7.9	5.8
0+40	8,144	66.9	29.5	10.6	4.5	3.3
	13,197	*	51.0	18.9	7.8	5.7
<u>WES 1 (20.5 Coverages)</u>						
0+10	8,326	55.5	31.1	10.4	4.7	3.2
	13,479	*	45.5	18.1	7.5	5.4
0+20	8,188	58.6	30.3	12.4	5.3	3.6
	13,273	*	51.4	21.9	8.8	6.1
0+30	8,136	62.5	30.3	11.8	5.2	3.7
	13,217	*	50.6	21.7	9.0	6.5
0+40	8,093	62.4	33.7	12.8	4.8	3.5
	13,141	*	56.9	22.8	8.7	5.8
<u>WES 1 (46.1 Coverages)</u>						
0+10	8,180	54.5	24.2	11.1	5.4	3.9
	13,344	*	42.5	20.5	9.7	7.0
0+20	8,040	66.1	37.4	15.4	5.6	3.5
	13,077	*	74.6	26.6	11.6	5.8
0+30	8,112	54.5	34.3	12.2	5.8	3.9
	13,260	*	62.2	20.9	10.6	6.5
0+40	8,021	67.0	40.4	11.8	6.0	3.6
	13,046	*	63.2	22.0	10.0	6.2

* Deflection exceeded range of velocity transducer.

TABLE A-1. FALLING WEIGHT DEFLECTOMETER DEFLECTION BASIN DATA
(CONTINUED)

Station No.	Force lbs.	Deflections				
		0-in. mils	12-in. mils	24-in. mils	36-in. mils	48-in. mils
<u>WES 2 (0 Coverages)</u>						
0+10	8,342	56.1	28.0	10.6	5.5	3.9
	13,543	*	54.3	18.5	9.6	6.1
0+20	8,323	53.0	27.6	10.0	6.0	3.8
	13,575	*	51.0	19.3	10.4	6.7
0+30	8,252	55.6	31.5	10.6	5.8	3.6
	13,464	*	58.7	20.5	9.8	6.4
0+40	8,339	45.7	26.4	10.0	5.6	3.7
	13,734	75.9	45.9	18.3	9.5	6.2
<u>WES 2 (6.5 Coverages)</u>						
0+10	8,048	*	30.1	10.4	4.8	3.6
	12,887	*	53.5	17.9	7.8	6.0
0+20	8,056	*	33.1	11.6	5.3	3.7
	12,915	*	55.3	19.7	8.7	6.2
0+30	8,053	*	33.5	11.8	5.3	3.9
	12,966	*	56.7	20.7	9.0	6.5
0+40	8,109	66.5	31.3	12.0	5.8	4.1
	13,213	*	53.3	22.8	9.8	7.0
<u>WES 2 (20.5 Coverages)</u>						
0+10	8,017	73.8	32.3	13.0	5.6	4.1
	12,958	*	55.9	22.6	9.5	6.7
0+20	8,085	66.9	32.7	12.4	5.9	4.1
	13,058	*	53.5	22.2	10.0	7.0

* Deflection exceeded range of velocity transducer.

TABLE A-1. FALLING WEIGHT DEFLECTOMETER DEFLECTION BASIN DATA
(CONTINUED)

Station No.	Force lbs.	Deflections				
		0-in. mils	12-in. mils	24-in. mils	36-in. mils	48-in. mils
<u>WES 2 (20.5 Coverages) Continued</u>						
0+30	8,088	60.6	34.4	13.0	6.4	4.1
	13,146	*	54.1	24.4	10.4	7.2
0+40	8,077	60.8	30.4	13.0	6.3	4.2
	13,213	*	53.1	23.6	10.7	7.3
<u>WES 3 (0 Coverages)</u>						
0+10	8,167	65.7	30.3	13.0	6.7	4.1
	13,241	*	56.1	20.5	11.8	6.5
0+20	8,180	64.3	35.4	13.4	7.3	4.6
	13,340	*	51.8	23.2	11.8	7.7
0+30	8,164	57.7	27.2	12.2	6.3	4.3
	13,472	*	52.2	21.2	11.9	7.0
0+40	8,204	56.3	23.2	10.2	5.7	3.9
	13,638	*	45.2	18.1	10.4	6.3
<u>WES 3 (6.5 Coverages)</u>						
0+10	7,902	*	29.1	13.8	5.5	3.8
	12,431	*	53.9	22.8	9.1	6.2
0+20	7,842	*	23.6	13.2	5.4	4.2
	12,224	*	41.3	19.1	8.0	6.3
0+30	6,141	*	22.0	11.4	5.4	3.8
	9,610	*	37.8	20.1	8.5	6.1
0+40	8,005	*	23.4	11.0	5.6	4.1
	12,756	*	43.1	19.9	9.0	6.3

* Deflection exceeded range of velocity transducer.

TABLE A-1. FALLING WEIGHT DEFLECTOMETER DEFLECTION BASIN DATA
(CONTINUED)

Station No.	Force lbs.	Deflections				
		0-in. mils	12-in. mils	24-in. mils	36-in. mils	48-in. mils
<u>WP-1 (0 Coverages)</u>						
0+05	8,803	62.8	18.9	3.9	1.3	2.3
	13,205	*	29.9	2.4	1.4	2.8
0+15	8,819	43.7	17.7	3.2	1.6	1.2
	13,236	60.4	28.0	5.0	1.7	2.4
0+25	8,851	47.4	23.5	3.5	1.9	1.1
	13,352	66.3	34.8	5.3	3.0	1.7
<u>WP-2 (0 Coverages)</u>						
0+05	8,994	20.9	9.4	3.2	1.5	1.5
	13,538	27.8	13.5	4.3	2.3	1.8
0+15	8,898	24.2	12.2	3.4	1.9	1.5
	13,538	31.3	17.6	4.7	2.7	2.1
0+25	8,867	23.2	11.3	3.5	2.1	1.5
	13,522	31.5	16.1	4.8	3.0	2.3
<u>WP-2 (46 Coverages)</u>						
0+05	8,612	*	42.9	10.6	1.5	1.7
0+15	8,596	*	62.6	9.1	1.0	1.8
	13,093	*	65.7	10.6	1.5	2.7
0+25	8,724	*	51.2	5.9	1.5	1.6
	13,363	*	50.4	7.9	2.2	2.5
<u>WP-2 (65.6 Coverages)</u>						
0+05	9,375	*	49.2	12.6	3.6	2.2
	13,888	*	52.4	14.6	3.5	2.5

* Deflection exceeded range of velocity transducer.

TABLE A-1. FALLING WEIGHT DEFLECTOMETER DEFLECTION BASIN DATA
(CONTINUED)

Station No.	Force lbs.	Deflections				
		0-in. mils	12-in. mils	24-in. mils	36-in. mils	48-in. mils
<u>WP-2 (65.6 Coverages) Continued</u>						
0+15	9,296	*	58.7	11.4	2.4	2.0
	13,761	*	63.4	12.6	3.0	2.9
0+25	9,200	*	41.7	5.5	2.2	3.4
	13,650	*	46.9	7.1	3.2	3.3
<u>WP-2 (87.7 Coverages)</u>						
0+05	8,787	67.7	35.4	9.8	2.4	1.6
	13,379	*	42.1	11.0	2.8	2.8
0+15	8,771	*	46.9	6.3	1.2	1.6
	13,284	*	49.2	8.7	2.0	2.4
0+25	8,708	*	31.1	4.7	1.6	2.8
	13,205	*	38.2	5.1	3.5	2.8
<u>WP-3 (0 Coverages)</u>						
0+05	9,200	45.7	23.6	6.3	2.5	2.4
	13,618	66.3	36.2	8.3	3.1	2.7
0+15	9,200	44.5	21.6	4.9	2.2	2.0
	13,665	63.3	33.9	7.7	2.7	2.5
0+25	9,184	55.7	28.0	4.3	2.6	2.6
	13,602	77.2	40.6	6.7	3.3	2.7
<u>WP-3 (12.3 Coverages)</u>						
0+05	8,464	*	62.6	16.1	2.4	1.6
	12,172	*	97.6	24.8	2.3	1.0

* Deflection exceeded range of velocity transducer.

TABLE A-1. FALLING WEIGHT DEFLECTOMETER DEFLECTION BASIN DATA
(CONTINUED)

Station No.	Force lbs.	Deflections				
		0-in. mils	12-in. mils	24-in. mils	36-in. mils	48-in. mils
<u>WP-3 (12.3 Coverages) Continued</u>						
0+15	8,168	*	77.2	21.7	4.4	2.4
	11,854	*	*	31.5	5.6	3.0
0+25	7,786	*	*	21.7	7.0	2.6
	11,314	*	*	31.5	12.2	3.0
<u>WP-4 (0 Coverages)</u>						
0+05	9,137	37.2	19.3	5.4	1.9	1.2
	13,427	52.4	28.8	8.5	2.6	1.8
0+15	9,121	32.1	14.3	3.9	1.5	1.3
	13,570	44.3	22.5	6.2	2.1	2.2
0+25	9,057	32.3	14.3	3.7	1.5	1.4
	13,475	44.5	22.6	5.9	2.0	1.3
<u>WP-4 (22.1 Coverages)</u>						
0+05	8,295	*	*	13.0	2.6	1.7
	11,965	*	*	20.0	4.5	2.8
0+15	8,692	*	58.0	7.9	3.1	1.3
	12,648	*	*	13.4	4.1	3.4
0+25	8,279	*	*	7.5	2.3	1.3
	11,886	*	*	11.0	4.8	2.3
<u>W-1 (0 Coverages)</u>						
0+05	9,081	36.5	8.5	5.1	3.7	2.9
	14,063	53.4	11.6	7.8	5.5	4.3

* Deflection exceeded range of velocity transducer.

TABLE A-1. FALLING WEIGHT DEFLECTOMETER DEFLECTION BASIN DATA
(CONTINUED)

Station No.	Force lbs.	Deflections				
		0-in. mils	12-in. mils	24-in. mils	36-in. mils	48-in. mils
<u>W-1 (0 Coverages) Continued</u>						
0+15	9,049	43.1	9.9	4.9	3.7	2.9
	13,955	59.7	15.6	7.5	5.6	4.3
0+25	9,033	35.8	7.1	5.2	3.8	2.8
	14,019	51.3	11.5	7.8	5.9	4.4
<u>W-1 (6.8 Coverages)</u>						
0+05	9,101	48.9	22.1	8.8	5.0	3.6
	13,982	69.5	32.6	13.5	7.5	5.4
0+15	8,930	62.1	25.2	8.2	5.4	3.5
	13,781	*	37.8	13.0	7.7	5.4
0+25	8,890	60.3	23.6	8.1	5.1	3.6
	13,721	*	35.2	13.0	8.1	5.4
<u>W-1 (13.6 Coverages)</u>						
0+05	8,941	76.5	33.4	11.5	6.7	3.6
	13,693	*	49.2	19.0	9.0	5.6
0+15	8,771	*	44.9	5.9	5.6	3.8
	13,518	*	55.3	9.5	9.1	6.0
0+25	8,815	*	36.4	11.5	5.9	3.8
	13,448	*	52.0	18.5	9.5	6.1
<u>W-1 (20.5 Coverages)</u>						
0+05	8,644	67.1	33.4	11.4	5.3	3.7
	13,371	*	49.4	19.7	8.8	5.7

* Deflection exceeded range of velocity transducer.

TABLE A-1. FALLING WEIGHT DEFLECTOMETER DEFLECTION BASIN DATA
(CONTINUED)

Station No.	Force lbs.	Deflections				
		0-in. mils	12-in. mils	24-in. mils	36-in. mils	48-in. mils
<u>W-1 (20.5 Coverages) Continued</u>						
0+15	6,491	*	33.5	11.6	5.7	3.2
	10,333	*	53.0	18.9	9.1	5.3
0+25	8,263	*	36.2	15.0	7.1	3.9
	13,066	*	56.3	20.2	11.7	6.3
<u>W-1 (27.3 Coverages)</u>						
0+05	9,200	*	48.2	17.9	6.5	3.7
	13,999	*	68.5	26.0	9.4	5.9
0+15	8,871	*	60.6	17.9	7.3	3.7
	13,594	*	*	26.8	9.7	5.7
0+25	8,673	*	70.1	28.4	11.8	4.1
	13,400	*	*	42.3	18.4	5.9
<u>W-1 (38.2 Coverages)</u>						
0+05	4,151	71.3	26.4	8.3	2.8	2.2
	9,176	*	50.6	16.6	6.9	5.0
0+15	3,432	*	37.1	8.7	2.6	1.5
	7,624	*	68.5	19.8	6.7	3.9
0+25	4,020	*	38.3	11.3	4.8	3.0
	8,673	*	*	26.3	11.2	6.0
<u>W-2 (0 Coverages)</u>						
0+05	9,160	48.2	28.4	11.0	5.9	4.6
	14,173	67.0	41.9	17.2	9.7	7.3

* Deflection exceeded range of velocity transducer.

TABLE A-1. FALLING WEIGHT DEFLECTOMETER DEFLECTION BASIN DATA
(CONTINUED)

Station No.	Force lbs.	Deflections				
		0-in. mils	12-in. mils	24-in. mils	36-in. mils	48-in. mils
<u>W-2 (0 Coverages) Continued</u>						
0+15	9,137	44.5	27.5	11.3	5.9	4.5
	14,106	62.8	41.3	17.5	9.8	7.2
0+25	9,149	45.0	25.9	9.7	5.3	3.8
	14,118	62.8	39.2	15.7	8.7	6.4
<u>W-2 (6.8 Coverages)</u>						
0+05	4,080	61.2	35.4	10.4	4.4	2.8
	8,390	*	76.4	20.9	9.9	7.2
0+15	4,028	52.7	31.9	9.3	5.0	2.5
	8,446	*	72.6	19.1	10.1	6.1
0+25	4,000	54.8	32.5	8.6	5.6	2.3
	8,390	*	70.3	33.5	9.6	5.7
<u>W-2 (13.6 Coverages)</u>						
0+05	3,583	*	58.7	12.3	4.6	3.3
0+15	3,899	68.0	30.5	11.6	5.1	3.0
0+25	3,822	60.3	32.9	9.7	4.2	2.4
<u>W-3 (0 Coverages)</u>						
0+05	8,827	46.1	17.0	7.8	4.2	3.2
	13,844	68.9	27.2	12.2	6.5	4.9
0+15	8,934	41.8	20.1	7.9	4.4	3.0
	13,884	60.9	30.9	12.2	6.8	4.9

* Deflection exceed range of velocity transducer.

TABLE A-1. FALLING WEIGHT DEFLECTOMETER DEFLECTION BASIN DATA
(CONCLUDED)

Station No.	Force lbs.	Deflections				
		0-in. mils	12-in. mils	24-in. mils	36-in. mils	48-in. mils
<u>W-3 (0 Coverages) Continued</u>						
0+25	8,875	42.2	18.4	7.1	4.1	2.8
	13,848	61.4	28.6	10.9	6.4	4.7
<u>W-3 (6.8 Coverages)</u>						
0+05	4,044	*	41.9	10.0	3.3	2.2
0+15	4,020	66.0	41.9	10.9	3.6	2.2
	8,267	*	*	24.2	6.4	4.2
0+25	3,958	*	51.2	10.7	3.0	1.8
	8,064	*	*	20.0	4.5	2.2
<u>W-3 (11.7 Coverages)</u>						
0+05	(Unable to use Station 0+05)					
0+15	4,004	*	47.2	10.1	2.6	2.0
0+25	2,300	*	45.1	8.2	2.3	2.2

* Deflection exceeded range of velocity transducer.

TABLE A-2. FALLING WEIGHT DEFLECTOMETER DEFLECTION BASIN DATA
NORTH FIELD

Station No.	Force lbs.	Deflections						
		0-in. mils	12-in. mils	18-in. mils	24-in. mils	36-in. mils	48-in. mils	60-in. mils
<u>NFF4 (Subgrade)^a</u>								
1+25	4,846	11.7	6.3	2.9	1.8	0.9	0.5	0.4
1+50	4,728	14.5	8.7	3.8	2.3	1.1	0.6	0.5
1+75	4,848	14.5	6.0	2.8	1.7	0.7	0.5	0.3
1+25	8,664	22.6	11.5	5.2	3.4	1.7	1.1	0.8
1+50	8,648	26.5	16.5	6.4	4.2	2.0	1.2	0.8
1+75	8,784	25.9	10.8	4.9	2.8	1.3	0.9	0.7
<u>NFF4 (Base Course)^b</u>								
1+25	5,160	19.9	6.2	3.2	2.1	1.6	1.0	0.7
1+50	4,840	23.8	7.3	3.4	2.0	1.3	1.0	0.7
1+75	4,816	23.3	6.8	3.8	2.5	1.7	1.1	0.7
1+25	9,080	27.5	12.6	6.3	4.0	2.7	1.9	1.3
1+50	8,832	35.6	12.9	6.2	3.9	2.6	1.8	1.3
1+75	8,872	34.7	12.4	7.1	4.2	2.8	1.9	1.3
1+25	11,720	32.0	16.9	8.8	5.5	3.9	2.6	1.8
1+50	11,584	43.6	16.3	7.7	4.3	3.1	2.2	1.5
1+75	11,720	42.2	16.3	8.5	4.7	3.2	2.1	1.5
<u>NFF4 (Before Traffic)</u>								
1+25	4,960	15.6	6.6	3.1	1.9	1.7	0.8	0.5
1+50	4,888	16.3	7.6	3.6	2.3	1.6	0.9	0.6
1+75	4,976	14.8	6.8	3.4	2.0	1.4	0.8	0.5
1+25	9,024	26.2	12.0	6.0	3.6	2.6	1.5	1.1
1+50	8,880	27.4	13.3	6.7	4.2	2.9	1.7	1.2
1+75	8,928	24.9	12.2	6.3	3.7	2.6	1.6	1.0

^a 17.7-in.-diameter plate.

^b 11.8-in.-diameter plate.

TABLE A-2. FALLING WEIGHT DEFLECTOMETER DEFLECTION BASIN DATA
NORTH FIELD (CONTINUED)

Station No.	Force lbs.	Deflections						
		0-in. mils	12-in. mils	18-in. mils	24-in. mils	36-in. mils	48-in. mils	60-in. mils
<u>NFF 4 (Before Traffic) Continued</u>								
1+25	11,904	37.4	16.1	7.3	4.3	3.1	1.9	1.3
1+50	11,736	39.1	18.1	8.2	5.1	3.5	2.0	1.4
1+75	11,760	34.7	16.1	7.5	4.3	3.1	1.9	1.2
<u>NFF4 (After Proof Testing - 2 Coverages, F-4)</u>								
1+25	8,688	26.2	11.7	6.7	4.2	2.8	1.6	1.1
1+50	8,680	25.8	11.5	7.0	4.5	3.2	1.8	1.2
1+75	8,672	25.6	12.0	6.9	4.1	2.8	1.5	1.0
1+25	13,976	43.8	19.1	10.6	6.5	3.6	2.4	1.6
1+50	13,992	43.2	18.9	11.1	6.9	4.7	2.7	1.8
1+75	14,016	42.9	19.5	10.9	6.4	2.8	2.3	1.5
<u>NFF4 (After F-4 Aircraft)</u>								
1+25	8,992	25.1	13.0	7.0	4.3	3.1	1.8	1.2
1+50	8,848	30.2	12.5	7.2	4.8	3.4	1.9	1.3
1+75	8,896	23.5	12.5	6.9	4.3	3.1	1.7	1.1
1+25	14,408	41.0	20.9	11.0	6.7	4.6	2.7	1.9
1+50	14,200	46.3	21.7	12.3	7.4	4.8	2.8	1.9
1+75	14,272	39.3	20.1	10.8	6.6	5.0	2.5	1.6
<u>NFF4 (10 Coverages)</u>								
1+25	9,312	27.9	12.2	7.1	4.6	3.2	2.0	1.4
1+50	9,168	32.2	14.2	8.5	5.5	4.0	2.7	1.6
1+75	9,168	27.7	13.0	7.8	5.0	3.5	1.9	1.3
1+25	14,576	47.0	19.9	10.9	6.9	4.9	2.8	1.9
1+50	14,352	54.0	22.7	12.7	7.9	5.4	3.5	2.1
1+75	14,672	46.7	20.9	12.0	7.4	4.9	2.7	1.7

TABLE A-2. FALLING WEIGHT DEFLECTOMETER DEFLECTION BASIN DATA
NORTH FIELD (CONCLUDED)

Station No.	Force lbs.	Deflections						
		0-in. mils	12-in. mils	18-in. mils	24-in. mils	36-in. mils	48-in. mils	60-in. mils
<u>NFF4 (20 Coverages)</u>								
1+25	9,032	29.4	13.3	7.5	4.7	3.3	1.9	1.3
1+50	8,904	35.9	15.1	8.7	5.5	4.0	2.4	1.6
1+75	8,920	30.0	13.7	8.0	5.0	3.4	1.9	1.2
1+25	14,528	44.8	20.9	11.8	7.2	5.0	2.8	1.9
1+50	14,136	60.9	25.1	13.7	8.0	5.4	3.1	2.2
1+75	14,424	50.9	22.3	12.5	7.4	5.0	2.6	1.7
<u>NFF4 (30 Coverages)</u>								
1+25	9,296	31.6	16.1	9.2	5.3	3.7	2.1	1.5
1+50	9,184	39.5	17.1	9.3	5.5	3.8	2.2	1.5
1+75	9,272	29.6	15.0	9.0	5.4	3.7	2.0	1.4
1+25	14,600	57.8	28.2	15.0	8.2	5.4	3.0	2.0
1+50	14,720	68.6	28.7	14.5	7.9	5.4	3.0	2.0
1+75	14,800	54.6	25.7	14.4	8.1	5.3	2.8	1.8
<u>NFF4 (50 Coverages)</u>								
1+25	9,096	37.8	16.7	8.5	5.0	3.6	2.2	1.5
1+50	8,936	55.5	21.2	9.8	5.3	3.8	2.3	1.6
1+75	9,120	30.1	15.0	8.7	5.3	3.8	2.1	1.4
1+25	14,120	62.8	27.5	13.3	7.5	5.2	3.1	2.2
1+50	11,720	68.8	26.9	12.5	6.7	4.7	2.8	2.0
1+75	14,424	51.8	25.0	13.7	8.0	5.4	2.9	2.0
<u>NFF4 (100 Coverages)</u>								
1+25	9,200	52.0	18.5	8.8	5.4	4.0	2.3	1.6
1+50	9,416	77.9	24.9	9.1	5.6	4.1	2.4	1.7
1+75	8,832	49.1	17.8	8.9	5.5	3.9	2.1	1.5
1+25	11,672	73.6	27.6	11.2	6.8	5.0	2.8	2.0
1+50	Overranged 12,000 and 15,000							
1+75	11,728	68.6	24.6	11.4	6.8	4.7	2.5	1.7

APPENDIX B
BISDEF PROGRAM

INTRODUCTION

The BISDEF program takes measured deflections from a deflection basin with critical estimates and ranges of layer modulus and computes the modulus values that best describe the airport deflection basin. A linearly layered elastic computer program developed by the Shell Oil Corporation is used as a subroutine to calculate the deflections. The program has been adapted to operate on a personal computer. The information provided herein is as follows:

- a. Flowchart
- b. Input guide from BINPUT program
- c. Example input file
- d. Example output file

FLOWCHART

A flowchart describing the logic of the program is presented on the following page.

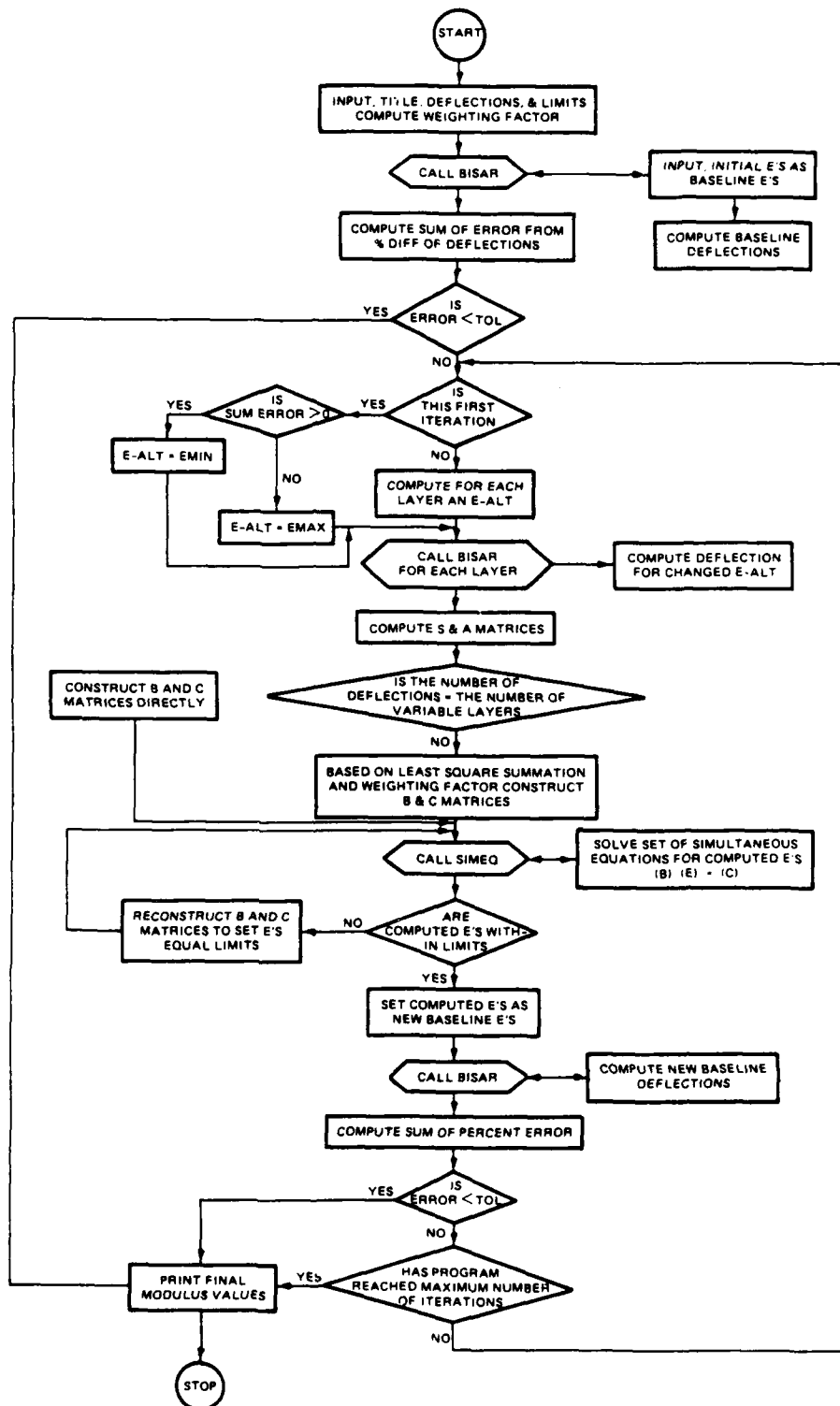


Figure B-1. Flow Chart for the BISDEF Program

INPUT GUIDE FROM BINPUT PROGRAM

THIS PROGRAM CREATES A DATA FILE FOR THE PAVEMENT
MODULUS BACK-CALCULATION PROGRAM "BISDEF"

ENTER A NAME FOR YOUR DATA FILE (10 CHARACTERS OR LESS)
-NFF4

INPUT: NUMBER OF PROBLEMS- 1

INPUT TITLE FOR PROBLEM NO. 1

--> NFF4 0 COV F4 STA 1+25

INPUT THE NUMBER OF SURFACE DEFLECTIONS FROM NDT
(MAXIMUM OF SEVEN READINGS).....--> 7

ARE SENSORS SPACED AT 1-FT INTERVALS?
(Y=YES, N=NO) --> Y

****MAGNITUDE AND LOCATION OF DEFLECTION READINGS****

GAGE NUMBER 1 :

DEFLECTION (MILS) --> 26.2

DISTANCE FROM CENTER OF LOADED AREA, (IN.) --> 3

GAGE NUMBER 2 :

DEFLECTION (MILS) --> 12

GAGE NUMBER 3 :

DEFLECTION (MILS) --> 6.0

GAGE NUMBER 4 :

DEFLECTION (MILS) --> 3.6

GAGE NUMBER 5 :

DEFLECTION (MILS) --> 2.6

GAGE NUMBER 6 :

DEFLECTION (MILS) --> 1.5

INPUT GUIDE FROM BINPUT PROGRAM (CONTINUED)

GAGE NUMBER 7 :

DEFLECTION (MILS) --> 1.1

*****ENTER LOAD INFORMATION*****

NUMBER OF LOADED AREAS.....--> 1

LOAD NUMBER 1 :

VERTICAL LOAD (LB) --> 9024

RADIUS OF LOADED AREA (IN).....--> 5.9

ENTER NUMBER OF LAYERS IN PAVEMENT SYSTEM --> 3

*****PAVEMENT INFORMATION*****

ENTER THE FOLLOWING FOR EACH SYSTEM LAYER

LAYER NUMBER 1 :

IS MODULUS (E) TO BE : 1) FIXED
2) COMPUTED

ENTER 1 OR 2 --> 2

TO COMPUTE THE LAYER MODULUS, BISDEF REQUIRES AN INITIAL MODULUS VALUE AND A RANGE (MINIMUM AND MAXIMUM MODULUS VALUES)!!!

WOULD YOU LIKE TO: 1) USE COMPUTER DEFAULT VALUES
OR

2) INPUT INITIAL E AND RANGE

ENTER 1 OR 2 --> 1

ENTER MATERIAL TYPE: 1) ASPHALTIC CONCRETE
2) PORTLAND CEMENT CONCRETE
3) HIGH-QUALITY STABILIZED BASE
4) BASE - SUBBASE, STABILIZED
5) BASE - SUBBASE, UNSTABILIZED
6) SUBGRADE

ENTER SELECTION (1-6) --> 1

INPUT GUIDE FROM BINPUT PROGRAM (CONTINUED)

LAYER THICKNESS (IN)..... --> 2.1

ENTER LAYER INTERFACE CONDITION RANGING FROM
0 (COMPLETE ADHESION) TO 1000 (FRICTIONLESS SLIP)--> 0

LAYER NUMBER 2 :

IS MODULUS (E) TO BE : 1) FIXED
2) COMPUTED
ENTER 1 OR 2 --> 2

TO COMPUTE THE LAYER MODULUS, BISDEF REQUIRES AN INITIAL MODULUS VALUE
AND A RANGE (MINIMUM AND MAXIMUM MODULUS VALUES)!!!

WOULD YOU LIKE TO: 1) USE COMPUTER DEFAULT VALUES
OR
2) INPUT INITIAL E AND RANGE
ENTER 1 OR 2 --> 1

ENTER MATERIAL TYPE: 1) ASPHALTIC CONCRETE
2) PORTLAND CEMENT CONCRETE
3) HIGH-QUALITY STABILIZED BASE
4) BASE - SUBBASE, STABILIZED
5) BASE - SUBBASE, UNSTABILIZED
6) SUBGRADE

ENTER SELECTION (1-6) --> 5

LAYER THICKNESS (IN)..... --> 6.2

ENTER LAYER INTERFACE CONDITION RANGING FROM
0 (COMPLETE ADHESION) TO 1000 (FRICTIONLESS SLIP)--> 0

LAYER NUMBER 3 :

IS MODULUS (E) TO BE : 1) FIXED
2) COMPUTED
ENTER 1 OR 2 --> 2

TO COMPUTE THE LAYER MODULUS, BISDEF REQUIRES AN INITIAL MODULUS VALUE
AND A RANGE (MINIMUM AND MAXIMUM MODULUS VALUES)!!

WOULD YOU LIKE TO: 1) USE COMPUTER DEFAULT VALUES
OR
2) INPUT INITIAL E AND RANGE
ENTER 1 OR 2 --> 1

INPUT GUIDE FROM BINPUT PROGRAM (CONCLUDED)

ENTER MATERIAL TYPE: 1) ASPHALTIC CONCRETE
2) PORTLAND CEMENT CONCRETE
3) HIGH-QUALITY STABILIZED BASE
4) BASE - SUBBASE, STABILIZED
5) BASE - SUBBASE, UNSTABILIZED
6) SUBGRADE

ENTER SELECTION (1-6) --> 6

BISDEF AUTOMATICALLY PUTS IN A STIFF LAYER BELOW
THIS FINAL (SUBGRADE) LAYER. BEST RESULTS ARE USUALLY
OBTAINED BY HAVING THIS STIFF LAYER AT A DEPTH OF 20-FT (240 IN.).
PLEASE ENTER A THICKNESS FOR THE SUBGRADE LAYER
REMEMBERING THAT THIS WILL SET THE LOCATION OF A RIGID
BOUNDARY IN BISDEF!!!

LAYER THICKNESS (IN). --> 231.7

ENTER LAYER INTERFACE CONDITION RANGING FROM
0 (COMPLETE ADHESION) TO 1000 (FRICTIONLESS SLIP) --> 0

EXAMPLE BISDEF INPUT FILE

```

      1
NFF4 0 COV F4 STA 1+25
      7
    26.20 12.00  6.00  3.60  2.60  1.50  1.10
      3.00 12.00 24.00 36.00 48.00 60.00 72.00
      1
    9024.00  5.900  0.00  0.00
      3
COMPUTE E
DEFAULT VALUES FOR INITIAL E AND RANGE
1  2.10  0.
COMPUTE E
DEFAULT VALUES FOR INITIAL E AND RANGE
5  6.20  0.
COMPUTE E
DEFAULT VALUES FOR INITIAL E AND RANGE
6 231.70  0.
```

EXAMPLE BISDEF OUTPUT FILE

* # ** # ** # *VERSION DRA-7.86.02* # ** # ** # *
 P R O B L E M N U M B E R - 1
 * # ** # ** # ** # ** # ** # ** # ** # ** # ** # ** # ** # *

NFF4 0 COV F4 STA 1+25

NUMBER OF VARIABLE LAYERS AND TARGET DEFLECTIONS - 3

VARIABLE LAYER NO.	SYSTEM LAYER NO.	ASSIGNED RANGE FOR LAYER MODULUS		
		ESTIMATED INITIAL MODULUS PSI	MINIMUM MODULUS PSI	MAXIMUM MODULUS PSI
1	1	350000.	200000.	1000000.
2	2	30000.	5000.	150000.
3	3	19736.	14736.	24736.

INITIAL PAVEMENT PARAMETERS

LAYER NO.	MATERIAL TYPE	MODULUS PSI	POISSON'S RATIO	THICK. IN.	INTERFACE VALUE
1	AC	350000.	0.35	2.10	0.
2	BASE OR SUBBASE	30000.	0.35	6.20	0.
3	SUBGRADE	19736.	0.40	231.70	0.
4	RIGID BOUNDARY	1000000.	0.50	SEMI-INF	

LOAD INFORMATION

LOAD NUMBER	LOAD POUNDS	RADIUS OF LOADED AREA, IN.	LOAD CO-ORDINATES X, IN.	Y, IN.
1	9024.	5.90	0.00	0.00

EXAMPLE BISDEF OUTPUT FILE (CONTINUED)

*****BISDEF OUTPUT SUMMARY*****

NUMBER OF ITERATIONS PERFORMED: 3

PREDICTED E DISREGARDING BOUNDARY CONDITIONS

LAYER NO.	MODULUS
1	1568.
2	143365.
3	15979.

PREDICTED E WITH BOUNDARY CONDITIONS CONSIDERED

LAYER NO.	MODULUS
1	200000.
2	42270.
3	15689.

DEFLECTIONS COMPUTED FOR FINAL MODULUS VALUES

POSITION	SENSOR OFFSET IN.	MEASURED DEFLECTION MILS	COMPUTED DEFLECTION MILS	DIFFERENCE	% DIFF.
1	3.0	26.2	25.8	0.4	1.6
2	12.0	12.0	12.1	-0.1	-0.4
3	24.0	6.0	5.8	0.2	2.6
4	36.0	3.6	3.5	0.1	4.1
5	48.0	2.6	2.3	0.3	11.4
6	60.0	1.5	1.6	-0.1	-9.8
7	72.0	1.1	1.2	-0.1	-11.4

ABSOLUTE SUM:	1.4	41.4
ARITHMETIC SUM:		-1.8
AVERAGE:	0.2	5.9

EXAMPLE BISDEF OUTPUT FILE (CONCLUDED)

FINAL MODULUS VALUES

LAYER NO.	MATERIAL TYPE	MODULUS PSI	POISSON'S RATIO	THICK. IN.	INTERFACE VALUE
1	AC	200000.	0.35	2.10	0.
2	BASE OR SUBBASE	42270.	0.35	6.20	0.
3	SUBGRADE	15689.	0.40	231.70	0.
4	RIGID BOUNDARY	1000000.	0.50	SEMI-INF	

REACHED MAX NO OF ITERATIONS
ABSOLUTE SUM OF % DIFF. NOT WITHIN TOLERANCE
CHANGE IN MODULUS VALUES WITHIN TOLERANCE

APPENDIX C

PROGRAM FOR CORRECTING FWD ISM DATA FOR TEMPERATURE

PROGRAM: FWDTCF

```

DATA A0/6.4832942E-01/,A1/-5.1830783E-02/,A2/4.9277325E-03/
DATA A3/-.00021081954/,A4/3.2681272E-06/
DATA B0/-9.6757755/,B1/3.6665256/,B2/-3.5506826E-01/
DATA B3/1.8453128E-02/, B4/-4.4352426E-04/
DATA D0/9.896776E-01/,D1/-5.820991E-02/
DATA D2/-1.692166E-03/
DATA E0/1.854619E-04/,E1/-9.401799E-04/
DATA E2/3.268749E-04/
DATA F0/-2.872853E-06/,F1/3.093604E-05/
DATA F2/-6.76536E-06/
DATA G0/3.461658E-08/,G1/-8.454449E-08/
DATA G2/3.507406E-08/
10  CONTINUE
    WRITE (*,100)
100  FORMAT(/,1X,'INPUT-PAVEMENT THICKNESS,SURF.+5DAY MEAN',/, '- ')
    READ(*,*) HI,S5
    IF(HI.LT.1.0E-06)GO TO 140
C    IF(HI.LT.3.) GO TO 151
    H=HI/2
    SL=A0+A1*H+A2*H**2.+A3*H**3.+A4*H**4.
    CP=B0+B1*H+B2*H**2.+B3*H**3.+B4*H**4.
    TD=SL*S5+CP
C    IF(TD.LT.30.OR.TD.GT.110) GO TO 131
    IF(TD.LT.30.OR.TD.GT.150) GO TO 131
    CO=D0+D1*HI+D2*HI**2.
    C1=E0+E1*HI+E2*HI**2.
    C2=F0+F1*HI+F2*HI**2.
    C3=G0+G1*HI+G2*HI**2.
    CF=CO+C1*TD+C2*TD**2.+C3*TD**3.
    CFD=1./CF
    WRITE (*,110)
110  FORMAT(/,1X,'PAV.THICK.',2X,'SURF.+5 DAY MEAN',2X,'MPTEMP',2X,
1'DSM CF',2X,'DEFL CF')
    WRITE(*,120)HI,S5,TD,CF,CFD
120  FORMAT(3X,F4.1,11X,F5.1,8X,F5.1,4X,F4.2,4X,F4.2)
    GO TO 10
131  WRITE (*,130)
130  FORMAT(/,1X,'TEMP IS OUT OF RANGE OF CURVES')
    GO TO 10
151  WRITE (*,150)
150  FORMAT(/,' THICKNESS OF LESS THAN 3 IN IS NOT CORRECTED FOR TEMP')
    GO TO 10
140  STOP
    END

```

REFERENCES

1. Rone, C. L., et al., Membrane Encapsulated Soil Layer (MESL) for Contingencies Surfaces, Technical Report No. TR 77-21, US Army Engineer Waterways Experiment Station, Vicksburg, Mississippi, April 1977.
2. Rone, C. L., et al., Evaluation of Material for Contingency Runways, Technical Report No. TR 78-46, US Army Engineer Waterways Experiment Station, Vicksburg, Mississippi, July 1979.
3. Beatty, D. N., et al., Preliminary Feasibility Study of Concepts of Contingency Surface Materials for Alternate Launch and Recovery Systems, Report No. ESL-TR-81-24, Air Force Engineering and Services Center, Tyndall Air Force Base, Florida, April 1981.
4. Baird, G. T., et al., Interim Crater Repair Test - North Field, Report No. ESL-TR-82-03, Air Force Engineering and Services Center, Tyndall Air Force Base, Florida, August 1982.
5. Rone, C. L., et al., Alternate Launch and Recovery Surfaces - State-of-the-Art Study, Report No. ESL-TR-83-13, Air Force Engineering and Services Center, Tyndall Air Force Base, Florida, February 1984.
6. Bush, A. J., et al., Design of Alternate Launch and Recovery Surfaces for Environmental Effects, Report No. ESL-TR-83-64, Air Force Engineering and Services Center, Tyndall Air Force Base, Florida, July 1984.
7. Styron, C. R., Performance Data for F-4 Operations on Alternate Launch and Recovery Surfaces, Report No. ESL-TR-83-96, Air Force Engineering and Services Center, Tyndall Air Force Base, Florida, July 1984.
8. Thompson, M. R., et al., Development of a Preliminary ALRS Stabilizer Material Pavement Analysis System, Report No. ESL-TR-83-34, Air Force Engineering and Services Center, Tyndall Air Force Base, Florida, March 1984.
9. Costigan, R. R., and Thompson, M. R., Response and Performance of Alternate Launch and Recovery Surfaces Containing Stabilized-Material Layers, Report No. ESL-TR-84-25, Air Force Engineering and Services Center, Tyndall Air Force Base, Florida, January 1985.
10. Bush, A. J., and Alford, S. J., Alternate Launch and Recovery Surface Test Section Design, Construction, and Evaluation, North Field, South Carolina, Air Force Engineering and Services Center, Tyndall Air Force Base, Florida, To be published.

REFERENCES (Continued)

11. Alexander, D. R., Bush, A. J., and McCaffrey, P. S., Jr., Spangdahlem ALRS Pavement Evaluation Support To Salty Demo 85, Phase I, Air Force Engineering and Services Center, Tyndall Air Force Base, Florida, To be published.
12. Hoffman, M. S., and Thompson, M. R., Mechanistic Interpretation of Nondestructive Pavement Testing Deflections, Report No. UILU-ENG-91-2010, University of Illinois, Urbana, Illinois, June 1981.
13. Green, J. L., and Hall, J. W., Nondestructive Vibratory Testing of Airport Pavements, Volume 1, Experimental Test Results and Development of Evaluation Methodology and Procedure, Report No. TR-S-75-14, U. S. Army Engineer Waterways Experiment Station, Vicksburg, Mississippi, September 1975.
14. Bush, Albert J., Nondestructive Testing for Light Aircraft Pavements, Phase II, Development of the Nondestructive Evaluation Procedure, Report No. FAA-RD-9-II, U. S. Department of Transportation, Federal Aviation Administration, Washington, D. C., November 1980.
15. Hall, J. W., Jr., Comparative Study of Nondestructive Pavement Testing - Macdill Air Force Base, Air Force Engineering and Services Center, Tyndall Air Force Base, Florida, September 1983.
16. Smith, Roger E., and Lytton, Robert L., Synthesis Study of Nondestructive Testing Devices for Use in Overlay Thickness Design of Flexible Pavements, FHWA Report RD/83/097, Federal Highway Administration, Washington, D. C., November 1983.
17. Bush, A. J., and Alexander D. R., Pavement Evaluation Using Deflection Basin Measurements and Layered Theory, Transportation Research Board, Washington, D. C., January 1985.
18. Lytton, R. L. et al. Determination of Asphaltic Concrete Pavement Structural Properties By Nondestructive Testing, NCHRP Project 10-27, Washington, D. C., April 1986.
19. Thompson, M. R., "Important Properties of Base and Subgrade Materials," unpublished paper presented to Conference on Crushed Stone for Road and Street Construction and Reconstruction, Arlington, Virginia, June 1984.
20. Walker, R. N., et al., "The South African Mechanistic Pavement Design Procedure," Proceedings Fourth International Conference on the Structural Design of Asphalt Pavements, Vol II, University of Michigan, Ann Arbor, Michigan 1977.

REFERENCES (Continued)

21. Barksdale, Richard D., "Laboratory Evaluation of Rutting in Base Course Materials," Proceedings Third International Conference on the Structural Design of Asphalt Pavements, Vol 1, University of Michigan, Ann Arbor, Michigan 1972.
22. Kondner, R. L., "Hyperbolic Stress-Strain Response: Cohesive Soils," Journal, Soils Mechanics and Foundations Division, American Society of Civil Engineers, Vol. 89, No. SM1, January 1963.
23. Duncan, J. M. and Chong, C. Y., "Non-Linear Analysis of Stress and Strain in Soils," Journal, Soil Mechanics and Foundations Division, American Society of Civil Engineers, Vol. 96, No. SM5, September 1970.
24. Khedr, S., Deformation Characteristics of Granular Base Course in Flexible Pavements, Transportation Research Record 1043, Transportation Research Board, Washington D.C., 1985.
25. Roberts, F. L. et al. Effects of Tire Pressures on Flexible Pavements, Report No. 372-1F, Texas Transportation Institute, Texas A&M University, College Station, Texas, August 1986.
26. Lentz, Rodney W., and Baladi, Gilbert Y., Constitutive Equation for Permanent Strain of Sand Subjected to Cyclic Loading, Transportation Research Record 810, Transportation Research Board, Washington D.C., 1981.
27. Lentz, Rodney W., and Baladi, Gilbert Y., Prediction of Permanent Strain in Sand Subjected to Cyclic Loading, Transportation Research Record 749, Transportation Research Board, Washington, D.C., 1980.
28. Baladi, G. Y. Vallejo, L. E., and Goitom, T., "Normalized Characterization Model of Pavement Materials," Properties of Flexible Pavement Materials, ASTM STP 807, J. J. Emery, Editor, American Society for Testing and Materials, 1983.
29. Brabston, W. N., Deformation Characteristics of Compacted Subgrade Soils and Their Influence in Flexible Pavement Structures, PhD Thesis, Texas A&M University, College Station, Texas, August 1982.
30. Barker, W. R., and Brabston, W. N., Development of a Structural Design Procedure for Flexible Airport Pavements, FAA-RD-74-199, Department of Transportation, Federal Aviation Administration, Washington D. C., September 1975.

REFERENCES (Continued)

31. Departments of the Navy, the Army, and the Air Force, Flexible Pavement Design for Airfields, Navy DM21.3, Army TM5-825.2, Air Force AFM 88-6 Chapter 2, August 1978.
32. U. S. Department of Transportation, Airport Pavement Design and Evaluation, AC 150/5320-6C, Federal Aviation Administration, Washington, D. C., December 1978.
33. International Civil Aviation Organization, Aerodrome Design Manual, Part 3, Pavements, Montreal, Quebec, Canada, 1983.
34. Pereira, A. T., Procedures for Development of CBR Design Curves, IR-S-77-1, U. S. Army Engineer Waterways Experiment Station, Vicksburg, Mississippi, June 1977.
35. Hall, J. W., Jr., and Elsea, D. R., Small Aperture Testing for Airfield Pavement Evaluation, MP S-74-3, U. S. Army Engineer Waterways Experiment Station, Vicksburg, Mississippi, February 1974.
36. Barber, V. C., et. al., The Deterioration and Reliability of Pavements, TR-S-78-8, U. S. Army Engineer Waterways Experiment Station, Vicksburg, Mississippi, July 1978.
37. Barker, W. R., Prediction of Pavement Roughness, MP GL-82-11, U. S. Army Engineer Waterways Experiment Station, Vicksburg, Mississippi, September 1982.
38. Baird, G. T., and Kirst, J. A., Nondestructive Pavement Testing System: Theory and Operation, ESL-TR-83-28, Air Force Engineering and Services Center, Tyndall Air Force Base, Florida, January 1983.
39. Nazarian, S., and Stokoe, K. H., II, "Nondestructive Testing of Pavements using Surface Waves," unpublished paper presented at Transportation Research Board, Washington, D. C., January 1984.
40. Peterson, D. F. et al. Asphalt Overlays and Pavement Rehabilitation - Evaluating Structural Adequacy for Flexible Pavement Overlays, Report No. 8-996, Utah Department of Transportation, January 1976.
41. ILLI-PAVE Users Manual, Civil Engineering Department, University of Illinois, Urbana-Champaign, May 1982.
42. Koninilijke/Shell Laboratorium, BISAR Users Manual; Layered Systems Under Normal and Tangential Loads, Amsterdam, Holland, 1972.

REFERENCES (Continued)

43. Chua, K. M., and Lytton, R. L., Load Rating of Light Pavement Structures, Report No. 284-6F, Texas Transportation Institute, Texas A&M University, College Station, Texas, December 1983.
44. Department of Defense, Military Standard Test Method for Pavement, Subgrade, Subbase, and Base Course Materials, MILSTD-621A, Washington, D. C., December 1964.
45. _____, "Test Methods for Bituminous Paving Materials," MIL-STD-620 A, Washington, D.C., January 1966.
46. American Society for Testing and Materials, Standard Test Method for Density of Soil and Soil-Aggregate in Place by Nuclear Methods (Shallow Depth), ASTM D 2922-81, Philadelphia, Pennsylvania, 1982.
47. _____, Standard Test Method for Density of Soil in Place by the Rubber-Balloon Method, ASTM D 2167, Philadelphia, Pennsylvania, 1982.
48. Horn, W. J., and Ledbetter, R. H., Pavement Response to Aircraft Dynamic Loads, Vol. 1, Instrumentation Systems and Testing Program. Report No. TR-S-75-11, U. S. Army Engineer Waterways Experiment Station, Vicksburg, Mississippi, June 1975.
49. Woodman, E. H., Pressure Cells for Field Use, Bulletin No. 40, U. S. Army Engineer Waterways Experiment Station, CE, Vicksburg, Mississippi, January 1955.
50. U. S. Army Engineer Waterways Experiment Station, CE, Soil Pressure Cell Investigation, Technical Memorandum No. 210-1, Vicksburg, Mississippi, July 1944.
51. Ahlvin, R. G. et al Multiple-Wheel Heavy Gear Load Pavement Tests, Volume 1, Basic Report, TR-S-71-17, U. S. Army Engineer Waterways Experiment Station, Vicksburg, Mississippi, November 1971.
52. Foxworthy, P. T., Concepts for the Development of a Nondestructive Testing and Evaluation System for Rigid Airfield Pavements, Ph.D. Thesis, University of Illinois, Urbana - Champaign, June 1985.
53. Bush, A. J. III, unpublished Memorandum For Record, Subject: Correction Factors for Deflections Measured on Pavements Containing Asphaltic Concrete Layers, U. S. Army Engineer Waterways Experiment Station, November 1979.

REFERENCES (Continued)

54. Kingham, R. I., and Kallas, B. F., "Laboratory Fatigue and Its Relationship to Pavement Performance," Proceedings, Third International Conference on the Structural Design of Asphalt Pavements, Vol. 1, University of Michigan, Ann Arbor, Michigan, 1972.
55. Asphalt Institute, "Asphalt Overlays and Pavement Rehabilitation", Manual Series No. 17, College Park, Maryland, 1969.
56. Elliott, R. P., and Thompson, M. R., Mechanistic Design Concepts for Conventional Flexible Pavements, Report No. UILU-ENG-85-2001, University of Illinois, Urbana, Illinois, February 1985.
57. Costigan, R. R., and Thompson, M. R., Response and Performance of Alternate Launch and Recovery Surfaces Containing Stabilized-Material Layers, ESL-TR-84-25, Air Force Engineering and Services Laboratory, Tyndall Air Force Base, Florida, January 1985.
58. Kelly, Henry F., Development of Mechanistic Flexible Pavement Design Concepts for the Heavyweight F-15 Aircraft, Ph.D. Thesis, University of Illinois, Urbana-Champaign, Illinois 1986.
59. Chou, Y. T., Hutchinson, R. L., and Ulery, H. H. Jr., "Design Method For Flexible Airfield Pavement", Asphalt Concrete Pavement Design and Evaluation, Transportation Research Record 521, Transportation Research Board, Washington, D. C., January 1974.

VITA

Albert Jasper Bush III [REDACTED]

[REDACTED] He received his B.S. in Agricultural Engineering from Mississippi State University in 1968. He began his career as a civil engineer in the Pavement Systems Division of the U. S. Army Engineer Waterways Experiment Station. He was assigned the development of expedient airfield surfacing for forward area airfields. In 1975, he was assigned to the Pavement Evaluation Section concentrating on the development of a nondestructive evaluation methodology for airfield pavements. He was the principal investigator on several major projects that led to the development of a procedure for evaluating the properties of layers within the pavement. He received his M.S. degree in Civil Engineering from Mississippi State University in 1979, authoring a thesis entitled "Comparison of Dynamic Surface Deflection Measurements on Rigid Pavements with the Model of an Infinite Plate on an Elastic Foundation." In 1980, he was selected by the U. S. Army Waterways Experiment Station for a Long-Term Training program at the University of Illinois in Urbana-Champaign, where he expects to receive his PhD degree in 1987.